# AFRRI Reports



199

Octobe

Decembe

Uniformed Services University of the Health Sciences

Armed Forces Radiobiology Institute

Bethesda, Maryland 20889-5

# REPORT DOCUMENTATION PAGE

Form Approved
OMB No. 0704-0188



| 1. AGENCY USE ONLY *(Leave blank)* | 2. REPORT DATE | 3. REPORT TYPE AND DATES COVERED |
|---|---|---|
| | 1991 January | Reprints/Technical |

**4. TITLE AND SUBTITLE**

AFRRI Reports, Oct-Dec 1990

**5. FUNDING NUMBERS**

NWED QAXM

**6. AUTHOR(S)**

**7. PERFORMING ORGANIZATION NAME(S) AND ADDRESS(ES)**

Armed Forces Radiobiology Research Institute
Bethesda, MD 20889-5145

**8. PERFORMING ORGANIZATION REPORT NUMBER**

SR90-25 - SR90-36

**9. SPONSORING/MONITORING AGENCY NAME(S) AND ADDRESS(ES)**

Defense Nuclear Agency
Washington, DC 20305

**10. SPONSORING/MONITORING AGENCY REPORT NUMBER**

**11. SUPPLEMENTARY NOTES**

**12a. DISTRIBUTION/AVAILABILITY STATEMENT**

Approved for public release; distribution unlimited.

**12b. DISTRIBUTION CODE**

**13. ABSTRACT** *(Maximum 200 words)*

This volume contains AFRRI Scientific Reports SR90-25 through SR90-36 for Oct-Dec 1990.



**14. SUBJECT TERMS**

**15. NUMBER OF PAGES**
105

**16. PRICE CODE**

| 17. SECURITY CLASSIFICATION OF REPORT | 18. SECURITY CLASSIFICATION OF THIS PAGE | 19. SECURITY CLASSIFICATION OF ABSTRACT | 20. LIMITATION OF ABSTRACT |
|---|---|---|---|
| UNCLASSIFIED | UNCLASSIFIED | UNCLASSIFIED | same as report |

CLASSIFIED BY:

DECLASSIFY ON:

## CONTENTS

**Scientific Reports**

*Free Radical Biology & Medicine*, Vol. 9, pp. 191–197, 1990
Printed in the USA. 

0891-5849/90 $3.00 + .00




## Original Contribution

# ESR STUDY OF ELECTRON TRANSFER REACTIONS BETWEEN γ-IRRADIATED PYRIMIDINES, ADRIAMYCIN AND OXYGEN

CARMEN M. ARROYO* and ALASDAIR J. CARMICHAEL†
Radiation Biochemistry Department, Armed Forces Radiobiology Research Institute, Bethesda MD 20814-5145

(*Received* 1 *March* 1990; *Revised and Accepted* 9 *May* 1990)

**Abstract**—Solid pyrimidine nucleic acid bases (cytosine, thymine, and uracil) were γ-irradiated (50 KGy) and dissolved in deaerated solutions of adriamycin in water and dimethylsulfoxide (DMSO). Analogous experiments using unirradiated pyrimidines as controls were also performed. In water only γ-irradiated cytosine showed a reaction with the adriamycin yielding a single ESR peak ($g$ = 2.0033) consistent with the adriamycin semiquinone radical. Since the unirradiated cytosine gave no reaction, the result suggests an electron transfer from cytosine radicals (generated by γ-radiolysis) to adriamycin. In DMSO the three γ-irradiated and unirradiated pyrimidines reacted with adriamycin yielding the adriamycin semiquinone radical observed by ESR. These results suggest that in DMSO an electron is transferred to adriamycin from the pyrimidine radicals and from the parent pyrimidine molecules. However, the process is on the order of $10^4$ times more efficient for the pyrimidine radicals. Superoxide radicals ($O_2^{\cdot}$) were formed following addition of oxygen to the deaerated DMSO solutions containing adriamycin semiquinone radicals. $O_2^{\cdot}$ was spin trapped using 5,5-dimethyl-1-pyrroline-*N*-oxide (DMPO). The results show a possible reaction sequence in which an electron transferred to adriamycin, by pyrimidine radicals and parent pyrimidine molecules, is subsequently transferred to dissolved oxygen.

**Keywords**—ESR, Spin trapping, γ-Radiolysis, Pyrimidines, Adriamycin, Oxygen, Free radicals

## INTRODUCTION

The direct effect of ionizing radiation on DNA generates mainly guanine and thymine radicals.[1-5] These radicals have been observed in solid DNA samples using electron spin resonance (ESR) spectroscopy. However, the exact fate of the guanine and thymine radicals when DNA is in solution is still unclear. One possibility of interest to this work, is the reaction of these radicals with other molecules in the solution generating products which may be harmful to cells. For this reason and as a model, the reaction between γ-irradiated pyrimidine bases with adriamycin was studied.

Adriamycin was chosen for two reasons: i) it is one of the most widely used antitumor agents functioning primarily through its ability to intercalate into DNA disrupting DNA and RNA synthesis.[6-8] The intercalated adriamycin is in close proximity to the DNA bases, therefore, knowledge about the direct interaction between bases and adriamycin is of interest. Furthermore, the direct interaction between γ-irradiated bases and adriamycin is of interest because of the possible enhancement of combined radiation and adriamycin therapies; ii) Adriamycin participates in oxidation reduction reactions via free radical mechanisms. Several reports have shown the formation of superoxide radicals ($O_2^{\cdot-}$) when adriamycin is incubated with cellular components.[9-12] In these cases adriamycin is first reduced forming the semiquinone radical which rapidly reacts with oxygen to form $O_2^{\cdot-}$. Superoxide is also formed via the oxidation of photoexcited adriamycin in air-saturated aqueous solutions and in air-saturated aqueous solutions containing pyrimidine bases.[13, 14] However, in the absence of oxygen the pyrimidines are oxidized, thus reducing the photoexcited adriamycin.[14]

Superoxide and the adriamycin semiquinone radical are potentially lethal to cells. The disproportionation of $O_2^{\cdot-}$ produces hydrogen peroxide which in the presence of trace amounts of metals generates hydroxyl radicals ($^{\cdot}OH$).[15-18] Hydroxyl radicals are powerful ox-

*Current Address: Carmen M. Arroyo, School of Medicine, MSTF 800, University of Maryland at Baltimore, 10 South Pine Street, Baltimore, MD 20201.
†Author to whom correspondence should be addressed.

idants with no known enzyme for their removal. On the other hand, the intercalation into DNA of the adriamycin semiquinone radical is known to cause DNA strand scission.[19]

Since intercalated adriamycin may be found in various environments, the reactions of adriamycin with pyrimidines (cytosine, thymine, and uracil) and with their radicals, formed by γ-radiolysis, were carried out by dissolution of the pyrimidines or their radicals in deaerated aqueous or dimethylsulfoxide solutions of adriamycin. In addition to providing an aprotic environment, DMSO allows the dissolution of larger amounts of pyrimidine bases. The reactions involving free radical intermediates were studied using ESR. The results show a possible reaction sequence in which an electron is transferred from the pyrimidines to adriamycin and subsequently to dissolved oxygen.

## MATERIALS AND METHODS

The pyrimidine bases and adriamycin were obtained from Sigma (St. Louis, MO). The spin trap 5,5-dimethyl-1-pyrroline-*N*-oxide (DMPO) was purchased from Aldrich (Milwaukee, WI). DMPO was purified using the method described by Buettner and Oberley.[20] In this method aqueous DMPO solutions are repeatedly treated with activated charcoal until free radical impurities are eliminated as verified by ESR. The DMPO concentration was measured spectophotometrically ($\lambda$ = 227 nm, $\epsilon = 8 \times 10^3\ M^{-1}\ cm^{-1}$).[21] For experiments in DMSO, samples of pure DMPO were dissolved directly into dry DMSO and contained no free radicals also verified by ESR. The DMSO was dried over calcium hydride overnight.

Pyrimidine base radicals were obtained by room temperature γ-radiation of cytosine, thymine, and uracil powders at a dose rate of 51 Gy/min to a total dose of 50 KGy. As observed by ESR, the pyrimidine radicals formed most likely originate from π-anions. Sevilla has shown that upon warming of glasses containing a mixture of π-cations and π-anions of 5-methyluracil (thymine) the ESR spectrum of the π-cation is lost, however, the spectrum for the π-anion persists.[22] In addition, spin density calculations have shown that the highest spin density for the pyrimidine anions is at the C(6) carbon.[22, 23]

Experiments requiring the absence of oxygen were carried out in an apparatus described by Russell et al.[24] and Evans.[25] This apparatus consists of a "U" tube connected to an ESR flat cell (60 × 10 × 0.25 mm) via a ground glass joint. Adriamycin was placed in one stem of the "U" tube and any one of the γ-irradiated pyrimidines (cytosine, thymine, or uracil) was placed in the other stem. Nitrogen-saturated water or DMSO were added to the adriamycin and the "U" tube was sealed. Nitrogen bubbling through the adriamycin solution was then continued for 20 min. Pure water was obtained from a Sybron/Barnstead NANO pure II water system and the DMSO was obtained from Aldrich (Gold Label or HPLC Grade). Therefore, unless the adriamycin contained trace metal impurities, which is unlikely as verified by the optical absorption spectrum of adriamycin solutions, there were virtually no trace metal ions in the solutions. Following deaeration with nitrogen, the adriamycin solution was transferred to the stem containing the γ-irradiated pyrimidine powder. The base was rapidly dissolved in the adriamycin solution by stirring with a magnetic stirring bar or a vortex mixer. After complete dissolution of the pyrimidine powder, the "U" tube was inverted and the reaction mixture was transferred into the ESR flat cell and its ESR spectrum recorded. Control experiments were done under identical conditions using nonirradiated pyrimidine bases. Control experiments were also carried out with adriamycin solutions alone and gave no ESR signals.

For reactions requiring oxygen, DMPO was added to the reaction mixture to a final concentration of 0.15 M prior to saturation with oxygen (1–2 min bubbling). The reaction mixture was then saturated with nitrogen (~2 min) to prevent the spin adduct ESR line broadening caused by dissolved oxygen.

The radical yields of adriamycin and of the solid γ-irradiated pyrimidines was determined by double integration of the first derivative ESR spectrum. For adriamycin radicals a solution of 3-carbamoyl-2,2,5,5-tetramethyl-1-pyrrolidone-1-yloxy free radical (3-CAR) was used as the standard. This stable nitroxide has been used previously as an ESR standard for determining unknown radical concentrations.[21] For the solid γ-irradiated pyrimidines, a homogeneous solid mixture of 3-CAR and KCl as described by Lion et al.[26] was used as the standard. Using the method described by Hall,[27] the accuracy of the double integrations was ±10%.

The ESR spectra were recorded on a Varian E-9 X-band spectrometer at 100 KHz magnetic field modulation. *g*-Value measurements were carried out using α,α′-diphenyl-β-pycrylhydrazyl (DPPH) as a standard ($g$ = 2.0036).

## RESULTS AND DISCUSSION

Room temperature γ-irradiation of cytosine, thymine, and uracil powders generates pyrimidine radicals which most likely originate mainly from π-anions. Spin density calculations have shown that the highest spin density for pyrimidine anions is at the C(6) carbon.[22, 23] Sevilla has shown that upon warming of glasses containing a mixture of π-cations and π-anions

of 5-methyluracil (thymine) the ESR spectrum of the π-cation is lost, however, the spectrum of the π-anion persists.[22]

When solid γ-irradiated pyrimidine bases are dissolved in oxygen-free adriamycin solutions, an electron is transferred from the pyrimidine to adriamycin (Fig. 1). Figure 1a shows the ESR spectrum obtained following dissolution of γ-irradiated cytosine (0.025 M) in deaerated aqueous adriamycin (7 mM) solutions. The single ESR line with $g = 2.0033$ is consistent with the previously observed adriamycin semiquinone radical in water.[11, 12] The semiquinone radical was observed only in the reaction involving γ-irradiated cytosine but not for γ-irradiated thymine or uracil. It is possible that the reaction in water may be more efficient for γ-irradiated cytosine. Since the control experiments involving adriamycin and nonirradiated cytosine (0.025 M) gave no ESR signals, it is concluded that the semiquinone adriamycin radical (Fig. 1a) is formed in the reaction between cytosine radicals (generated by γ-radiolysis) and adriamycin. The result of similar experiments carried out in deaerated adriamycin solutions in DMSO is shown in Fig. 1b. In this case the reaction occurs following dissolution of any one of the γ-irradiated pyrimidine bases (cytosine, thymine, or uracil) in the adriamycin (3.5 nM) solution. Although an ESR spectrum for the reduced adriamycin radical in DMSO has not been reported, the hyperfine structure observed in Fig. 1b is similar to that of the chemically reduced adriamycin analog, daunomycin, semiquinone radical.[28, 29] In addition to the ESR spectrum of the adriamycin semiquinone radical, a single ESR line with $g = 2.00$ is observed in Fig. 1b. This additional ESR spectrum is typical of charge transfer processes between organic molecules.[30] It must be noted that control experiments under the same conditions using nonirradiated pyrimidines also yield the adriamycin semiquinone radical. Therefore, the result shown in Fig. 1b suggests that in DMSO an electron is transferred to adriamycin from pyrimidine radicals (produced by γ-radiolysis) and from the parent pyrimidine molecules. However, as will be shown in other experiments in this work, the electron transfer process is on the order of $10^5$ times more efficient for the pyrimidine radicals than for the parent pyrimidine molecules. When DMSO solutions containing the adriamycin semiquinone radical are saturated with oxygen in the presence of added spin trap DMPO (0.15 M), the semiquinone ESR spectrum rapidly disappears and a new ESR spectrum is obtained (Fig. 1c). This twelve-line ESR spectrum has hyperfine coupling constants, $a_N^{\beta} = 0.127$ mT, $a_H^{\beta} = 0.103$ mT and $a_H^{\gamma} = 0.013$ mT, corresponding to the $O_2^{\cdot-}$ spin adduct of DMPO (DMPO–$O_2^{\cdot-}$).[31] This result suggests that an electron

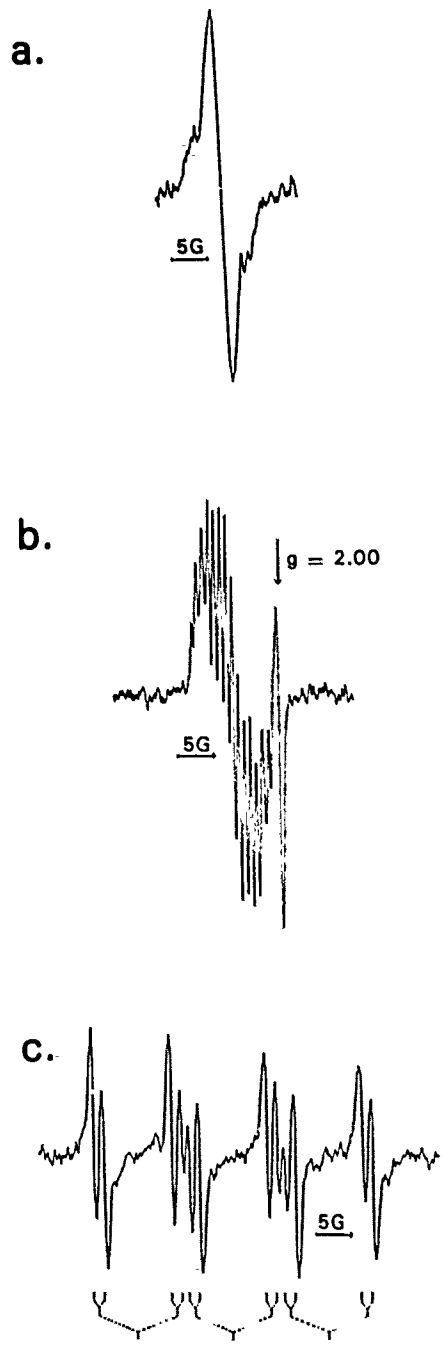


Fig. 1. (a) ESR spectrum of the adriamycin semiquinone radical in water. Spectrum obtained following dissolution of γ-irradiated cytosine (0.025 M) in deaerated aqueous adriamycin solutions. (b) ESR spectrum of the adriamycin semiquinone radical in deaerated DMSO. Spectrum obtained following dissolution of any one of the γ-irradiated pyrimidine bases in deaerated adriamycin solutions. Cytosine, 0.09 M; thymine, 0.4 M; uracil, 0.4 M. (c) ESR spectrum of the DMPO $O_2^{\cdot-}$ spin adduct in DMSO. Spectrum obtained following the addition of DMPO (0.15 M) to the deaerated DMSO solution of adriamycin containing the semiquinone radical formed in (b). After the addition of DMPO the solution was saturated with oxygen. Instrument settings: magnetic field, 340.0 mT; modulation amplitude, 0.1 mT for (a), 0.05 mT for (b) and (c); microwave power, 4 mW for (a), 0.4 mW for (b) and 10 mW for (c); receiver gain, $3.2 \times 10^5$ for (a), $5 \times 10^5$ for (b) and $6.3 \times 10^4$ for (c).

was transferred from the semiquinone radical to dissolved oxygen yielding $O_2^{\cdot-}$. In an analogous experiment in water using γ-irradiated cytosine to generate the semiquinone radicals, the ESR spectrum of the DMPO–$O_2^-$ was not observed. However, it is known that DMPO–$O_2^-$ is unstable in water and rapidly decomposes forming DMPO–OH.[32, 33] The DMPO–OH ESR spectrum consists of a 1:2:2:1 quartet ($a_N = a_H^\beta = 1.49$ mT) and is different from the DMPO–$O_2^-$ ESR spectrum.[29] Because the yield of adriamycin semiquinone radicals was low when produced in water in the reaction between cytosine radicals and adriamycin, it is possible that the yield of DMPO–$O_2^-$ and of its decomposition product, DMPO–OH, are too low in the reaction mixture to be observed by ESR. It is also possible that the DMPO–$O_2^-$ was not observed in the aqueous reaction mixture due to the decomposition of DMPO–$O_2^-$ by $O_2^{\cdot-}$.[34]

The electron transfer in DMSO from pyrimidine radicals and parent pyrimidine molecules to adriamycin is not immediate and can be followed over a period of time. Therefore, it is important to determine whether there are differences between the ability of cytosine, thymine, and uracil radicals to reduce adriamycin and also if there are differences between the parent pyrimidines' ability to reduce adriamycin. For this purpose, powder samples of γ-irradiated cytosine, thymine, and uracil adjusted to contain an equal quantity of radicals ($1.5 \times 10^{15}$), were each dissolved in different adriamycin (3.5 nM) in DMSO. Analagous control experiments using nonirradiated cytosine, thymine, and uracil were also studied. Figure 2 shows, as a function of time, the formation of adriamycin semiquinone radicals originating from the pyrimidine radicals and parent pyrimidine molecules. The adriamycin semiquinone radicals originating only from the reactions involving the pyrimidine radicals was determined as the difference in the results obtained from the experiments using nonirradiated pyrimidines (controls) and those using γ-irradiated pyrimidines. Control experiments using deaerated solutions containing only adriamycin gave no ESR signals. The results in Figure 2 also indicate that the difference between the reduction of adriamycin by thymine or uracil radicals is small and that the process is more efficient for cytosine radicals. It must be noted that the initial concentration of pyrimidine radicals (2.5 μM) dissolved in the deaerated adriamycin solutions, is slightly larger than the adriamycin semiquinone radical yield at 30 min originating from cytosine radicals, therefore, explaining the curvature observed in the data obtained from the experiment involving cytosine radicals (Fig. 2).

Although in DMSO the electron transfer to adriamycin occurs from pyrimidine radicals and parent pyrimidine molecules, the quantity of pyrimidine radicals ($1.5 \times 10^{15}$) dissolved is smaller than the quantity of parent pyrimidine molecules ($5.4 \times 10^{19}$ for cytosine and uracil; $8.1 \times 10^{19}$ for thymine). Figure 3a shows the adriamycin semiquinone yield normalized for the initial concentration of pyrimidine radicals dissolved in the deaerated adriamycin solution. Likewise, Fig. 3b (plotted on the same scale as Fig. 3a) shows the adriamycin semiquinone radical yield in the controls (Fig. 2) normalized for the pyrimidine molecules present. The results indicate that the electron transfer to adriamycin is approximately $10^5$ times more efficient from pyrimidine radicals than from parent pyrimidine molecules.

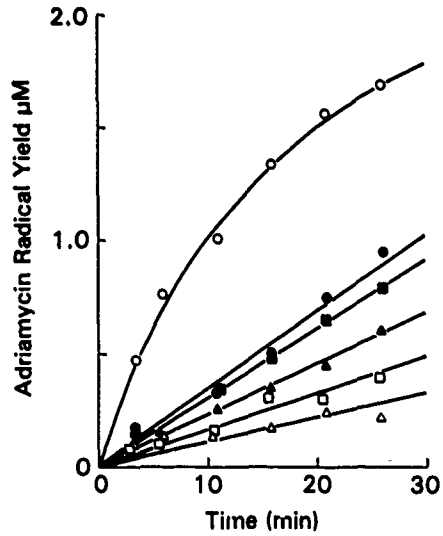


Fig. 2. Adriamycin radical yield as a function of time. γ-Irradiated pyrimidine bases, containing parent pyrimidine molecules and pyrimidine radicals, were dissolved in deaerated adriamycin (3.5 mM) solutions in DMSO. Open symbols correspond to reactions between pyrimidine radicals and adriamycin. Closed symbols to the reaction between neutral pyrimidines and adriamycin. The amount of γ-irradiated pyrimidines was adjusted to contain equal number of pyrimidine radicals ($1.5 \times 10^{15}$). (○) cytosine radicals; (□) thymine radicals; (△) uracil radicals; (●) cytosine; (■) thymine; (▲) uracil.

The reaction between pyrimidine radicals and adriamycin in DMSO is far more efficient than the reaction using parent pyrimidines. In order to determine the optimal adriamycin concentration for the electron transfer process, from pyrimidine radicals to adriamycin, a fixed quantity of pyrimidine radicals was dissolved in several deaerated adriamycin solutions (0.8–7 mM). The increase in intensity of the adriamycin semiquinone radical ESR spectrum was measured at various time intervals. The intensity of the ESR spectrum is directly proportional to the adriamycin semiquinone radical yield. Figure 4 shows the semiquinone radical yield in time following the dissolution of γ-

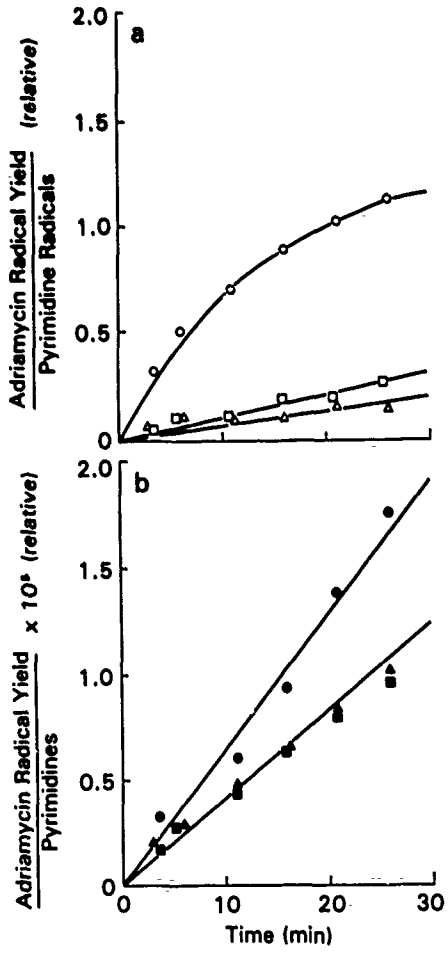


Fig. 3. Adriamycin radical yield (normalized for the quantity of pyrimidine radicals or neutral pyrimidines) vs. time. Reaction conditions are the same as in Fig. 2. (a) Normalized for pyrimidine radicals: (○) cytosine; (□) thymine; (△) uracil. (b) Normalized for neutral pyrimidines: (●) cytosine; (■) thymine; (▲) uracil.

irradiated thymine (0.4 M) in the deaerated adriamycin solutions. The results indicate that the maximum interaction between thymine radicals and adriamycin occurs using 3.5 mM adriamycin (Fig. 4, Insert). Similar results were obtained in experiments using γ-irradiated cytosine and uracil.

Pyrimidine radicals generated by γ-radiolysis of pyrimidine powders are unstable when dissolved and rapidly disappear. This property, in addition to the observed results (Figs. 2 and 3) showing that the reduction of adriamycin occurs over a period of time and most likely via a direct interaction between the pyrimidine radicals and adriamycin, suggests that a pyrimidine–adriamycin complex may be formed prior to the electron transfer to adriamycin. It is conceivable that such a complex could stabilize the pyrimidine radicals sufficiently for their reaction with adriamycin to occur.

Since the reaction between cytosine radicals and adriamycin yields adriamycin radicals approaching the initial concentration of cytosine radicals dissolved (Fig. 2), it is probable that most of the pyrimidine radicals rapidly interact with adriamycin prior to their decomposition. In addition, the results shown in Fig. 3 suggest that if the formation of such a complex were possible, this interaction would have to occur approximately $10^5$ times more efficiently for pyrimidine radicals than for parent pyrimidine molecules.

A possible mechanism for the electron transfer from pyrimidine radicals ($P^{\cdot}$) to adriamycin (ADR) can be explained following the reaction scheme for the oxidation or reduction of organic molecules by free radicals described by Steenken[35]:

$$P^{\cdot} + ADR \longrightarrow P{-}\overset{\cdot}{A}DR \longrightarrow P^{+} + ADR^{\cdot -} \quad (1)$$

$$P^{\cdot} + ADR \longrightarrow P{-}\overset{\cdot}{A}DR \longrightarrow P^{-} + ADR^{\cdot +} \quad (2)$$

In general, the mechanism first involves the covalent bonding between $P^{\cdot}$ and ADR to form an inter-

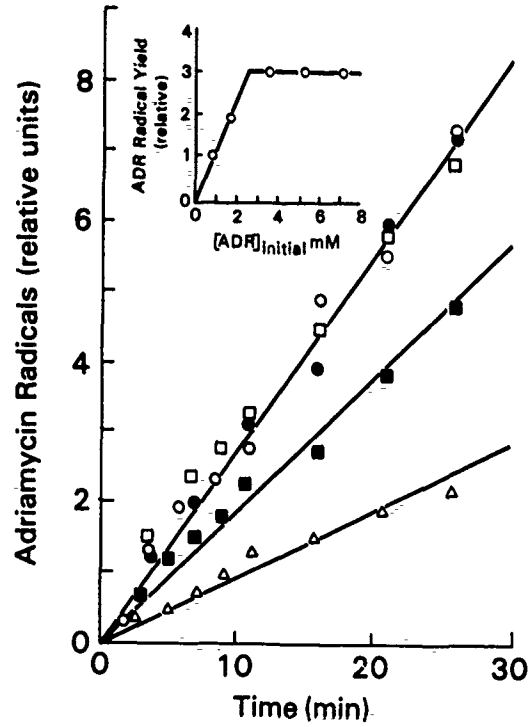


Fig. 4. Adriamycin radical yield in deaerated DMSO solutions as a function of time. A constant amount of γ-irradiated thymine was dissolved in various deaerated adriamycin solutions in DMSO. Thymine concentration: 0.4 M. Adriamycin concentrations: (●) 6.9 mM; (○) 5.2 mM; (□) 3.5 mM; (■) 1.7 mM; (△) 0.86 mM. Insert: adriamycin radical yield at any time (t) versus initial concentration of adriamycin.

mediate, P–ADR$^{\cdot}$, which subsequently undergoes heterolysis leading to the products in reaction (1) or (2) depending on whether the electron pair shared by P–ADR$^{\cdot}$ goes to ADR [reaction (1)] or to the pyrimidine [reaction (2)]. The experimental results shown in this work favor the mechanism given in reaction (1) in which adriamycin is reduced forming the semiquinone radical. Pyrimidine radicals in which the highest spin density is at the C(6) carbon are considered reducing species.[35] Figure 1b shows the ESR spectrum of the adriamycin semiquinone radical indicating that adriamycin is reduced by the pyrimidine radicals. In addition, Fig. 1b also shows an ESR spectrum ($g$ = 2.00) upfield from the semiquinone radical ESR spectrum which is characteristic of a charge–transfer type complex between organic molecules.[30] This suggests that a species similar to P–ADR$^{\cdot}$ is formed. It is conceivable that a similar mechanism could apply for the reaction between the parent pyrimidine molecules and adriamycin. However, as shown in Figs. 2 and 3 this process is less efficient than the process involving pyrimidine radicals.

Fluorescence-quenching experiments were attempted to confirm the presence of an intermediary pyrimidine adriamycin complex in deaerated DMSO solutions. The results of these experiments showed no appreciable quenching of the adriamycin emission spectrum, even at pyrimidine concentrations 100 times larger than the adriamycin concentration. However, the ESR spectrum ($g$ = 2.00) in Fig. 1b upfield from the semiquinone radical ESR spectrum supports the formation of such a complex.

Although the experiments in this work have shown that in an aprotic environment (DMSO) the reduction of adriamycin by the parent pyrimidine molecules is not an efficient process, it is possible that this may not be the case when adriamycin is intercalated into hydrophobic regions of DNA. Whereas the pyrimidine and adriamycin molecules in solution are in rapid motion possibly making strong complex formation more difficult, the adriamycin intercalated into DNA is locked into position nearby the nucleic acid bases. This proximity could facilitate a direct interaction between the bases and adriamycin. A similar argument could be made for the pyrimidine radicals formed by the effects of ionizing radiation on DNA. However, the results suggest that the subsequent reactions following a base–adriamycin interaction is far more efficient for the pyrimidine radicals than for the parent pyrimidine molecules.

Finally, the results obtained in this work show that it may be possible at least for pyrimidine radicals formed by the effects of ionizing radiation on DNA, to react with molecules other than oxygen in solution.[16] In this case the pyrimidine radicals react with a DNA intercalating agent, adriamycin, forming the adriamycin semiquinone radical. This radical intercalated into DNA causes DNA strand scission.[19] Furthermore, the adriamycin semiquinone radical was shown to react with dissolved oxygen. This reaction generates $O_2^{\cdot}$ which may disproportionate and lead to the formation of hydroxyl radicals which are known to cause irreversible DNA damage and are also lethal to cells.

## REFERENCES


1. Hüttermann, J.; Voit, K.; Oloff, H.; Köhnlein, W.; Gräslund, A.; Rupprecht, A. Specific formation of electron gain and loss centres in X-irradiated oriented fibers of DNA at low temperatures. *Faraday Discussions Chem. Soc. 78*: 135–149; 1984.
2. Gräslund, A.; Rupprecht, A.; Ehrenberg, A. Structure of radicals from nucleic acids. In: Huttermann, J.; Kohnlein W.; Teoule, R., eds. *Effects of ionizing radiation on DNA. Physical, chemical and biological aspects*. Berlin: Springer-Verlag; 1975: 71–79.
3. Gräslund, A.; Ehrenberg, A.; Rupprecht, A.; Tjäldin, B.; Ström, G. ESR kinetics of free radical conversion in γ-irradiated oriented DNA. *Rad. Res. 61*: 488–503; 1975.
4. Gräslund, A.; Ehrenberg, A.; Rupprecht, A.; Ström, G. Ionic base radicals in γ-irradiated DNA. *Biochem. Biophys. Acta 254*:172–186.
5. Arroyo, C. M.; Carmichael, A. J.; Swenberg, C. E.; Myers, L. S., Jr. Neutron-induced free radicals in oriented DNA. *Int. J. Rad. Biol. 50*: 789–793; 1986.
6. DiMarco, A.; Arcamone, F.; Zumino, F. In: Corcoran, J. W.; Hahn, R. E., eds. *Antibiotics*. Vol. 3. Berlin: Springer-Verlag; 1975: 101–128.
7. Cheng, C. C.; Zbinden, G.; Zee-Chang, R. K. Y. Comparison of antineoplastic activity of aminoethylaminoanthraquinones and anthracycline antibiotics. *J. Pha* · *Sci. 68*: 393–396; 1979.
8. Johnson, R. K.; Zee-Chang, R. K. Y.; Lee, W. W.; Acton, E. M.; Henry, D. W.; Cheng, C. C. Experimental antitumor activity of anthraquinones. *Cancer Treat. Rep. 63*: 425–429; 1979.
9. Goo[illegible]an, J.; Hochstein, P. Generation of free radicals and lipid peroxidation by redox cycling of adriamycin and daunomycin. *Biochem. Biophys. Res. Commun. 77*: 797–803; 1977.
10. Bachur, N. R.; Gordon, S. L.; Gee, M. V. Anthracycline antibiotic augmentation of microsomal electron transport and free radical formation. *Mol. Pharmacol. 13*: 901–910; 1977.
11. Kalyanaraman, B.; Perez-Reyes, E.; Mason, R. P. Spin trapping and direct electron spin resonance investigations of the redox metabolism of quinone anticancer drugs. *Biochem. Biophys. Acta 630*: 119–130; 1980.
12. Sato, S.; Iwaizumi, M.; Handa, K.; Tamura, Y. Electron spin resonance study on the mode of generation of free radicals of daunomycin, adriamycin, and carboquone in NAD(P)H-microsome system. *Gann 68*: 603–608; 1977.
13. Carmichael, A. J.; Mossoba, M. M.; Riesz, P. Photogeneration of superoxide by adriamycin and daunomycin. An electron spin resonance and spin-trapping study. *FEBS Lett. 164*: 401–405; 1983.
14. Carmichael, A. J.; Riesz, P. Photoinduced reactions of anthraquinone antitumor agents with peptides and nucleic acid bases. An electron spin resonance and spin-trapping study. *Arch. Biochem. Biophys. 237*:433–444; 1985.
15. Bors, W.; Saran, M.; Czapski, G. In: Bannister, W.; Bannister, J. V., eds. *Biological and clinical aspects of superoxide and superoxide dismutase*. New York: Elsevier/North Holland; 1980.
16. Aust, S. D.; Morehouse, L. A.; Thomas, C. E. Role of metals

in oxygen radical reactions. *J. Free Radical Biol. Med. 1*: 3–25; 1985.
17. Carmichael, A. J. Reaction of vanadyl with hydrogen peroxide. An ESR and spin trapping study. *Free Radical Res. Commun. 10*: 37–45, 1990.
18. Carmichael, A. J. Vanadyl-induced Fenton-like reaction in RNA. An ESR and spin-trapping study. *FEBS Lett. 261*: 165–170; 1990.
19. Lown, J. W.; Sim, S. K.; Majumdar, K. C.; Chang, R. Y. Strand Scission of DNA by bound adriamycin and daunomycin in the presence of reducing agents. *Biochem. Biophys. Res. Commun. 76*: 705–710; 1977.
20. Buettner, G. R.; Oberley, L. W. Considerations in the spin trapping of superoxide and hydroxyl radicals in aqueous systems using 5,5-dimethyl-1-pyrroline-1-oxide. *Biochem. Biophys. Res. Commun. 83*: 69–74; 1978.
21. Kalyanaraman, B.; Felix, C. C.; Sealy, R. C. Photoionization of melanin precursors: An electron spin resonance investigation using the spin trap 5,5-dimethyl-1-pyrroline-1-oxide (DMPO). *Photochem. Photobiol. 36*: 5–12; 1982.
22. Sevilla, M. D. An electron spin resonance study of the photoionization of thymine. The thymine cation and anion radicals. *J. Phys. Chem. 75*: 626–631; 1971.
23. Sevilla, M. D.; Van Paemel, C. An ESR study of pyrimidine, pyrimidine nucleoside, and halopyrimidine anions. *Photochem. Photobiol. 15*: 407–409; 1972.
24. Russell, G. A.; Janzen, E. G.; Strom, E. T. Electron-transfer process. I. The scope of the reaction between carbanions or nitranions and unsaturated electron acceptors. *J. Am. Chem. Soc. 86*: 1807–1814; 1964.
25. Evans, C. A. Spin trapping. *Aldrichim. Acta 12*: 23–29; 1979.
26. Lion, Y.; Dennis, G.; Mossoba, M. M.; Riesz, P. ESR of spin-trapped radicals in γ-irradiated polycrystalline DL alanine. A quantitative determination of radical yield. *Int. J. Radiat. Biol. 43*: 71–83; 1983.
27. Hall, P. L. Errors in the determination of ESR spin concentrations by numerical double integration. *J. Phys. D. 5*: 673–675; 1972.
28. Lown, J. W., and Chen, H. H. Electron paramagnetic resonance characterization and conformation of daunomycin semiquinone intermediate implicated in anthracycline metabolism, carditoxicity, and anticancer action. *Can. J. Chem. 59*: 3212–3217; 1981.
29. Schreiber, J.; Mottley, C.; Sinha, B. K.; Kalyanaraman, B.; Mason, R. P. One-electron reduction of daunomycin, daunomycinone, and 7-deoxydaunomycinone by Xanthine/xanthine oxidase system: detection of semiquinone free radicals by electron spin resonance. *J. Am. Chem. Soc. 109*: 348–351; 1987.
30. Carrington, A.; McLachlan, A. D. *Introduction to magnetic resonance*. Chapter 8. New York: Harper and Row; 1969; 128–129.
31. Buettner, G. R. Spin trapping: ESR parameters of spin adducts. *Free Radical Biol. Med. 3*: 259–303; 1987.
32. Finkelstein, E. G.; Rosen, G. M.; Rauckman, E. J. Production of hydroxyl radical by decomposition of superoxide spin trapped adducts. *Mol. Pharm. 21*: 262–265; 1982.
33. Finkelstein, E. G.; Rosen, G. M.; Rauckman, E. J.; Paxton, J. Spin trapping of superoxide. *Mol. Pharm. 16*: 676–685; 1979.
34. Samuni, A.; Murali Krishna, C.; Riesz, P.; Finkelstein, E.; Russo, A. Superoxide reaction with nitroxide spin adducts. *Free Radical Biol. Med. 6*: 141–148; 1989.
35. Steenken, S. Addition-elimination paths in electron-transfer reactions between radicals and molecules. Oxidation of organic molecules by the OH radical. *J. Chem. Soc., Faraday Trans. 1 83*: 113–124; 1987.
36. Gregoli, S.; Olast, M.; Bertinchamps, A. Radiolytic pathways in γ-irradiated DNA. Influence of chemical conformation factors. *Rad. Res. 89*: 238–254; 1982.

*Free Rad. Res. Comms.*, Vol. 9, No. 3-6, pp. 287-296
Reprints available directly from the publisher
Photocopying permitted by license only



# ENDOTHELIAL CELLS AS A SOURCE OF OXYGEN-FREE RADICALS. AN ESR STUDY

C.M. ARROYO, A.J. CARMICHAEL*, B. BOUSCAREL, J.H. LIANG and W.B. WEGLICKI

*Department of Medicine, George Washington University, Washington, D.C., and *Radiation Biochemistry Department, Armed Forces Radiobiology Research Institute, Bethesda, Maryland, USA*

Endothelial cells were subjected to anoxia/reoxygenation in order to simulate some of the free radical mechanisms occurring in ischaemia/reperfusion. With ESR and spin trapping using the spin traps 5,5-dimethyl-1-pyrroline-1-oxide (DMPO) and 3,3,5,5-dimethyl-1-pyrroline-1-oxide ($M_4PO$), the results show that upon reoxygenation of endothelial cells, following a period of anoxia, these cells generate superoxide ($O_2^-$). Cytotoxicity of the spin traps was measured by standard trypan blue exclusion methods. Cell injury or death was measured at various times during reoxygenation by lactate dehydrogenase (LDH) release. Experiments using oxypurinol, SOD, CAT and a combination of SOD and CAT show that while oxypurinol partially prevents spin adduct formation, the combination of SOD and CAT is more effective in doing so. These results suggest that the majority of the oxygen radicals produced by endothelial cells are done so exogenously. The results also suggest that endothelial cells are not only a source of oxygen radicals but also a target.

KEY WORDS: Endothelial cells, oxygen radicals, ESR, spin trapping

## INTRODUCTION

In various organs, reperfusion injury following a period of ischemia is, in a substantial proportion, caused by oxygen free radicals.[1,2] Evidence suggests that the oxygen-centered radicals are generated by a similar xanthine oxidase mediated pathway. The fact that different organs demonstrate a similar biochemical mechanism for this injury suggests that the injury may originate from common cellular sources. Possible cellular sources are circulating neutrophils and endothelial cells. Circulating neutrophils are a well-recognized oxygen free radical generating system.[3,4] Endothelial cells, because of their location at the blood-tissue barrier, have been postulated as the initial site of tissue injury during reperfusion.[5] However, it remains unclear if whether initial site refers to the endothelial cells being the target of the reactive free radicals, a source of the reactive free radicals or a combination of both. The role of oxygen metabolites in neutrophil-dependent endothelial cell injury was first suggested by Sacks *et al.*[5] Their experiments showed that neutrophils stimulated with zymosan-activated serum would induce the release of $^{51}Cr$ from cultured endothelial cells. Furthermore, the $^{51}Cr$ release was inhibited by superoxide dismutase and catalase suggesting that superoxide and hydrogen peroxide played an important role in the cell damage. Neutrophils

Current address: Dr. Carmen Arroyo, Pharmacology Department, University of Maryland at Baltimore, 20 N. Pine St., Baltimore, Maryland 21201, USA.

stimulated by phorbol esters are known to generate superoxide radicals.[3] In addition, Weiss *et al.*[6] has confirmed the ability of reactive oxygen products from activated human neutrophils to damage cultured endothelial cells. With regard to endothelial cells being a possible source of oxygen centered radicals a recent study by Zweier *et al.*[7] has shown, using the technique of spin trapping and the spin trap 5,5 dimethyl-1-pyrroline-N-oxide (DMPO), that oxygen-centered radicals were formed during re-oxygenation of endothelial cell suspensions which had been subjected to anoxia. Although in the study by Zweier *et al.*, scavenging experiments using ethanol implied that ·OH radicals were formed and experiments with SOD and catalase suggested that the ·OH radicals originated from superoxide ($O_2^{\cdot-}$), it was concluded, following xanthine oxidase inhibition studies, that the $O_2^{\cdot-}$ was produced endogenously in the endothelial cells.

However, several points were not addressed in this study: (1) How exogenously added SOD suppressed the spin trapping of endogenously generated oxygen radicals. It is well known that exogenously added SOD does not enter cells.[8] (2) How catalase suppresses the spin trapping of oxygen centred radicals. It is known that DMPO reacts with $O_2^{\cdot-}$ and that the DMPO-$O_2^{\cdot-}$ adduct decomposes forming DMPO-OH.[3] Catalase in turn reacts with hydrogen peroxide, a product of the dismutation of $O_2^{\cdot-}$.[3] Although DMPO-OH was observed suggesting the possible production of $O_2^{\cdot-}$ or ·OH, it is known that this spin adduct may also be formed in the presence of $O_2$ at room temperature and more rapidly at higher temperatures (37 °C) by processes other than the reaction of $O_2^{\cdot-}$ and ·OH with DMPO.[9,10] There is also the inherent problem of the DMPO-OH and other nitroxides short-lifetime with cells that has not been addressed.[11] Finally, nothing was mentioned with regard to the origin of additional spin adducts observed in the ESR spectra. It appears that a reasonable amount of the reduction product of DMPO, DMPO-H, was generated in these studies simultaneously with the DMPO-OH.

Therefore, of interest to the present study is to determine whether endothelial cells are actually a source of oxygen centered radicals. In an effort to circumvent the possibility of misassignment of the trapped radicals due to possible artifacts associated with using DMPO, in the present study two spin traps were used: 3,3,5,5-tetramethyl-1-pyrroline-N-oxide ($M_4PO$) and 5,5 dimethyl-1-pyrroline-N-oxide (DMPO). It is also of interest to verify free radical-induced cell damage, following reoxygenation of anoxic cells, via molecular assays more sensitive than trypan blue exclusion. For this purpose, lactate dehydrogenase (LDH) release from the cells was studied.[12]

## METHOD

### *Endothelial Cell Culture System*

Bovine pulmonary arterial endothelial cells (CCL # 207, American Type Culture Collection, Rockville, Md) were cultured in medium 199 supplemented with 18% fetal bovine serum (GIBCO Grand Island, NY). Primary cultures were maintained on a standard growth medium with penicillin (50 units/ml) and streptomycin (505 g/ml) (Mediatech, Washington, D.C.). Confluent plates were harvested by trypsinizing with 0.25% trypsin-EDTA (Sigma, St. Louis, MO), centrifuged at 900 rpm (5 minutes). The pellet was washed twice with potassium phosphate buffer (120 mM KCl and

10 mM $K_2HPO_4/KH_2PO_4$, pH 7.2) at room temperature, then resuspended in the phosphate buffer (6–7 million cells per ml).

The spin trapping studies were performed by using two different spin trapping agents 5,5′-dimethyl-1-pyrroline-N-oxide (DMPO) and 3,3,5,5-tetramethyl-1-pyrroline-N-oxide ($M_4PO$) obtained from the Aldrich Co. DMPO as supplied usually contains colored impurities. These were removed using the method described by Buettner and Oberley.[13] Activated charcoal was successively added to a 10 % solution of the nitrone in 10 mM phosphate buffer, pH 7.2, and stirring for 30 min at room temperature. The charcoal was filtered and filtrate was monitored by ESR at high receiver gain ($1 \times 10^5$) for nitrone impurities. $M_4PO$ was also further purified by charcoal treatment. Anaerobic preparations were achieved by removing the solution above settled cells and adding an identical volume of solution previously purged with nitrogen for 15 to 20 min. Anaerobic conditions were maintained by keeping the cell suspension under a gentle stream of nitrogen gas. Reoxygenation was produced by rapidly removing the nitrogen saturated solution above the cells and replacing it with an equal volume of solution previously purged, for 15 to 20 min, with a gas mixture containing 95 % $O_2$ and 5 % $CO_2$. Reoxygenated conditions were maintained by gently exposing the surface of the solutions to an atmosphere consisting of the $O_2/CO_2$ mixture. The experiments were done in the dark to prevent photolytic degradation of $M_4PO$ or DMPO.

The ESR spectra were recorded on a Bruker IBM ER 100 X-band spectrometer at 100-kHz magnetic field modulation. The ESR spectra were obtained using a quartz flat cell ($60 \times 10 \times 0.25$ mm). The microwave power was maintained at 10 mW to avoid saturation and the modulation amplitude was set at 1 G. Hyperfine coupling constants were measured directly from the spectra using a 10 G marker for calibration. These parameters were also obained by computer simulation, generating theoretical ESR spectra which match the experimentally obtained ESR spectra. The concentration of spin adducts was determined by double integration of the first derivative ESR spectrum. An aqueous solution of 3-carbamoyl-2,2,5,5-tetramethyl-1-pyrrolidine-1-yloxy (Aldrich) was used as the nitroxide standard. This nitroxide has previously been used as a standard for determining unknown free radical concentrations.[14] The accuracy of the double integrations, $\pm$ 10 %, was determined using the method described by Hall.[15]

*In vitro* anoxia/reoxygenation of the cells was used as a model to simulate some of the processes occurring in ischemia/reperfusion. During culture, the cells were normally exposed to atmosphere consisting of 95 % air and 5 % $CO_2$. Anoxia was produced with an atmosphere of 95 % $N_2$ and 5 % $CO_2$, while reoxygenation was produced by restoration of the 95 % air, 5 % $CO_2$. These atmospheres were produced in a homemade gas chamber approx. 1 l). The chamber was initially purged with each experimental gas for 1 minute at a flow rate of 5 L/min. The experimental time points were taken beginning at the end of each purging. End points were then determined.

Oxypurinol was obtained from Burroughs Wellcome Co. (Research Triangle Park, NC) and was dissolved and used at the desired concentration. Optimal doses of superoxide dismutase (SOD) from bovine erythrocytes, (EC 1.15, 1.1, Boehringer Mannheim Biochemicals, Indianapolis, IN), 5000 Units/mg protein, and catalase (CAT), 5000 Units/mg protein, (Sigma Chemical Co.) were determined individually and together in a dose response fashion. To provide a suitable control for the active SOD, SOD was inactivated according to a modification of the method of Hodgson and Fridovich[16] with overnight dialysis in a glycerine buffer pH 10 with 10 mM $H_2O_2$.

Similarly, CAT was inactivated by overnight dialysis in 10 mM aminotriazole and 50 mM $H_2O_2$.

## RESULTS

Concentrated suspension of $2 \times 10^7$ cells in 0.5 ml were made anoxic by incubation under anaerobic conditions at 37 °C for 45 min. The cells were then reoxygenated by addition of aerobic solutions of DMPO or $M_4PO$ and exposure to atmospheric air. The final concentration of DMPO or $M_4PO$ used was 50 mM. Cells were then immediately transferred to the ESR flat cell and spectra were obtained. When fresh oxygenated buffer containing 50 mM $M_4$ PO (same identical preparation added to the cells) was monitored, no ESR signal was observed. The spectra of the reoxygenated cells exhibited complex patterns (Figure 1A). The seven line spectrum observed can be explained as two different overlapping ESR spectra which can be simulated as shown in Figure 1C and 1D. Spectrum C consists of a triplet of doublets with hyperfine splittings of $A_N = 15.6$ G and $A_H^\beta = 6.5$ G; this spectrum can be attributed to $M_4PO$-$O_2^-$. A similar spectrum was obtained in a X/XO solution containing $M_4PO$ or in the photochemical production of $O_2^-$ using riboflavin. The spectral simulation of a triplet with hyperfine splitting constant of $a_N = 18$ G is shown in Figure 1D. The

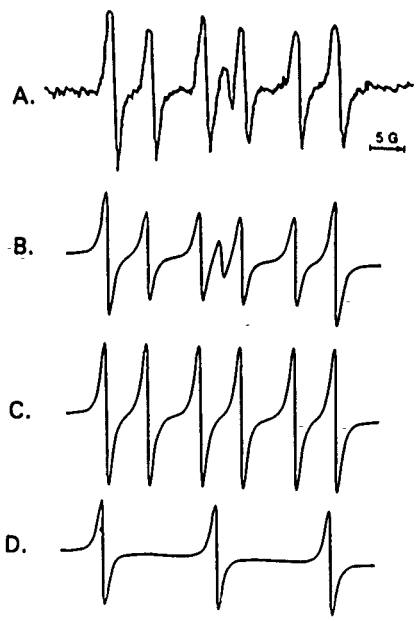


FIGURE 1 ESR spectra of preparations of endothelial cells ($1.9 \times 10^7$) in the presence of 50 mM $M_4PO$. A. Reoxygenation following 45 min anoxia at 37 °C. B. Computer simulated spectrum that best fits the experimental spectrum (A). This spectrum is the addition of spectra C and D. C. Simulated spectrum consisting of a triplet of doublets. Hyperfine splittings used in this simulation: $a_N = 15.0$ G and $a_H = 6.5$ G. D. Simulated spectrum of a triplet using $a_N = 18.0$ G as the hyperfine splitting constant. ESR spectra were recorded with a mircowave power of 10 mW and a modulation amplitude of 1 G.

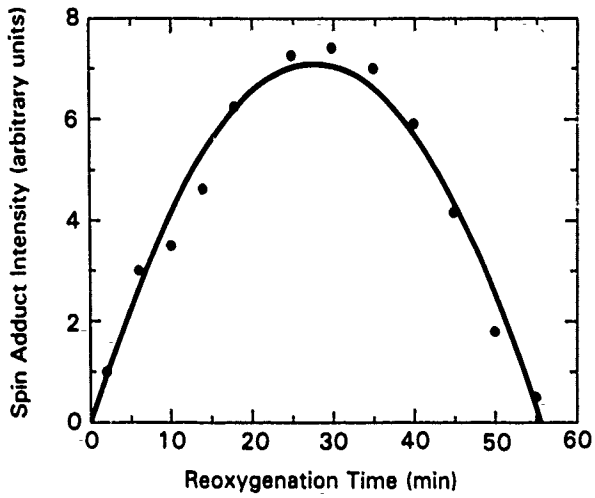


FIGURE 2 Time course of the appearance of $M_4PO$ adducts under identical cell concentration ($2 \times 10^7$ cells in 0.5 ml) but different reoxygenation time. The concentration of oxygen used in this study was approximately 140 mm/Hg. ESR spectra were recorded every 2 min as described in Figure 1.

simulated spectrum that best fits the experimental spectrum (Figure 1A) is shown in Figure 1B. This spectrum is the addition of the simulated spectra shown in Figure 1C and 1D. These measurements were repeated many times with different preparations of cells and different reoxygenation times. Each time different prominent signals were observed depending on the amount of cells used and the reoxygenation time, with no signal observed in controls. When DMPO (50 mM) was used instead of $M_2PO$ a signal similar to that reported by Zweier[7] was obtained.

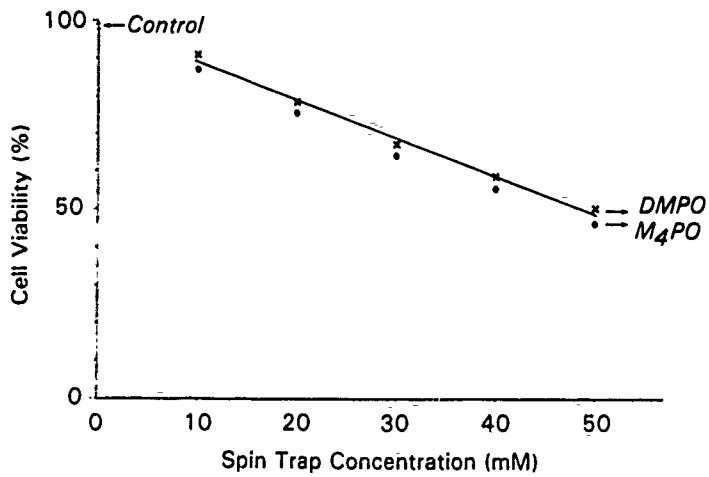


FIGURE 3 Percent of cell viability as a function of $M_4PO$ or DMPO concentration. Spin trap cytotoxicity assay was measured by a standard trypan blue exclusion.

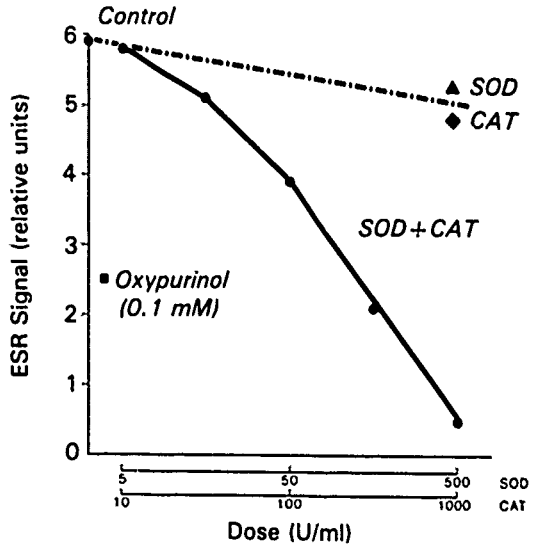


FIGURE 4 Protective effects of varying doses of SOD/CAT, SOD, CAT and oxypurinol in preventing free radical generation monitored by ESR signal intensity. (○) control; (▲) SOD 500 U/ml; (◆) catalase 1000 U/ml; (■) oxypurinol (0.1 mM).

Time course of the appearance of the $M_4PO$ adducts under identical cell concentration ($2 \times 10^7$ cells/0.5 ml) but different reoxygenation time is shown in Figure 2. The concentration of oxygen used in this study was approximately 140 mg/Hg. These measurements indicated that as early as 1 min after reoxygenation a spin adduct signal was observed. The maximum intensity of the spin adducts observed was at 30 min of reoxygenation. After 50 min of reoxygenation there was no observable signal. A rough quantitation of the maximum observed radical concentration was 1.1 $\mu$M was observed in a preparation of $2.1 \times 10^7$ cells per 0.5 ml with 50 mM $M_4PO$.

To determine the fate of the spin adducts observed in Figure 1A, identical experiments were performed to measure the time course of the endothelial free radical generation. The time course of appearance of the $M_4PO$ spin adduct signals in a preparation of $1.9 \times 10^7$ endothelial cells in 0.5 ml exposed to 45 min 37 °C anoxia followed by reoxygenation was measured. Immediately after reoxygenation ESR spectra were recorded every two minutes for a period of 1 hr. In time, the seven line spectrum in Figure 1A begins to change generating different hyperfine patterns that could be degradation products of $M_4PO$ or of its spin adducts. Further investigation of this observation is currently being done to determine the nature of these processes.

Spin trap cytoxicity was measured by a standard trypan blue exclusion test. The endothelial cells were seeded into the wells of a 24-well culture dish at $2.5 \times 10^6$ cells per well in 1 ml of culture medium. Each well was treated with a different molar concentration of $M_4PO$ or DMPO ranging from 0–50 mM. The spin trapping agents were allowed to settle onto the endothelial cell monolayer for 30 minutes. Cells were stained with 0.02 % trypan blue in phosphate buffer and cell counts of 100 cells were performed after 3 min with a standard laboratory light microscope. Figure 3 shows the percent of cell viability as a function of $M_4PO$ or DMPO concentration. Cell counts performed in the first 3 min after staining showed that only 48 % of the cells

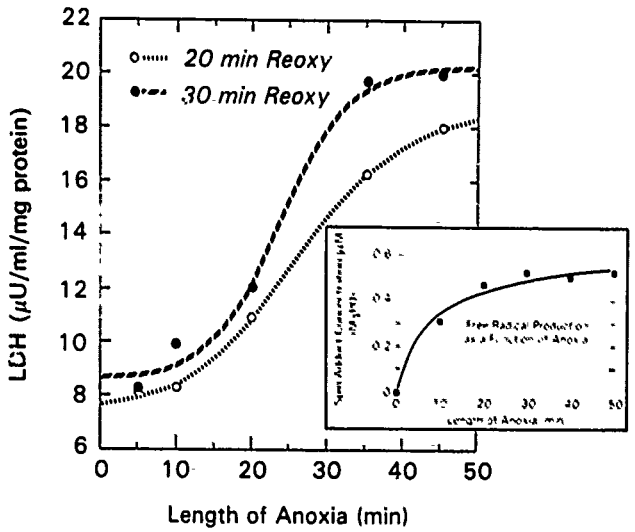


FIGURE 5 Correlation, assessed by the release of LDH, between increasing degree of cell injury with increasing periods of anoxia at 20 min and 30 min reoxygenation. Insert: Radical production monitored by spin adduct concentration as a function of the length of anoxia.

took up trypan blue after being exposed to 50 min of $M_4PO$ for 30 min. 50 % of the cells took up the dye when 50 mM DMPO was introduced for 30 min. Cells not subjected to the spin traps continued to exclude the dye with > 92 % of the cells excluding dye even after 30 min. Figure 4 shows the protective effects of varying doses of SOD and CAT as well as the effect of doses of each agent by itself. The optimal combined doses of SOD and CAT were 500 U/ml and 1000 U/ml, respectively. Neither SOD or CAT alone demonstrated significant inhibition of the ESR signal adducts. Administration of SOD and CAT together substantially and significantly reduced the $M_4PO$-adduct signals, while neither SOD or CAT alone was effective. The combination of SOD and CAT was equally effective whether administered before the anoxia period or after anoxia just prior to reoxygenation. Inactivated SOD and inactivated CAT had no effect. Oxypurinol (0.1 mM) also provided significant protection but was significantly less effective than SOD and CAT. Since it is known that exogenously added SOD and CAT do not enter the cells, in addition to the observation that oxypurinol only partially surpresses the formation of spin adducts and is less effective than the combination of SOD and CAT, the results suggest that the majority of the oxygen-centered radicals are formed exogenously to the endothelial cells.

The effect of the duration of anoxia on cell injury was examined (Figure 5) at 20 and 30 minutes of reoxygenation. Cell injury increased with an increasing duration of reoxygenation. Also, cell injury increased with an increasing duration of anoxia as measured by the release of LDH. This indicator of cell injury shows a close relationship with the ESR data collected: the maximum intensity of the spin adducts observed was at 30 min of reoxygenation when the cells were made anoxic at 37 °C for 45 min.

Thirty minutes of reoxygenation increased the generation of ESR adducts over that seen with 20 min of reoxygenation. These studies suggest that the generation of $M_4PO$ adducts (free radicals) in reoxygenated endothelial cells parallels gradually increasing

cellular damage as radical production continues. In the presence of combined doses of SOD and CAT 500 U/ml and 1000 U/ml, respectively, cell damage was prevented consistent with an inhibition of free radical generation. Since cell death appears to correlate with radical production, therefore suggesting, that the observed free radical spin adducts may have represented free radicals contributing to cell injury and cell death.

## DISCUSSION

These experiments clearly demonstrate that the endothelial cell alone is capable of producing $O_2^-$ upon reoxygenation following anoxia and that this correlates with substantial cellular injury. Interestingly, neither SOD alone nor CAT alone prevented the generation of $M_4$PO-adducts whereas combination of these two enzymes was very effective. Superoxide dismutase rapidly dismutates superoxide to hydrogen peroxide, which itself is toxic to cells and also has been shown to be an inhibitor of SOD activity.[17] The superoxide radical may also inhibit catalase.[18] Although these properties could explain the need for both scavenging enzymes to be present in order to see inhibition, they are unlikely to occur in the short time frame of the experiments since the $H_2O_2$ inactivation of SOD is slow and the $O_2^-$ inhibition of catalase is not strong. An exact explanation for the requirement of both enzymes to suppress spin adduct formation is unclear at this time. The fact that SOD and CAT together were as effective when administered just before reoxygenation as when administered before anoxia confirms that the radical production occurs primarily at reoxygenation. Therefore, these studies suggest that the ongoing generation of free radicals in reoxygenated endothelium induce gradually increasing cellular damage as radical production continues.

The ability of oxypurinol to partially inhibit the radical production, as measured by spin adduct formation, suggests that XO is one source of oxygen free radical generation within the endothelial cell at reoxygenation. The fact that oxypurinol was less effective than SOD and CAT combined strongly suggests that the majority of free radicals are generated by other sources that are not inhibited by oxypurinol. However, it must be noted that oxypurinol is a good hydroxyl radical scavenger and in this manner could possibly prevent the observed oxygen radical spin adduct formation. Since exogenously added SOD and CAT do not enter the cells, the results suggest that the production of oxygen-centred radicals that are not inhibited by oxypurinol occurs exogenously to the endothelial cells.

Other studies suggest that the endothelial cell may act as a trigger for postischemic injury. Jarash *et al.*[19] using immunofluorescent techniques, reported that XO was an important constituent of microvascular endothelial cells from a variety of organs.[19] Del Maestro[20] observed direct evidence of microvascular endothelial cell injury in response to the exogenous generation of the superoxide with X/XO. Therefore, it appears that the initial injury occurs within or near the intravascular space. For instance, SOD is effective in preventing postischemic reperfusion injury in the cold-preserved, allotransplanted kidney when administered intravascularly at the time of reperfusion. On the other hand, when the kidney is stored in a high concentration of SOD and SOD is not added to the vascular stream at reperfusion, no protection is found.[21]

The technique of spin trapping involves producing the unstable free radical of

interest and allowing it to react with a diamagnetic compound (a nitroso or nitrone compound) to form a more stable free radical which can be observed by electron spin resonance (ESR). The observation of a stable free radical, however, is no guarantee that the radical of interest has been trapped. Spectral artifacts can arise due to nitroxide impurities or nucleophilic addition to nitrone compounds followed by oxidation of the nitroxide. The triplet spectrum observed in these studies reflects another way in which spin trapping artifacts may arise, that of direct reduction of a nitrone spin trap to a nitroxide free radical. Though nitrone spin traps have been used extensively, little attention has been given to the possibility of this reduction, though reduction of the spin adduct has been proposed as a decay process.[22]

The reduction of the spin trap itself or of the spin adduct is particularly important in biological systems because of the presence of endogenous reducing agents such as ascorbate. Therefore, the data presented here must be viewed critically to ensure that conclusions are not drawn on the basis of artifacts. The fact that the triplet signal of the $M_4PO$ was generated in the presence of the endothelial cells only when they were subjected to anoxia followed by reoxygenation, implies that some biological reducing agents are generated during anoxia/reoxygenation, an important part of the conditions observed in ischemic and reperfused tissue.

In the present study we showed that bovine pulmonary artery endothelial cells could be a source of toxic oxygen products, including $O_2^-$, OH and other species undefined. A likely explanation, which is consistent with the published data, is that superoxide generation from activated XO within the endothelial cells trigger the biochemical mechanism at reperfusion. The fact that superoxide generation from anoxia/reperfusion conditions can be observed by spin trapping ($M_4PO$-$O_2^-$ adduct) establishes its independence as a source.

## *References*


1. Frank, L. and Massaro, D. Oxygen toxicity. *Am. J. Med.*, **69**, 117–126, (1980).
2. Arroyo, C.M., Kramer, J.H., Dickens, B.F. and Weglicki, W.B. Identification of free radicals in myocardial ischemia/reperfusion by spin trapping with nitrone DMPO. *FEBS Lett.*, **221**, 101–104, (1988).
3. Rosen, G.M., Britigan, B.E., Cohen, M.S., Ellington, S.P. and Barber, M.J Detection of phagocyte-derived free radicals with spin trapping techniques: effect of temperature and cellular metabolism. *Biochem. Biophys. Acta*, **969**, 236–241, (1988).
4. Sanumi, A., Black, C.D.V., Krishna, C.M., Malech, H.L., Bernstein, E.F. and Russo, A. Hydroxyl radical production by stimulated neutrophils reappraised. *J. Biol. Chem.*, **263**, 13797–13801, (1988).
5. Sacks, T., Moldow, C.F., Craddock, P.R., Bowers, T.K. and Jacob, H.S. Oxygen radicals mediate endothelial cell damage by complement-stimulated granulocytes. *J. Clin. Invest.*, **61**, 1161–1172, (1978).
6. Weiss, S.J., Young, J., LoBuglio, A.F., Slivka, A. and Nimeh, N.F. Role of hydrogen peroxide in neutrophile-mediated destruction of cultured endothelial cells. *J. Clin. Envest.*, **68**, 714–724, (1980).
7. Zweier, J.L., Kuppusamy, P. and Lutty, G.A. Measurement cell free radical generation: evidence for a central mechanism of free radical injury in postischemic tissues. *Proc. Natl. Acad. Sci. USA*, **85**, 4046–4050, (1988).
8. Oberley, L.W., Leuthauser, S.W.C., Pasternack, R.F., Oberley, T.D. and Schutt, L. Anticancer activity of metal compounds with superoxide dismutase activity. *Agents and Actions*, **15**, 535–538, (1984).
9. Bannister, J.V. and Thornalley, P.J. The production of hydroxyl radicals by adriamycin in red blood cells. *FEBS. Lett.*, **157**, 170–172, (1983).
10. Carmichael, A.J., Makino, K. and Riesz, P. Quantitative aspects of ESR and spin trapping of hydroxyl radicals and hydrogen atoms in gamma-irradiated aqueous solutions. *Rad. Res.*, **100**, 222–234, (1984).

11. Samuni, A., Carmichael, A.J., Russo, A., Mitchell, J.B. and Riesz, P. On the spin trapping and ESR detection of oxygen-derived radicals generated inside cells. *Proc. Natl. Acad. Sci. USA*, **83**, 7593–7597, (1986).
12. Toth, K.M., Harlan, J.M., Beehler, C.J., Berger, E.M., Parker, N.B., Linas, S.L. and Repine, J.E. Dimethylthiourea prevents hydrogen peroxide and nutrophil mediated damage to lung endothelial cells in vitro and disappears in the process. *Free Rad. Biol. Med.*, **6**, 457–466, (1989).
13. Buettner, G.R. and Oberley, L.W. Considerations in spin trapping of superoxide and hydroxyl radicals in aqueous solutions using 5,5-dimethyl-1-pyrroline-1-oxide. *Biochem. Biophys. Res. Comm.*, **83**, 69–74, (1978).
14. Kalyanaraman, B., Felix, C.C. and Sealy, R.C. Photoionization of melanin precursors: An electron spin resonance investigation using the spin trap 5,5-dimethyl-1-pyrroline-1-oxide (DMPO). *Photochem. Photobiol.*, **36**, 5–12, (1982).
15. Hall, P.L. Errors in determination of ESR spin concentrations by numerical double integrations. *J. Phys. D: Appl. Phys.*, **5**, 673–675, (1972).
16. Hodgson, E.K. and Fridovich, I. The interaction of bovine erythrocyte superoxide dismutase with hydrogen peroxide: inactivation of the enzyme. *Biochem.*, **14**, 5294–5299, (1968).
17. Freeman, B.A., Young, S.L. and Craspo, J.D. Liposome-mediated augmentation of superoxide dismutase in endothelial cells prevents oxygen injury. *J. Biol. Chem*, **258**, 12534–12542, (1983).
18. Kono, Y. and Fridovich, I. Superoxide radical inhibits catalase. *J. Biol. Chem.*, **257**, 5751–5754, (1982).
19. Jarash, E.D., Bruder, G. and Heid, H.W. Significance of xanthine oxidase in capillary endothelial cells. *Acta Physiol. Scand. [Suppl]*, **548**, 39–46, (1986).
20. DelMaestro, R.F., Thaw, H.H., Bjork, J., Planker, M. and Arfors, K.E. Free radicals as mediators of tissue injury. *Acta Physiol. Scand. [suppl]*, **492**, 43–57, (1980).
21. Koyoma, I., Bulkley, G.B. and Im, M.J. The role of oxygen free radicals in mediating reperfusion injuiry of cold preserved ischemic kidneys. *Transplan*, **40**, 590–595, (1985).
22. Giotta, G.J. and Wang, H.H. Reduction of nitroxide free radicals by biological materials. *Biochem. Biophys. Res. Comm.*, **46**, 1576–1580, (1972).

Accepted by Prof. E.G. Janzen

INT. J. RADIAT. BIOL., 1990, VOL. 58, NO. 3, 397–415



# Yields of radiation-induced base products in DNA: effects of DNA conformation and gassing conditions

A. F. FUCIARELLI†‡§, B. J. WEGHER‡, W. F. BLAKELY‡ and M. DIZDAROGLU†

†Center for Chemical Technology, National Institute of Standards and Technology, Gaithersburg, MD 20899, USA
‡Radiation Biochemistry Department, Armed Forces Radiobiology Research Institute, Bethesda, MD 20814-5145, USA

*(Received 5 October 1989; revision received 17 January 1990; accepted 28 March 1990)*

Gas chromatography–mass spectrometry with selected-ion monitoring was used to measure the yields of radiation-induced base products in aqueous solutions of native or heat-denatured DNA irradiated in the dose range 20–100 Gy. These DNA solutions were saturated with nitrous oxide, nitrogen, air or 20% oxygen in nitrous oxide during irradiation. The products measured were as follows: 5,6-dihydrothymine; 5-hydroxy-5,6-dihydrothymine; 5,6-dihydroxy-5,6-dihydrothymine (thymine glycol); 5-hydroxy-5,6-dihydrocytosine; 5,6-dihydroxy-5,6-dihydrocytosine (cytosine glycol); 4,6-diamino-5-formamidopyrimidine; 7,8-dihydro-8-oxoadenine (8-hydroxyadenine); 2,6-diamino-4-hydroxy-5-formamidopyrimidine; and 7,8-dihydro-8-oxoguanine (8-hydroxyguanine). In oxygenated solutions, 5,6-dihydrothymine, 5-hydroxy-5,6-dihydrothymine and 5-hydroxy-5,6-dihydrocytosine were not formed. The yields of all products, other than 5,6-dihydrothymine, were greater in irradiated DNA samples from $N_2O$-saturated solutions than from $N_2$-saturated solutions. In $N_2$-saturated solutions the yield of 8-hydroxyadenine was low and 8-hydroxyguanine was undetectable. Yields of pyrimidine products in heat-denatured DNA were greater than those in native DNA using all types of gases. However, the effects of DNA conformation on the yields of purine products were dependent on the type of gas used to saturate the irradiated DNA solutions. Yields of formamidopyrimidines were generally lower in solutions of DNA irradiated in the native than in the heat-denatured conformation. In air-saturated solutions of DNA, yields of 8-hydroxypurines were not influenced greatly by DNA conformation. In DNA solutions saturated with $N_2O/O_2$, 8-hydroxypurine formation was more favourable in the heat-denatured conformation than in the native conformation. On the other hand, in deoxygenated solutions, formation of 8-hydroxypurines was favoured in the native conformation. Data indicate that DNA conformation and the type of gas used to saturate the irradiated solutions have a profound influence on yields of base products in DNA.

## 1. Introduction

Interaction of highly reactive radicals generated by water radiolysis (i.e. ·OH, H-atoms and $e_{aq}^-$) with the purine and pyrimidine constituents of DNA leads to several types of stable products (for reviews see Téoule and Cadet 1978, Cadet and Berger 1985, von Sonntag and Schuchmann 1986, von Sonntag 1987). For

§To whom correspondence should be addressed, at Department of Radiation Medicine, Massachusetts General Hospital, 55 Fruit Street, Boston, MA 02114, USA.

example, H-atom and $e_{aq}^-$ addition at the C(5)–C(6) double bond of thymine results in the formation of the 5,6-dihydrothymine moiety in deoxygenated DNA solutions (Nishimoto *et al.* 1983, Dizdaroglu 1985a, Furlong *et al.* 1986, Téoule and Guy 1987, Hubbard *et al.* 1989). Hydroxyl radical addition to the C(5) of pyrimidines results in the formation of 5-hydroxy-5,6-dihydropyrimidine moieties under deoxygenated conditions (Dizdaroglu 1985a, Téoule and Guy 1987). On the other hand, •OH radical-induced formation of 5,6-dihydroxy-5,6-dihydrothymine (thymine glycol) has been reported in both oxygenated and deoxygenated solutions of DNA irradiated *in vitro* (Téoule *et al.* 1977, Schellenberg and Shaeffer 1986; West *et al.* 1982a, Rajagopalan *et al.* 1984, Dizdaroglu 1985a, Teebor *et al.* 1987, Téoule and Guy 1987) and *in vivo* (Breimer and Lindahl 1985, Leadon and Hanawalt 1983). The analogous product resulting from the cytosine moiety in DNA, 5,6-dihydroxy-5,6-dihydrocytosine (cytosine glycol), has also been detected (Dizdaroglu 1985a). In the case of purines, addition to the N(7)–C(8) bond leads to the formation of 7,8-dihydro-8-oxopurines (8-hydroxypurines) and formamidopyrimidines (FAPy) in irradiated solutions of DNA (Bonicel *et al.* 1980, West *et al.* 1982b, Chetsanga and Grigorian 1983, Kasai *et al.* 1984, Dizdaroglu 1985a,b).

The yields of radiation-induced purine and pyrimidine products are affected by the type of gas used to saturate the DNA solutions during irradiation. This is expected because the type of gas present during irradiation will influence both the types and yields of radicals that are available to react with the DNA substrate (see von Sonntag (1987) for a review). For example, the reaction of oxygen with organic radicals, resulting in the formation of peroxyl radicals, occurs at diffusion-controlled rates and prevents the formation of several types of products including 5,6-dihydrothymine, 5- and 6-hydroxy-5,6-dihydropyrimidines and the 8,5′-cyclopurine nucleosides(tides) (for reviews see Téoule and Cadet 1978, Cadet and Berger 1985, von Sonntag and Schuchmann 1986, von Sonntag 1987). In $N_2O$-saturated aqueous solutions, conversion of $e_{aq}^-$ to hydroxyl radicals results in a doubling of the hydroxyl radical yield as compared with $N_2$-saturated solutions (Dainton and Peterson 1962). As a result the initial yields of secondary radicals formed in $N_2O$-saturated solutions may be greater than those for $N_2$-saturated solutions; therefore, greater yields of products might be anticipated. For example, Raleigh *et al.* (1976) observed that the yield of 8,5′-cycloadenosine-5′-monophosphate in irradiated solutions of adenosine-5′-monophosphate saturated with $N_2O$ was twice that observed in $N_2$-saturated solutions. Though the yields of the 8,5′-cycloadenosine moiety in irradiated solutions of polyadenylic acid and that of 8,5′-cyclo-2′-deoxyadenosine in DNA were greater in $N_2O$-saturated than in $N_2$-saturated solutions, a doubling in product yield was not observed (Fuciarelli *et al.* 1985). Studies addressing the influence of the type of gas used to saturate solutions of DNA during irradiation on both the type and yield of products have, with few exceptions, yet to be completed. This is a result of the analytical limitations inherent in the types of methods previously available to assess product yield. However, development of a methodology to measure the yields of several types of radiation-induced purine and pyrimidine products using gas chromatography–mass spectrometry with selected-ion monitoring (GC–MS/SIM) now makes such studies feasible (Dizdaroglu 1986).

The yield of radiation-induced damage in DNA has been found to be influenced by DNA conformation. In this respect chromophore destruction (e.g. loss of absorption at 260 nm) was found to be greater in heat-denatured DNA solutions

than in native DNA solutions (Weissburger and Okada 1961), and a shouldered dose–response curve for chromophore destruction in polynucleotides was observed (Ward and Urist 1967, Ward and Kuo 1978), which could be removed by nicking the DNA with DNase prior to irradiation (Ward 1975). These data, in addition to a 9–12-fold higher efficiency of product formation at doses lower than 200 Gy in heat-denatured DNA than in solutions containing native DNA (Swinehart *et al.* 1974), led to the development of the shielded base hypothesis (Ward 1975, Ward and Kuo 1978). This hypothesis suggests that the probability of reaction of hydroxyl radicals with purines and pyrimidines in native DNA is lower than that for denatured DNA, as a result of internalization of the bases within the native DNA structure. With respect to analysis of the yields of several types of radiation-induced pyrimidine and purine products, this hypothesis has received support from some studies (Dirksen *et al.* 1988, Hubbard *et al.* 1989) but not others (Frenkel *et al.* 1981, Fuciarelli *et al.* 1985, Furlong *et al.* 1986). Methodology incorporating GC–MS/SIM has two distinct advantages, which may provide a better understanding of the effects of DNA conformation on product yield. First, many radiation-induced products of pyrimidines and purines are measured in the same DNA sample during one chromatographic run. Second, and more importantly, the effects of DNA conformation can be assessed at doses lower than those used for other techniques of analysis, thereby minimizing artefacts due to loss of DNA conformation resulting from radiation-induced strand scission as discussed by Ward (1975).

This study represents the first detailed analysis of the effects of DNA conformation and the type of gas used to saturate solutions during irradiation on the yields of several radiation-induced pyrimidines and purines.

## 2. Methods and materials†

### 2.1. *Preparation of irradiated DNA samples*

Calf thymus DNA (0·5 mg cm$^{-3}$) was dissolved in 30 mmol dm$^{-3}$ phosphate buffer (pH 7·0). A portion of this solution was denatured by heating the solution to 95°C for 5 min followed by rapid cooling in ice-water. Aliquots of these solutions were exposed to a graded series of doses of ionizing radiation at a dose rate of 166 Gy min$^{-1}$ as measured by Fricke dosimetry (Fricke and Hart 1966) in a $^{60}$Co $\gamma$-ray source (Gammacell-220, Atomic Energy of Canada, Ltd). The solutions were bubbled with either air, $N_2$, $N_2O$ or $N_2O/O_2$ (4:1) for 20 min prior to, and then throughout, the irradiation interval. Irradiated and untreated solutions of DNA were then dialysed extensively against deionized water in SpectraPor6 dialysis membranes (molecular weight cut-off 1000, Fisher Scientific Co.). The quantity of DNA recovered following dialysis was measured spectrophotometrically (assuming that 1·0 $OD_{260}$ = 50 $\mu$g DNA cm$^{-3}$), by a modified Burton's assay (Burton 1968) and gravimetrically following lyophilization. The Burton's assay was calibrated using ultra-high-purity DNA (Sigma). Measurements of the DNA amount by spectrophotometric assay and by modified Burton's assay were in good agreement. Gravimetric measurements tended to be higher and were not used in the analysis of the data. Following lyophilization, the internal standards, 6-azathymine and 8-aza-adenine, were added to each 2·5 mg DNA sample. The optimal amount of internal standard added to these samples was determined from preliminary measurements.

† Mention of commercial products does not imply recommendation or endorsement by the National Institute of Standards and Technology, nor does it imply that the products identified are necessarily the best available for the purpose.

### 2.2. *Hydrolysis and derivatization*

Conditions for optimal hydrolysis of irradiated DNA samples containing modified purines and pyrimidines were determined previously (Fuciarelli *et al.* 1989). From these data, hydrolysis of the 2·5 mg DNA sample in 1·0 ml of 88% formic acid at 150°C for 40 min was judged optimal. The formic acid was removed by lyopilization and the samples were then derivatized by trimethylsilylation in a 0·2 ml mixture of bis(trimethylsilyl)trifluoroacetamide (BSTFA) containing 1% trimethylchlorosilane and acetonitrile (1:1) in polytetrafluoroethylene-capped hypovials (Pierce) by heating for 30 min at 130°C.

### 2.3. *Analysis by gas chromatography–mass spectrometry*

A mass selective detector (model 5970B) controlled by a computer work station (model 59970C) and interfaced to a gas chromatograph (Hewlett-Packard model 5890A) was used for analysis. The injection port and the GC–MS interface were kept at 250°C and 270°C, respectively. The ion source was maintained at 250°C. Separations were carried out on a fused silica capillary column (12·5 m × 0·32 mm) coated with crosslinked 5% phenyl methyl silicone gum phase (film thickness 0·17 μm) (Hewlett-Packard). The column temperature was increased from 120°C to 250°C at a rate of 8°C $min^{-1}$ after 2 min at 120°C. Helium was used as a carrier gas at an inlet pressure of 5 kPa. Samples were injected using the split mode. Mass spectra were obtained at 70 eV. A chromatogram, representative of the data generated in this series of experiments, has been previously published and the product yields were determined as previously described (Fuciarelli *et al.* 1989).

## 3. Results

Yields of the radiation-induced products of purines and pyrimidines were determined from the slopes generated from dose–yield curves, some of which are illustrated in Figures 1–3. The yields of the products from DNA solutions irradiated in either the heat-denatured or native conformation saturated with air, $N_2$, $N_2O$ or $N_2O/O_2$ are listed in Table 1, with the corresponding standard error associated with each measurement. Figure 4 illustrates the combined yields of the

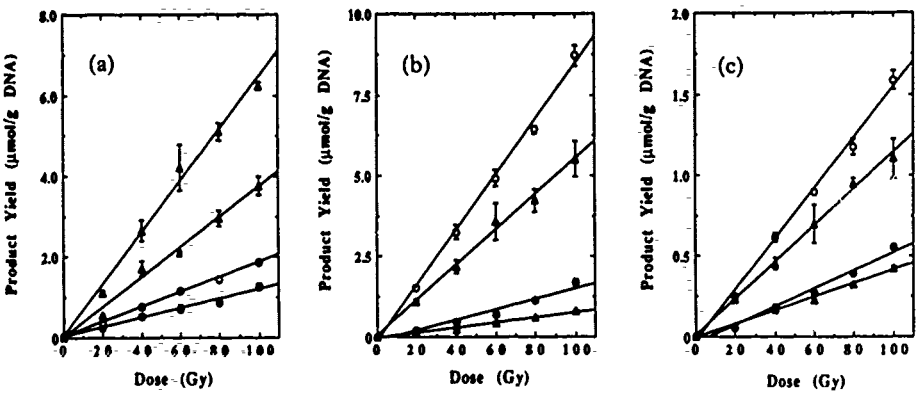


Figure 1. Yields of (a) 5,6-dihydrothymine, (b) 5-hydroxy-5,6-dihydrothymine and (c) 5-hydroxy-5,6-dihydrocytosine from aqueous solutions of DNA saturated with $N_2O$ (○,●) or $N_2$ (△,▲) and irradiated in the native (solid symbols) or heat-denatured (open symbols) conformation (0·5 mg $cm^{-3}$ DNA in 30 mmol $dm^{-3}$ phosphate buffer, pH 7·0).

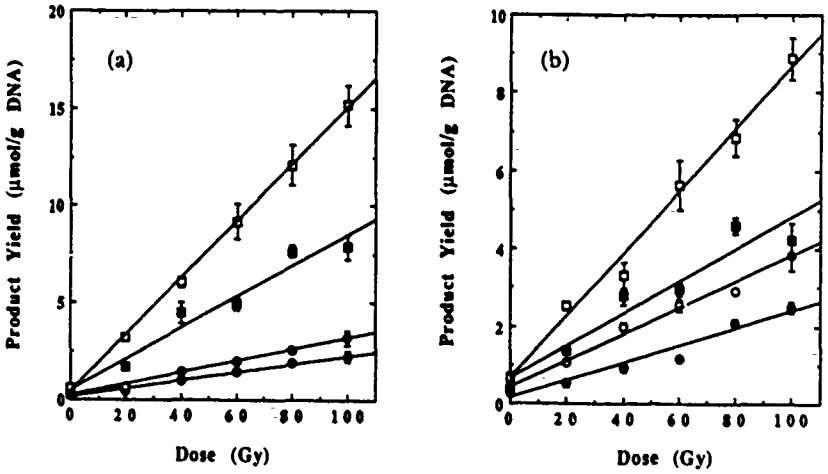


Figure 2. Yields of (a) thymine glycol and (b) cytosine glycol from aqueous solutions of DNA saturated with air (□,■) or $N_2O$ (○,●) and irradiated in the native (solid symbols) or heat-denatured (open symbols) conformation (0·5 mg cm$^{-3}$ DNA in 30 mmol dm$^{-3}$ phosphate buffer, pH 7·0).

radiation-induced pyrimidine (top) and purine (bottom) products in native and heat-denatured samples of DNA saturated with the four types of gases. The total yield of the purine and pyrimidine products measured is greater in oxygenated solutions than in deoxygenated solutions, and their combined yields in either air or $N_2O/O_2$ are similar for both native and heat-denatured samples of DNA. In samples of native DNA irradiated in oxygenated solutions the total yield of such products is greater by factors of approximately 1·8 and 3·5 than in $N_2O$-saturated or $N_2$-saturated solutions, respectively. Similarly, for samples of heat-denatured DNA, the total yield of the same products under oxygenated conditions is greater by factors of approximately 1·8 and 2·0 than in $N_2O$-saturated and $N_2$-saturated solutions, respectively. For $N_2$-saturated solutions the total yield of hydroxyl radical addition products is less than that measured in $N_2O$-saturated solutions (Figure 4). However, this fact may not be apparent in Figure 4 because the yield of 5,6-dihydrothymine is included. Ratios of the yields of each product for DNA samples irradiated in the native or heat-denatured conformations under selected pairs of conditions of gas saturation are presented in Table 2.

The logarithm of the product yield ratio (i.e. yield in heat-denatured DNA/yield in native DNA) from data presented in Table 1 is plotted for each product to illustrate the effects of DNA conformation on the yields of the radiation-induced products of purines and pyrimidines (Figure 5). In this manner a positive value indicates that the yield of the product is greater in heat-denatured DNA than in native DNA. A negative value, on the other hand, indicates that the product yield is greater in native DNA. Furthermore, when the yield is identical in native and heat-denatured DNA, the value of the ratio approaches zero.

### 3.1. *Measurement of pyrimidine products*

3.1.1. *Product formation in the absence of oxygen.* Of the pyrimidine products measured, 5,6-dihydrothymine and the 5-hydroxy-5,6-dihydropyrimidines were not detected in DNA samples irradiated in the presence of air or $N_2O/O_2$ (Table 1).

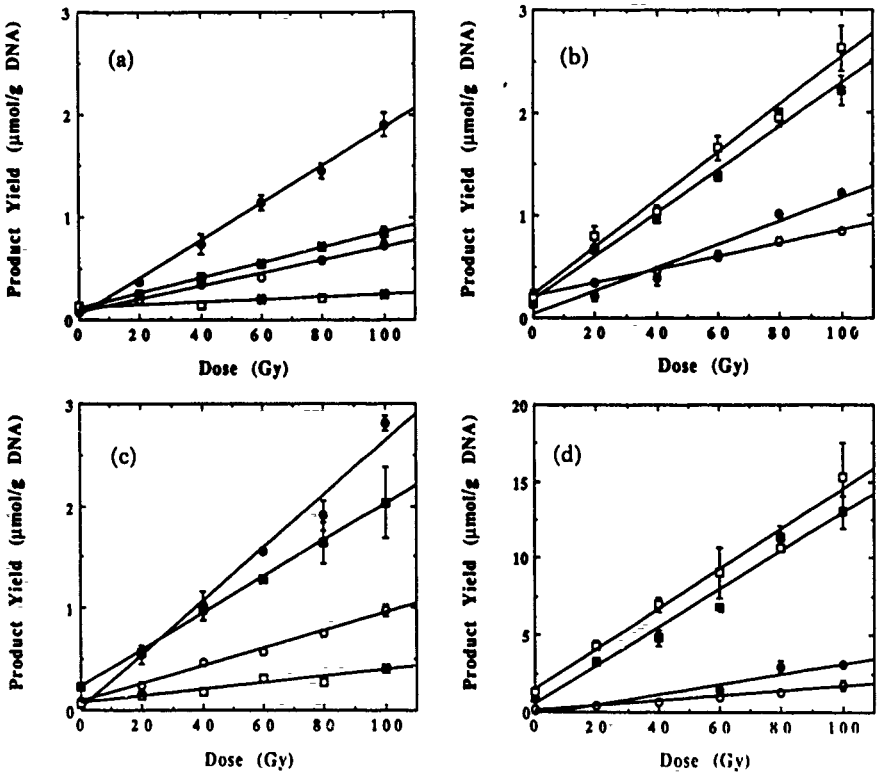


Figure 3. Yields of (a) FAPy-adenine, (b) 8-hydroxyadenine, (c) FAPy-guanine, and (d) 8-hydroxyguanine from aqueous solutions of DNA saturated with air (□,■) or $N_2O$ (○,●) and irradiated in the native (solid symbols) or heat-denatured (open symbols) conformation (0·5 mg cm$^{-3}$ DNA in 30 mmol dm$^{-3}$ phosphate buffer, pH 7·0).

In the case of the 5,6-dihydrothymine moiety the product yield ratio was a factor of 3·18 (±0·21) (native) and 3·44 (±0·17) (heat-denatured) greater in $N_2$-saturated than in $N_2O$-saturated solutions (Table 1 and Figure 1(a)). The higher yield of 5,6-dihydrothymine in the presence of $N_2$ was expected, because this product results from the reaction of H-atom and $e_{aq}^-$ with thymine (Téoule and Cadet 1978, Nishimoto *et al.* 1983, von Sonntag 1987). The yields of 5,6-dihydrothymine were also greater in heat-denatured than in native DNA with a product yield ratio of 1·57 (±0·08) for $N_2O$-saturated and 1·70 (±0·10) for $N_2$-saturated conditions (Figures 1(a), 4 and 5, and Table 1). The yields of the 5-hydroxy-5-dihydropyrimidines from native and heat-denatured samples of DNA irradiated in either $N_2O$-saturated or $N_2$-saturated solutions are also illustrated in Figure 1. The yield of 5-hydroxy-5,6-dihydrothymine was greater in $N_2O$-saturated than in $N_2$-saturated solutions (product yield ratios of 2·03 (±0·20) for native DNA and 1·56 (±0·06) for heat-denatured DNA (Table 2)), and the yield was greater in heat-denatured than in native DNA (product yield ratios of 5·26 (±0·47) for $N_2O$-saturated and 6·84 (±0·40) for $N_2$-saturated solutions (Figures 1(b), 4 and 5, and Table 1)). In the case of 5-hydroxy-5,6-dihydrocytosine, acid-induced deamination leads to the formation of 5-hydroxy-5,6-dihydrouracil (Dizdaroglu 1985a) whose

Table 1. Product yield ($\times 10^2 \mu mol\, J^{-1}$)† measured in samples of DNA irradiated in the native (ds) or heat-denatured (ss) conformation ($0{\cdot}5\, mg\, cm^{-3}$ DNA in $30\, mmol\, dm^{-3}$ phosphate buffer pH 7·0)

| | Gassing condition | | | | | | | |
|---|---|---|---|---|---|---|---|---|
| | DNA conformation (Air) | | DNA conformation ($N_2O/O_2$) | | DNA conformation ($N_2O$) | | DNA conformation ($N_2$) | |
| | ds | ss | ds | ss | ds | ss | ds | ss |
| Pyrimidine products | | | | | | | | |
| 5,6-Dihydrothymine | ND | ND | ND | ND | 0·56 (0·028) | 0·88 (0·010) | 1·78 (0·081) | 3·03 (0·110) |
| 5-Hydroxy-5,6-dihydrothymine | ND | ND | <0·01 | <0·01 | 0·77 (0·066) | 4·05 (0·100) | 0·38 (0·019) | 2·60 (0·076) |
| 5-Hydroxy-5,6-dihydrocytosine | ND | ND | <0·01 | <0·01 | 0·26 (0·014) | 0·74 (0·019) | 0·20 (0·010) | 0·54 (0·014) |
| Cytosine glycol | 1·99 (0·240) | 3·79 (0·200) | 2·56 (0·110) | 3·22 (0·076) | 1·07 (0·100) | 1·63 (0·081) | 0·26 (0·062) | 1·33 (0·085) |
| Thymine glycol | 3·81 (0·330) | 6·95 (0·710) | 4·34 (0·120) | 5·84 (0·200) | 1·02 (0·033) | 1·43 (0·003) | 0·38 (0·052) | 0·66 (0·076) |
| Purine products | | | | | | | | |
| FAPy-adenine | 0·36 (0·005) | 0·06 (0·010) | 0·59 (0·024) | 0·45 (0·028) | 0·87 (0·019) | 0·31 (0·010) | 0·29 (0·014) | 0.13 (0·002) |
| 8-Hydroxyadenine | 1·00 (0·004) | 1·09 (0·052) | 1·58 (0·028) | 2·40 (0·100) | 0·53 (0·062) | 0·31 (0·005) | 0·09 (0·010) | 0·05 (0·011) |
| FAPy-guanine | 0·85 (0·400) | 0·19 (0·042) | 0·36 (0·033) | 0·49 (0·028) | 1·24 (0·078) | 0·41 (0·014) | 0·68 (0·024) | 0·16 (0·019) |
| 8-Hydroxyguanine | 5·92 (0·480) | 6·20 (0·006) | 4·67 (0·010) | 7·05 (0·370) | 1·62 (0·200) | 0·75 (0·033) | <0·01 | <0·01 |

†Product yields are presented with standard errors in parentheses. ND = not detected.

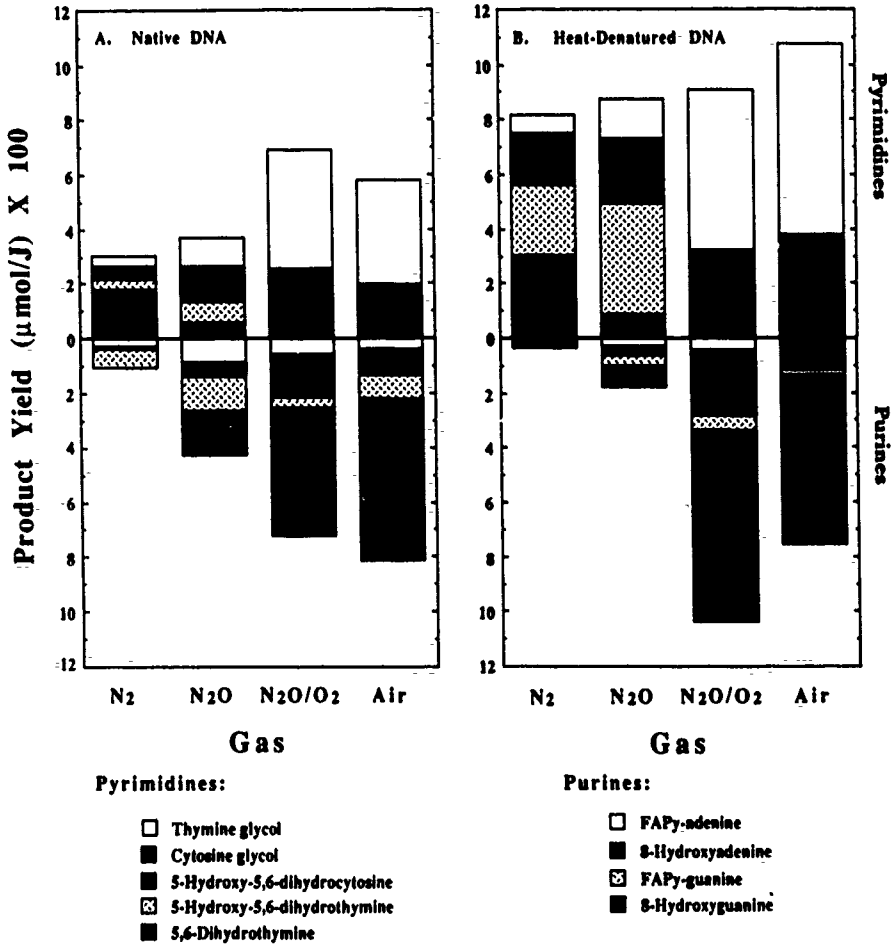


Figure 4. Summation of product yields calculated from the slopes of the linear regression analysis of dose–yield plots including, and similar to, data illustrated in Figures 1–3. Pyrimidine products are illustrated in the upper portion, and purine products are illustrated in the lower portion, of Figures 4A and 4B.

yield was taken to represent that of the former product. The yield of 5-hydroxy-5,6-dihydrocytosine was also greater in $N_2O$-saturated than in $N_2$-saturated solutions (product yield ratios of 1·30 (±0·09) for native DNA and 1·37 (±0·05) for heat-denatured DNA (Table 2)), and the yield was greater in heat-denatured than in native DNA samples (product yield ratios of 2·85 (±0·17) for $N_2O$-saturated and 2·70 (±0·15) for $N_2$-saturated solutions (Figures 1(c), 4 and 5, and Table 1)).

3.1.2. *Formation of pyrimidine glycols.* In contrast to the pyrimidine products discussed earlier, pyrimidine glycols were detected in DNA samples irradiated in solutions saturated with any of the types of gases tested (Table 1 and Figure 4). Figures 2(a) and 2(b) illustrate the yields of the pyrimidine glycols from irradiated DNA samples, both in heat-denatured and native DNA conformations for air-saturated and $N_2O$-saturated aqueous solutions for thymine glycol and cytosine glycol, respectively. Under the conditions of acid hydrolysis used, the yield of

Table 2. Ratios of the yields of radiation-induced purine and pyrimidine products measured in DNA samples from solutions† saturated with selected pairs of gases

| | DNA conformation | | | | | | | |
|---|---|---|---|---|---|---|---|---|
| | Native | | | | Heat-denatured | | | |
| Gassing Condition A / Gassing Condition B: | $\frac{N_2O/O_2}{N_2O}$ | $\frac{Air}{N_2}$ | $\frac{N_2O}{N_2}$ | $\frac{N_2O/O_2}{Air}$ | $\frac{N_2O/O_2}{N_2O}$ | $\frac{Air}{N_2}$ | $\frac{N_2O}{N_2}$ | $\frac{N_2O/O_2}{Air}$ |
| Pyrimidine products | | | | | | | | |
| 5,6-Dihydrothymine | — | — | 0·31 | — | — | — | 0·29 | — |
| 5-Hydroxy-5,6-dihydrothymine | — | — | 2·03 | — | — | — | 1·56 | — |
| 5-Hydroxy-5,6-dihydrocytosine | — | — | 1·30 | — | — | — | 1·37 | — |
| Cytosine glycol | 2·39 | 7·65 | 4·12 | 1·29 | 1·98 | 2·85 | 1·23 | 0·85 |
| Thymine glycol | 4·25 | 10·00 | 2·68 | 1·14 | 4·08 | 10·53 | 2·77 | 0·84 |
| Purine products | | | | | | | | |
| FAPy-adenine | 0·68 | 1·24 | 3·00 | 1·64 | 1·45 | 0·46 | 2·38 | 7·50 |
| 8-Hydroxyadenine | 2·98 | 11·11 | 5·89 | 1·58 | 7·74 | 23·19 | 6·20 | 2·20 |
| FAPy-guanine | 1·25 | 1·25 | 1·82 | 0·42 | 1·20 | 1·19 | 2·57 | 2·58 |
| 8-Hydroxyguanine | 2·88 | — | — | 0·79 | 9·40 | — | — | 1·14 |

†0·5 mg cm$^{-3}$ DNA in ) mmol dm$^{-3}$ phosphate buffer pH 7·0.

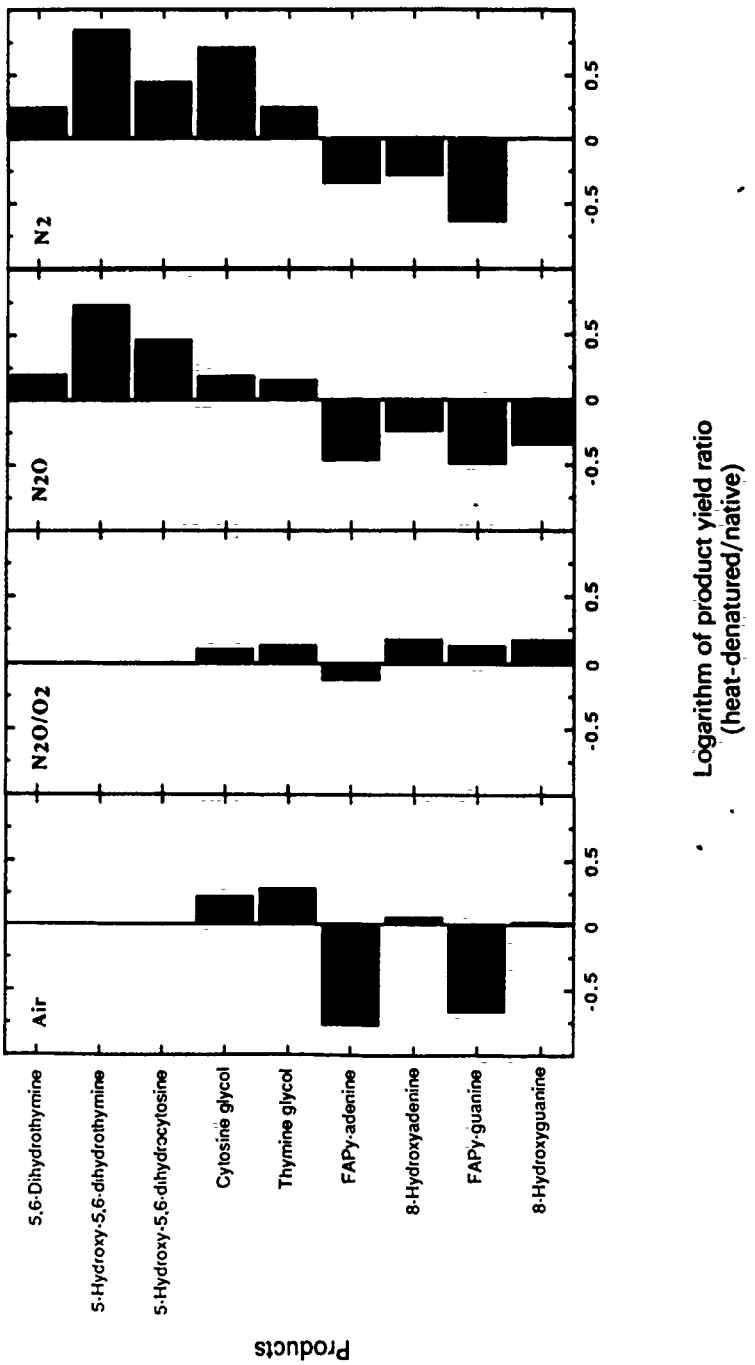


Figure 5. Logarithm of product yield ratio for DNA irradiated in the native or heat-denatured conformation in solutions saturated with air, $N_2$, $N_2O$ or $N_2O/O_2$. Measurements of product yields are taken from Table 1.

cytosine glycol was given by the summation of the yields of 5-hydroxycytosine and 5-hydroxyuracil (Dizdaroğlu *et al.* 1986, Fuciarelli *et al.* 1989). The yields of the pyrimidine glycols in DNA samples irradiated under oxygenated conditions were greater than the yields under deoxygenated conditions (Figures 2 and 4; Tables 1 and 2). For example, the ratio of product yields of thymine glycol from DNA samples irradiated in $N_2O/O_2$ were factors of 4·25 (±0·18) (native) and 4·08 (±0·16) (heat-denatured) greater than those irradiated in $N_2O$ alone (Table 2). Similarly, in irradiated samples of DNA, the ratio of product yield of cytosine glycol under $N_2O/O_2$ were factors of 2·39 (±0·25) (native) and 1·98 (±0·11) (heat-denatured) greater than the yields in $N_2O$ (Table 2). In addition, in irradiated samples of native DNA, the yields of pyrimidine glycols were greater in $N_2O/O_2$-saturated than in air-saturated solutions by factors of 1·14 (±0·10) and 1·29 (±0·16) for thymine glycol and cytosine glycol, respectively (Table 2). On the other hand, the product yield ratios of the pyrimidine glycols in samples of heat-denatured DNA were factors of 1·19 (±0·04) and 1·18 (±0·07) greater in air-saturated than in $N_2O/O_2$-saturated solutions for thymine glycol and cytosine glycol, respectively. The yields of pyrimidine glycols were also greater in samples of DNA irradiated in $N_2O$-saturated than in $N_2$-saturated solutions. The ratios of the yields of thymine glycols were 2·68 (±0·38) and 2·17 (±0·25) for native and heat-denatured solutions, respectively. For cytosine glycol the ratios of the yields were 4·12 (±1·05) and 1·23 (±0·10) for native and heat-denatured solutions, respectively (Table 2). With respect to the effects of DNA conformation, the yields of pyrimidine glycols were greater in heat-denatured solutions of DNA than in solutions containing DNA in the native conformation (Figures 2, 4, and 5, and Table 1). The yields of pyrimidine glycols in heat-denatured DNA solutions were generally from 1·26- to 1·90-fold greater than those in native DNA solutions (except for cytosine glycol in $N_2$-saturated solutions where the ratio of product yields was 5·12) (Figure 5).

### 3.2. *Measurement of purine products*

3.2.1. *Formamidopyrimidines.* The formamidopyrimidines, more correctly referred to as 4,6-diamino-5-formamidopyrimidine (FAPy-adenine) and 2,6-diamino-4-hydroxy-5-formamidopyrimidine (FAPy-guanine) were detected under all conditions of irradiation described in these experiments (Table 1 and Figure 4). Examples of the yields of these products as a function of radiation dose are presented in Figures 3(a) (FAPy-adenine) and 3(c) (FAPy-guanine) from samples of DNA irradiated in $N_2O$-saturated and air-saturated solutions. Generally, the differences in the yields of the formamidopyrimidines resulting from irradiation using the different types of gases described were not as distinct as those observed with the pyrimidine products discussed earlier. Some trends were apparent, although a marked dependency on conformation was evident. For example, the yields of the formamidopyrimidines in irradiated native DNA were greatest in $N_2O$-saturated solutions and lowest in $N_2$-saturated (FAPy-adenine) or $N_2O/O_2$-saturated (FAPy-guanine) (Table 1 and Figure 4). On the other hand, yields of the formamidopyrimidines for samples of DNA irradiated in the heat-denatured conformation were greatest in $N_2O/O_2$-saturated and lowest in air-saturated (FAPy-adenine) or $N_2$-saturated (FAPy-guanine) solutions (Table 1 and Figure 4). The yields of the formamidopyrimidines were from 1·82 to 3·00-fold higher in

DNA samples irradiated in $N_2O$-saturated solutions than in samples irradiated in $N_2$-saturated solutions.

3.2.2. *7,8-Dihydro-8-oxypurines (8-hydroxypurines).* Formation of the 8-hydroxypurines predominated under oxygenated conditions (i.e. saturation with either air or $N_2O/O_2$) for both heat-denatured and native DNA samples (Table 1 and Figure 4). In $N_2$-saturated solutions the yield was very much reduced for 8-hydroxyadenine and below the limits of detectability for 8-hydroxyguanine (Table 1). The yields of 8-hydroxyadenine and 8-hydroxyguanine from DNA samples, irradiated in the native and heat-denatured forms in air-saturated or $N_2O$-saturated solutions, are shown as a function of radiation dose in Figures 3(b) and 3(d), respectively. The ratio of product yields of 8-hydroxyadenine were factors of 1·58 (±0·08) (native) and 2·20 (±0·14) (heat-denatured) greater in $N_2O/O_2$-saturated than in air-saturated solutions. On the other hand, the ratios of the yields of 8-hydroxyguanine in $N_2O/O_2$-saturated solutions to that of air-saturated solutions were 0·79 (±0·06) (native) and 1·14 (±0·06) (heat-denatured). The effects of DNA conformation on the yield of 8-hydroxypurines were dependent on the type of gas used to saturate the DNA solutions during irradiation. For samples of DNA irradiated in air-saturated solutions, the ratio of the yields of the 8-hydroxypurines in native or heat-denatured samples was 1·09 (±0·07) and 1·05 (±0·09) for 8-hydroxyadenine and 8-hydroxyguanine, respectively (Figure 5). A significantly higher yield of 8-hydroxypurine occurred in heat-denatured DNA samples irradiated under $N_2O/O_2$, as compared with native samples with ratios of yields of 1·52 (±0·07) and 1·51 (±0·08) for 8-hydroxyadenine and 8-hydroxyguanine, respectively (Figure 5). On the other hand, for deoxygenated solutions the yield of 8-hydroxypurines was greater in samples of DNA irradiated in the native conformation. In $N_2O$-saturated solutions the ratio of product yields of 8-hydroxyadenine and 8-hydroxyguanine in samples of heat-denatured DNA were 0·58 (±0·07) and 0·46 (±0·06) of those in native DNA samples, respectively (Figure 5). Similarly, the yield of 8-hydroxyadenine in samples of heat-denatured DNA irradiated in $N_2$-saturated solutions was 0·56 (±0·14) of that measured in samples of irradiated native DNA.

3.3. *Reduction versus oxidation of DNA base radicals*

The products, 5-hydroxy-5,6-dihydroxypyrimidines/pyrimidine glycols and formamidopyrimidines/8-hydroxypurines, result from reduction/oxidation of the same 5-OH-adduct radical of pyrimidines and 8-OH-adduct radical of purines, respectively (Téoule 1987, Steenken 1989). The extent of the reduction/oxidation reactions of the OH-adduct radicals may be compared by listing the ratio of the yields of the corresponding products. In deoxygenated solutions, thymine 5-OH-adduct radicals tend to be reduced when the DNA is in the heat-denatured conformation (Table 3). Cytosine 5-OH-adduct radicals tend to be oxidized in both native and heat-denatured samples of DNA. Adenine 8-OH-adduct radicals tend to undergo reduction, whereas oxidation is the preferred reaction of guanine 8-OH-adduct radicals (Table 3). In oxygenated solutions, 5-hydroxy-5,6-dihydropyrimidines are not formed because of the reactions of 5-OH-adduct radicals with molecular oxygen to yield pyrimidine glycols (von Sonntag 1987). On the other hand, there is evidence that purine radicals might not react with oxygen (Steenken 1989). Hence, a comparison of reduction/oxidation reactions of purine

Table 3. Ratio of yields of products resulting from reduction/oxidation of base OH-adduct radicals

| | Gassing condition | | | | | | | |
|---|---|---|---|---|---|---|---|---|
| | DNA conformation† (Air) | | DNA conformation† ($N_2O/O_2$) | | DNA conformation† ($N_2O$) | | DNA conformation† ($N_2$) | |
| | ds | ss | ds | ss | ds | ss | ds | ss |
| Pyrimidine products | | | | | | | | |
| 5-Hydroxy-5,6-dihydrothymine/thymine glycol | — | — | — | — | 0·77 | 2·83 | 1·00 | 3.92 |
| 5-Hydroxy-5,6-dihydrocytosine/cytosine glycol | — | — | — | — | 0·25 | 0·46 | 0·74 | 0·40 |
| Purine products | | | | | | | | |
| FAPy-adenine/8-hydroxyadenine | 0·36 | 0·06 | 0·37 | 0·19 | 1·63 | 0·99 | 3·22 | 2·60 |
| FAPy-guanine/8-hydroxyguanine | 0·14 | 0·03 | 0·08 | 0·07 | 0·77 | 0·55 | — | — |

†ds = native conformation; ss = heat-denatured conformation.

radicals in terms of the resulting products in oxygenated solutions might be appropriate. Table 3 clearly indicates that 8-OH-adduct radicals of purines preferentially undergo oxidation in samples of DNA irradiated in both the native and heat-denatured conformations in both air-saturated and $N_2O/O_2$-saturated solutions.

## 4. Discussion

The yields of primary radicals in aqueous solutions exposed to ionizing radiation can be altered by saturating the solutions with different types of gases during the irradiation interval (for a review see von Sonntag 1987). Several radiobiological end-points are altered by such changes; the classic case being the enhancement of radiation sensitivity of cells in oxygenated (i.e. air-saturated) as compared with deoxygenated (i.e. $N_2$-saturated) conditions (Koch 1984). At the molecular level, differences in the yields of several radiation-induced DNA base products are also known to occur as a function of oxygen concentration (Fuciarelli *et al.* 1988) and several DNA base products are known to be formed exclusively in deoxygenated solutions (for reviews see Téoule and Cadet 1978, Cadet and Berger 1985, von Sonntag and Schuchmann 1986, von Sonntag 1987). Characterization of radiation-induced molecular changes to the purine and pyrimidine constituents of isolated DNA provides a first step for elucidating the importance of base damage at the cellular level.

The presence of oxygen in the irradiated solution markedly affects overall product yield and influences the types of products that are ultimately formed. Under oxygenated conditions, pyrimidine glycols and 8-hydroxypurines constitute >90% of those products measured using GC-MS/SIM methodology (Table 1 and Figure 4). By comparison, these products represent only 39–55% and 18–22% of the total product yield in $N_2O$-saturated and $N_2$-saturated solutions, respectively. To illustrate further the influence of oxygen on product yield, in $N_2$-saturated solutions the yield of 8-hydroxyadenine is less than one-tenth that observed in oxygenated solutions and 8-hydroxyguanine is not detectable. Therefore, oxidation of both 5-OH-adduct radicals of pyrimidines and 8-OH-adduct radicals of purines occurs readily under oxygenated conditions.

In solutions saturated with $N_2O$, conversion of hydrated electrons to hydroxyl radicals effectively doubles the yield of hydroxyl radicals relative to $N_2$-saturated solutions (Dainton and Peterson 1962). In this environment the increased yield of hydroxyl radicals can be evoked to explain the approximate two-fold increase in the yield of 8,5′-cycloadenosine-5′-monophosphate from adenosine-5′-monophosphate observed in $N_2O$-saturated as compared with $N_2$-saturated solutions (Raleigh *et al.* 1976). However, the ratio of the yield of 8,5′-cyclodeoxypurine nucleosides in $N_2O$-saturated solutions over that formed in $N_2$-saturated solutions was reduced in nucleic acids (Fuciarelli *et al.* 1985). Similarly, because the ratio of the yields of products in $N_2O$-saturated solutions over those in $N_2$-saturated solutions for many of the products of DNA bases measured in this study was less than a factor of 2 (Table 2), this suggests that their formation was influenced by other factors in addition to the primary radical yield. These include the type of gas used during irradiation, and DNA conformation (as shown in this study), but may also include factors such as ionization state, hydrogen bonding, base stacking relationships within the DNA and the oxidizing or reducing properties of the solution.

The shielded base hypothesis (Ward 1975, Ward and Kuo 1978) predicts a shift

in the probability of radical attack toward the sugar-phosphate backbone in native, as compared with heat-denatured, DNA because of internalization of the purine and pyrimidine bases. This hypothesis adequately predicts the effects of conformation on product yield for pyrimidine products formed in DNA that was irradiated in aqueous solution (Figure 5). Similar observations were made by Swinehart *et al.* (1974), who reported a 9–12-fold greater yield of ring saturated pyrimidine products in single-stranded $\phi$X174 DNA than native *E. coli* DNA, and by Hubbard *et al.* (1989) who reported an 8-fold higher yield of 5,6-dihydrothymine (compared with only a 1·7-fold higher yield as measured by GC–MS/SIM) in heat-denatured DNA samples than in native DNA samples exposed to ionizing radiation in $N_2$-saturated aqueous solutions. On the other hand, Furlong *et al.* (1986) reported that the yield of 5,6-dihydrothymine was greater in DNA samples irradiated in the native than in the heat-denatured conformation. This latter observation contrasts not only with the data of Hubbard *et al.* (1989), but also with the data presented in Figure 1, which illustrates that 5,6-dihydrothymine was formed in higher yield in heat-denatured DNA than in native DNA. Thus, without exception, the yields of the pyrimidine products measured in the present study were higher in heat-denatured DNA than in native DNA; an observation which is consistent with the shielded base hypothesis.

The shielded base hypothesis, however, is not an adequate model for predicting the effects of conformation on the yield of radiation-induced purine products (Figure 5). For the formamidopyrimidines there is a general trend toward greater product yields in samples of DNA irradiated in the native than in the heat-denatured conformation, using the four types of gases mentioned for saturation (Figure 5). However, for the 8-hydroxypurines the pattern of product distribution is influenced by the type of gas used to saturate the solutions during irradiation. Under oxygenated conditions the yield of the 8-hydroxypurines is greater in DNA samples irradiated in the heat-denatured than in the native conformation (Figure 5). However, under deoxygenated conditions the yields of the 8-hydroxypurine moieties are greater in DNA samples irradiated in the native than in the heat-denatured conformation (Figure 5). This might reflect prevention of the restitution reactions involving purine radicals due to steric hindrance, thus resulting in higher yields of 8-hydroxypurines in samples of DNA irradiated in the native conformation. On the other hand, based on this idea, steric hindrance would be expected to be reduced in DNA samples irradiated in the heat-denatured conformation and, therefore, the ability of the purine radicals to restitute would be enhanced, resulting in a lower yield of radiation-induced DNA base products.

A discussion of the effects of conformation on radiation-induced purine products is not complete without mentioning the effects of DNA conformation on the yields of the 8,5′-cyclo-2′-deoxynucleoside moieties. Using immunochemical techniques, Fuciarelli *et al.* (1985) observed a greater yield of 8,5′-cyclo-2′-deoxyadenosine in DNA samples irradiated in the native than in the heat-denatured conformation. However, in contrast to this observation, Dirksen *et al.* (1988), using GC–MS/SIM methodology, reported a higher yield of both epimers of the 8,5′-cyclo-2′-deoxyadenosine and 8,5′-cyclo-2′-deoxyguanosine moieties in DNA samples irradiated in the heat-denatured than in the native conformation.

Further understanding of the effects of DNA conformation on product yield must acknowledge the influence of the microenvironment at the site of the DNA target molecule, which might include factors such as hydrogen bonding and

ionization state of the DNA molecule and their ability to direct radical attack and influence product distribution as demonstrated in model systems (Fujita and Steenken 1981, Hazra and Steenken 1983, Raleigh and Fuciarelli 1985, Fuciarelli *et al.* 1987, Vieira and Steenken 1987). The use of GC–MS/SIM methodology to address the effects of DNA conformation on the yields of radiation-induced products has the distinct advantage of measuring both purine and pyrimidine products at radiation doses that minimize radiation-induced strand scission preventing denaturation of the DNA. Therefore, a broader understanding of the factors contributing to the effect of DNA conformation on product yield is feasible using this technique.

A comparison of the yields of DNA base products obtained with GC–MS/SIM methodology to those obtained using other assay techniques deserves comment. As illustrated in this study, product yields may be sensitive to DNA conformation and the type of gas used to saturate the solutions during irradiation. However, many parameters including, the type, concentration, and pH of the buffer, in addition to the concentration of the DNA, might affect the product yields. Hence, product yields may only be directly comparable when all of the conditions under which the irradiations were performed are identical. This happens infrequently in the literature and, therefore, comparison of absolute product yields with other reports may be inappropriate, although we by no means imply that the conditions under which the irradiations in this study were performed are optimal.

The data presented in Figures 2 and 3 reveal that low levels of radiation-induced purine and pyrimidine products can be measured by GC–MS/SIM in unirradiated samples of DNA as was previously reported (Dizdaroglu and Bergtold 1986). Several other researchers, using different methodologies for measuring DNA base products, have reported similar observations (Frenkel *et al.* 1981, Kasai *et al.* 1986, Richter *et al.* 1988). Indeed, Kasai *et al.* (1986) demonstrated that 8-hydroxyguanine can be measured in nuclear DNA isolated from HeLa cells, mouse liver, and *S. tryphimurium* that had not been treated with oxygen radical generating agents, suggesting that modifications to the purine and pyrimidine moieties in DNA arise in *in vivo*, as a result of normal oxidative processes in the cell. Given that cellular systems have developed repair processes, as exemplified by thymine glycol *N*-glycosylase (Higgins *et al.* 1987) and cytosine photoproduct *N*-glycosylase (Weiss *et al.* 1989) activities, it may be reasonable to assume that a portion of the altered DNA base products measured may represent an intrinsic level of oxidative damage that is routinely found in cells. Further DNA damage may occur as these repair processes are terminated by disruption of tissues and cells when isolating nuclear DNA. The generation of peroxides in homogenized mammalian tissues provides support for this argument (Cutler 1985). Finally, the methodology used to measure product formation (i.e. chemical hydrolysis) might also contribute to the low background of modified purine and pyrimidine products.

In summary, methodology incorporating gas chromatography–mass spectrometry was used for quantitative measurement of radiation-induced base damage in DNA. The effects of DNA conformation and the type of gas used to saturate the solutions during irradiation were found to affect both the types and yields of radiation-induced purine and pyrimidine products in DNA.

## Acknowledgements

This research was supported in part by the Armed Forces Radiobiology

Research Institute of the Defense Nuclear Agency, under Research Work Units 00105 and 00150. The views expressed in this article are those of the authors and do not reflect the official views or position of the Department of Defense or the US Government. The authors thank Mr W. E. Jackson for assistance with statistical analysis of the data, and Dr J. F. Ward for helpful discussions.

## References

BONICEL, A., MARIAGGI, N., HUGHES, E. and TÉOULE, R., 1980, *In vitro* gamma irradiation of DNA: identification of radiation-induced chemical modification of the adenine moiety. *Radiation Research*, **83**, 19–26.

BREIMER, L. H. and LINDAHL, T., 1985, Thymine lesions produced by ionizing radiation in double-stranded DNA. *Biochemistry*, **24**, 4018–4022.

BURTON, K., 1968, Determination of DNA concentration with diphenylamine. *Methods in Enzymology, Nucleic Acids, Part B*, edited by L. Grossman and K. Moldzie (Academic Press, New York), vol. 12, pp. 163–166.

CADET, J. and BERGER, M., 1985, Radiation-induced decomposition of the purine bases within DNA and related model compounds. *International Journal of Radiation Biology*, **47**, 127–143.

CHETSANGA, C. J. and GRIGORIAN, C., 1983, A dose–response study on opening of imidazole ring of adenine in DNA by ionizing radiation. *International Journal of Radiation Biology*, **44**, 321–331.

CUTLER, R. G., 1985, Peroxide-producing potential of tissues: Inverse correlation with longevity of mammalian species. *Proceedings of the National Academy of Sciences, USA*, **82**, 4798–4802.

DAINTON, F. S. and PETERSON, D. B., 1962, Forms of H and OH produced in the radiolysis of aqueous systems. *Proceedings of the Royal Society*, **A267**, 443–463.

DIRKSEN, M.-L., BLAKELY, W. F., HOLWITT, E. and DIZDAROGLU, M., 1988, Effect of DNA conformation on hydroxyl radical-induced formation of 8,5′-cyclopurine 2′-deoxyribonucleoside residues in DNA. *International Journal of Radiation Biology*, **54**, 195–204.

DIZDAROGLU, M., 1985a, Application of capillary gas chromatography-mass spectrometry to chemical characterization of radiation-induced base damage to DNA: implications for assessing DNA repair processes. *Analytical Biochemistry*, **144**, 593–603.

DIZDAROGLU, M., 1985b, Formation of an 8-hydroxyguanine moiety in deoxyribonucleic acid on gamma-irradiation in aqueous solution. *Biochemistry*, **24**, 4476–4481.

DIZDAROGLU, M., 1986, Chemical characterization of ionizing radiation-induced damage to DNA. *BioTechniques*, **4**, 536–546.

DIZDAROGLU, M. and BERGTOLD, D. S., 1986, Charactization of free radical-induced base damage in DNA at biologically relevant levels. *Analytical Biochemistry*, **156**, 182–188.

DIZDAROGLU, M., HOLWITT, E., HAGAN, M. P. and BLAKELY, W. F., 1986, Formation of cytosine glycol and 5,6-dihydroxycytosine in deoxyribonucleic acid on treatment with osmium tetroxide. *Biochemical Journal*, **235**, 531–536.

FRENKEL, K., GOLDSTEIN, M., DUKER, N. H. and TEEBOR, G. W., 1981, Identification of the *cis*-thymine glycol moiety in chemically oxidized and irradiated deoxyribonucleic acid by high-pressure liquid chromatography analysis. *Biochemistry*, **20**, 7566–7571.

FRICKE, J. and HART, E. J., 1966, Chemical dosimetry. *Radiation Dosimetry*, Vol. II, *Instrumentation*, 2nd edn, edited by F. H. Attix and W. C. Roesch (Academic Press, New York), pp. 167–239.

FUCIARELLI, A. F., MILLER, G. G. and RALEIGH, J. A., 1985, An immunochemical probe for 8,5′-cycloadenosine-5′-monophosphate and its deoxy analog in irradiated nucleic acids. *Radiation Research*, **104**, 272–283.

FUCIARELLI, A. F., SHUM, F. Y. and RALEIGH, J. A., 1987, Intramolecular cyclization in irradiated nucleic acids. Correlation between high-performance liquid chromatography and an immunochemical assay for 8,5′-cycloadenosine in irradiated poly A. *Radiation Research*, **110**, 35–44.

FUCIARELLI, A. F., KOCH, C. J. and RALEIGH, J. A., 1988, Oxygen dependence of product formation in irradiated adenosine-5′-monophosphate. *Radiation Research*, **113**, 447–457.

FUCIARELLI, A. F., WEGHER, B. J., GAJEWSKI, W., DIZDAROGLU, M. and BLAKELY, W. F., 1989, Quantitative measurement of radiation-induced base products in DNA using gas chromatography–mass spectrometry. *Radiation Research*, **119**, 219–231.

FUJITA, S. and STEENKEN, S., 1981, Pattern of OH radical addition to uracil and methyl- and carboxyl-substituted uracils. Electron transfer of OH adducts with N,N,N',N'-tetramethyl-*p*-phenylene-diamine and tetranitromethane. *Journal of the American Chemical Society*, **103**, 2540–2545.

FURLONG, E. A., JORGENSEN, T. J. and HENNER, W. D., 1986, Production of dihydrothymidine stereoisomers in DNA by gamma-irradiation. *Biochemistry*, **25**, 4344–4349.

HAZRA, D. K. and STEENKEN, S., 1983, Pattern of OH radical addition to cytosine and 1-, 3-, 5-, and 6-substituted cytosines. Electron transfer and dehydration reactions of the OH adducts. *Journal of the American Chemical Society*, **105**, 4380–4386.

HIGGINS, S. A., FRENKEL, K., CUMMINGS, A. and TEEBOR, G. W., 1987, Definitive characterization of human thymine glycol N-glycosylase activity. *Biochemistry*, **26**, 1683–1688.

HUBBARD, K., IDE, H., ERLANGER, B. F. and WALLACE, S. S., 1989, Characterization of antibodies to dihydrothymine, a radiolysis product of DNA. *Biochemistry*, **28**, 4382–4387.

KASAI, H., TANOOKA, H. and NISHIMURA, S., 1984, Formation of 8-hydroxyguanine residues in DNA by X-irradiation. *Gann*, **75**, 1037–1039.

KASAI, H., CRAIN, P. F., KUCHINO, Y., NISHIMURA, S., OOTSUYAMA, A. and TANOOKA, H., 1986, Formation of 8-hydroxyguanine moiety in cellular DNA by agents producing oxygen radicals and evidence for its repair. *Carcinogenesis*, **7**, 1849–1851.

KOCH, C. J., 1984, A thin-film culturing technique allowing rapid gas-liquid equilibration (6 sec) with no toxicity to mammalian cells. *Radiation Research*, **97**, 434–442.

LEADON, S. A. and HANAWALT, P. C., 1983, Monoclonal antibody to DNA containing thymine glycol. *Mutation Research*, **12**, 191–200.

NISHIMOTO, S., IDE, H., WADA, T. and KAGIYA, T., 1983, Radiation-induced hydroxylation of thymine promoted by electron-affinic compounds. *International Journal of Radiation Biology*, **44**, 585–600.

RAJAGOPALAN, R., MELAMEDE, R. J., LASPIA, M. F., ERLANGER, B. F. and WALLACE, S. S., 1984, Properties of antibodies to thymine glycol, a product of the radiolysis of DNA. *Radiation Research*, **97**, 499–510.

RALEIGH, J. A. and FUCIARELLI, A. F., 1985, Distribution of damage in irradiated 5'-AMP: 8,5'-cycloAMP, 8-hydroxyAMP and adenine release. *Radiation Research*, **102**, 165–175.

RALEIGH, J. A., KREMERS, W. and WHITEHOUSE, R., 1976, Radiation chemistry of nucleotides: 8,5'-cyclonucleotide formation and phosphate release initiated by hydroxyl radical attack on adenosine monophosphates. *Radiation Research*, **65**, 414–422.

RICHTER, C., PARK, J.-W. and AMES, B. N., 1988, Normal oxidative damage to mitochondrial and nuclear DNA is extensive. *Proceedings of the National Academy of Sciences, USA*, **85**, 6465–6467.

SCHELLENBERG, K. A. and SHAEFFER, J., 1986, Formation of methyl ester of 2-methylglyceric acid from thymine glycol residues: A convenient new method for determining radiation damage to DNA. *Biochemistry*, **25**, 1479–1482.

STEENKEN, S., 1989, Purine bases, nucleosides, and nucleotides: Aqueous solution redox chemistry and transformation reactions of their radical cations and $e^-$ and OH adducts. *Chemical Reviews*, **89**, 503–520.

SWINEHART, J. L., LINN, W. S. and CERUTTI, P. A., 1974, Gamma-ray-induced damage in thymine in mononucleotide mixtures, and in single- and double-stranded DNA. *Radiation Research*, **58**, 166–175.

TEEBOR, G., CUMMINGS, A., FRENKEL, K., SHAW, A., VOITURIEZ, L. and CADET, J., 1987, Quantitative measurement of the diastereoisomers of *cis* thymidine glycol in gamma-irradiated DNA. *Free Radical Research Communications*, **2**, 303–309.

TÉOULE, R., 1987, Radiation-induced DNA damage and its repair. *International Journal of Radiation Biology*, **51**, 573–589.

TÉOULE, R. and CADET, J., 1978, Radiation-induced degradation of the base component in DNA and related substances-final products. *Effects of Ionizing Radiation on DNA*, edited by J. Hütterman, W. Köhnlein, R. Téoule and A. J. Bertinchamps (Springer-Verlag, New York), pp. 171–203.

TÉOULE, R. and GUY, A., 1987, Quantitative measurements of modified thymine residues in DNA chains by formic acid hydrolysis. *Nucleosides and Nucleotides*, **6**, 301–305.

TÉOULE, R., BERT, C. and BONICEL, A., 1977, Thymine fragment damage retained in the DNA polynucleotide chain after gamma irradiation in aerated solutions. II. *Radiation Research*, **72**, 190–200.

VIEIRA, A. J. S. C. and STEENKEN, S., 1987, Pattern of OH radical reaction with $N^6$,$N^6$-dimethyladenosine. Production of three isomeric OH adducts and their dehydration and ring-opening reactions. *Journal of the American Chemical Society*, **109**, 7441–7448.

VON SONNTAG, C., 1987, *The Chemical Basis of Radiation Biology* (Taylor & Francis, New York).

VON SONNTAG, C. and SCHUCHMANN, H.-P., 1986, The radiolysis of pyrimidines in aqueous solutions: an updating review. *International Journal of Radiation Biology*, **49**, 1–34.

WARD, J. F., 1975, Molecular mechanisms of radiation-induced damage to nucleic acids. *Advances in Radiation Biology*, edited by J. T. Lett and H. Adler (Academic Press, New York), vol. 5, pp. 181–239.

WARD, J. F. and KUO, I., 1978, Radiation damage to DNA in aqueous solution: a comparison of the response of the single-stranded form with that of the double-stranded form. *Radiation Research*, **75**, 278–285.

WARD, J. F. and URIST, M. M., 1967, Gamma-irradiation of aqueous solutions of polynucleotides. *International Journal of Radiation Biology*, **12**, 209–218.

WEISS, R. B., GALLAGHER, P. E., BRENT, T. P. and DUKER, N. J., 1989, Cytosine photoproduct-DNA glycosylase in *Escherichia coli* and cultured human cells. *Biochemistry*, **28**, 1488–1492.

WEISSBURGER, E. and OKADA, S., 1961, Radiosensitivity of single- and double-stranded deoxyribonucleic acid. *International Journal of Radiation Biology*, **3**, 331–333.

WEST, G. J., WEST, I. W.-L. and WARD, J. F., 1982a, Radioimmunoassay of a thymine glycol. *Radiation Research*, **90**, 595–608.

WEST, G. J., WEST, I. W.-L. and WARD, J. F., 1982b, Radioimmunoassay of 7,8-dihydro-8-hydroxyadenine. *International Journal of Radiation Biology*, **42**, 481–490.

# CHARACTERISTICS OF NONCOVALENT AND COVALENT INTERACTIONS OF (+) AND (-) *ANTI*-BENZO[a]PYRENE DIOL EPOXIDE STEREOISOMERS OF DIFFERENT BIOLOGICAL ACTIVITIES WITH DNA.

N.E. GEACINTOV, M. COSMAN, V. IBANEZ, S.S. BIRKE and C.E. SWENBERG[1]
*Chemistry Department, New York University, New York, NY, 10003, and [1]Radiation Biochemistry Department, Armed Forces Radiobiology Research Institute, Bethesda, MD 20814*

**ABSTRACT.** The (+) and (-) enantiomers of *anti*-7,8-diol-9,10-epoxy-7,8,9,10-tetrahydrobenzo[a]pyrene (BPDE) are characterized by striking differences in their tumorigenic and mutagenic activities. The covalent binding of these isomers leads to DNA adducts with different distributions of conformations. The adducts derived from (+)-BPDE cause significant unwinding of supercoiled DNA, while those derived from (-)-BPDE do not. The conformations of these covalent lesions are different from those of classical intercalation complexes and include external binding modes and adducts which exhibit some though not all characteristics of intercalative binding. New insights into these different adducts are obtained from studies of oligonucleotides of defined base composition and sequence modified covalently at the exocyclic amino group of guanine by *cis* and *trans* addition of (+)-BPDE and (-)-BPDE.

## 1. INTRODUCTION

Polycyclic aromatic hydrocarbons (PAH) are characterized by varying degrees of tumorigenic and mutagenic activities. It is well established that these compounds are metabolically activated to epoxide and diol epoxide derivatives, which are the ultimate mutagenic and tumorigenic forms of these molecules [1,2]. Mutations probably constitute the initial first steps in the complex, multi-stage phenomenon of chemical carcinogenesis [3]. The detailed molecular mechanisms by which PAH diol epoxides and other chemical carcinogens induce mutations are not yet well understood. Subtle structural differences, such as the stereochemical properties of the PAH diol epoxide molecules, can manifest themselves in terms of dramatic differences in their biological activities [1]. The formation of covalent adducts with cellular DNA in specific genomic sequences is critical for the expression of the mutagenic potentials of PAH diol epoxides [4-8]. Experimental [9-13] and theoretical [14,15] studies have shown that base composition and sequence effects can play an important role in determining the chemical reactivities of PAH diol epoxides and the characteristics of the DNA adducts formed *in vitro*.



*B. Pullman and J. Jortner (eds.), Molecular Basis of Specificity in Nucleic Acid-Drug Interactions*, 433–450.

The most biologically active metabolites of the ubiquitous environmental pollutant benzo[a]pyrene (BP) are the bay-region diol epoxide derivatives in which an epoxide ring bridges the 9,10-positions of BP with two -OH groups located at the 7 and 8 positions. [1]. There are four different stereoisomers of this metabolite. The most tumorigenic isomer is the (+) enantiomer of the diastereomer *trans*-7,8-dihydroxy-*anti*-9,10-epoxy-7,8,9,10-tetrahydrobenzo[a]pyrene, or BPDE (known also as *anti*-BPDE, BPDE 2, or BPDE I). Unlike (+)-BPDE, the (-) enantiomer is not tumorigenic to any significant extent [1]. Both enantiomers are mutagenic, but their activities are different from one another in mammalian [16] and in bacterial [17] cell systems. These pairs of *anti*-BPDE enantiomers, denoted here by (+)-BPDE and (-)-BPDE, constitute a fascinating example of structure-biological activity relationships. Brookes and Osborne [16] proposed that the conformational properties of covalent adducts derived from the chemical binding of these two isomers to DNA are different from one another, and that these differences may be of critical importance in the processing of these adducts by the cellular machineries of repair and replication. The mechanisms of interaction of these BPDE stereoisomers with DNA in aqueous model systems, and the properties of the noncovalent complexes and covalent adducts formed, have been studied extensively (reviewed in 18-20].

The relationships between biological activities, chemical structure, steric characteristics, and reactivities of chemical carcinogens and their metabolites with DNA, have long been subjects of intense interest to researchers in the field of chemical carcinogenesis [2]. In this article we discuss and review the differences in the interactions of (+)-BPDE and (-)-BPDE with nucleic acids, and the characteristics of the covalent adducts formed. Recent results obtained with supercoiled DNA and with oligodeoxynucleotides of defined base composition and sequence have provided new insights into the characteristics of the covalent BPDE-DNA lesions.

## 2. Characteristics of Reaction and Binding of BPDE with Nucleic Acids.

### 2.1 REACTION PATHWAYS IN AQUEOUS DNA SOLUTIONS

The hydrophobic BPDE stereoisomers and similar PAH diol epoxides are known to form noncovalent complexes with DNA. Such physical BPDE-DNA complexes are formed on time scales of milliseconds, while the covalent binding reactions occur on time scales of minutes [21]. The dominant reaction of the BPDE enantiomers is hydrolysis to the tetraols BPT (7,8,9,10-tetrahydrotetrahydroxybenzo[a]pyrene). This reaction is catalyzed by DNA under conditions of relatively low ionic strengths [18, and references quoted therein]. Only 16-20% of (+)-BPDE and 4-5% of the (-)-BPDE molecules form covalent addition products with native double-stranded DNA. The reaction pathways of BPDE in aqueous solutions are summarized in Fig. 1.

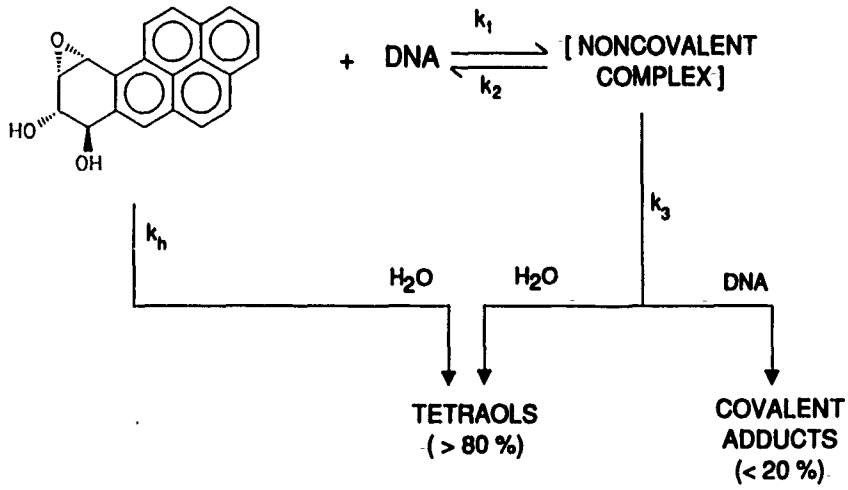


Fig. 1

The characteristics of the non-covalent BPDE-DNA complexes are consistent with those of classical intercalation complexes because of the following observations: (1) unwinding of supercoiled DNA [22,37], and (2) the pyrenyl residues are oriented parallel to the planes of the DNA bases [23]. The association constants K ($M^{-1}$) characterizing the formation of these noncovalent complexes appear to be approximately equal for (+)-BPDE and (-)-BPDE [24,25]. The formation of BPT is by far the dominant reaction pathway of BPDE in aqueous DNA solutions.

Most recently, the chemical adduct distribution of the two enantiomers of BPDE with calf thymus DNA has been reinvestigated by Cheng et al. [26]; in the case of (+)-BPDE, the major adduct (~94%) involves *trans* opening of the BPDE epoxide ring and covalent adduct formation between the C-10 position of BPDE and the exocyclic amino group of guanine in DNA. In the case of (-)-BPDE, a similar *trans*-dG adduct is also formed (63%), with lesser amounts of a *cis*-adduct (22%) and a *trans* -N6-adenine adduct (15%) [26].

## 2.2. BASE-SEQUENCE SELECTIVITIES

2.2.1. *Noncovalent Complex Formation and Reaction Kinetics.* Based on the reaction scheme in Fig. 1, it can be shown [27] that the overall reaction rate constant (k) of BPDE molecules in aqueous DNA solutions can be approximated by the following equation:

$$k = \frac{k_h + k_3 K[DNA]}{1 + K[DNA]} \quad (1)$$

where $k_h$ is the reaction rate constant in the absence of DNA, $k_3$ is the rate constant for reaction of BPDE molecules at DNA binding sites, and $K = k_1/k_2$ is the apparent association constant averaged over all types of different noncovalent binding sites [12]. The quantity [DNA] denotes the concentration of binding sites expressed in units of DNA nucleotides.

The reactivity of BPDE with DNA can be expressed in terms of $f_{cov}$, the fraction of BPDE molecules which react by forming covalent adducts with DNA rather then by reacting with water to form tetraols.

A comparison of the base sequence dependences of the parameters $k_3(s^{-1})$, $f_{cov}$, and $K(M^{-1})$ obtained with synthetic polynucleotides is summarized in Fig. 2.

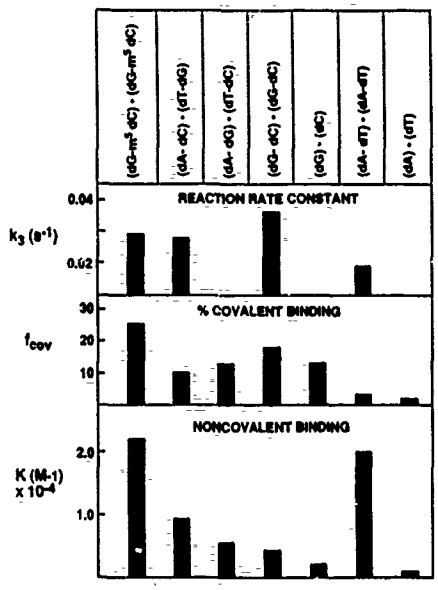


Fig. 2

In these studies [12], racemic mixtures of BPDE ((±)-BPDE), rather then the resolved enantiomers were used because of the greater availability of (±)-BPDE. Roche has shown that $f_{cov}$ for (+)-BPDE is larger than for (-)-BPDE by factors of ~5 in poly(dG-dC)·(dG-dC) and in poly(dG)·(dC). For the adenine-containing polymers, the values of $f_{cov}$ are comparable for (+)-BPDE and (-)-BPDE [28].

The noncovalent association constant K is highest in poly(dG-$m^5$dC)·(dG-$m^5$dC) and in poly(dA-dT)·(dA-dT) sequences, and is lowest in the non-alternating polymers poly(dG)·(dC) and poly(dA)·(dT). The reaction rate constant of physically bound BPDE, $k_3$, is uniformly

higher for all dG-containing polymers, reflecting the preferred reactions of BPDE with guanine [10]. Values of $k_3$ are not listed for any of the non-alternating polynucleotides; the reactions at these sequences do not appear to involve the formation of pre-reaction physical complexes [12], and thus Eq. (1) is not appropriate in these cases. The values of the covalent binding efficiency factor $f_{cov}$ are significantly higher for all polymers which contain guanine than for those which do not (Fig. 2). Again this fact reflects the preference for the covalent binding of both BPDE enantiomers to guanine rather than to adenine [26].

2.2.3. *Relationship Between Noncovalent Complex and Covalent Adduct Formation*. It is evident from the data shown in Fig. 2, that there is no obvious and direct correlation between noncovalent complex formation (which is presumed to be intercalative in nature [12]) and the efficiency of covalent adduct formation. It is often assumed that intercalation is an important pre-requisite for covalent adduct formation, and thus for the manifestation of the biological activities of PAH diol epoxides [19,27,29]. While this hypothesis is not supported by the data in Fig. 2, it is likely that in a complex cellular environment the value of K may be important. Large values of K for any particular PAH diol epoxide tend to keep these reactive molecules associated with the DNA where they can ultimately undergo chemical reactions to form mutagenic adducts with guanine or adenine [27]. If the K values are small, a greater fraction of the PAH diol epoxide molecules will be located in complexes with other cellular macromolecules and in the aqueous phases of the cell. In these other environments they can be deactivated by reacting with glutathione or other agents which serve to detoxify these mutagenic compounds. Thus, the ability of these compounds to form noncovalent complexes with DNA, whether intercalative or not, may be important because high values of K increase the probability of reaction with DNA.

In the case of native DNA, which contains all possible sequence, the results summarized in Fig. 2 suggest that a higher fraction of BPDE molecules which have not yet reacted can be found at alternating dA-dT sequences. However, covalent binding reactions at dG can still occur efficiently; the residence time of any given BPDE molecule at a particular noncovalent binding site is expected to be quite short, of the order of several milliseconds, or less. Since the covalent binding and hydrolysis reactions occur on time scale of minutes, any particular BPDE molecule has the opportunity to sample many different DNA binding sites during its lifetime by physically diffusing from site to site and, finally, reacting with guanine [12].

## 2.3. CHARACTERISTICS OF COVALENT ADDUCTS.

2.3.1. *Types of Adduct Conformations*. Two different types of BPDE-DNA binding sites have been identified based on linear dichroism and other spectroscopic techniques [18-20].

Site I-type conformations are characterized by mean tilts of the long axis of the pyrenyl residues of 25-30° with respect to the aver-

age orientations of the planes of the DNA bases; these site I conformations are characterized by broadened and red shifted absorption spectra (~10 nm with respect to the absorption spectra of BPDE molecules in aqueous solutions). Such red shifts are usually attributed to extensive $\pi$ - electron stacking interactions between the pyrenyl residues and DNA bases; however, other causes for these effects cannot be excluded. In linear dichroism experiments in which the DNA molecules are oriented in hydrodynamic flow gradients, any BPDE molecules bound to the DNA either noncovalently or covalently, contribute to the linear dichroism (LD) signal [18,20]. The LD spectra above 300 nm resemble the absorption spectra of the pyrenyl residues, but are either negative or positive in sign, depending on the mean orientation of the pyrenyl long axis with respect to the planes of the DNA bases. Site I adducts contribute *negative* LD signals because, on the average, the long axes of the pyrenyl residues are tilted close to the planes of the DNA bases.

Site II adducts, in contrast to Site I adducts, are considerably more exposed to the aqueous solvent environment [30-32]. The red shift in the absorption spectrum is only 2-3 nm, and the LD spectrum again resembles the absorption spectrum, but is positive in sign. Taken together, these characteristics suggest that the long axes of the planar pyrenyl residues, on the average, are tilted away from the DNA base planes at relatively large angles ( $> 65^{o}$).

2.3.2. *Conformations of Noncovalent Complexes and Covalent Adducts Derived from (+)-BPDE- and (-)-BPDE.* The complexes formed when either enantiomer binds to native DNA are of the Site I-type, and intercalative in nature [23]. Linear dichroism measurements indicate that there is a pronounced change in orientation of (+)-BPDE as a result of the chemical binding reaction, whereas the apparent changes in conformations of the (-)-BPDE pyrenyl residues appear to be less pronounced [25].

Examples of LD spectra obtained from the covalent binding of (+)-BPDE or (-)-BPDE to poly(dG)•(dC) are shown in Fig. 3.

The adducts derived from (-)-BPDE are characterized by an absorption spectrum with maxima at 338 and 353 nm (Fig. 3A), which constitutes a 9-10 nm red shift with respect to the absorption spectrum of free BPDE in aqueous solutions. The LD spectrum is negative in sign with the minima occurring at the same wavelength as the absorption maxima (Fig. 3C). The (-)-BPDE-poly(dG)•(dC) adducts are clearly of the site I-type.

The adducts derived from (+)-BPDE are characterized by a positive LD spectrum (Fig. 3D) which resembles the absorption spectrum (Fig. 3B), with maxima at 329 and 345 nm in both cases. These maxima are red-shifted by only 1-2 nm with respect to free BPDE, suggesting that $\pi$-stacking interactions are not occurring to any significant extent; a small negative Site I LD signal with a minimum at 260 nm is also observed (Fig. 3D). Overall, the LD spectrum is attributed mainly to Site II adducts with a small contribution from site I adducts. Similar effects are observed with the alternating poly(dG-dC)•(dG-dC). In the case of(+)-BPDE bound covalently to calf thymus DNA, site II

adducts are even more dominant than in the case of poly(dG)•(dC), whereas in (-)-BPDE-DNA adducts the Site I:Site II distribution is about 2:1 [32].

2.3.3 *Adduct Conformations and Biological Activities.* The conformations of covalent native DNA adducts derived from nearly 20 different PAH diol epoxides have been examined by linear dichroism techniques [18,33]. All of the highly tumorigenic isomers give rise to adducts which are predominantly of the Site II-type, whereas all less active or inactive isomers give rise predominantly to Site I adducts. This empirical correlation between biological activity and adduct conformation has been observed for PAH diol epoxide molecules which are known to bind predominantly to N2 of guanine. The conformations of DNA adducts derived from other PAH diol epoxides which bind extensively to adenine [7,34] have not yet been studied, and may well be different.

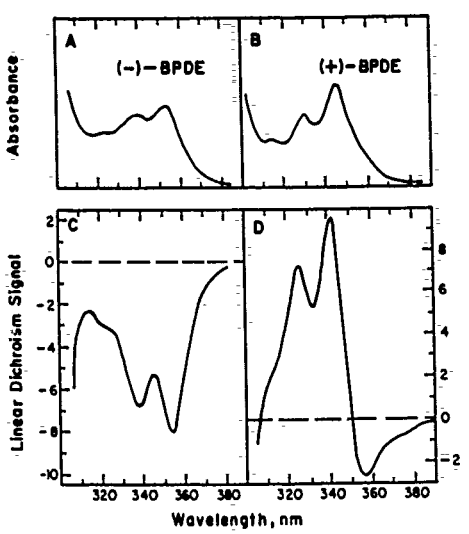


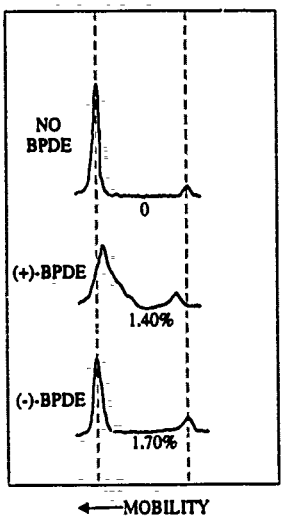


Fig. 3 (left). Characteristic absorption and linear dichroism spectra of BPDE enantiomers covalently bound to poly(dG)•(dC).

Fig. 4 (right). Electrophoretic agarose gel patterns of PIBI 30 supercoiled DNA covalently modified with (+)-BPDE or (-)-BPDE with 1.4% and 1.7% of bases modified, respectively.

### 3. Unwinding of Supercoiled DNA Induced by (+)-BPDE and (-)-BPDE.

The unwinding of supercoiled DNA by drugs and carcinogens can provide information on the mechanism of complex formation and DNA damage, *e.g.* the formation of single strand breaks. The unwinding of supercoiled DNA by racemic BPDE via noncovalent complex formation [22] and covalent adduct formation [35-37], has been previously investigated. It is well established that adducts derived from the covalent binding of (±)-BPDE to SV40 DNA [35] and ϕX174 DNA [36] cause the removal of left-handed supercoils and a decreased electrophoretic mobility on agarose gels. Based on such results, Drinkwater *et al.* [35] proposed a covalent intercalative binding model for racemic BPDE. Gamper and co-workers [36] suggested that the unwinding may be due to a disruption of base pairing at BPDE binding sites, with the aromatic hydrocarbon residues lying in the minor or the major groove.

We have investigated the unwinding of supercoiled DNA using (+)-BPDE and (-)-BPDE enantiomers instead of (±)-BPDE, and supercoiled PIBI 30 DNA (2926 base pairs, superhelical density $\sigma \approx -0.04$). Utilizing a kinetic flow linear dichroism method [37], we have observed that both enantiomers when bound *noncovalently* to DNA cause reversible unwinding (data not shown); this is in agreement with the earlier observations of Meehan *et al.* [22]. However, the effects of *covalently* bound (+)-BPDE and (-)-BPDE residues are dramatically different from one another. Typical densitometer traces of gel electrophoresis patterns obtained with unmodified PIBI 30, and the same DNA sample modified covalently by either (+)-BPDE or (-)-BPDE are shown in Fig. 4.

The unmodified DNA is characterized by two electrophoretic bands of different mobilities. The higher mobility, more intense band is due to the supercoiled form, while the slower and smaller band is attributed to the relaxed nicked form ($\sigma = 0$). The shape of the highly supercoiled DNA is more compact than that of the relaxed DNA, and thus its electrophoretic mobility is higher than that of the nicked form. The covalently bound (+)-BPDE causes a significant decrease and broadening of the electrophoretic mobilities of PIBI30, while adducts arising from the (-) enantiomer clearly are much less effective, since the mobility distribution of the modified DNA is somewhat broadened but otherwise unaffected even at a high level of binding (1.7% of all PIBI 30 nucleotides modified).

Based on the results shown in Fig. 4, we conclude that the previously observed unwinding of supercoiled DNA induced by covalently bound residues derived from (±)-BPDE [35,36] was predominantly caused by the (+) enantiomer.

The striking difference in unwinding effects produced by (+) and (-) BPDE indicates that the covalently bound (+)-BPDE residues cause significant changes in the tertiary structure of DNA, while those arising from (-)-BPDE do not. It is interesting to note that simi-

lar effects are observed with the anti-tumor agent cis-dichlorodiammineplatinum (II) (cis-DPP) and its inactive isomer trans-DPP [38]. While cis-DPP causes significant unwinding of supercoiled DNA, trans-DPP does not.

Based on results of linear dichroism measurements on supercoiled DNA [37] covalently modified with either (+)-BPDE or (-)-BPDE, the adduct conformations appear to be similar in linear and in supercoiled DNA (data not shown). Unexpectedly, the external Site II adducts derived from (+)-BPDE cause extensive unwinding, while the Site I adducts derived from (-)-BPDE do not, even though the conformations of these Site I adducts resemble those of classical intercalation complexes in several respects. These results are in accord with previous conclusions that covalent adduct conformations other than intercalative ones can cause significant unwinding of supercoiled DNA [37]. Indeed other causes of duplex unwinding not involving the formation of intercalation complexes have been documented [39].

It is known that racemic BPDE, upon covalent binding to native DNA, gives rise to a bend or kink at the binding site [40]. Eriksson *et al.* [41] have provided evidence that such effects are caused by (+)-BPDE, but not by (-)-BPDE. Thus, the observed unwinding effects may be due to the formation of such kinks, and/or flexible hinge joints. The lack of unwinding of supercoiled DNA by the covalent binding of (-)-BPDE is difficult to rationalize since the pyrenyl residues appear to be at least partially stacked with the DNA bases. A more thorough understanding of these complex effects must await a detailed elucidation of the structures of these covalent BPDE-DNA adducts.

## 4. Synthesis and Characterization of Defined Covalent BPDE-Oligodeoxynucleotide Adducts.

The characteristics of covalent adducts derived from the reactions of the tumorigenic (+)-BPDE and non-tumorigenic (-)-BPDE with native linear DNA, synthetic polynucleotides, and supercoiled DNA, are strikingly different from one another. However, in order to achieve a deeper understanding of these characteristics on a more detailed molecular level, it is necessary to extend these investigations to DNA of well defined base composition and sequence. We have therefore initiated a series of studies on the characteristics of covalent adducts derived from the binding of (+)-BPDE and (-)-BPDE to oligonucleotides of defined base composition and sequence. Our initial studies have focused on single strands containing a single dG residue, the primary site of attack of both enantiomers, and the characteristics of the duplexes formed with modified strands.

### 4.1. SYNTHESIS AND IDENTIFICATION

Initial studies in our laboratory have shown that pyrimidine-guanine-pyrimidine sequences in oligonucleotides 9-11 bases long can be efficiently modified with either of the two BPDE enantiomers at the

single dG residues; the details of the synthesis and chemical characterization of the adducts are described more fully elsewhere [42]. Only a brief summary is provided here.

4.1.1. *Reaction Yields.* Both (+)-BPDE and (-)-BPDE form predominantly *cis* and *trans* addition products with the exocyclic amino group of guanine (defined in Fig. 5).

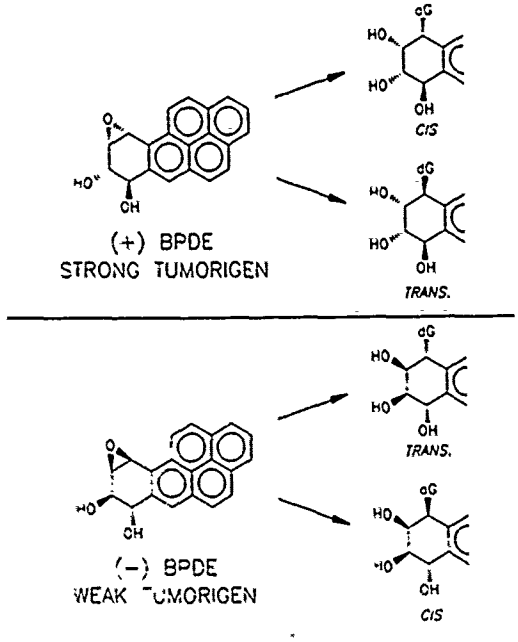


Fig. 5

Good levels of covalent binding were achieved with the 9-mer sequence d(ATATGTATA) and 11-mer sequence d(CACATGTACAC). The reaction yields, or fraction of BPDE molecules which react by covalently binding to the oligonucleotides, were 34 - 45% in the case of (+)-BPDE and 15% - 20% in the case of (-)-BPDE.

4.1.2. *Isolation and Characterization of Addition Products.* The adducts were characterized by basically following methods similar to those of Cheng *et al.* [26]. The BPDE-oligonucleotide adducts were separated from the unmodified oligonucleotides by HPLC methods utilizing an ODS-Hypersil preparatory column and a 0-90% methanol/20 mM sodium phosphate (pH = 7.0) buffer gradient in 60 minutes (24 ± 1 C°) with a 3.0 ml/min flow rate. Typical elution profiles of the

oligonucleotide d(ATATGTATA) modified with (+)-BPDE or (-)-BPDE are shown in Fig. 6. Three major elution peaks corresponding to the

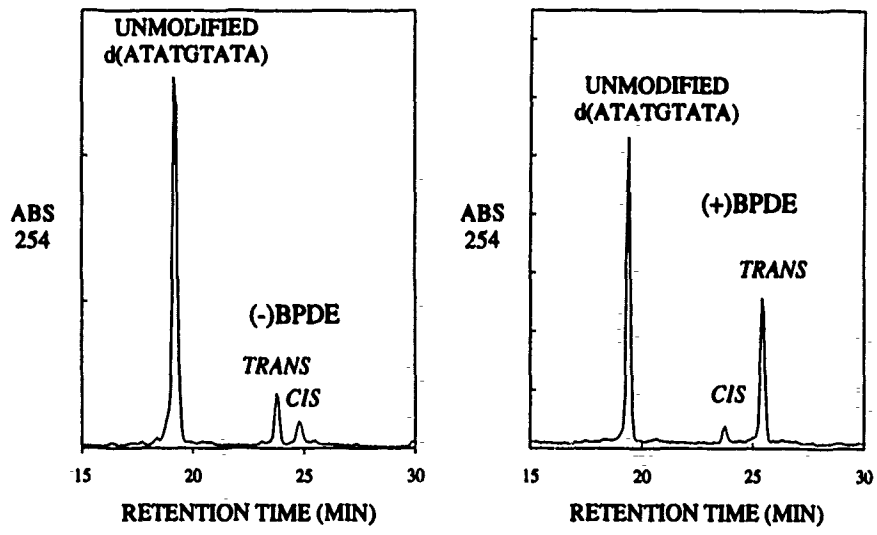


Fig. 6

unmodified oligonucleotide, and two elution peaks corresponding to BPDE-modified oligonucleotides are observed (minor elution peaks were also observed at later elution times and are not shown in Fig. 6).

Each of the elution peaks were collected and subjected to enzyme hydrolysis [42] for adduct analysis and identification. The enzyme hydrolysates were separated by HPLC using an ODS-Hypersil analytical column with a linear 0-90% methanol/buffer gradient in 60 min and a flow rate of 1.5 ml/min. The retention times of the BPDE-nucleoside adducts were compared with those of BPDE-N2-dG and BPDE-N6-dA standards prepared by the methods of Cheng *et al.* [26]. The *cis* and *trans* assignments shown in Fig. 6 were further confirmed by comparing the CD spectra (data not shown) of each of the eluates with those published by Cheng *et al.* [26]. With both enantiomers, the yield of N2-dG adducts was dominant over the yield of BPDE-dA adducts. We shall therefore focus our attention here only on the *cis* and *trans* BPDE-N2-dG adducts. With the oligonucleotide d(ATATGTATA) and (+)-BPDE, the relative yield of *trans/cis* adducts was about 7:1, whereas in the case of (-)-BPDE the *trans/cis* adduct ratio was only 2:1. Thus, in each case, *trans* addition dominates, although this effect is much less pronounced in the case of (-)-BPDE. Out of these four adducts, only the (-) *cis*-BPDE-N2-dG adduct was found to be chemically unstable upon storage in the dark.

4.2. PROPERTIES OF BPDE-OLIGONUCLEOTIDE ADDUCTS

4.2.1. *Absorption Spectra of Single-Stranded BPDE-Oligonucleotide Adducts.* The absorption spectra of the (+)-*trans*-N2-dG and (+)-*cis*-N2-dG BPDE-d(ATATGTATA) adducts are shown in Fig. 7.

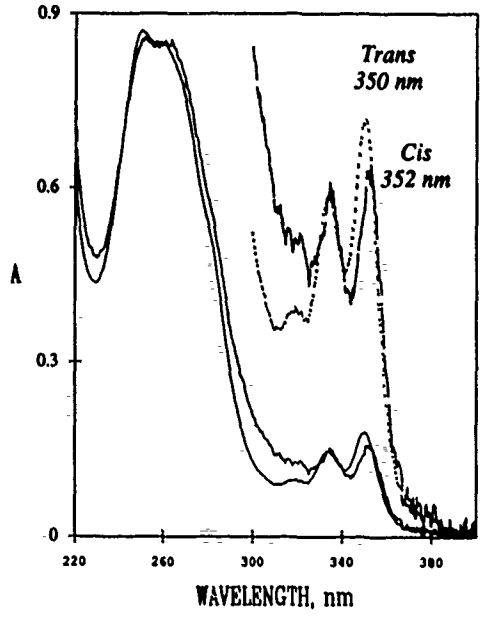


Fig. 7

The longest wavelength absorption band of the (+)-*trans* adduct displays a maximum at 350 nm, while the corresponding maximum of the *cis* adduct is at 352 nm. The (-)-*trans* and (-)-*cis* adducts display absorption maxima at 350 and 353 nm, respectively. These 6-9 nm red shifts in the absorption spectra relative to free BPDE in buffer solution suggests that there are significant base stacking interactions between the pyrenyl residues and the DNA bases. Upon heating to 80 $C^{o}$, the absorbance maxima shift from 350 - 353 nm to 346 - 348 nm, suggesting that these stacking interactions are disrupted at the higher temperatures.

4.2.2. *Changes in Absorption Spectra Upon Stoichiometric Addition of the Complementary Strands.* Upon addition of the complementary strand d(TATACATAT) to any of the four N2-dG-BPDE-d(ATATGTATA) adducts described in the above paragraph, there were no perceptible changes within the absorption band of the pyrenyl residues above 300 nm. These results suggest that this 9-mer is not capable of forming good duplexes when the single dG is modified with BPDE.

It was therefore of interest to construct a longer oligonucleotide with the same central d(..TAT..) motif, but with a few dC residues instead of dT residues in the flanking regions in order to provide extra stability upon duplex formation with the complementary strand. We selected the 11-mer d(CACATGTACAC) which, upon reaction with either (+)-BPDE or (-)-BPDE gave rise to the sets of four adducts described for the sequence d(ATATGTATA) in the above paragraphs. Interestingly, upon addition of the complementary strand d(GTGTACATGTG), the absorption maxima of the pyrenyl residues of the (+)-*trans* and (-)-*trans*-adducts blue-shifted from 350 nm to 346 nm; these absorption characteristics are reminiscent of the external Site II adducts observed when (+)-BPDE binds to native DNA, poly(dG-dC)•(dG-dC), or poly(dG)•(dC) (see above). On the other hand, when the complementary strands are added to the (+)-*cis*- and (-)-*cis*-BPDE-N2-dG adducts of the modified sequence d(CACATGTACAC), the absorption maxima remain approximately at the same positions near 352-353 nm. These results suggest that there are considerable base stacking interactions in both the single-stranded and double-stranded DNA. The absorption characteristics of these adducts are reminiscent of the Site I-type conformations observed when (-)-BPDE binds to high molecular weight DNA or polynucleotides.

4.2.3. *Melting Curves - the Destabilization of Duplex DNA by BPDE.* The unmodified 9-mer d(ATATGTATA) and 11-mer d(CACATGTACAC) in the duplex form (titrated with their respective complements) exhibit classical two-state helix coil melting curves (Figs. 8A and 8B) with $T_m$ values of 20 and 39 C, respectively, and hyperchromicities of 16 ± 1% in both cases.

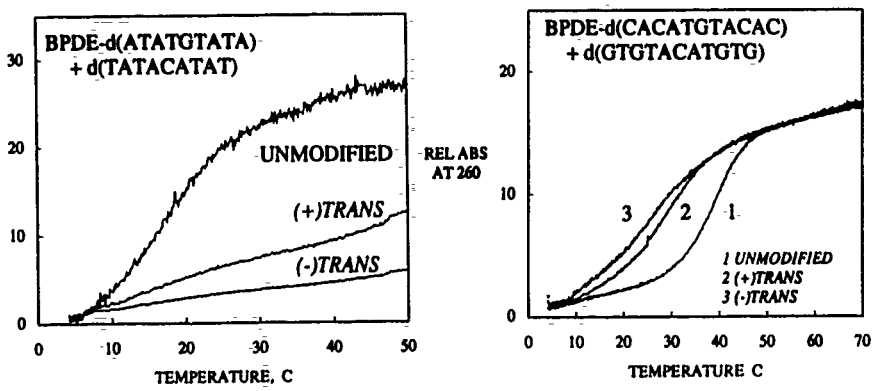


Fig. 8. Melting curves of modified oligonucleotides.

In the case of the modified 9-mer duplex, the presence of the covalently bound BPDE residues appears to disrupt base pairing and duplex formation, as is evident from the melting curves obtained with the (+)-*trans* and (-)-*trans* 9-mer adducts (Fig. 8A); neither of the *cis* adducts displayed any hyperchromicity upon heating (data not shown).

The modified (+)-*trans* and (-)-*trans*-11-mer adducts are characterized by well defined helix coil transition curves with significantly lower $T_m$ values (27 and 25 C, respectively). In the case of the (+)-*trans* 11-mer adduct, the hyperchromicity is the same as in the case of the unmodified 11-mer; however, the large decrease in the $T_m$ value suggests a significant loss in hydrogen-bonding in the covalent adduct. In the case of the (-)-*trans* 11-mer adduct, the hyperchromicity is lowered from 15% to 11% upon covalent adduct formation, suggesting a small decrease in base stacking interactions as well as a loss in base pairing. The (+)-*cis* adduct exhibited a low $T_m$ (27 C) and the hyperchromicity was 12%.

It is evident that the covalent binding of (+)-BPDE or (-)-BPDE has a tendency to destabilize duplex DNA, regardless of the *cis* or *trans* conformation of the adducts. This effect can be minimized by introducing additional dC-dG base pairs on either side of the BPDE-modified oligonucleotide residues.

## 5. Conclusions

The preparation of stereochemically defined oligonucleotides modified at specific dG residues with either (+)-BPDE or (-)-BPDE has allowed, for the first time, a comparison of the spectroscopic characteristics of *cis* and *trans* BPDE-N2-dG adducts incorporated in sequences 9-11 bases long. The spectroscopic properties of these BPDE-oligonucleotide adducts suggest that the Site I and Site II conformations observed with higher molecular weight DNA modified with (+)-BPDE and (-)-BPDE may, in part, correspond to such *cis* and *trans* adducts, respectively. The characteristics of DNA adducts derived from the covalent binding of the tumorigenic (+)-BPDE and non-tumorigenic (-)-BPDE are quite different from one another in the relative proportions of Site I and Site II adducts, and in the unwinding of supercoiled DNA. How these differences manifest themselves biologically remains to be elucidated.

## 6. ACKNOWLEDGEMENTS

This work was supported by the Department of Energy (Grants DEFG02-86ER60405 and DEFG02-88ER60674) and in part by Grant CA 20851 from the US Public Health Service, Department of Health and Human Resources, awarded by the National Cancer Institute. We wish to thank Dr. D. Patel for suggesting the sequence of the 11-mer oligonucleotide described in this work.

## 7. REFERENCES


1. Conney, A.H. (1982) 'Induction of microsomal enzymes by foreign chemicals and carcinogenesis by polycyclic aromatic hydrocarbons', G.H.A. Clowes memorial lecture, Cancer Research 42, 4875-4917.
2. Singer, B. and Grunberger, D. (1983) Molecular Biology of Mutagens and Carcinogens, Plenum Press, New York.
3. Loeb, L.A. (1989) Endogenous carcinogenesis: molecular oncology in the twenty-first century-presidential address. Cancer Res. 49, 5489-5496.
4. Yang, J.-L, Maher, V.M., and McCormick, J.J. (1987) 'Kinds of mutations formed when a shuttle vector containing adducts of (±)-7b,8a-dihydroxy-9a,10a-epoxy-7,8,9,10-tetrahydrobenzo[a] pyrene replicates in human cells, Proc. Natl. Acad. Sci. USA 84, 3787-3791.
5. Kootstra, A., Lew, L.K., Nairn, R.S., and McLeod, M.C. (1989) 'Preferential modification of GC boxes by benzo[a]pyrene-7,8-diol-9,10-epoxide', Mol. Carcinogenesis 1, 239-244.
6. Boles, T.C. and Hogan, M.E. (1984) 'Site specific carcinogen binding to DNA, Proc. Natl. Acad. Sci. USA 81, 5623-5627.
7. Reardon, D.B., Bigger, C.A.H., Strandberg, J., Yagi, H., Jerina, D.M., and A. Dipple (1989) 'Sequence selectivity in the reaction of optically active hydrocarbon dihydrodiol epoxides with rat h-*ras* DNA', Chem. Res. Toxicol. 2, 12-14.
8. Warpehoski, M.A. and Hurley, L.H. (1988) 'Sequence selectivity of DNA covalent modification', Chem. Res. Toxicol. 1, 315-333.
9. Maher, V.M., Yang, J.-L., Ma, M.C.-M. and McCormick, J. (1989) 'Comparing the frequency and spectra of mutations induced when an SV-40 based shuttle vector containing covalently bound residues of structurally related carcinogens replicates in human cells', Mutation Res. 220, 83-92.
10. MacLeod, M.C. and Zachary, K.L. (1985) 'Involvement of the exocyclic amino group of deoxyguanine in DNA-catalyzed carcinogen detoxification', Carcinogenesis 6, 147-149.
11. Chen, F.M. (1986) 'Binding of enantiomers of *trans*-7,8-dihydroxy-*anti*-9,10-epoxy-7,8,9,10-tetrahydrobenzo[a]pyrene to polynucleotides, J. Biomol. Struct. and Dynamics 4, 401-418.
12. Geacintov, N.E., Shahbaz, M., Ibanez, V., Moussaoui, K. and Harvey, R.G. (1988) 'Base-sequence dependence of noncovalent complex formation and reactivity of benzo[a]pyrene diol epoxide with polynucleotides.' Biochemistry 27, 8380-8387.
13. Kim, S.-K., Geacintov, N.E., Zinger, D., and Sutherland, J.C. (1988) 'Fluorescence spectral characteristics and fluorescence decay profiles of covalent polycyclic aromatic carcinogen-DNA adducts', in R.M. Sweet and A.D. Woodhead (eds), Synchrotron Radiation in Structural Biology, Basic Life Sciences, Vol, 51, Plenum Press, New York, pp. 187-205.

14. Miller, K.J., Taylor, E.R., and Dommen, J. (1985) A mechanism for the stereoselectivity and binding of benzo[a]pyrene diol epoxides, in R.G. Harvey (ed.) Polycyclic Hydrocarbons and Carcinogenesis, ACS Symposium Series 283, American Chemical Society, Washington, D.C., pp. 239-288
15. Zakrzewska, K. and Pullman, B. (1987) 'Sequence selectivity, a test of the nature of the covalent adduct formed between benzo[a]pyrene and DNA', J. Biomol. Struct. Dynamics 4, 845-858.
16. Brookes, P. and Osborne, M.R. (1982) Mutation in mammalian cells by stereoisomers of *anti*-benzo[a]pyrene diol epoxide in relation to the extent and nature of the DNA reaction products', Carcinogenesis 3, 1223-1226.
17. Stevens, C.W., Bouck, N., Burgess, J.A., and Fahl, W.E. (1985) Benzo[a]pyrene diol-epoxides: differential mutagenic efficiency in human and bacterial cells', Mutation Res. 152, 5-14.
18. Geacintov, N.E. (1988) 'Mechanisms of reaction of polycyclic aromatic epoxide derivatives with nucleic acids', in S.K. Yang and B.D. Silverman (eds.) Polycyclic Aromatic Hydrocarbon Carcinogenesis: Structure Activity Relationships, CRC Press, Boca Raton, FL, Vol. 2, pp. 181-206.
19. Harvey, R.G. and Geacintov, N.E. (1988) 'Intercalation and binding of carcinogenic hydrocarbon metabolites to nucleic acids', Accts. Chem. Res. 21, 66-73.
20. Gräslund, A. and Jernström, B. (1989) 'DNA-carcinogen interaction: covalent DNA-adducts of benzo[a]pyrene 7,8-dihydrodiol 9,10-epoxides studied by biochemical and biophysical techniques', Quart. Rev. Biophys. 22, 1-37.
21. Geacintov, N.E., Yoshida, H., Ibanez, V., and Harvey, R.G. (1981) Non-covalent intercalative binding of 7,8-dihydroxy-9,10-epoxy-benzo[a]pyrene to DNA, Biochem. Biophys. Res. Comm. 100, 1569-1577.
22. Meehan, T., Gamper, H. and Becker, J.F. (1982) 'Characterization of reversible physical binding of benzo[a]pyrene derivatives to DNA', J. Biol. Chem. 257, 10479-10485.
23. Roche, C.J. Geacintov, N.E., Ibanez, V., and Harvey, R.G. (1989) 'Linear dichroism properties and orientations of different ultraviolet transition moments of benzo[a]pyrene derivatives bound noncovalently and covalently to DNA', Biophys. Chem. 33, 277-288.
24. MacLeod, M.C. and Zachary, K. (1985) 'Catalysis of carcinogen-detoxification by DNA: comparison of enantiomeric diol epoxides', Chem. Biol. Interactions 54, 45-55.
25. Geacintov, N.E., Yoshida, H., Ibanez, V., Jacobs, S.A. and Harvey, R.G. (1984) Conformations of adducts and kinetics of binding to DNA of the optically pure enantiomers of anti-benzo[a]pyrene diol epoxide', Biochem. Biophys. Res. Comm. 122, 33-39.
26. Cheng, S.C., Hilton, B.D., Roman, J.M. and Dipple, A. (1989) 'DNA adducts from carcinogenic and noncarcinogenic enantiomers of benzo[a]pyrene dihydrodiol epoxide', Chem. Res. Toxicol. 2, 324-340.

27. Geacintov, N.E. (1986) 'Is intercalation a critical factor in the covalent binding of mutagenic and tumorigenic polycyclic aromatic diol epoxides to DNA? Carcinogenesis 7, 759-766.
28. Roche, C.J. (1987) The Physical and Covalent Interactions of Polycyclic Aromatic Hydrocarbon Epoxide Derivatives with Nucleic Acids. Ph.D. Dissertation, New York University.
29. LeBreton, P.R. (1985) 'The intercalation of benzo[a]pyrene and 7,12-dimethyl-benz[a]anthracene metabolites and metabolite model compounds in DNA', in R.G. Harvey (ed.) Polycyclic Hydrocarbons and Carcinogenesis, ACS Symposium Series 283, American Chemical Society, Washington, D.C., pp.64-84.
30. Kolubayev, V., Brenner, H.C., and Geacintov, N.E. (1987) Stereoselective covalent binding of enantiomers of *anti*-benzo[a]pyrene diol epoxide to DNA as probed by optical detection of magnetic resonance', Biochemistry 26, 2638-2641.
31. Kim, S.-K., Brenner, H.C., Soh, B.J., and Geacintov, N.E. (1989) 'Fluorescence spectroscopy of benzo[a]pyrene diol epoxide-DNA adducts. Conformation-specific emission spectra', Photochem. Photobiol. 50, 327-337.
32. Zinger, D., Geacintov, N.E., and Harvey, R.G. (1987) Conformations and selective photodissociation of heterogeneous benzo[a]pyrene diol epoxide enantiomer-DNA adducts', Biophys. Chem. 27, 131-138.
33. Carberry, S.E., Geacintov, N.E., and R.G. Harvey (1989) 'Reactions of stereoisomeric non-bay-region benz[a]anthracene diol epoxides with DNA and conformations of non-covalent complexes and covalent adducts', Carcinogenesis 10, 97-103.
34. Bigger, C.A.H., Strandberg, J., Yagi, H., Jerina, D.M. and Dipple, A. (1989) 'Mutagenic specificity of a potent carcinogen, benzo[c]phenanthrene (4*R*,3*S*)-dihydrodiol (2*S*,1*R*)-epoxide, which reacts with adenine and guanine in DNA', Proc. Natl. Acad. Sci. USA 86, 2291-2295.
35. Drinkwater, N.R., Miller, J.A., Miller, E.C., and N.-C. Yang (1978) Covalent intercalative binding to DNA in relation to the mutagenicity of hydrocarbon epoxides and N-acetone-2-acetylamine fluorene', Cancer Res. 38, 3247-3255.
36. Gamper, H.B., Straub, K., Calvin, M., and Bartholomew, J.C. (1980) DNA alkylation and unwinding induced by benzo[a]pyrene diol epoxide: Modulation by ionic strength and superhelicity', Proc. Natl. Acad. Sci. USA 77, 2000-2004.
37. Yoshida, H. and Swenberg, C.E. (1987) 'Kinetic flow dichroism study of conformational changes in supercoiled DNA induced by ethidium bromide and noncovalent and covalent binding of benzo[a]pyrene diol epoxide', Biochemistry 26, 1351-1358.
38. Scovell, W.M. and Collert, F. (1985) Unwinding of supercoiled DNA by *cis*- and *trans*-diamminedichloroplatinum(II): influence of the torsional strain on DNA unwinding', Nucl. Acids Res. 13, 2881-2895.
39. Bauer, W.R. (1978) 'Structures and reaction of closed duplex DNA' Ann. Rev. Biophys. Bioeng. 7, 287-313.

40. Hogan, M.E., Dattagupta, N., and Whitlock, J.P. Jr. (1981) 'Carcinogen-induced alteration of DNA structure', J. Biol. Chem. 256, 4504-4513.
41. Eriksson, M., Nordén, B., Jernström, B., and Gräslund, A. (1988) 'Binding geometries of benzo[a]pyrene diol epoxide isomers covalently bound to DNA. Orientational distribution', Biochemistry 27, 1213-1221.
42. Cosman, M., Ibanez, V., Geacintov, N.E. and Harvey, R.G. (1990) 'Preparation and isolation of adducts in high yield derived from the binding of two benzo[a]pyrene-7,8-dihydroxy-9,10-oxide stereoisomers to the oligonucleotide d(ATATGTATA)'. Submitted for publication.
43. McLaughlin, L.W. and Piel, N. (1984) 'Chromatographic purification of synthetic oligonucleotides', in M.J. Gait (ed.), Oligonucleotide Synthesis: A Practical Approach, IRL Press, Oxford, pp. 117-133.

Reprinted from THE JOURNAL OF BURN CARE & REHABILITATION, St. Louis
Vol. 10, No. 5, pp. 410-417, Sept./Oct., 1989, (Printed in the U.S.A.)




# Bone Marrow Myelopoiesis in Rats After 10%, 20%, or 30% Thermal Injury

Dale F. Gruber, PhD, and Ann M. Farese, MA
*Bethesda, Maryland*

**The high incidence of serious opportunistic infections that follow thermal injuries is well documented. Normal levels of functioning leukocytes are essential to the host's ability to resist infection. This study examined alterations in murine granulopoiesis after the inducement of a standardized, sublethal, third-degree burn covering 10%, 20%, or 30% of the dorsal body surface area. Significant alterations arose in peripheral leukocyte concentrations after inducement of uncomplicated thermal injury. In general, within the first day of injury, all three trauma levels produced a peripheral leukocytosis that lasted for 35 days or more. The leukocytoses that followed 20% and 30% injuries were similar and in numerous respects paralleled previously reported human peripheral responses after similar levels of thermal trauma. Differential examinations of peripheral blood demonstrated the peripheral leukocytosis to be due primarily to the influx of morphologically mature-appearing polymorphonuclear neutrophils. Premature bone marrow release did not appear to be a factor as immature polymorphonuclear neutrophils were seldom greater than 2% of polymorphonuclear neutrophil totals. Bone marrow granulopoietic activity was examined by in vitro clonal cell culture techniques and assessed over a period of 35 days after injury. Granulocyte-macrophage colony forming cells (GM-CFC), indicative of marrow progenitor cell concentrations, were significantly increased for 28 to 35 days after 10% injury and 11 to 14 days after 20% or 30% injury. Normal or increased progenitor cell concentrations and a lack of morphologically appearing premature forms suggest that the leukocytosis is the result of injury-induced alteration(s) in polymorphonuclear neutrophil margination or release mechanisms. The rat model and its human thermal-injury parallel may be valuable in the assessment of quantitative and qualitative myelopoietic lesions after the inducement of standardized levels of thermal trauma or the initiation of therapy. (J BURN CARE REHABIL 1989;10:410-17)**

Burn injury is the second most common cause of accidental death in the United States.[1] Because of this ignominious distinction, considerable efforts over the past 30 years have been dedicated to the pathophysiologic exploration of thermal injury. The application of acquired knowledge has resulted in a steady increase in survival rates. Despite the development of new topical and systemic antibiotics and therapeutic interventions,[2-3] patients with thermal injuries remain predisposed to infection. Systemic sepsis arising from invasive bacteria remains the primary cause of death in patients hospitalized for thermal injuries.[4] Patients with burns exhibit profoundly altered resistance capabilities.[5] Once dermal integrity,[6-7] the first line of resistance, is compromised, wound areas become substrates for microbial colonization. Once a locus of infection becomes established the containment, repair, and resolution of the infection or injury is largely dependent on the presence of properly functioning inflammatory cells. The host's primary circulating inflammatory cell is the polymorphonuclear neutrophil (PMN). Although responsible for first-line nonspecific resistance, PMNs possess short biological half-lives which

*From the Department of Experimental Hematology, Armed Forces Radiobiology Research Institute, Defense Nuclear Agency.*
*Supported by Armed Forces Radiobiology Research Institute, Defense Nuclear Agency, under work unit 00130.*
*Views presented in this article are those of the authors, no endorsement by the Defense Nuclear Agency has been given or should be inferred.*
*Research was conducted according to the principles enunciated in the "Guide for the Care and Use of Laboratory Animals" prepared by the Institute of Laboratory Animal Resources, National Research Council.*
*Reprint requests: Dale F. Gruber, PhD, Department of Experimental Hematology, AFRRI, Wisconsin Ave., Bethesda, MD 20814-5145.*
*30/1/13951*

necessitate continuous replenishment by bone—marrow—resident progenitor cells, termed granulocyte-macrophage colony-forming cells (GM-CFC). Granulocyte-macrophage colony-forming cells' responses to trauma and/or to infection are vital to the overall level of host resistance. Patients who have died as a result of burn wounds were unable to increase GM-CFC concentrations in reponse to infection. This suggests that bone marrow failure may be a major contributing factor in the development of fatal infections.[8] Despite reports that suggest bone marrow dysfunction after trauma,[8-10] there is relatively little information on GM-CFC regulation after increases in burn injury. Trauma-induced alterations in bone marrow progenitor cell concentrations could affect the formation of PMNs during critical periods after trauma. Polymorphonuclear neutrophil production and differentiation in the bone marrow normally takes between 11 and 14 days.[13,14] Alteration of PMN production times, mechanisms of release, diminution of numbers, or functional alterations may contribute to increased incidence of infection that may arise 2 to 3 weeks after injury. The obvious importance of bone marrow in both clinical evaluations and inflammation responses prompted our examination of murine marrow GM-CFC capabilities after the inducement of 10%, 20%, or 30% body surface area (BSA) thermal injury.

## MATERIALS AND METHODS

### Animals

Male Cr:CDBR rats *(Rattus norvegicus)* obtained commercially (Charles River Breeding Laboratory, Wilmington, Mass.) were quarantined on arrival and screened for evidence of disease before being released to experiments. Animals were maintained in a facility accredited by the American Association for Accreditation of Laboratory Animal Care, in plastic microisolator cages with hardwood chip bedding, and they were provided with commercial rodent chow and acidified water (pH 2.5) ad libitum. Animal holding rooms were maintained at 70° ± 2° F with 50% ± 10% relative humidity with at least 10 air changes per hour of 100% conditioned fresh air. Animals were on a 12-hour light/dark full-spectrum photoperiod with no twilight. Most experiments were conducted on animals 10 to 12 weeks old with weights of 300 to 350 gm.

### Thermal Injury

Animals were anesthetized with Nembutal (pentobarbital sodium) 50 mg/ml, 0.1 ml/10 gm body weight, intraperitoneally. The rats' dorsal epidermis was shaved, hair remover (Nair, Carter Products, New York, N.Y.) was applied for 7 minutes, after which the excess depilating agent was washed off with tepid water. Rats were placed in plastic templates with openings that corresponded to 10%, 20%, or 30% of the total body surface area (TBSA) as calculated by Meeh's formula.[13] Thermal scald injuries were induced in a manner similar to that reported by Walker and Mason.[14] The templates and depilated dorsi of the rats were immersed in 96° C water for 10 seconds. The depth of injuries was determined by histologic cross-section examinations of skin biopsy specimens fixed in 10% buffered formalin and stained with hematoxylin and eosin. Histologic results verified that the burn injuries were of full thickness over the entire exposed areas. Immediately after thermal trauma, rats received 5 ml sterile lactated Ringer's solution (Baxter-Travenol Laboratories, Deerfield, Ill.) intraperitoneally.

### Granulocyte-Macrophage Colony-Forming Cell (GM-CFC) Assay

Committed granulocyte-macrophage hematopoietic progenitor cells were assayed by a modification of the semisolid agar technique described by Bradley and Metcalf[15] and by Pluznik and Sachs.[16] The upper agar medium mixture for cell suspensions consisted of equal volumes of 0.66% agar (Bacto-agar, Difco, Detroit, Mich.) and double-strength CMRL medium 1066 (10X, GIBCO, Grand Island, N.Y.) supplemented with 10% heat-inactivated (56° C, 30 minutes) fetal bovine serum (FBS, Hyclone Labs, Logan, Utah), 5% tryptic soy broth (Difco), 5% heat-inactivated (56° C, 30 minutes) horse serum (Hyclone), 2% sodium pyruvate (100X, GIBCO), 1% penicillin/streptomycin (GIBCO), 0.06% wt/vol L-asparagine, 0.06% wt/vol L-serine (Calbiochem, LaJolla, Calif), and 0.44% wt/vol sodium bicarbonate (Fisher Scientific, Silver Spring, Md). The lower agar medium feeder layer consisted of equal volumes of 1% agar and supplemented CMRL. Endotoxin-stimulated sera, the source of the colony-stimulating factor (5% vol/vol) were added to the lower feeder layer. Colonies (greater than 50 cells) were quantitated after 10 days' incubation at 37° C in a humidified environment with 7.5% carbon monoxide and air.

### White Blood Cell Differentials

Slides for differential examination were prepared by the slide push method, air-dried, and stained with Wright Giemsa stain (American Scientific Products, McGaw Park, Ill.). Differential counts were per-

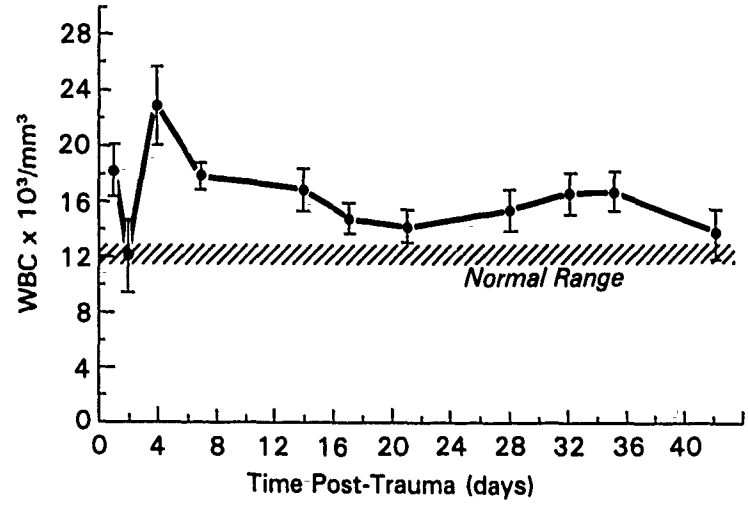


**Figure 1.** Leukocyte composition of heparinized peripheral blood samples after 10% BSA thermal injury. Results are expressed in white blood cells × $10^3/mm^3$ subsequent to the administration of a 10% dorsal scald injury. Each data point represents the mean ± SEM of a minimum of six individual samples. Normal is 11.86 ± 0.4.

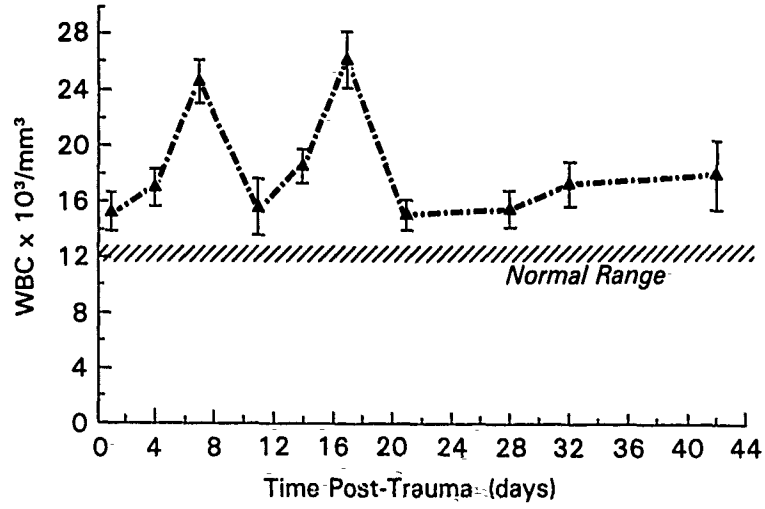


**Figure 2.** Leukocyte composition of heparinized peripheral blood samples after 20% BSA thermal injury. Results are expressed in white blood cells × $10^3/mm^3$ subsequent to the administration of a 20% dorsal scald injury. Each data point represents the mean ± SEM of a minimum of six individual samples. Normal is 11.86 ± 0.4.

formed under oil immersion (100×). One hundred white blood cells were counted and each cell type was reported as a percentage.

### Statistical Analysis

All data are presented as mean ± standard deviation. Statistical differences were determined with the Student *t* test. *P* values less than 0.05 were considered statistically significant.

## RESULTS

Animals with burns to 10% BSA demonstrated peripheral leukocytosis on day 1 after injury (Figure 1). Leukocyte levels returned to normal on day 2 and increased significantly on Day 4 to levels greater than 90% above baseline. On day 7, leukocyte concentrations retreated to levels 50% above normal and for the remaining 35 days of the examination period

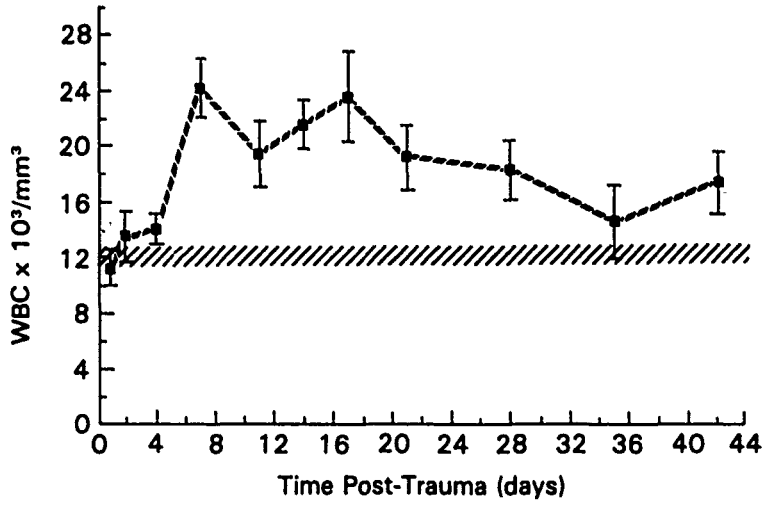


**Figure 3.** Leukocyte composition of heparinized peripheral blood samples after 30% BSA thermal injury. Results are expressed in white blood cells × $10^3/mm^3$ subsequent to the administration of a 30% dorsal scald injury. Each data point represents the mean ± SEM of a minimum of six individual samples. Normal is 11.86 ± 0.4.

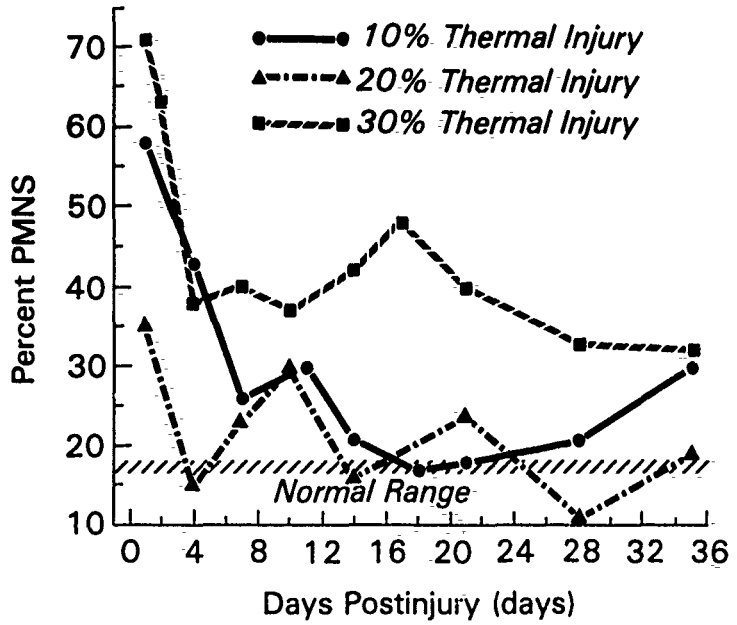


**Figure 4.** Differential analysis of peripheral blood smears. Results are expressed as percentage of granulocytes subsequent to the 10%, 20%, or 30% dorsal scald injury. Each data point represents the mean ± SEM of a minimum of six individual samples. Normal is 17.3 ± 0.7.

were 14% to 40% above normal. Animals with 20% and 30% BSA burns demonstrated a temporal peripheral leukocytosis (Figures 2 and 3) similar to that reported for human patients with burns.[17] An initial leukocytosis phase was followed by a moderate reduction around day 11 and a second elevation to levels almost 100% above normal on day 17. After day 17 the leukocytosis levels began decreasing but were still evident (22% to 60% above normal) 42 days after injury. Differential analysis showed PMNs to be the principal cellular components responsible (Figure 4). Immature cells (metas, myelocytes,

**Table 1.** Progenitor cell (GM-CFC) concentration of rat femoral marrow subsequent to 10%, 20%, or 30% dorsal scald injury

| | Days after burn | | | | | |
|---|---|---|---|---|---|---|
| **Burn** | **1** | **2** | **4** | **7** | **8** | **11** |
| 10% | −21% | 39% | | 107% | 179% | 103% |
| | NS | $p < 0.01$ | | $p < 0.001$ | $p < 0.001$ | $p < 0.001$ |
| 20% | 159% | 47% | 46% | 31% | | −14% |
| | $p < 0.001$ | $p = 0.006$ | $p = 0.003$ | $p = 0.05$ | | NS |
| 30% | 102% | 106% | 73% | 86% | | 44% |
| | $p < 0.001$ | $p < 0.001$ | $p < 0.001$ | $p < 0.001$ | | $p = 0.01$ |

Results are expressed as percent of increase or decrease (−) compared with normal baseline concentrations of 29 ± 2 GM-CFC/$10^5$ cultured cells. *p* Values were determined by the Student *t* test.

blasts) constituted less than 2% of the total PMNs counted. Thermal injuries to 10% and 20% BSAs caused increases (27% to 50%) in leukocyte levels 1 day after injury. After 30% BSA injury, leukocyte levels were slightly lower (−6%) than normal. Leukocyte levels were increased significantly 4 days after injury: 10% injury by 90%, 20% by 41%, and 30% by 17%. By day 7, leukocyte levels after 20% and 30% injuries had increased to levels that were greater than 100% above normal.

## GM-CFC after 10% thermal injury

Bone marrow from normal rats produced 29 ± 2 GM-CFCs/$10^5$ bone marrow cells cultured. One day after 10% injury, GM-CFCs decreased by 21% (Table 1) but rebounded on day 2 to 39% above normal ($p < 0.01$). Granulocyte-macrophage colony-forming cell concentrations continued to increase and on day 8 reached experimental maximums, 179% above normal ($p < 0.001$), 8 days after injury. After day 8 GM-CFC levels began to decrease gradually and reached normal 35 days after injury.

## GM-CFC after 20% thermal injury

One day after 20% BSA thermal injury GM-CFC levels were 159% ($p < 0.001$) above normal (Table 1). On days 2 and 4 GM-CFC decreased to levels that were 47% ($p = 0.006$) and 46% ($p = 0.003$) above normal, respectively. Granulocyte-macrophage colony-forming cell levels were 31% ($p = 0.05$) above normal on day 7 before returning to essentially normal levels on Days 11 to 42.

## GM-CFC after 30% thermal injury

One day after injury, GM-CFC levels were 102% ($p < 0.001$) of normal (Table 1). GM-CFCs increased to maximal levels on Day 3, 161% ($p < 0.001$) of normal. Four days after injury GM-CFC levels began decreasing and by Day 14 (interrupted only by a second increase [73% above normal, $p < 0.001$] on Day 21) had returned to near normal levels.

## Absolute Granulocytes

In 10% thermal injuries absolute granulocyte numbers increased greater than threefold on day 1 before decreasing on a nadir of 0.5-fold above normal on day 17. Absolute granulocytes began increasing after day 17 and were greater than one fold above normal 35 days after injury.

In 20% thermal injuries the pattern of absolute granulocytes was similar but of less magnitude than that after 30% injury. Absolute granulocytes after 20% injuries never increased above 1.5-fold. Previous investigators have suggested that the fluctuations may be a result of margination of cellular reserves or the production of cell-specific inhibitory factors.[18]

Absolute granulocyte numbers (Figure 5) were greatest after 30% BSA injury. Absolute numbers were above normal for 35 days and demonstrated significant increases on days 1 (less than threefold), 7 (greater than threefold), and 17 (greater than fourfold). After day 17 absolute granulocyte numbers began decreasing but were still 1.5-fold above normal 35 days after injury.

## Blood Differentials

Morphologic examinations demonstrated that the PMN population comprised neutrophils almost exclusively, with no significant increases in eosinophils or basophils. Mean PMN percentage from peripheral blood differentials of normal rats was 17.3% ± 0.7%. Experimental injuries caused peripheral neutrophilia (Figure 4) within 1 day of application. Ten percent injury caused more than a twofold increase, 20% more than a onefold increase, and

| Days after burn | | | | | |
|---|---|---|---|---|---|
| 14 | 17 | 21 | 28 | 35 | 42 |
| 93% | 63% | 54% | 32% | 7% | 19% |
| $p < 0.001$ | $p < 0.001$ | $p < 0.001$ | $p = 0.05$ | NS | NS |
| 25% | −10% | 24% | −7% | −28% | 5% |
| NS | NS | NS | NS | NS | NS |
| 24% | 21% | 73% | 2% | −4% | |
| NS | NS | $p < 0.001$ | NS | NS | |

30% more than a threefold increase. After day 1 PMN percentages began decreasing for all three types of burn injuries. In general, 10% and 20% injuries resembled each other between days 7 and 21. Neutrophilia was most evident after the inducement of 30% BSA injury, threefold above normal on day 1, onefold on day 7, and onefold to twofold above normal through 35 days.

## DISCUSSION

This report examines granulopoietic precursor cell concentrations in a rat thermal injury model after 10%, 20%, or 30% BSA thermal injury. Experimental injuries resulted in significant alterations in circulating neutrophil and marrow progenitor cell (GM-CFC) concentrations. Normal PMN circulating concentrations are, in large measure, dependent upon normal levels and function of myeloid precursor cells as well as normal release mechanisms. In the physiologic steady state, the rate of granulopoiesis equals the rates of utilization and destruction. Any alterations in the steady state rates could produce significant alterations in peripheral leukocyte concentrations. After burn trauma, humans[8] and mice[17] demonstrate depressed stem cell levels. Depending on the extent of injury, the initial reduction period could be hours to days, after which the marrow often becomes hyperactive. Results following 10%, 20%, and 30% experimental burn injuries in this report corroborate previous reports of marrow hyperactivity. Bone marrow samples from mice[17] demonstrate increased tritiated thymidine uptake largely paralelling increases we report in rat GM-CFC concentrations after 10% thermal injury. Likewise, GM-CFC concentrations after 20% and 30% thermal injuries were also significantly increased and comparable to autoradiograms that have suggested increased uptake patterns 24 to 48 hours after injury.[17]

The process of granulopoiesis is highly dynamic because of the nature of PMN effector functions in combination with their short biologic half-life. Normal human beings for example, are reported to produce up to $1.6 \times 10^9$ PMN/kg/day.[8] Production dynamics[11] and biologic half-life combine to make the immediate period after burn critically important to recovery. Investigators report increased susceptibility of thermally injured mice to infection with *Pseudomonas aeruginosa*.[18] Within 2 minutes of injury, there were sixfold reductions in the number of organisms necessary to induce a $LD_{50}$.

Burn injury reports have described both leukopenia and leukocytosis after burn injury.[1,7,19,21] The peripheral leukocytosis has been reported to be proportional to burn size,[22] and it has been suggested that it is due to marginating PMNs and fluid volume shifts.[23] Elevated PMN levels occur despite quantitative reductions in marrow cellularity[20,21] and activity.[21] Through the margination process, the host transiently alters concentrations of peripheral blood elements. Masked by the phenomenon of demargination, long-term GM-CFC depressions could place the host at risk. Estimates of turnover times of the mature PMN storage pool in human beings is 5 days, and accelerated outflow rates of postmitotic PMNs could deplete marrow reserves within 2 to 3 days.[19] Investigators have suggested that human beings are most susceptible to infection on days 3 to 7 after burn.[5] In addition to GM-CFC suppression and depletion of marrow reserves, there have been reports of trauma-induced replacement PMNs lacking the qualitative functional capabilities exhibited by normal circulating PMNs.[24] The peripheral leukocytosis phenomenon, although different in some quantitative and temporal respects, has been reported in mice,[10,17] rats,[20,25] canines,[23] and human beings[19,26] after burn injury. The rat has long served as a model of thermal injury.[14] McCarthy and Odell[27] investi-

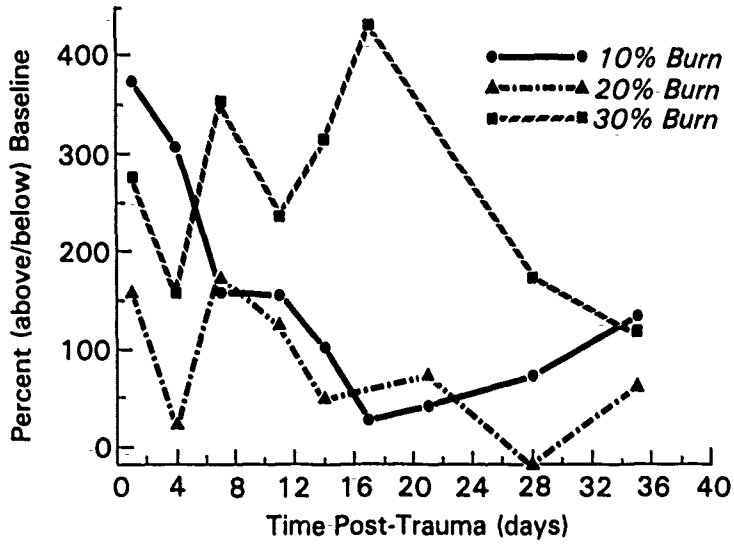


**Figure 5.** Changes in absolute numbers (number of white blood cells × differential percentage) of granulocytes after 10%, 20%, or 30% thermal injuries. Results are expressed as percent of change over baseline (12 × 17.3) for six to ten experimental measures per data point.

gated rat lekuocyte levels after 20% or 50% thermal injuries and reported long-term decreases. In contrast to their findings, other investigators have reported a peripheral leukocytosis following 30% or 60% thermal injuries.[20,25] Our observations on 20% thermal injury concur qualitatively and temporally with the previous observations of Eurenius and Brouse.[20] After 20% or 30% injury, experimental animals had bimodal leukocytosis patterns similar to those previously reported.[20,25] Early leukocytosis has been reported as being due to the shifting of PMNs from marginal pools into the peripheral circulation;[20,28] whereas it has been suggested that the secondary leukocytosis, 5 to 10 days later, is a response to wound-induced inflammatory changes.[26] Bimodal response patterns, as reported here, may reflect the interaction of multiple regulatory mechanisms. Serum factors, such as leukocytosis inducing factor, or complement products, among others, cause demargination[29-30] which increases peripheral leukocyte concentrations. Increased peripheral leukocyte concentrations may then be reduced by burn toxins,[31] serum inhibitors, cell-line-specific regulatory factors (chalones),[32] or precipitated plasma proteins. Complement or complement fractions may act dualistically, mobilizing marrow reserves while also acting as chemotaxins[33-34] promoting rapid egress of circulating PMNs to inflammation sites and decreasing peripheral levels.

Peripheral neutrophil concentrations, although clinically useful, are not indicative of marrow progenitor cell status after injury.[8,17] Reductions in tritiated thymidine uptake, reflecting reductions in DNA synthesis, have been reported in mouse bone marrow within hours of 17% to 25% thermal injury.[17] Radioisotopic techniques are, however, somewhat indiscriminate in that all cells in the process of division are labeled. A more accurate assessment of bone marrow granulocyte-macrophage proliferative potential may be the in vitro soft-agar clonogenic assay. Our findings after 30% thermal injury to rats concurred in large measure with those reported by McEuen et al.,[9] who used a methylcellulose support system to examine GM-CFC levels and reported significantly increased GM-CFC concentrations for a period of 7 days after injury. Circulating stem cells have also been examined in the peripheral blood of surviving and deceased subjects with burns.[8] Stem cells in survivors were increased and elevated above normal levels, whereas stem cell numbers in deceased subjects were significantly decreased by day 15.

Mechanisms of granulopoietic regulation after trauma will require extensive investigation because of the many factors that have direct or indirect regulatory effects. The experimental models examined in this report do not appear to demonstrate decreased progenitor cell concentrations subsequent to 10%, 20%, and 30% thermal injuries. Progenitor cell concentrations (GM-CFC) were significantly increased in the marrow for 1 to 4 weeks after injury. Neutrophil concentrations in the peripheral blood were in-

creased for 6 weeks after trauma. On the basis of quantitative assessments of bone marrow and peripheral blood samples from these models, there does not appear to be trauma-induced inhibition of either production or margination. Nevertheless, clinical infections remain even in light of quantitative PMN increases. Consideration must be given to lesions in other cellular qualitative functions. Further information on the qualitative functions of leukocytes is critical to the proper understanding and management of infectious sequelae after trauma.

We greatly appreciate Dr. T. J. MacVittie's scientific input and critique of this manuscript. We also gratefully acknowledge the technical assistance of T. A. Davis and K. P. O'Halloran.

## REFERENCES

1. Artz CP. Epidemiology, causes and prognosis. In: Artz CP, Moncrief JA, Pruitt BA Jr, eds. Burns, a team approach. Philadelphia: WB Saunders, 1979:17-22.
2. Alexander JW, Meakins JL. A physiological basis for the development of opportunistic infections in man. Ann Surg 1972;176:273-87.
3. Allgower M, Durig M, Wolff G. Infection and trauma. Surg Clin North Am 1980;60:133-44.
4. Burke JF, Quinby WC, Bondoc CC, et al. Immunosuppression and temporary skin transplantation in the treatment of massive third-degree burns. Ann Surg1975;182:183-97.
5. Artz CP. Burn infections. South Med J 1963;56:1071-4.
6. Moncrief JA: Burns. N Engl J Med 1973;288:444-54.
7. Lindberg RB, Curreri PW, Pruitt BA Jr. IV carbenicillin for burn sepsis. J Infect Dis 1970;122:34-43.
8. Peterson VM, Robinson WA, Wallner SF, et al. Granulocyte stem cells are decreased in humans with fatal burns. J Trauma 1985;25:413-8.
9. McEuen DD, Ogawa M, Eurenius K. Myelopoiesis in the infected burn. J Lab Clin Med 1977;89:540-3.
10. Gamelli RL, Hebert JC, Foster RS Jr. Effect of burn injury on granulocyte and macrophage production. J Trauma 1985;25:615-9.
11. Cartwright GE, Athens JW, Wintrobe MM. The kinetics of granulopoiesis in normal man. Blood 1964;24:780-803.
12. Spitznagel JK. Microbial interactions with neutrophils. Rev Infect Dis 1983;5:806-22.
13. Quiring DP. Surface-area determination. In: Glasser O, ed. Medical Physics. Chicago: Year Book, 1944:1491-3.
14. Walker HL, Mason AD Jr. A standard animal burn. J Trauma 1968;8:1049-51.
15. Bradley TR, Metcalf D. The growth of mouse bone marrow cells *in vitro*. Aust J Exp Med Sci 1966;448:287-300.
16. Pluznik DH, Sachs L. The cloning of normal mast cells in tissue culture. J Cell Physiol 1965;66:219-324.
17. Asko-Seljavaara S. Granulocyte kinetics in burned mice. Scand J Plast Reconstr Surg 1974;8:185-91.
18. McRipley RJ, Garrison DW. Increased susceptibility of burned rats to *Pseudomonas aeruginosa*. Proc Soc Exp Biol Med 1963;115:336-8.
19. McIver MA. A study in extensive cutaneous burns. Ann Surg 1933;97:670-82.
20. Eurenius K, Brouse RO. Granulocyte kinetics after thermal injury. Am J Clin Pathol 1973;60:337-42.
21. Asko-Seljavaara S. Inhibition of bone marrow cell proliferation in burned mice: an *in vitro* study of the effect of fluid replacement and burn serum on bone marrow cell growth. Scand J Plast Reconstr Surg 1974;8:192-7.
22. Wolach B, Coates TD, Hugli TE, et al. Plasma lactoferrin reflects granulocyte activation via complement in burn patients. J Lab Clin Med 1984;103:284-93.
23. Alexander JW, Wixon D. Neutrophil dysfunction and sepsis in burn injury. Surg Gynecol Obstet 1970;130:431-8.
24. McManus AT. Examination of neutrophil function in a rat model of decreased host resistance following burn trauma. Rev Infect Dis 1983;5:898-907.
25. Heideman M. The effect of thermal injury on hemodynamic, respiratory, and hematologic variables in relation to complement activation. J Trauma 1979;19:239-43.
26. Sevitt S. Burns: pathology and therapeutic applications. London: Butterworth, 1957:220-8.
27. McCarthy MD, Odell J. Myelograms relating to anemia and hematopoiesis following thermal injury in rats. Proc Soc Exp Biol Med 1957;94:489-93.
28. Craddock CG. Production, distribution and fate of granulocytes. In: Williams JH, Beutler E, Erslev AJ, Rundles RW, eds. Hematology. New York: McGraw-Hill, 1972:607-18.
29. Marsh JC, Levitt M. Neutrophilia-inducing activity in the plasma of neutropenic human beings. Blood 1971;37:647-56.
30. Gordon AS, Neri RO, Siegel CD, et al. Evidence for a circulating leukocytosis-inducing factor (LIF). Acta Haematol 1960;23:323-41.
31. Kremer B, Allgower M, Scholmerich J, et al. Burn toxin. In: Ninnemann JL, ed. The immune consequences of thermal injury. Baltimore: Williams and Wilkins, 1981:90-118.
32. Rytomaa T. Role of chalone in granulopoiesis. Br J Haematol 1973;24:141-5.
33. Oliveira B, Osler AG, Siraganian RP, et al. The biologic activities of guinea pig antibodies. I. Separation of gamma1 and gamma2 immunoglobulins and their participation in allergic reactions of the immediate type. J Immunol 1970; 104:320-8.
34. Sandberg AL, Osler AG, Shin HS, et al. The biologic activities of guinea pig antibodies. II. Modes of complement interaction with gamma1 and gamma2 immunoglobulins. J Immunol 1970;104:329-34.

IMMUNOPHARMACOLOGY AND IMMUNOTOXICOLOGY, 11(2&3), 151-163 (1989)

# AMINOPHYLLINE INDUCED OXIDATIVE METABOLISM IN ISOLATED CANINE POLYMORPHONUCLEAR LEUKOCYTES

Dale F. Gruber*, Kevin P. O'Halloran and
Ann M. Farese
Armed Forces Radiobiology Research Institute
Bethesda, Maryland 20814-5145

## ABSTRACT

Adenosine reportedly mediates myocardial and skeletal blood flow, bronchoconstriction, and cellular production of toxic oxygen radicals. Cellular effects of adenosine can be antagonized by the methylxanthines, which are widely used in the clinical treatment of obstructive airway diseases. Methylxanthine compounds such as aminophylline and theophylline inhibit the cyclic nucleotide phosphodiesterase of smooth muscle, reversing pathogenic states of bronchoconstriction. Recent techniques in flow cytometry allow examination of individual cells for the electrophysiological and metabolic cellular side effects of methylxanthine therapy. We report that the flow cytometric examination of isolated canine peripheral neutrophils, in the presence of therapeutic concentrations of aminophylline resulted in small but significant membrane depolarization and almost fivefold increases in baseline cytosolic H2O2 levels. If aminophylline is capable of direct *in vitro* activation of isolated canine neutrophils it may have the capacity to potentiate neutrophil activation *in vivo*: indirectly by competing with circulating modifiers, such as adenosine, for cell surface receptor sites and directly by the induction of toxic oxygen radicals as demonstrated here. H2O2 induction by aminophylline and other xanthine derivatives may become clinically important in instances of vascular occlusion, stasis, or instances of reperfusion where neutrophils may become activated. In an activated state, neutrophils could contribute to pathogenecity and tissue damage by indiscriminantly releasing oxygen-reactive species.

## INTRODUCTION

Neutrophils are central cellular elements in nonspecific inflammatory resistance. To adequately perform the many functions required of them, neutrophils must be responsive to a considerable array of extracellular bioregulatory signals. The presence (or absence) of bioregulatory substances in the extracellular milieu largely influence a cell's functional responses at any instant. Adenosine, a purine nucleoside formed by the cleavage of adenosine monophosphate (AMP) by 5'-nucleotidase, has been reported to be a biological response modifier. Adenosine levels increase after traumata such as ischemia (1), hypoxia (2), or neural overstimulation, and (3) mediate cellular function by modulating stimulus-response coupling and cyclic AMP concentrations in a large variety of cell types (4). Physiological concentrations of adenosine are also reported to modulate the metabolic capacity of neutrophils to produce toxic oxygen radicals such as superoxide anion (SO) (5). The availability of adenosine antagonists and analogs has facilitated investigations of the cellular and biological effects of adenosine. Substituted xanthine derivatives i.e., methylxanthines, theophylline, and aminophylline have been prophylactically administered as adenosine antagonists (6). Recognized primarily for their ability to stimulate bronchidilation, methylxanthines also mobilize intracellular calcium, inhibit phosphodiesterase, antagonize adenosine receptor-coupling (7), alter cellular aggregation, lysosomal enzyme release and SO formation (8). The formation of toxic oxygen radicals are of particular interest since the high reactivity of the reduced oxygen forms have led to their implication as mediator substances in a number of pathological conditions (9). The possibility of oxygen-radical-mediated tissue damage being augmented by methylxanthines prompted our investigation of the *in vitro* effects of substituted xanthines on isolated canine peripheral neutrophils. Canine neutrophils were selected for examination because of the data base that exists for ischemia, hyperdynamic sepsis, and radiation injury modeling systems. The pharmacological effects of aminophylline were examined for effects on the electrophysiological state of neutrophil membranes and cytosolic $H_2O_2$ production levels and were compared to levels induced by reference concentrations of phorbol myristate acetate (PMA).

## MATERIALS AND METHODS

### Reagents

Aminophylline (American Quinine, Shirley, NY), PMA, xanthine oxidase, dimethylsulfoxide (Sigma Chemical Company, St. Louis, MO); Hanks' balanced salt solution (HBSS), phosphate-buffered saline (PBS), HEPES buffer, and trypan blue (Grand Island Biological Company, Grand Island, NY); dichlorofluorescein diacetate (DCFH-DA) (Eastman Kodak Company, Rochester, NY); di-pentyl-oxocarbocyanine (Molecular Probes, Inc., Junction City, OR); ammonium chloride (Fisher Scientific, Silver Spring, MD); propidium iodide (Calbiochem, La Jolla, CA). Stock solutions of DCFH-DA (5mM) were stored in absolute ethanol. PMA was dissolved in dimethylsulfoxide at 0.01 M and stored at -70°C. Fetal bovine serum (FBS) (Hyclone Labs, Logan, UT) was heat-inactivated (56°C, 60 minutes) and filtered (0.45 um) before use.

### Animals

Hra beagles (*Canis familiaris*, 10-12 kg, 1-2 years old) were used in these experiments. Dogs were quarantined on arrival and screened for evidence of disease before being released for experimentation. Dogs were kenneled in an AAALAC-accredited facility and provided commercial dog chow and tap water *ad libitum*. Animal holding rooms were maintained at 70°F +/- 2°F with 50% +/- 10% relative humidity with at least 10 air changes/hour of 100% conditioned fresh air. The dogs were maintained on a 12-hour light/dark full-spectrum lighting cycle with no twilight.

### PMN Isolation

Peripheral blood (5 ml) was drawn monthly from the lateral saphenous vein into syringes containing preservative-free heparin (10 U/ml). Blood was washed in HBSS without Ca++ and Mg++ (400xg, 10 minutes, room temperature). Contaminating red blood cells were lysed with 0.83% $NH_4Cl$ (10 minutes, 4°C) and the leukocytes polleted. The cell pellet was minimally resuspended in PBS supplemented with 0.2% heat-inactivated FBS. Wright's stained blood smears were prepared for differential and morphological examination.

### Flowcytometric Measurement of Intracellular H2O2 Production

H2O2 production was measured as described by Bass et al. (10). DCFH-DA, a nonpolar, nonfluorescent compound diffused through cell membranes, was hydrolysed by cellular esterases to nonfluorescent, intracellularly trapped 2',7'-dichlorofluorescein (DCFH). The H2O2 produced by activated PMNs oxidizes DCFH to the fluorescent analogue 2',7'-dichlorofluorescin (DCF). PMNs (10e6 cells/ml) were incubated with 5 uM DCFH-DA in PBS supplemented with 0.2% FBS for 10 minutes at 37°C and stimulated with PMA (100 ng/ml) or other reagents. DCF levels were measured flowcytometrically on a FACS Analyzer. The percent change in H2O2 production was determined by

$$\frac{\text{Mean fluorescent intensity (Fl), experimental} - \text{Fl, control}}{\text{Fl, control}}$$

### Flowcytometric Assay of Membrane Potential

DiOC5(3) is a lipophilic dye that freely diffuses through cellular membranes. Alterations in membrane potentials are reflected by changes in intracellular dye concentration. PMNs (10e6 cells/ml) were resuspended in HBSS supplemented with glucose (1 mg/ml) and incubated with 10e-8 M DiOC5(3) for 10 minutes at 37°C. Cell suspensions were placed on ice to inhibit further dye uptake. Under these conditions, stable fluorescence patterns were maintained for 30 minutes. Cells were stimulated with 100 ng/ml PMA for 10 minutes at 37°C. Flowcytometric analysis of cellular fluorochrome concentrations were assessed, in the manner described previously for measurement of H2O2 production.

### Statistical Analysis

All data are presented as the mean +/- standard error. Statistical differences were determined using the Student's t-test. P values <0.05 were considered statistically significant.

## RESULTS

Activation of PMNs, with respect to membrane alterations and production of H2O2, were evaluated on the basis of

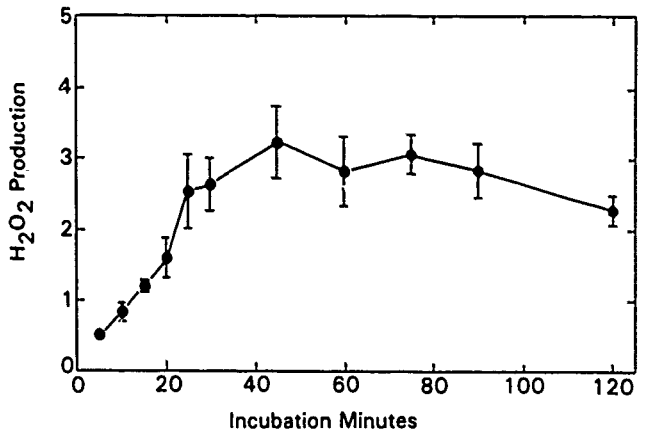


Figure 1. Canine PMN H202 production as a function of time and 37 C. Data is represented by changes (increases) in mean channel fluorescence measured between 5 and 120 minutes. Individual assays are reported as the mean fluorescent increases of a minimum of 10,000 gated events. Data points represent the mean fluorescence intensity (+/- SEM) from 12 to 21 animals.

the differences in mean channel fluorescence detected at varying times following PMN stimulation with either aminophylline or PMA. Except for isotonic lysis (room temperature) and dye loading (37°C), cells were maintained at 4°C. The combined processes of dye loading and 37°C incubation resulted in low-level metabolic activation of PMNs the magnitude of which, over a 2-hour period, did not generally exceed baseline levels more than threefold (figure 1). PMA responses were examined as a cellular membrane and metabolic reference standard. Figure 2 demonstrates the in vitro canine neutrophil H202 responses that occurred over 2-hours in the presence of an optimal concentration of PMA (100 ng/ml). H202 responses to PMA increased almost linearly for 60 minutes before leveling off at magnitudes in excess of 50 times control values. Compared to temperature controls, aminophylline incubation (10E-4 M, final concentration) resulted in significant ($p<0.05$) reduction in cellular cytosolic H202 production when examined at 5 and 10 minutes. By 15 minutes,

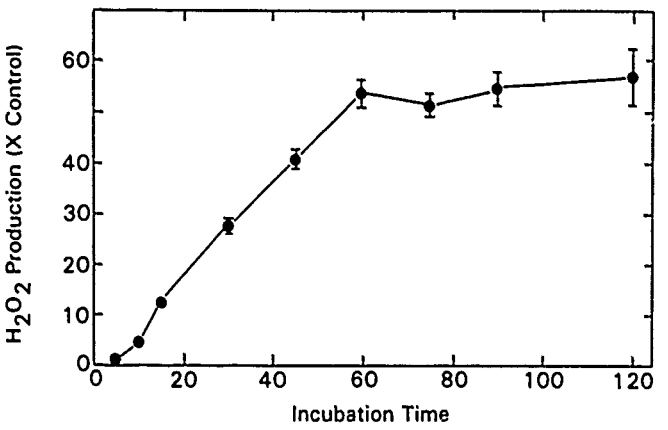


Figure 2. Canine cytosolic PMN H202 production following 5 to 120 minutes stimulation with PMA (100 ng/ml, final concentration). Data points represent the increases (x control) in mean fluorescence intensity (+/- SEM) of a minimum of 10,000 gated events from 10 to 20 animals.

cytosolic H202 production had significantly increased ($p<0.05$), and reached an experimental maximum at 60 minutes ($p<0.001$) which was almost 5-times control and approximately 30% of PMA. Both treatments exhibited kinetic similarities, increasing to experimental maxima at 60 minutes before leveling off (figure 3). Based on metabolic induction of H202, aminophylline did not appear to degrade when kept refrigerated at 4°C for up to four weeks. Refrigerated samples from original aliquots retained metabolic stimulating capabilities statistically indistinguishable from freshly opened aminophylline (figure 4). Preincubation of PMNs for 10 minutes with aminophylline and subsequent stimulation with PMA resulted in H202 response levels that were not significantly different from those of PMA alone, suggesting that aminophylline did not pharmacologically interfere with the PMNs' ability to respond to PMA (table 1).

Alterations in membrane potential have been reported to occur early after receptor-ligand interaction and have been suggested as being representative of an early in-

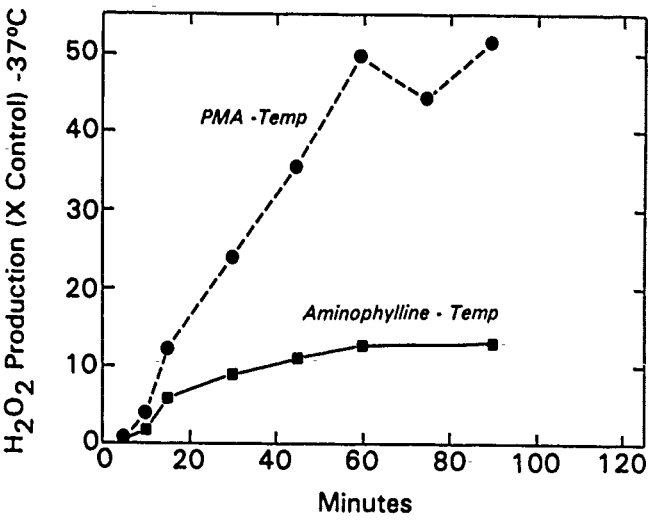


Figure 3. Canine PMN H202 production between 5 and 90 minutes following stimulation with either PMA (100 ng/ml) or aminophylline (10E-4 M). Data points represent the mean fluorescent intensity increases (temperature controls subtracted) of a minimum of 10,000 gated events from 10 to 12 animals.

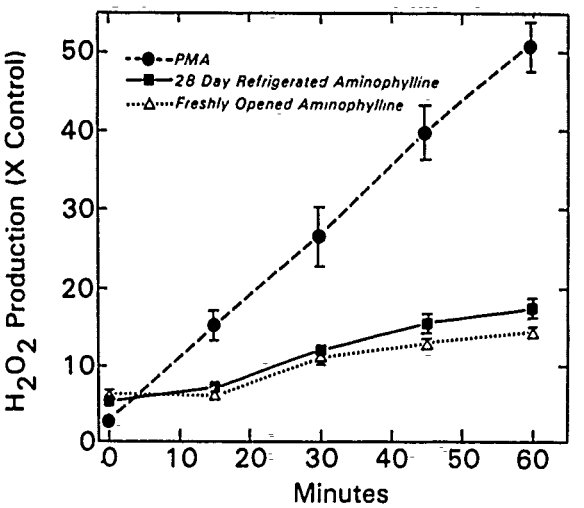


Figure 4. Canine PMN H202 production over a period of 60 minutes following stimulation with PMA (100 ng/ml) or one of two aminophylline (10E-4 M) types, freshly opened or 28 day refrigerated. Data points represent the mean fluorescent intensity (+/- SEM) increases of a minimum of 10,000 gated events from 10 to 12 animals.

Table 1. Demonstrates the effects a 10 minute 37 C preincubation of aminophylline (final concentration, 10e-4 M), on PMN production of H2O2 upon subsequent stimulation with PMA for 15 minutes.

**Aminophylline (10e-3M) Preincubation and PMA**

| Stimulation (Minutes) | 10 | 15 | 30 | 45 | 60 | 90 | 120 |
|---|---|---|---|---|---|---|---|
| PMA only<br>Mean<br>SEM | 4.54<br>0.36 | 12.68<br>0.46 | 27.29<br>1.28 | 40.86<br>1.87 | 53.68<br>2.65 | 54.73<br>3.28 | 57.25<br>5.50 |
| Aminophylline Preincubation and Subsequent PMA Stimulation | 3.99<br>3.54<br>3.95<br>4.18<br>5.00<br>6.19<br>9.07<br>7.53 | 7.68<br>6.75<br>12.09<br>8.51<br>18.54<br>23.18<br>12.08<br>21.53<br>13.72<br>19.34<br>5.69<br>7.11<br>6.33<br>7.58 | 39.64<br>62.64<br>27.25<br>58.05<br>18.29<br>28.60<br>27.87<br>24.71 | 49.84<br>84.27<br>45.01<br>86.07<br>26.74<br>38.67<br>31.34<br>32.36 | 60.67<br>91.61<br>67.70<br>114.10<br>43.72<br>52.27<br>45.89<br>45.48 | 41.92<br>56.83<br>45.26<br>55.51 | 32.47<br>65.30<br>42.03<br>58.36 |
| Mean<br>SEM | 5.43<br>0.70 | 12.13<br>1.64 | 35.88<br>5.74 | 49.29<br>8.26 | 65.18<br>8.97 | 49.88<br>3.70 | 49.54<br>7.49 |

flammatory state preceding the metabolic and other cellular effects of neutrophil activation (11). Table 2 demonstrates that aminophylline concentrations, considered within therapeutic ranges, resulted in slight but significant reductions in membrane depolarization (0.063 +/- 0.005) when compared to normal values (-0.07 +/-0.03). Aminophylline levels were considerably less than levels that were PMA induced (0.455 +/-0.016). Preincubation of PMNs with aminophylline resulted in a significant reduction (44%) in the level of membrane depolarization, which could be subsequently achieved with PMA stimulation.

## DISCUSSION

Aminophylline, present *in vitro* at final concentrations considered within *in vivo* therapeutic ranges, re-

Table 2. The fluorescent dye DiOC5-(3) partitions between cellular cytosol and extracellular fluid as a function of the electrophysiological state of the cellular membrane. Based on differences in fluorescent partitioning alterations in the electrophysiological state of cellular membranes are demonstrated. Hyperpolarization (-) of the cells interior, relative to its exterior, results in increased fluorescence whereas depolarization (+) causes decreased fluorescence. Membrane potential data are results of PMNs being incubated for 10 minutes at 37 C with either aminophylline or PMA alone, or an aminophylline preincubation followed by PMA stimulation.

**Canine Neutrophil Membrane Potential Alteration**

| Subjects | 37°C | Aminophylline | PMA | Aminophylline and PMA |
|---|---|---|---|---|
| 1 | +0.02 | +0.07 | +0.44 | +0.20 |
| 2 | -0.07 | +0.07 | +0.42 | +0.23 |
| 3 | -0.01 | +0.04 | +0.43 | +0.30 |
| 4 | -0.12 | +0.06 | +0.51 | +0.26 |
| 5 | -0.18 | +0.07 | +0.43 | +0.26 |
| 6 | -0.07 | +0.07 | +0.50 | +0.29 |
| Mean | -0.07 | +0.06 | +0.46 | +0.26 |
| SEM | -0.03 | +0.01 | +0.02 | +0.02 |
| (vs. 37°C) | | $p < 0.01$ | $p < 0.001$ | $p < 0.001$ |

sulted in significant electrophysiological and metabolic alterations of separated canine peripheral blood neutrophils. Compared to either normal temperature controls or cells stimulated by PMA, aminophylline significantly altered the membrane potentials of neutrophils. Aminophylline-induced increases in cytosolic levels of $H_2O_2$ occurred within 15 minutes and at 60 minutes reached experimental maximums that were almost 5-times that of normal temperature controls but only 30% of those induced by PMA.

Methylxanthines, such as 1,3-dimethylxanthine (theophylline) and the diethylamine salt (aminophylline), have been used clinically in the treatment of obstructive airway diseases, primarily because of their ability to inhibit cellular cAMP phosphodiesterase, resulting in the

relaxation of bronchiolar smooth muscle (12). Patients whose blood levels were between 10 and 20 ug/ml plasma demonstrate reductions of 10-12% in cellular phosphodiesterase activity (13). At concentration levels 10-100 times lower than those inhibiting phosphodiesterase, methylxanthines compete with biological mediators, such as adenosine, for A1 and A2 cell surface receptors (14). The competition of methylxanthines with adenosine for A1 and A2 cell surface receptors may have important biological implications. It has been suggested that increased levels of extracellular adenosine modulate the production of SO, mediating indiscriminate toxic-radical-mediated tissue damage (15). Methylxanthines may upset the level of adenosine bioregulation, thereby becoming clinically and pathologically important.

Damaged cells release adenine nucleotides (16,17,) which undergo biodegradation to adenosine. Adenosine levels increase to pharmacologic mediator levels between 0.01 uM and 10 uM (15,18), exerting effects through specific cellular surface receptors (14). Depending on the type, or ratio, of cell-surface receptors stimulated, adenosine and/or its phosphate analogs induce smooth muscle relaxation or contraction. Contraction of perivascular smooth muscle could result in localized vascular stasis. Sequestration and activation of phagocytic cellular elements, particularly neutrophils, could result in tissue damage because of the indiscriminate release of toxic oxygen radicals (19). Under normal conditions, the host usually has adequate serum and cellular mechanisms to protect against oxidant-mediated damage. One reported protective mechanism involves alterations in endogenous extracellular adenosine concentrations. Increases in extracellular adenosine concentrations modulate the production of toxic oxygen radicals, i.e., SO (15). Adenosine levels, following trauma or ischemia, increase up to 30-times normal levels within minutes (20,21). If not modulated, toxic radicals could contribute significantly to pathological circumstances. Although short-lived, toxic radicals are extremely reactive and are capable of the lipid peroxidation of lysosomal, mitochondrial, and plasma membranes, resulting in serious, possibly lethal, alterations of cellular structure and/or function.

We have demonstrated that aminophylline *in vitro* is capable of modifying the electrophysiological state of neutrophil membranes and the mechanism(s) of oxidative metabolism that resulted in the production of significant levels of H202. Previous reports suggested that methyl-

xanthines and adenosine utilize similar surface receptors. Based on information presented it appears that the biological or functional end points of the adenosine or methylxanthine receptor stimulations differ considerably. There does not appear to be cellular metabolic additivity between aminophylline and PMA, suggesting differences in receptors or disparities in the mechanisms of signal transduction. Both mechanisms remain as areas to be further investigated.

ACKNOWLEDGMENTS

The authors wish to acknowledge the excellent technical assistance of R.T. Brandenburg and L.M. Konradi.

FOOTNOTE

Supported by the Armed Forces Radiobiology Research Institute, Defense Nuclear Agency, under work unit 00082. Views presented in this paper are those of the authors; no endorsement by the Defense Nuclear Agency has been given or should be inferred. Research was conducted according to the principles enunciated in the "Guide for the Care and Use of Laboratory Animals." prepared by the Institute of Laboratory Animal Resources, National Research Council.

REFERENCES

1. Miller, W.L., Thomas, R.A., Berne, R.M. and Rubio, R. Adenosine production in the ischemic kidney. Circ. Res.,43:390,1978

2. Mentzer, R.M. Jr., Rubio, R. and Berne R.M., Release of adenosine by hypoxic canine lung tissue and its possible role in pulmonary circulation. Am. J. Pathol.,229:1625,1975.

3. Sattin, A., Increase in the content of adenosine 3′, 5′- monophosphate in mouse forebrain during seizures and prevention of the increase by methylxanthines. J. Neurochem.,18:1087,1971.

4. Baer, H.P. and Drummond, G.I., Physiological and Regulatory Functions of Adenosine and Adenine Nucleotides, Raven Press, New York 1979.

5. Cronstein, B.N., Rosenstein, E.D., Kramer, S.B., Weissman, G. and Hirschhorn R., Adenosine; a physiologic modulator of superoxide anion generation by human neutrophils. Adenosine acts via an A2 receptor on human neutrophils. J. Immunol., 135:1366,1985.

6. Holgate, S.T., Mann, J.S. and Cushley, M.J., Adenosine as a bronchoconstrictor mediator in asthma and its antagonism by methylxanthines. J. Allergy Clin. Immunol.,74:302,1984.

7. Rall, T.W., in The Pharmacological Basis of Therapeutics, edited by A.G. Gilman, L.S. Goodman, and A. Gilman, p.592, Macmillan Publishing Co., New York, 1980.

8. Schmeichel, C.J., and Thomas, L.L., Methylxanthine bronchodilators potentiate multiple human neutrophil functions. J. Immunol.,130:1910,1987.

9. Slator, T., Free-radical mechanisms in tissue injury. Biochem. J.,222:1,1984.

10. Bass, D. A., Parce, J. W., Dechatelet, L. R., Szejda, P., Seeds, M. C., Thomas, M., Flow cytometric studies of oxidative product formation by neutrophils: a graded response to membrane stimulation. J. Immunol. 130:1910,1983.

11. Korchak, H.M. and Weissmann, G., Changes in membrane potential of human granulocytes antecede the metabolic responses to surface stimulation. Proc. Natl. Acad. Sci.,75:3818,1978.

12. Webb-Johnson, D.C. and Andrews, J.L., Bronchodilation therapy. N. Engl. J. Med.,297:476,1977.

13. Polson, J.B., Krzanowski, J.J., Goldman, A.L., and Szentivanyi, A., Inhibition of human pulmonary phosphodiesterase activity by therapeutic levels of theophylline. Clin. Exp. Pharmacol. Physiol.,8:535, 1978.

14. Fredholm, B.B. and Persson, C.G.A., Adenosine-induced bronchoconstriction in asthma; specificity and relationship to airway reactivity. Eur. J. Pharmacol.,81:673,1982.

15. Cronstein, B.N., Kramer, S.B., Weissmann, G. and Hirschhorn, R., Adenosine: a physiological modulator of superoxide anion generation by human neutrophils. J. Exp. Med.,158:1160,1983.

16. Pearson, J.D. and Gordon, J.L., Vascular endothelial and smooth muscle cells in culture selectively release adenine nucleotides. Nature,281:384,1979.

17. Henderson, J.F., in Physiological and Regulatory Functions of Adenosine and Adenine Nucleotides, edited by H.P. Baer and G.I. Drummond, p.315, Raven Press, New York, 1979.

18. Holgate, S.T., Mann, J.S. and Cushley, M.J., Adenosine as a bronchoconstrictor mediator in asthma and its antagonism by methylxanthines. J. Allergy Clin. Immunol.,74:302,1984.

19. Simpson, P.J., Fantone, J.C. and Lucchesi, B.R., in Oxygen Radicals and Tissue Injury, edited by B. Halliwell, p.63, FASEB, Bethesda, 1987.

20. Winn, H.R., Welsh, J.E., Rubio, R. and Berne, R.M., Changes in brain adenosine during bicuculline-induced seizures in rats. Circ. Res.,47;568,1980.

21. Schultz, V. and Lowenstein, J.M., The purine nucleotide cycle. J. Biol. Chem.,253:1938,1978.

*Journal of Biological Response Modifiers*
8:462–467 © 1989 Raven Press, Ltd., New York



Short Communication

# Xanthine Oxidase Potentiation of Reactive Oxygen Intermediates in Isolated Canine Peripheral Neutrophils

Dale F. Gruber, Kevin P. O'Halloran, and Ann M. Farese

*Experimental Hematology Department, Armed Forces Radiobiology Research Institute, Bethesda, Maryland, U.S.A.*

**Summary:** Oxygen-derived free radicals are believed to contribute to reperfusion injury based, in part, upon results conferred by the pharmacologic administration of allopurinol. Allopurinol inhibits xanthine oxidase (XO) activity in ischemic tissues. The possible role of XO as a pathologic mediator prompted examination of its effects on isolated peripheral canine neutrophils. In contrast to neutrophils alone, or following stimulation with phorbol myristate acetate (PMA), it was determined that XO affected both the membrane potential and the metabolism significantly. Membrane potential assay showed that at 5–10 min, PMA depolarized 89–96% of the canine neutrophils between 32–48%. Incubation with 0.5 U/ml XO involved fewer cells (54–86%), but at substantially increased cellular depolarization levels (76–90%). Metabolic assay showed that XO concentrations as low as 0.124 U induced significant cellular $H_2O_2$ production compared with temperature controls. At 0.25–0.5 U XO/$10^6$ cells, cytosolic $H_2O_2$ increases were almost three times those of PMA. **Key Words:** Canine—$H_2O_2$—Membrane depolarization—Neutrophils—Oxygen radicals—Xanthine oxidase.

Exposure of polymorphonuclear neutrophils (PMN) to soluble or insoluble stimuli, i.e., chemoattractants, bacteria, or opsonized particles, initiates a complex series of responses that may include the secretion of granules and lysosomal enzymes and the production, or release, of reactive oxygen intermediates (ROI) (1,2). It is in part by way of these specialized mechanisms that professional phagocytes are able to fulfill their bactericidal role (3). In the absence of adequate in vivo protective mechanisms, an inappropriate elaboration of ROI could result

Received December 5, 1988; accepted April 14, 1989.
Address correspondence and reprint requests to Dr. D. F. Gruber at Experimental Hematology Department, Armed Forces Radiobiology Research Institute, Wisconsin Avenue, Bethesda, MD 20814-5145, U.S.A.

in lipid peroxidation and damage of normal healthy tissue (4,5). Xanthine oxidase (XO) has been reported to be one of the substrates necessary in the acellular production of reactive oxygen radicals (6–9). XO's participation in acellular generation of ROI and its presence as a normal breakdown product of tissue xanthine dehydrogenase prompted our examination of its effects on the membrane potential and metabolism, i.e., $H_2O_2$ production of separated canine peripheral neutrophils in comparison with changes initiated by phorbol myristate acetate (PMA), a potent stimulator of the respiratory burst in human PMNs (1).

## MATERIALS AND METHODS

### Reagents

The following reagents were used: PMA, xanthine oxidase, dimethylsulfoxide (Sigma Chemical Co., St. Louis, MO, U.S.A.); Hanks' balanced salt solution (HBSS), phosphate-buffered saline (PBS), and trypan blue (GIBCO, Grand Island, NY, U.S.A.); dichlorofluorescein diacetate (DCFH-DA) (Eastman Kodak Company, Rochester, NY, U.S.A.); dipentyloxocarbocyanine [DiOC5(3)] (Molecular Probes Inc., Junction City, OR, U.S.A.); ammonium chloride (Fisher Scientific, Silver Spring, MD, U.S.A.); propidium iodide (Calbiochem, La Jolla, CA, U.S.A.). Stock solutions of DCFH-DA and DiOC5(3) were stored in absolute ethanol at concentrations of 5 and 1 m*M*, respectively. PMA was dissolved in dimethylsulfoxide at 0.01 *M* and stored at −70°C. Fetal bovine serum (FBS) (Hyclone Labs, Logan, UT, U.S.A.) was heat-inactivated (56°C, 60 min) and filtered (0.45 μm) before use.

### Animals

Hra beagles (*Canis familaris*), 1–2 years old weighing 10–12 kg, were used in these experiments. Canines were quarantined on arrival and screened for evidence of disease or parasitic infestation before being released for experimentation. Unless prescribed by protocol, canines were not medicated during the experiment or for 30 days before. Canines were kenneled in an AAALAC-accredited facility, provided commercial lab chow, and allowed access to tap water ad libitum. Animal holding rooms were maintained at 70 ± 2°F with 50 ± 10% relative humidity using at least 10 changes/h of 100% conditioned fresh air. Animals were maintained on a 12 hour light/dark full-spectrum photoperiod with no twilight.

### Neutrophil Isolation

Peripheral blood (5 ml once a month) was drawn from the lateral saphenous vein into heparinized (10 U/ml blood) syringes. Peripheral blood was washed in HBSS without $Ca^{2+}$ and $Mg^{2+}$ (400 *g*, 10 min, 21°C). Contaminating red blood cells were lysed with 0.83% $NH_4Cl$ (10 min, 4°C) and washed. The leukocyte pellet was resuspended in PBS supplemented with 0.2% heat-inactivated FBS. Viability of cells isolated in this manner was >95% when assessed by trypan blue or propidium iodide exclusion.

### Membrane Potential Assay

Alterations in membrane potential were determined by measuring changes in the intracellular concentrations of DiOC5(3), which partitions between cells and aqueous media as a function of transmembrane potential. Cellular fluorescence intensity varies as a function of membrane potential, decreasing as the membrane depolarizes. PMN aliquots ($10^6$ cells/ml) were resuspended in glucose-supplemented (5 mg/ml) HBSS and incubated with $10^{-8}$ *M* DiOC5(3) for 10 min at 37°C. Cells aliquots were stimulated with PMA (100 ng/ml) or XO (0.5 U/ml) for 10 min at 37°C. Changes in resting membrane potential (t = 0 min) were analyzed by flow cytometry using a FACS analyzer interfaced to a Consort 30 computer system. Green fluorescence was monitored between 515 and 545 nm after excitation by a mercury arc lamp equipped with a 485/22 nm excitation filter. PMNs were distinguished from other cellular types based on coulter volume and right-angle light scatter properties. Quantitation of membrane depolarization was determined by the following formula:

(fluorescence at 0 min − fluorescence at 10 min)/fluorescence at 0 min

### Measurement of Intracellular $H_2O_2$ Production

$H_2O_2$ production was measured as described previously by Bass et al. (10). Cells ($10^6$/ml) were incubated for 10 min at 37°C with 5 μ*M* DCFH-DA in $Ca^{2+}$/$Mg^{2+}$-free PBS supplemented with 0.2% FBS. DCFH-DA diffused through cellular membranes and was hydrolyzed by cellular esterases to nonfluorescent 2′,7′-DCFH, which is intracellularly trapped. Cells were then stimulated with PMA, uricase, or XO and analyzed. Cells capable of producing intracellular $H_2O_2$ oxidize DCFH to the fluorescent analogue DCF PMNs were distinguished from other cellular types on the basis of coulter volume(s) and right-angle light scatter properties. DCF levels were measured as described for membrane potential, and the percent change in $H_2O_2$ production was determined by the following formula:

100 × [(mean fluorescence intensity (FL) experimental − FL control)/FL control]

### Statistical Analysis

All data are presented as the mean ± SEM. Statistical differences were determined using Student's *t* test, and any p values <0.05 were considered statistically significant.

## RESULTS

PMA alters the membrane potential of isolated, normal peripheral canine neutrophils. Assays of individual samples were run in triplicate. Flow cytometric analyses of membrane potential changes demonstrated that 89–96% of the cellular population (determined by right-angle light scatter to be granulocytes) was depolarized at 10 min between 32 and 48% (change in cellular fluorescence × 100) with

an average change of 41% in comparison with 37°C controls (Table 1). Quantitatively, although fewer cells were stimulated by XO (range 54–86%, mean 70%) than by PMA, responding cells exhibited a substantially increased depolarization (range 76–90%, mean 70%).

Figure 1 depicts cytosolic $H_2O_2$ that was stimulated by XO at final concentrations of 0.025–0.5 U/ml when examined at 15 min. Figure 2 demonstrates cellular $H_2O_2$ production of PMNs examined 10–35 min after stimulation with 0.5 U XO/ml. $H_2O_2$ production was apparent for 15 min, after which the responses begin to decrease.

## DISCUSSION

The in vitro biological effects of XO on canine PMNs include significant membrane and metabolic effects. In comparison with membrane depolarization characteristics demonstrated by PMA, XO involved fewer PMNs but at significantly enhanced response levels. In addition to the membrane effects, XO also enhanced PMN $H_2O_2$ production three times that of PMA maxima.

Alterations in cellular transmembrane potentials have been suggested as being among the earliest events following appropriate levels of stimulus-response coupling (11). DiOC5(3) and other closely related lipophilic cations are able to assess the electrophysiological state of cellular membranes by differences in potential-dependent fluorescent partitioning coefficients. PMA stimulates a loss of cellular fluorescence representative of electrophysiological membrane depolarization and has been used by investigators as a reference standard (12). In vitro, XO induced greater effects on PMN membranes than did PMA and although reacting with fewer PMNs was able to depolarize them to a greater extent.

Different lots of XO have been examined and, although active (compared with controls), have demonstrated significant variability. Older lots of XO demonstrated the highest activities. Recent lots of XO, although significantly active, were unable to stimulate to PMA maxima. The liquid vehicle (2.3 *M* ammonium

**TABLE 1.** *Alterations in canine neutrophil membrane potentials following stimulation by phorbol myristate acetate (PMA) or xanthine oxidase (XO)*

| | PMA[a] | | XO[b] | |
|---|---|---|---|---|
| Subject | Response | Percent early responders | Response | Percent early responders |
| 1 | 0.32 | 89 | 0.81 | 72 |
| 2 | 0.38 | 90 | 0.81 | 79 |
| 3 | 0.45 | 96 | 0.85 | 86 |
| 4 | 0.46 | 95 | 0.76 | 62 |
| 5 | 0.36 | 94 | 0.81 | 63 |
| 6 | 0.48 | 89 | 0.84 | 54 |
| 7 | | | 0.90 | 61 |
| 8 | | | 0.87 | 84 |
| Mean ± SEM | 0.41 ± 0.03 | 92 ± 1 | 0.83 ± 0.02 | 70 ± 4 |

[a] PMA, final concentration 100 ng/ml.
[b] XO, final concentration 0.5 U/ml.

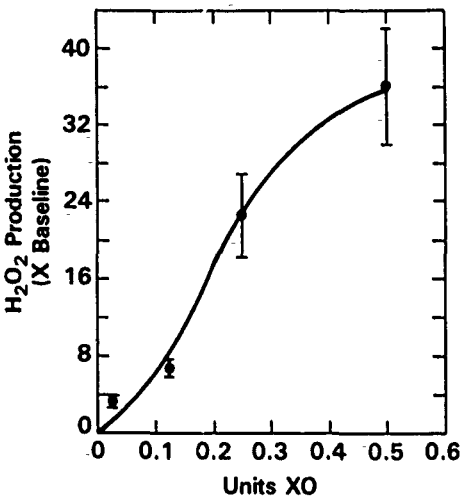


FIG. 1. Canine PMN $H_2O_2$ production (×baseline) following 15 min stimulation with xanthine oxidase (XO) between 0.0025 and 0.5 U/ml. Data points represent the mean fluorescense intensity (±SEM) of a minimum of 10,000 events gathered from 12 to 21 animals.

sulphate) had no effect on PMN cellular membranes or metabolism (results not shown). Uricase, a common enzyme contaminant of XO preparations, was determined to have small, significant, direct effects and little or no priming ability (results not shown).

The reasons for the lot-to-lot manufacturer variability will require further investigation. Despite the reagent variability, XO remains an interesting biological moiety based on these results and others suggesting substantial XO increases in mice following their inoculation with Ehrlich carcinoma cells, bacteria, or protozoa (13). The mechanisms by which XO participates within inflammatory pro-

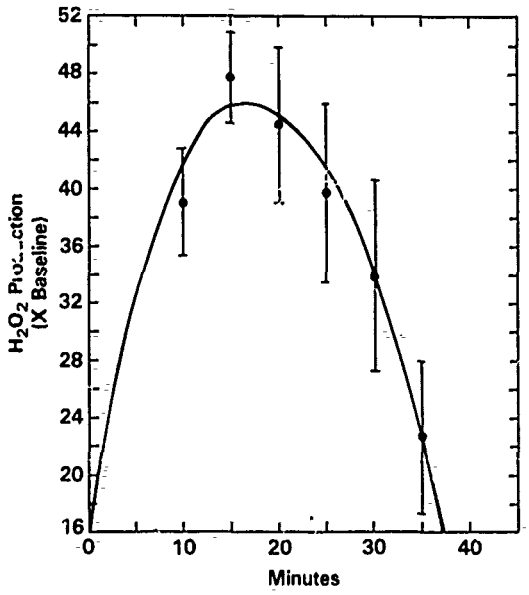


FIG. 2. Canine PMN $H_2O_2$ production (×baseline) between 10 and 35 min following stimulation with 0.5 U XO/ml, final concentration. Data points represent the mean fluorescence intensity (±SEM) of a minimum of 10,000 events from 10 to 12 animals.

cesses deserve further examination, since inappropriate in vivo XO levels could generate toxic oxygen radical forms and destruction of healthy tissue.

**Acknowledgment:** This work was supported by the Armed Forces Radiobiology Research Institute, Defense Nuclear Agency, under work unit 00082. Views presented in this paper are those of the authors; no endorsement by the Defense Nuclear Agency has been given or should be inferred. Research was conducted according to the principles enunciated in the "Guide for the Care and Use of Laboratory Animals" prepared by the Institute of Laboratory Animal Resources, National Research Council.

## REFERENCES

1. DeChatelet LR, Shirley PS, Johnston RB Jr. Effect of phorbol myristate acetate on the oxidative metabolism of human polymorphonuclear leukocytes. *Blood* 1976;45:545–54.
2. Goldstein IM, Roos D, Kaplan HB, et al. Complement and immunoglobulins stimulate production by human leukocytes independently of phagocytosis. *J Clin Invest* 1975;56:1155–63.
3. Babior B, Kipnes R, Curnette J. Biological defense mechanisms: the production by leukocytes of superoxide, a potential bactericidal agent. *J Clin Invest* 1973;52:741–4.
4. Frank L. Oxygen toxicity in eukaryotes. In: Oberly LW, ed. *Superoxide dismutase*. Boca Raton: CRC Press Inc, 1985:1–43.
5. McCord JM. The role of superoxide in postischemic tissue injury. In: Oberly LW, ed. *Superoxide dismutase*. Boca Raton: CRC Press Inc, 1985:143–50.
6. McCord JM, Fridovich I. The reduction of cytochrome c by milk xanthine oxidase. *J Biol Chem* 1968;243:5753–60.
7. Bindoli A, Cavallini L, Rigobello MP, et al. Modification of the xanthine-converting enzyme of perfused rat heart during ischemia and oxidative stress. *Free Radical Biol Med* 1988;4:163–7.
8. Roy RS, McCord JM. Superoxide and ischemia: conversion of xanthine dehydrogenase to xanthine oxidase. In: Greenwald R, Cohen G, eds. *Oxyradicals and their scavenger systems*, vol 2. New York: Elsevier, 1983:145–53.
9. Mellgren RL. Canine cardiac calcium-dependent proteases: resolution of two forms with different requirements for calcium. *FEBS Lett* 1980;109:129–33.
10. Bass DA, Parce JW, Dechatelet LR, et al. Flow cytometric studies of oxidative product formation by neutrophils: a graded response to membrane stimulation. *J Immunol* 1983;130:1910–7.
11. Korchak HM, Weissmann G. Changes in membrane potential of human granulocytes antecede the metabolic responses to surface stimulation. *Proc Natl Acad Sci USA* 1978;75:3818–22.
12. Seligmann B, Chused TM, Gallin JI. Human neutrophil heterogeneity identified using flow microfluorometry to monitor membrane potential. *J Clin Invest* 1981;68:1125–31.
13. Tubaro E, Lotti B, Santiangeli C. Xanthine oxidase increases in polymorphonuclear leucocytes and macrophages in mice in three pathological situations. *Biochem Pharmacol* 1980;29:1945–8.

RADIATION RESEARCH 123, 268–274 (1990)



# Radiation-Induced Binding of DNA from Irradiated Mammalian Cells to Hydroxyapatite Columns[1]

KATHRYN D. HELD,* JANE MIRRO,* DEBORAH C. MELDER,† WILLIAM F. BLAKELY,‡
NANCY L. OLEINICK,§ AND SONG-MAO CHIU§

*Department of Radiation Medicine, Massachusetts General Hospital, Harvard Medical School, Boston, Massachusetts 02114, †Pharmacology Department, Mayo Clinic and Mayo Foundation, Rochester, Minnesota 55905, ‡Radiation Biochemistry Department, Armed Forces Radiobiology Research Institute, Bethesda, Maryland 20814-5145, and §Division of Biochemical Oncology, Case Western Reserve University, Cleveland, Ohio 44106

HELD, K. D., MIRRO, J., MELDER, D. C., BLAKELY, W. F., OLEINICK, N. L., AND CHIU, S.-M. Radiation-Induced Binding of DNA from Irradiated Mammalian Cells to Hydroxyapatite Columns. *Radiat. Res.* 123, 268–274 (1990).

In experiments designed to measure radiation-induced DNA damage using the DNA unwinding–hydroxyapatite chromatography technique, we observed that under some experimental conditions a significant proportion of the test DNA became tightly bound to the hydroxyapatite (HA) and could not be released even with a high concentration of phosphate buffer. Approximately 5–10% of DNA from unirradiated cells binds to the HA. With increasing radiation doses in air, the fraction of bound DNA increases, reaching about 30% at about 35 Gy. The binding exhibits many of the characteristics of a radiation-induced cell lesion: the proportion of DNA retained by the HA is less when cells are irradiated under hypoxic conditions or in the presence of the thiol radioprotector dithiothreitol; and the binding decreases when an incubation period is allowed between irradiation and harvest of the cells for assay. Studies to determine the nature of the lesion responsible for the binding demonstrated that lesion production requires a component found in cells since no binding was observed with irradiated isolated DNA or nuclear matrix; the binding is not a result of the production of DNA–protein crosslinks; and the bound DNA is single-stranded, based on its sensitivity to nuclease $S_1$. Because of the dose dependence of the binding of DNA to HA, the slopes of the dose–response curves for DNA damage determined with this assay depend on the method used to calculate the fraction of double-stranded DNA. Our demonstration that the bound DNA is single-stranded guides the choice of the method for data analysis. 

## INTRODUCTION

The DNA unwinding–hydroxyapatite chromatography technique (*1–3*) can be used to study production of DNA single-strand breaks by various agents including ionizing radiation. The technique is based on the observation that, although the time required for complete unwinding of large DNA molecules at high pH is long, strand separation is accelerated if breaks are introduced into the DNA (*1–3*). Thus, if the DNA is allowed to unwind in alkali for a fixed time, and the unwinding is then terminated by neutralization, the amount of single-stranded DNA formed by unwinding is proportional to the number of breaks in the starting sample. After unwinding, the DNA is fragmented to minimize renaturation, and the single- and double-stranded DNA fractions are separated on hydroxyapatite (HA) columns.

We have been using this assay to study the modification of radiation-induced DNA damage by sulfhydryl-containing radioprotectors (*4*). In the course of these studies it became apparent that under certain experimental conditions a significant proportion of the test DNA became tightly bound to the HA columns and could not be eluted even with a high concentration of phosphate buffer. Some characteristics of the binding and experiments designed to elucidate the nature of the lesion responsible for the binding are described here.

## MATERIALS AND METHODS

### *Cell Culture and Irradiation*

Chinese hamster lung fibroblasts, V79-367, obtained from Dr. Bruce F. Kimler, were used unless otherwise indicated. The cells were maintained in monolayer culture in exponential growth in Eagle's minimal essential medium (MEM) supplemented with 10% fetal calf serum, 10 mmol $dm^{-3}$ Hepes buffer, 100 U penicillin/ml, and 100 μg streptomycin/ml at 37°C in an atmosphere of 95% air/5% $CO_2$. Under these conditions the V79 cells have a generation doubling time of slightly less than 12 h.

DNA was radiolabeled by incubation of cells in growth medium containing $1.48 \times 10^3$ Bq/ml (0.04 μCi/ml) [$^{14}$C]thymidine ($1.98 \times 10^9$ Bq/mmol) or $1.48 \times 10^4$ Bq/ml (0.4 μCi/ml) [$^3$H]thymidine ($7.4 \times 10^{11}$ Bq/mmol) plus 2 μmol $dm^{-3}$ unlabeled thymidine for 18 h, followed by a 1- to 2-h growth period in medium lacking radiolabeled thymidine. In a few experiments, cellular protein and lipids were radiolabeled by overnight incubation of cells in medium containing $3.7 \times 10^3$ Bq/ml (0.1 μCi/ml) [$^{14}$C]amino acid mixture or $1.85 \times 10^4$ Bq/ml (5 μCi/ml) [*methyl*-$^3$H]choline chloride ($2.96 \times 10^{12}$ Bq/mmol). All radiolabeled compounds were

[1] The views presented in this paper are those of the authors, no endorsement by the Defense Nuclear Agency has been given or should be inferred.



0033-7587/90 $3.00

obtained from New England Nuclear. Cells were harvested by trypsinization, washed by centrifugation, and resuspended in phosphate-buffered saline (PBS) or complete medium at about $1 \times 10^6$ cells/ml. In most experiments, the cells were placed in a glass irradiation vessel on ice and gassed with oxygen or nitrogen (<20 ppm oxygen) prior to and during irradiation. In a few experiments where strict control of the gaseous environment was not required, cell suspensions were placed in a plastic petri dish for irradiation. Cells were irradiated using either a G.E. Maxitron 300 X-ray machine operated at 300 kVp and 20 mA, dose rate 1.07 Gy/min, or a Picker X-ray machine operated at 280 kVp, dose rate 1.46 Gy/min. Details of the gassing and irradiation procedures have been published (*4*).

DNA was isolated from V79 cells and purified by standard methods, essentially as described previously for bacterial DNA (*5*). Nuclear matrix was prepared as described previously from Chinese hamster V79-379 cells cultured in McCoy's 5A medium supplemented with 10% calf serum (*6*). DNA and nuclear matrix were irradiated in petri dishes in the same manner as intact cells.

### *DNA Unwinding–Hydroxyapatite Chromatography*

The DNA unwinding–hydroxyapatite chromatography technique developed by Ahnström and associates (*1–3*) was used as described previously (*4*). In brief, the procedure is as follows. Cells were irradiated, 0.5 ml of a solution containing 0.03 mol $dm^{-3}$ NaOH, 0.97 mol $dm^{-3}$ NaCl, pH 11.8, was added to each 50-$\mu$l cell sample, and cell lysis and DNA unwinding were allowed to proceed on ice in the dark for 30 min. Lysis and unwinding were terminated by addition of 1.0 ml of 0.02 mol $dm^{-3}$ $NaH_2PO_4$, pH 4.8, and the samples were sonicated, sodium dodecyl sulfate (SDS) was added, and the samples were frozen overnight.

New columns were prepared for each experiment by measuring 150 ± 10 mg hydroxyapatite powder into 3-ml syringes. In most of the experiments high-resolution hydroxyapatite (Calbiochem, La Jolla, CA) was used. However, in some experiments fast-flow HA (Calbiochem) and DNA grade Bio-Gel HTP (Bio-Rad, Richmond, CA) were used for purposes of comparison. Although the different preparations of hydroxyapatite yielded quantitatively different results, the qualitative agreement of increasing DNA binding with increasing radiation dose was apparent with all of the hydroxyapatites. The HA-containing syringes were placed at 60 ± 0.5°C, and the HA was hydrated by washing three times with 2.0 ml of 0.012 mol $dm^{-3}$ potassium phosphate buffer, pH 6.8. The thawed cell lysates were applied onto the top of the columns and washed three times with 1.0 ml 0.012 mol $dm^{-3}$ potassium phosphate. Single-stranded DNA was eluted with four 1.0-ml washes of 0.12 mol $dm^{-3}$ potassium phosphate buffer containing 0.4% SDS, pH 6.8, at 60°C. Double-stranded DNA was then eluted with four 1.0-ml washes of 0.25 mol $dm^{-3}$ potassium phosphate buffer also containing SDS and at 60°C. Scintiverse II scintillation cocktail (Fisher Scientific Co., Springfield, NJ) was added to each sample and radioactivity was counted. After all HA columns had drained, the HA was dried and transferred to a scintillation vial, cocktail was added, and the radioactivity remaining in the HA was counted. Under the conditions used here the counting efficiencies were the same for all samples; therefore, data are presented as cpm rather than being converted to dpm. The percentage DNA bound to the HA was calculated as

$$\% \text{ cpm bound to HA} = (100) \text{ cpm in HA/total cpm from column,}$$

where the "total cpm from column" was the sum of the cpm in all washes plus the cpm bound to the HA. On occasion, an aliquot of each input sample was also counted, and the total cpm recovered from each column was equal to the total cpm loaded onto the column.

The experiments presented here were conducted in two different laboratories—Mayo Clinic (data in figures) and Massachusetts General Hospital (data in tables)—over a period of about 5 years. The data may show some quantitative inconsistency between data sets and over time, for unknown reasons, but within a series of experiments the results are quite consistent quantitatively and all experiments are in qualitative agreement.

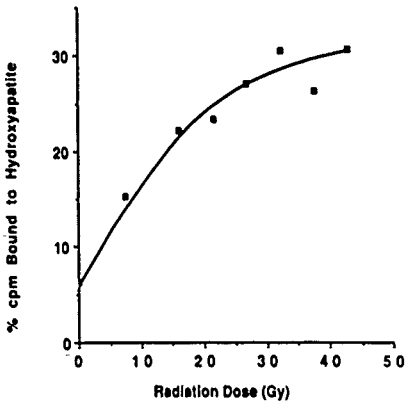


FIG. 1. Fraction of radioactive DNA bound to the HA columns as a function of radiation dose. Chinese hamster V79 cells were irradiated in air in complete medium, then subjected to the DNA unwinding–HA chromatography assay, as described under Methods and Materials. Data are means of 16 experiments. Error bars have been deleted to simplify the figure, but the SD averages 5.25% cpm.

Deoxyribonuclease (DNase) I (Type IV from bovine pancreas, EC 3.1.21.1), Pronase E (protease XXV), lipase (Type I from wheat germ, EC 3.1.1.3), nuclease $S_1$ (EC 3.1.30.1), and dithiothreitol were obtained from Sigma Chemical Co. (St. Louis, MO).

## RESULTS AND DISCUSSION

### *Characteristics of DNA Binding to HA*

In studies using the DNA unwinding–hydroxyapatite chromatography assay, one generally assumes that negligible amounts of DNA are washed through the columns in the initial washes or remain bound to the HA following elution with a high concentration of phosphate buffer. This appears to be the case for DNA from unirradiated cells, but the data in Fig. 1 show that radiation induces binding of DNA to HA which cannot be eluted with a high concentration of phosphate buffer. About 5–10% of the DNA from unirradiated V79 cells binds to the HA, but upon irradiation of the cells in air, the fraction bound increases in a radiation dose-dependent manner, reaching 30–40% bound after high radiation doses (e.g., 40 Gy). The data presented in Fig. 1 are for cells suspended in MEM during irradiation, but similar results were obtained when cells were suspended in PBS. If the cells are irradiated in a nitrogen atmosphere rather than in air, the binding of DNA to HA decreases about threefold at low radiation doses, although at very high doses (>80 Gy) the binding reaches a maximum of about 30% DNA bound (data not shown). If cells are irradiated in the presence of the sulfhydryl-containing radioprotector dithiothreitol (DTT), the amount of

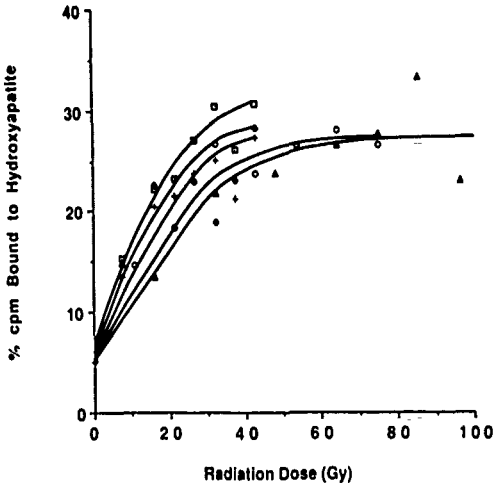


FIG. 2. Binding of DNA from cells irradiated in air in the presence of DTT to HA columns. Experiments were conducted as described for Fig. 1. Data points obtained in the presence of DTT are presented as the means of three or four experiments; data for irradiation in the absence of DTT are repeated from Fig. 1. (□) No DTT; (♦) 1 m*M* DTT; (+) 5 m*M* DTT; (○) 10 m*M* DTT; (▲) 50 m*M* DTT.

DNA bound to HA is less than the amount bound from cells irradiated in the absence of DTT at low radiation doses (Fig. 2). The extent of the reduction in DNA binding is dependent on DTT concentration (Fig. 2).

The sensitivity of the DNA unwinding assay, i.e., the radiation dose range over which it can be used, can be varied by changing the alkaline unwinding conditions used during the experiments. For the work presented here we used conditions which gave intermediate sensitivity. However, in a few experiments we have used alkaline unwinding conditions which increase or decrease the radiation dose sensitivity (e.g., longer unwinding times at higher temperatures, decreased salt concentration, or increased pH). In all cases, the radiation dose-dependent binding of DNA to HA was observed, although the dose range over which it occurred was shifted in accord with the dose range used.

### *Nature of the Lesion Responsible for the Binding of DNA to HA*

We questioned whether the binding of DNA to HA would occur if isolated DNA rather than cells were irradiated. Therefore, isolated DNA and nuclear matrix preparations were irradiated under the same conditions as used for irradiation of cells, and then the DNA was subjected to unwinding, neutralization, and HA chromatography. The results (Table I) indicate that the radiation-induced binding of DNA to HA does not occur when either isolated DNA or nuclear matrix is irradiated. Furthermore, no binding of DNA to HA was seen when nuclear matrix isolated from irradiated cells was exposed to unwinding and HA chromatography (data not shown).

TABLE I
Binding to HA of DNA from Cells, Isolated DNA, and DNA from Nuclear Matrix

| | Percentage cpm bound to hydroxyapatite | | |
|---|---|---|---|
| | 0 Gy | 14.6 Gy | 29.2 Gy |
| Cells | 11.3 ± 2.8[a] | 17.9 ± 5.3 | 20.4 ± 7.8 |
| Isolated DNA | 5.8 ± 0.8 | 6.7 ± 1.1 | 8.1 ± 1.3 |
| Nuclear matrix | 7.0 ± 2.8 | 7.0 ± 2.5 | 6.6 ± 2.6 |

[a] Mean ± SD of three experiments.

We next asked whether or not the binding was a result of crosslinks between DNA and other cell components. Of particular interest are proteins and lipids since hydroxyapatite can be used to fractionate both of those types of molecules (*7*). Cells were irradiated and treated as usual up to the stage of applying the lysates to the columns. At that time the lysates were treated with Pronase or lipase for 30 min at 37°C, followed by HA chromatography. The results (Table II) indicate that neither enzyme treatment significantly decreased the radiation-induced binding of DNA to HA. We were concerned, however, that Pronase and lipase might not have had sufficient opportunity to digest their substrates under the conditions just described. Therefore, in subsequent experiments, DNA from irradiated cells was loaded onto HA in columns, the column contents were expelled into a small beaker, buffer containing Pronase or DNase was added, and the mixture was stirred at 37°C for 2 h. The suspension was then centrifuged and the HA pellet was counted. When the HA was treated with Pronase, the radiolabel remained bound to the HA rather than being released into the supernate; however, when the DNA-containing HA was treated with DNase, no radiolabel remained in the HA pellet (data not shown). These results

TABLE II
Lack of Effect of Pronase and Lipase on the Radiation-Induced Binding of DNA to HA

| | Percentage cpm bound to hydroxyapatite | | |
|---|---|---|---|
| | 0 Gy | 14.6 Gy | 29.2 Gy |
| Control | 11.4 ± 1.8[a] | 27.8 ± 8.3 | 40.9 ± 4.7 |
| Pronase-treated[b] | 14.8 ± 1.8 | 23.9 ± 5.4 | 32.0 ± 2.6 |
| Lipase-treated | 13.3 ± 2.4 | 19.4 ± 2.7 | 31.8 ± 8.6 |

[a] Mean ± SD of three experiments.
[b] Enzyme treatments were at 10 or 100 μg/ml for 30 min at 37°C.

TABLE III
Investigation of Possible Binding of Proteins or Lipids to the HA Column with the Bound DNA

| Radioactive precursor | Percentage cpm bound to hydroxyapatite | | |
|---|---|---|---|
| | 0 Gy | 14.6 Gy | 29.2 Gy |
| [$^3$H]- or [$^{14}$C]Thymidine | 10.2 ± 1.9[a] | 24.9 ± 8.9 | 33.5 ± 7.6 |
| [$^{14}$C]Amino acids | 4.9 ± 2.5 | 6.3 ± 3.3 | 6.7 ± 4.4 |
| [$^3$H]Choline | 2.1 ± 0.7 | 3.5 ± 0.5 | 4.0 ± 0.5 |

[a] Mean ± SD of three experiments.

confirm that the radiolabel bound to the HA was indeed in DNA and that the binding of DNA to HA was not sensitive to Pronase and therefore was not likely to be a result of crosslinking of DNA to protein.

Further studies to investigate the possibility of crosslinking were performed by dual-labeling cellular DNA and proteins or lipids by growth in radiolabeled thymidine and amino acids or choline, respectively. Cells were then irradiated and treated as usual. Radiolabeled proteins were not bound to HA in the radiation dose-dependent manner characteristic of the binding of DNA (Table III). There was a suggestion of a dose-dependent binding of [$^3$H]choline material to HA (Table III); however, the total amount of binding was quite low and therefore was not studied further.

The results of these studies suggest that covalent binding of DNA to proteins is not responsible for the binding of DNA to HA. Such findings are consistent with the observation that DNA binding is greater when cells are irradiated in air, while production of DNA–protein crosslinks is enhanced when irradiation is under hypoxic conditions (*8–10*).

In an attempt to ensure that the radiation-induced binding was not caused by a large DNA aggregate that was resistant to sonication, we analyzed DNA samples from cells exposed to 0, 30, and 60 Gy of irradiation in air by electrophoresis on agarose gels. There was no evidence that high molecular weight DNA was retained preferentially in the irradiated samples (data not shown). This suggests that DNA aggregates are not responsible for the binding to HA.

The results presented here do not entirely eliminate the possibility that DNA–lipid crosslinks are involved in the binding of DNA to HA, nor do they address the possibility that DNA–DNA crosslinks are involved. Additional studies of both possibilities are underway.

To date, most attempts to remove bound DNA from the HA matrix in order to analyze it further have been unsuccessful. These attempts have included treating HA columns containing bound DNA with 0.5 mol dm$^{-3}$ phosphate buffer, 2 mol dm$^{-3}$ KCl, 10 mmol dm$^{-3}$ DTT, 10 mmol dm$^{-3}$ citrate or Pronase and lipase (as mentioned above and in Table II), increasing the concentration of SDS in the buffer, and increasing the temperature of the columns during chromatography to 75°C. Furthermore, a digestion with 100 μg/ml proteinase K in 1% SDS for 60 min at 37 or 60°C prior to chromatography did not prevent the binding of DNA to HA. Treatment of cell lysates with added copper and iron or with the metal chelator EDTA prior to HA chromatography did not alter the binding.

Because nuclease $S_1$ preferentially digests single-stranded DNA with minimal effect on double-stranded DNA, we used it to determine whether the cpm bound to the HA were in single- or double-stranded DNA. Prior to loading on HA columns, cell lysates were treated for varying times with nuclease $S_1$ (1500 U/sample) at 37°C. Table IV shows that $S_1$ had no effect on recovery of DNA in double-stranded fractions or on binding of DNA to HA when unirradiated samples were treated. However, treatment of irradiated DNA with nuclease $S_1$ decreased the percentage of single-stranded DNA and completely prevented all binding of DNA to HA. The radioactivity lost from the single-stranded DNA washes and the HA was all found in the prewashes (0.012 mol dm$^{-3}$ phosphate), which normally contain only minimal radioactivity. This result shows that the DNA bound to HA is single-stranded. However, it does not necessarily mean that the binding of radiolabel to HA is a result of single-strand breaks. Recall that single-strand breaks were produced in isolated DNA or in nuclear matrix DNA, yet neither showed binding of DNA to HA when irradiated. Some lesion other than or in addition to a single-strand break must cause the radiation-induced binding of DNA to HA. Furthermore, although the lesion clearly is in single-stranded DNA, single-stranded DNA from unirradiated cells (single-stranded DNA created by heat denaturation of lysed cell samples) does not bind to HA (data not shown), so production of the lesion involved depends on radiation.

*Impact of DNA–Hydroxyapatite Binding on Data Analysis*

Typically, the fraction of double-stranded (DS) DNA recovered during HA chromatography is calculated using

$$\% \text{ DS DNA} = (100)\, \text{cpm}_{DS}/(\text{cpm}_{DS} + \text{cpm}_{SS}), \quad (1)$$

where $\text{cpm}_{DS}$ is the total radioactivity eluted by 0.25 mol dm$^{-3}$ buffer (double-stranded DNA) and $\text{cpm}_{SS}$ is the total activity eluted by 0.12 mol dm$^{-3}$ buffer (single-stranded DNA). The percentage of double-stranded DNA plotted as a function of radiation dose then gives a straight line on a semilog graph. The slope of this line is a measure of the radiosensitivity of the DNA. An example of such a graph is shown in the line for Eq. (1) of Fig. 3. This method of analy-

TABLE IV
Effect of Nuclease $S_1$ on Binding of DNA to HA[a]

| | Percentage cpm[b] | | | |
|---|---|---|---|---|
| Prewashes | 0.12 mol $dm^{-3}$ washes | 0.25 mol $dm^{-3}$ washes | HA | |
| 0 Gy; no nuclease | 1.8 ± 1.5 | 3.0 ± 0.6 | 92.4 ± 1.6 | 2.8 ± 0.2 |
| 40 Gy; no nuclease | 4.5 ± 0.4 | 48.7 ± 10.1 | 33.6 ± 4.7 | 13.3 ± 5.8 |
| 0 Gy; + nuclease[c] | 3.3 ± 0.3 | 1.3 ± 1.0 | 93.7 ± 1.1 | 1.7 ± 0.1 |
| 40 Gy; + nuclease | 60.6 ± 3.8 | 7.3 ± 1.7 | 31.2 ± 2.0 | 0.8 ± 0.2 |

[a] Mean ± SD of three replicates in a single typical experiment.
[b] Percentage cpm in each set of washes is expressed relative to the total cpm of all washes. Note that this differs slightly from the use of "total cpm" elsewhere in the paper (see Materials and Methods), where cpm in prewashes was excluded because it was minimal.
[c] Nuclease $S_1$ used at 1500 U/sample.

sis assumes either that no DNA is bound to the HA or that the binding is independent of DNA strandedness, i.e., that both double- and single-stranded DNA are bound to the HA in amounts proportional to the amounts eluted.

However, because the binding of DNA to HA is dependent on radiation dose, the slope of the dose–response curve will differ if one calculates the percentage of double-stranded DNA in a different manner. Figure 3 also shows the same data analyzed by

$$\%\ \text{DS DNA} = (100)\ \text{cpm}_{DS}/\text{total cpm} \qquad (2)$$

and

$$\%\ \text{DS DNA} = (100)\ [1 - (\text{cpm}_{SS}/\text{total cpm})], \qquad (3)$$

where total cpm is the sum of all radioactivity eluted from the column by 0.12 and 0.25 mol $dm^{-3}$ buffer and bound to the HA. The second method of analysis (Eq. (2)) implies that all the double-stranded DNA is eluted by the 0.25 mol $dm^{-3}$ buffer; i.e., the HA-bound DNA must be single-stranded, as shown in Table IV. In contrast, use of Eq. (3) assumes that all the single-stranded DNA is eluted in the 0.12 mol $dm^{-3}$ buffer, so the HA-bound DNA is double-stranded, which is not the case, as shown in Table IV.

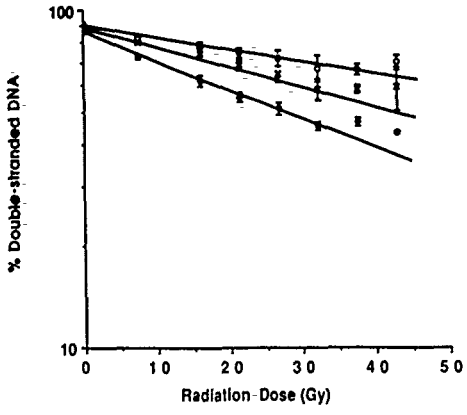


FIG. 3. Dose–response curves for DNA damage determined using the DNA unwinding–HA chromatography method on V79 cells irradiated in air. Percentage double-stranded DNA was calculated using the three different equations given in the text. The same raw data are used for all three curves. Data points are means ± SD of three replicate determinations. (X) Equation (1), (♦) Eq. (2), (O) Eq. (3).

Thus the results shown in Fig. 3 illustrate that systematic differences are introduced into the data analysis depending upon the analysis method used, and therefore values of $D_0$, and perhaps parameters such as oxygen enhancement ratio and protection factor which are derived from $D_0$'s, may depend on the equation used for analysis. Investigators using the DNA unwinding–hydroxyapatite technique must use only one method of data analysis when comparing sets of data obtained on different days. Furthermore, care must be exercised when comparing data obtained in laboratories that have analyzed their data by different methods. Unfortunately, most papers in the literature using the DNA unwinding–hydroxyapatite chromatography technique do not state clearly what method was used to calculate the percentage of double-stranded DNA. The data presented in Table IV show that the DNA bound to the HA is single-stranded. Therefore, Eq. (2) would be the preferred method of data analysis since it assumes all bound DNA is single-stranded.

Although the phenomenon of DNA binding to HA described here has been observed in all of the authors' laboratories, some other laboratories have not reported this result. In particular, Olive *et al.* (*11, 12*) have reported that >95 or 98% of the radioactivity is recovered from HA columns. We initially suspected this difference was due to the type of hydroxyapatite used. However, when we performed experiments using HA kindly supplied by Dr. Olive, we obtained the same radiation-induced binding of DNA to HA as described here.

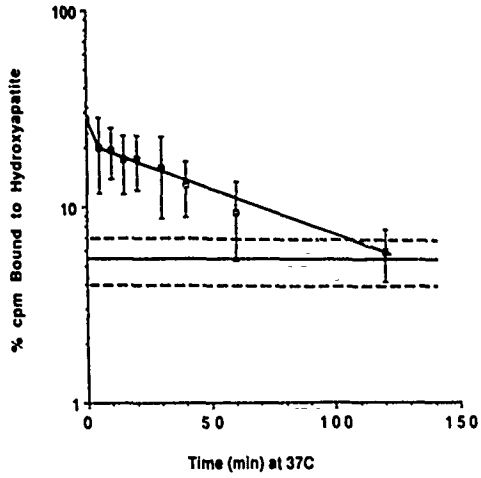


FIG. 4. Reversal of radiation-induced binding of DNA to HA by post-irradiation incubation of cells at 37°C prior to cell lysis and DNA damage assay. Cells were irradiated in air in complete medium with 42.8 Gy. Data points are means ± SD from five experiments. Dashed lines represent means ± SD of unirradiated controls in the same experiments.

An additional point of comparison between laboratories is that we always use freshly prepared HA columns for every experiment, because re-using columns introduced more experiment-to-experiment variation in our hands. However, some laboratories re-use HA columns multiple times (*3*) or even use only "used" columns, i.e., columns saturated with DNA (personal communication from K. Erixon to W. F. Blakely). Since the binding of DNA to HA appears to saturate (Figs. 1 and 2), and that DNA will not elute off the column even with a high concentration of phosphate buffer, the first time a column is used one might expect to see DNA binding; however, in subsequent re-uses of the column if all sites of binding are saturated no additional sticking would be seen.

### *"Repair" of the Radiation-Induced Binding of DNA to Hydroxyapatite*

The radiation-induced binding of DNA to HA was reversed by incubating irradiated cells in medium at 37°C, i.e., conditions which allow rejoining of DNA strand breaks, before cell lysis and DNA unwinding (Fig. 4). Although Fig. 4 shows data only for cells irradiated in air in medium without additive, 'repair' of the DNA binding to HA was also observed after irradiation of cells in hypoxic conditions, in PBS rather than in medium, and in the presence of DTT (data not shown). The 'repair' kinetics shown in Fig. 4 appears to be biphasic, and the 'repair' was complete to control levels in about 2 h. Although the data are too limited to quantify rates of repair of the components with precision, the reversal of binding appears to occur on a time scale slower than that of repair of single-strand breaks (e.g., single-strand break repair half-time is usually 2–4 min for the fast component (*13*)). On the other hand, the reversal of the DNA binding to HA may be on a time scale similar to that of repair of DNA double-strand breaks (half-time about 10 min for the fast component (*14*)).

## CONCLUSIONS

We have presented data indicating that ionizing radiation induces a lesion in cellular DNA which causes binding of DNA to hydroxyapatite. The binding has many of the properties characteristic of a cellular lesion which alters cell survival: it is dependent on radiation dose; it results in an OER of about 3; its formation is prevented by an SH-containing radioprotector; and it is "repaired" or reversed during a postirradiation incubation period. Our attempts to elucidate the nature of this lesion have not been successful, although the results suggest that the binding is not the result of DNA crosslinks to protein and the bound DNA is in the single-stranded form. However, we have not ruled out the possibility that DNA–DNA crosslinks are involved somehow in the binding; this possibility is being investigated. We believe that the binding is important for two reasons. First, on a practical note, we suggest that investigators using the DNA unwinding–hydroxyapatite chromatography technique must be aware of the problems caused by the binding and analyze their data accordingly. Second, because the binding shows many of the properties of a cellular lesion, its "repairability" being most interesting, the nature of this lesion should be determined and its biological relevance assessed.

## ACKNOWLEDGMENTS

We thank Dr. Peggy Olive for providing hydroxyapatite for the comparison experiments and for helpful discussions. This work was supported in part by the Mayo Foundation, by PHS Grants RO1 CA42167 (K.D.H.), RO1 CA15378 (N.L.O. and S.M.C.), and P30 CA43703 (N.L.O. and S.M.C.) from the National Cancer Institute, DHHS, and by the Armed Forces Radiobiology Research Institute, Defense Nuclear Agency work units 00150 and 00105 (W.F.B.).

RECEIVED: September 2, 1988; ACCEPTED: March 20, 1990

## REFERENCES

1. G. AHNSTRÖM and K. ERIXON, Radiation induced strand breakage in DNA from mammalian cells. Strand separation in alkaline solution. *Int. J. Radiat. Biol.* **23**, 285–289 (1973).
2. G. AHNSTRÖM and K.-A. EDVARDSSON, Radiation-induced single-strand breaks in DNA determined by rate of alkaline strand separation and hydroxylapatite chromatography: An alternative to velocity sedimentation. *Int. J. Radiat. Biol.* **26**, 493–497 (1974).
3. G. AHNSTRÖM and K. ERIXON, Measurement of strand breaks by alkaline denaturation and hydroxyapatite chromatography. In *DNA Repair: A Laboratory Manual of Research Procedures* (E. C. Fried-

berg and P. C. Hanawalt, Eds.), Vol. 1, Part B, pp. 403–418. Dekker, New York, 1981.

4. K. D. HELD, G. D. BREN, and D. C. MELDER, Interactions of radioprotectors and oxygen in cultured mammalian cells. II. Effects of dithiothreitol on radiation-induced DNA damage and comparison with cell survival. *Radiat. Res.* **108**, 296–306 (1986).

5. K. D. HELD, R. W. SYNEK, and E. L. POWERS, Radiation sensitivity of transforming DNA. *Int. J. Radiat. Biol.* **33**, 317–324 (1978).

6. S.-M. CHIU, L. R. FRIEDMAN, N. M. SOKANY, L.-Y. XUE, and N. L. OLEINICK, Nuclear matrix proteins are crosslinked to transcriptionally active gene sequences by ionizing radiation. *Radiat Res.* **107**, 24–38 (1986).

7. T. L. BROOKS, *Hydroxylapatite*. Behring Diagnostics, La Jolla, CA, 1981.

8. A. J. FORNACE and J. LITTLE, DNA cross-linking induced by X-rays and chemical agents. *Biochim. Biophys. Acta* **477**, 343–355 (1977).

9. R. E. MEYN, S. C. VAN ANKEREN, and W. T. JENKINS, The induction of DNA-protein crosslinks in hypoxic cells and their possible contribution to cell lethality. *Radiat. Res.* **109**, 419–429 (1987).

10. L. Y. XUE, L. R. FRIEDMAN, and N. L. Oleinick, Repair of chromatin damage in glutathione-depleted V-79 cells: Comparison of oxic and hypoxic conditions. *Radiat. Res.* **116**, 88–99 (1988).

11. P. L. OLIVE, Inhibition of DNA synthesis by nitroheterocycles. II. Mechanisms of cytotoxicity. *Br. J. Cancer* **40**, 94–104 (1979).

12. P. L. OLIVE, A. P. S. CHAN, C. S. CU, and S. H. MACPHAIL, Extending the range of sensitivity for detecting DNA strand breaks. *Br. J. Radiol.* **61**, 69–72 (1988).

13. W. F. BLAKELY, J. F. WARD, and E. I. JONER, A quantitative assay of deoxyribonucleic acid strand breaks and their repair in mammalian cells. *Anal. Biochem.* **124**, 125–133 (1982).

14. W. G. WOODS, Quantitation of the repair of gamma-radiation-induced double-strand DNA breaks in human fibroblasts. *Biochim Biophys. Acta* **655**, 342–348 (1981).

PROSTAGLANDINS LEUKOTRIENES AND ESSENTIAL FATTY ACIDS

Prostaglandins Leukotrienes and Essential Fatty Acids (1990) 39, 247–252
© Longman Group UK Ltd 1990

0952-3278/90/0039–0247/$10.00



# Behavioral and Physiological Effects of Leukotriene $C_4$

M. R. Landauer*, H. D. Davis* and T. L. Walden†

*Departments of Behavioural Sciences* and Radiation Biochemistry†, Armed Forces Radiobiology Research Institute, Bethesda, MD 20814–5145, USA (Reprint requests to MRL)*

*ABSTRACT.* **Leukotriene $C_4$ ($LTC_4$), a lipoxygenase metabolite of arachidonic acid, is a biological mediator of vasoregulation, pulmonary activity, shock, and inflammation, that has been demonstrated to have radioprotective efficacy. The effects of $LTC_4$ on locomotor activity, rectal temperature and hematocrit were examined. Subcutaneous administration of doses of 1.0 μg $LTC_4$/mouse or less did not affect locomotor activity. Doses of 5 or 10 μg $LTC_4$/mouse, however, resulted in almost complete cessation of locomotion within 12–14 min following treatment. At these doses, activity was suppressed for 2 h with complete recovery by 3 h postinjection. While a dose as high as 10 μg $LTC_4$ did not affect rectal temperature, 5 and 10 μg $LTC_4$ resulted in hematocrit increases of 10% and 40% respectively. Hematocrit returned to baseline within 1 h after a 5 μg pretreatment of $LTC_4$, and by 3 h following a 10 μg pretreatment. The duration of $LTC_4$-induced locomotor suppression did not correlate with previously determined durations of $LTC_4$-induced radioprotection.**

## INTRODUCTION

The leukotrienes have emerged as an important class of biological mediators, although little information is available regarding their effects on behavioral processes. They have physiological roles in vasoregulation (1–7), neurotransmission (8, 9), hormonal regulation (9, 10), smooth muscle contraction (9, 11), and may also participate in inflammatory processes (9, 12), anaphylactic shock (9, 11) and asthma (9, 13). The peptide leukotrienes are derived from arachidonic acid through the lipoxygenase pathway and consist of leukotrienes (LT) $C_4$, $D_4$, and $E_4$. Some biological activities attributed to $LTC_4$ may be indirect through its conversion to $LTD_4$ or $LTE_4$. Each of these compounds is biologically active and generally elicits biological responses through interaction with specific receptors on the cell surface of the target tissue (14). Some biological activities are induced directly by $LTC_4$. Others may be mediated its conversion to $LTD_4$ or $LTE_4$. Activation of the receptor sometimes initiates synthesis of other eicosanoids or biological mediators (9, 11, 12). Unlike prostaglandins (15), leukotrienes are not capable of crossing the blood/brain barrier (16), although they may be synthesized by brain tissue (12, 17).

Responses to eicosanoids may vary from tissue to tissue and between species. $LTC_4$, for example, results in vasodilation and increased blood flow in the skin of humans (7), but is vasoconstrictive in the dog coronary artery (18, 19). Direct administration of $LTC_4$ into the brain has been shown to alter behavior in rats (20).

$LTC_4$ has recently been shown to protect V79AO3 Chinese hamster fibroblasts in culture (21), and mouse hematopoietic stem cells in vivo from damage by ionizing radiation (22). It also enhances the survival of mice exposed to an otherwise lethal dose of gamma radiation (23). Leukotriene treatment must be administered prior to irradiation to elicit protection (22, 23). In mice, optimal radioprotection of hematopoietic stem cells is induced by $LTC_4$ treatment 5–15 min before radiation exposure. A pretreatment of 10 μg $LTC_4$ per mouse provides a dose reduction factor (DRF) of 1.6 for exogenous spleen colony forming units (CFU-S), and a DRF of 2.0 for granulocyte macrophage progenitor stem cells (22).

Radioprotectors are advantageous for both civil defense and clinical use. In a civil defense setting, agents that maximize protection from radiation in-

Date received 11 July 1989
Date accepted after revision 2 October 1989

jury with minimal suppression of behavior are required. In the clinic, behavioral side effects are less critical, and compounds that selectively protect normal tissues can be used to enhance the therapeutic efficacy of radio- and chemotherapy.

Because of the important biological roles and the significant radioprotection afforded by $LTC_4$ (22), we have investigated the time course of some behavioral and physiological responses of this compound. In this paper we describe the effects of subcutaneous administration of $LTC_4$ on locomotor behavior. Further, because $LTC_4$ is known to affect body temperature (20) and hematocrit (5) in rats, these parameters were monitored to determine if alterations in behavior were associated with these measures.

## MATERIALS AND METHODS

### Subjects

Male CD2F1 male mice, 10–12 weeks old (20–25 grams) were obtained from Charles River Breeding Laboratory (Raleigh, NC). They were quarantined on arrival and representative animals were screened for evidence of disease. Mice were housed in groups of 8–10 in Micro-Isolator cages on hardwood chip contact bedding in an AAALAC accredited facility. Rooms were maintained at 21 +/− 1 C with 50% relative humidity on a reversed 12–12 hr light-dark cycle with lights off at 2 pm. Commercial rodent chow (Wayne Rodent Blox) and acidified water (pH, 2.5) were freely available. All mice were euthanized by inhalation of carbon dioxide at the end of the experiment.

### Drug

$LTC_4$ was the generous gift of Dr. J. Rokach (Merok-Frosst Laboratories, Pointe Claire-Dorval, Canada). It was dissolved in physiological saline, and administered to mice subcutaneously (s.c.) in the nape of the neck in a volume of 100 $\mu$l. Each animal received a single injection of either the saline vehicle or 0.1, 1, 5 or 10 $\mu$g $LTC_4$ (N = 9–10/group).

### Locomotor activity measurement

A computerized Digiscan Animal Activity Monitory (Model RXYZCM-16, Omnitech Electronics, Columbus, Ohio) was used to quantitate locomotor behavior. This system has been previously used to monitor the effects of a number of radioprotective agents on locomotor activity, including prostaglandins (24, 25). Briefly, the apparatus used an array of infrared photodetectors spaced 2.5 cm apart to determine total distance travelled (horizontal activity; ambulation) and vertical sensors to record the number of vertical movements (vertical activity; rearing). The test chamber consisted of a 20 × 20 × 30.5 cm Plexiglas arena. The horizontal and vertical detectors were positioned 1.3 and 6.3 cm, respectively, above the floor of the arena.

Immediately following injection of $LTC_4$, animals were placed into the activity monitor where horizontal and vertical activity were recorded every 2 min for 1 h to ascertain the behavioral onset of the drug. Thereafter, activity was recorded at 1 h intervals for the next 2 h, after which time all groups had returned to control levels. All testing took place during the dark portion of the light-dark cycle. After each test, the apparatus was cleaned with a 50% alcohol solution.

### Temperature measurement

Rectal temperatures were monitored using a Thermistar Thermometer (Model 8110–20, Cole-Parmer, Chicago, IL) thermister probe (Model #423, Yellow Springs Instruments, Yellow Springs, OH). The probe was inserted 2 cm into the rectum and secured in place to the tail by a 2.5 cm strip of adhesive tape. It remained in place during the 3 h measurement period during which time the mice were restrained. The study was conducted in an environmentally controlled room set at 22° C. Mice received either s.c. injection of the saline vehicle (N=7) or 10 $\mu$g $LTC_4$ (N=7). The rectal temperature was recorded every 5 min for the first hour and at 30 min intervals for the next 2 h.

### Hematocrit

Animals received a s.c. injection of 0 (saline vehicle), 0.1, 1.0, 5.0, or 10.0 $\mu$g $LTC_4$ in saline (N=5–17/group). Mice were anesthetized with methoxyflurane (Pitman-Moore, Inc., Washington Crossing, N.J.) and blood samples for hematocrit determinations were obtained from the retro-orbital sinus. Measurements were made in duplicate and each animal was bled only once, at 0, 10, 60, or 120 min following $LTC_4$ treatment.

### Statistical analysis

One-way analysis of variance was used to determine significance levels for the effects of $LTC_4$ on locomotor activity and rectal temperature. Post hoc comparisons were made using Dunnett's test. Mean values of the hematocrit were compared to the control group using Student's t-tests.

## RESULTS

### Locomotor activity

$LTC_4$ produced a dose-dependent decrease in

locomotor activity. Doses of 0.1 and 1.0 μg did not significantly alter locomotor behavior compared to control values. Doses of 5.0 and 10.0 μg, however, resulted in pronounced reductions in locomotion. At these dosages, both ambulation and rearing were significantly reduced from control values within 6 min of injection and maximal effect (a decrement of 95–100%) was observed at 12–14 min. During the second hour, postinjection locomotor activity was approximately 50% of controls. All animals fully recovered locomotor performance by the third hour following drug administration. Since the time course and magnitude of the response for both horizontal and vertical activity were very similar, only one parameter (vertical activity) is illustrated in Figures 1 and 2.

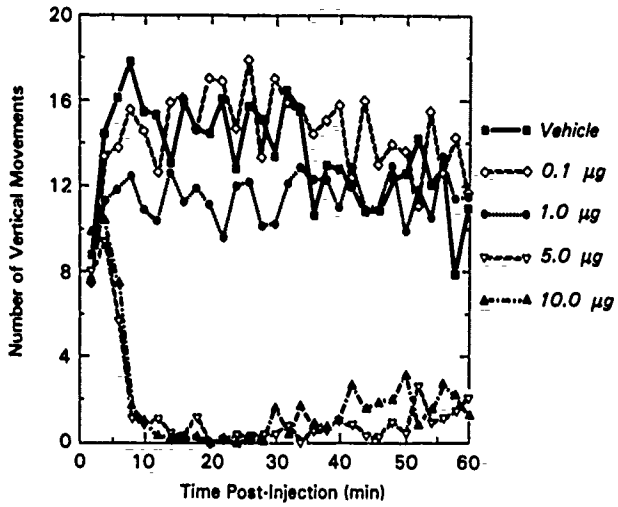


Fig. 1 Time course of leukotriene $C_4$ as a function of dose on vertical activity (rearing) during the first 60 min after injection (N= 9–10/group). Activity counts are presented in 2 min intervals. $LTC_4$ was administered subcutaneously immediately prior to assessment of locomotor activity. Maximal effect was reached 12–14 min postinjection. Similar results were obtained for horizontal activity (data not shown).

**Rectal temperature**

There were no significant differences in the rectal temperature of mice treated with saline or 10 μg $LTC_4$ (Fig. 3). The temperature of both the control and $LTC_4$ treated mice decreased as a function of time and is likely related to the duration of restraint.

**Hematocrit**

A dose-dependent increase in the hematocrit was observed in animals receiving $LTC_4$ (Table). Although no change in hematocrit was observed following doses of 0.1 or 1.0 μg/mouse, administration of 5.0 and 10.0 μg $LTC_4$ resulted in a 10% and 40% increase compared to controls, at 10 min postinjection. At 1 h after drug administration the 5.0 μg group had returned to control levels. Mice receiving 10.0 μg still had a 10% elevation in hematocrit at 2 h postinjection, and returned to normal by the third hour following treatment.

## DISCUSSION

Doses of $LTC_4$ which have previously been shown to be radioprotective (5 to 10 μg $LTC_4$/mouse which is equivalent to 200 to 400 μg/kg body weight) (22, 23) resulted in a rapid reduction in locomotor activity and significant increases in the hematocrit, although rectal temperature remained unaffected. The decrease in locomotor behavior was dose dependent. While doses of 1 μg or less did not alter locomotor activity, administration of 5 and 10 μg $LTC_4$ resulted in almost total cessation of ambulation and rearing within 10–15 min after single s.c. injection. The animals did not fully recover from this reduction in activity until 3 h post-injection. Although this is the first study to report the effects of

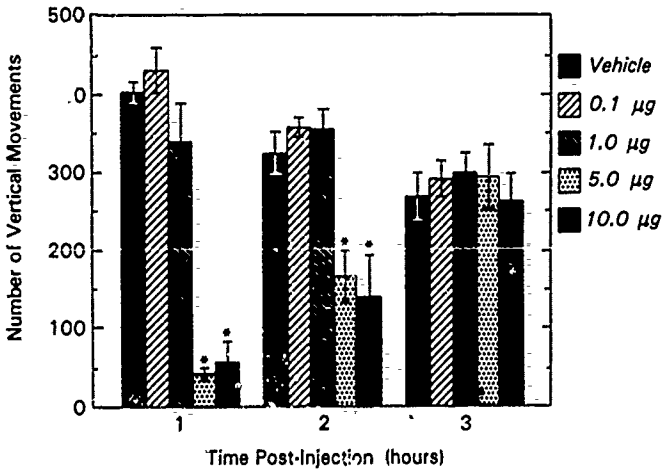


Fig. 2 Duration of action of the effects $LTC_4$ on vertical activity (rearing). By 3 h postinjection all groups had returned to control levels (N= 9–10/group). Horizontal activity showed a similar pattern of recovery (data not shown).
**Significantly ($p < 0.01$) from vehicle control group.

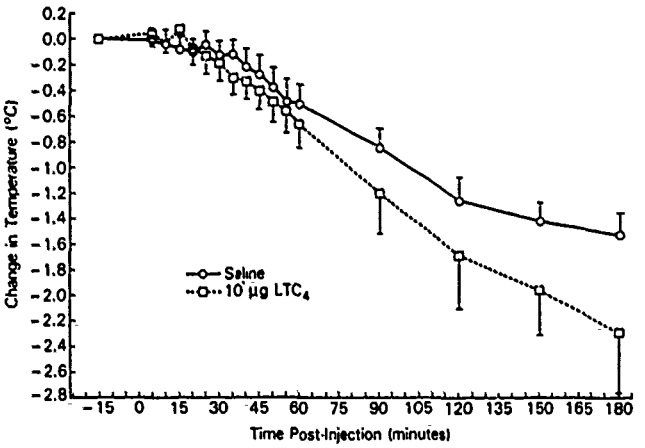


**Fig. 3** Effect of $LTC_4$ (10 $\mu$g/mouse) on rectal temperature, expressed as the change in temperature from baseline levels taken 15 min prior to drug administration. There were no significant differences between the control mice and the $LTC_4$ group at any during the 3 h recording period (N=7/group).

**Table** Effect of $LTC_4$ on hematocrit

| ug LTC4 per mouse | Time Post-Treatment 10 min | 60 min | 120 min | 180 min |
|---|---|---|---|---|
| 0.0 | 49.6 +/- 0.4 | — | — | — |
| 0.1 | 48.8 +/- 0.4 | 48.5 +/- 0.6 | — | — |
| 1.0 | 50.0 +/- 0.1 | 48.3 +/- 0.5 | — | — |
| 5.0 | 55.0 +/- 0.3*** | 48.6 +/- 1.1 | — | — |
| 10.0 | 69.6 +/- 1.4*** | 63.0 +/- 1.9*** | 54.8 +/- 1.3*** | 50.2 +/- 1.3 |

*** significantly different from control, $p < 0.0001$, t-test (N = 5–17/group)

s.c. administration of $LTC_4$ on locomotor behavior in mice, Brus et al (20) found that intracerebroventricular (ICV) administration of 1 $\mu$g of this compound to rats produced locomotor deficits that were apparent at 1 and 30 min after injection but not at 1 h. No decrease in locomotor activity was observed in mice in the present study following s.c. administration of 1 $\mu$g $LTC_4$.

Other eicosanoids such as prostaglandins of the E series result in a similar suppression of locomotor activity of rats (26), and we have recently described (24, 25) the decrease in locomotor behavior of mice treated with 16,16-dimethyl prostaglandin $E_2$ ($DiPGE_2$). Pretreatment with 40 $\mu$g/mouse $DiPGE_2$ provided a dose reduction factor (DRF) of 1.72 for animal survival following gamma irradiation (27). $DiPGE_2$ reduction of locomotor activity was dose dependent and required up to 30 h after administration of 40 $\mu$g/mouse to return to normal.

The decrease in ambulation and rearing by $LTC_4$ is comparable to that observed for 200 mg/kg of WR-2721, a thiol radioprotective agent with a DRF at this dose of approximately 1.6 (28–30). Although $LTC_4$ contains a thiol ether, the radioprotective action is not believed to act by a thiol free radical scavenging mechanism (22). In terms of radioprotective efficacy, five times more endogenous spleen colonies (E-CFU) survive irradiation when animals are pretreated with 10 $\mu$g $LTC_4$ than for mice receiving equivalent doses of $LTD_4$ or $LTE_4$ (22). This indicates that the radioprotection is attributable to the effects of $LTC_4$ rather than its conversion to $LTD_4$ or to $LTE_4$. The extent to which $LTC_4$ mediated behavioral effects may be due to other leukotrienes has yet to be determined.

Subcutaneous administration of doses of $LTC_4$ (10 $\mu$g) that induced radioprotection (22), reduced locomotor activity, and elevated the hematocrit, did not significantly affect rectal temperature. A similar lack of temperature response was observed in rats receiving 1 $\mu$g $LTC_4$ by ICV (31) or intrapreoptic administration (32). A decrease in body temperature, however, was observed in rats 10 min following an ICV injection of 7.5 $\mu$g $LTC_4$ (20). Possible effects of leukotrienes on temperature elevation have been implied from $LTC_4$ measurements in tissue biopsies of women with dysmenorrhea (33).

Although $LTC_4$ can be produced by nerve tissue (9, 17) and act as a neurotransmitter (8), it is not capable of crossing the blood/brain barrier (16). Therefore, it is unlikely that the rapid onset in suppression of locomotor behavior is the result of a

direct action on the central nervous system. The decreased activity observed in the present study may either result from intermediate messengers produced by the leukotriene, or in response to the physiologioal action of $LTC_4$. Some physiological responses to leukotrienes are mediated by inducing synthesis of other eicosanoids, such as thromboxanes and prostaglandins (11) that in turn produce the biological response. Prostaglandins are known to cross the blood/brain barrier (15) and to suppress locomotor activity (24–26).

Leukotrienes have direct potent activity on constriction of tracheal and bronchial smooth muscle (9, 11) and also vasoactivity (1, 4, 7, 17). Within 10 min after treatment with doses of $LTC_4$ that produced a behavioral decrement (5 and 10 $\mu$g/mouse), hematocrit levels had increased by at least 10% and 40% respectively. Increases in hematocrit and mean arterial blood pressure have been reported previously following intravenous administration of $LTC_4$ to rats (5, 6). Moreover, $LTC_4$ is known to promote plasma leakage from the vasculature (1). The short latency for the reduction in locomotor activity may reflect the rapid physiological responses induced by $LTC_4$. A 10% or greater elevation in hematocrit would likely increase resistance to blood flow, in turn reducing oxygen delivery. $LTC_4$ has been previously shown to decrease coronary flow (18, 19) with a concomitant reduction in contractile force (34). A reduction of blood flow to the heart could affect locomotor activity, although we have not determined if $LTC_4$ induces vasoconstriction of mouse coronary arteries. However, a decrease in the quantity of blood obtained from mice by cardiac puncture was observed at times corresponding to the increase in hematocrit and optimal period for radioprotection following administration of $LTC_4$ (T. L. Walden, Jr., unpublished).

Maintenance of the duration of the locomotor decrement does not appear to be associated with the physiological responses producing the hematocrit elevation. With 5 $\mu$g $LTC_4$, locomotor behavior was reduced by 88% within 1 h and 50% by 2 h post-treatment (Fig. 2). In a parallel study (Table), the hematocrit, after 5 $\mu$g $LTC_4$, had returned to normal within 1 h. In addition, the duration of the radioprotective action of $LTC_4$ (22) does not follow the same time course as that found for the suppression of locomotor behavior. Administration of 10 $\mu$g $LTC_4$ 5–15 min prior to radiation exposure resulted in optimal radioprotection to mouse hematopoietic stem cells. At this dose, the protective activity was lost by 90 min post-treatment (22), while locomotor activity did not return to control level until 3 h after $LTC_4$ administration.

The toxic effects of radioprotectors are well established and occur at both the cellular and tissue levels (35). We have observed that the onset of behavioral toxicity as measured by locomotor activity decrements corresponds to the optimal pre-radiation treatment time for a variety of radioprotective compounds including $LTC_4$ (this study), $DiPGE_2$ (24, 25), WR-2721 (28–30) and glucan (36). The duration of the radioprotective effect for each of these is shorter than the behavioral decrement. We are continuing to explore the use of the locomotor activity test as an effective means to predict the optimal pre-radiation time for administration of radioprotectant compounds.

It may also be possible to mitigate the behavioral toxicity of $LTC_4$ without altering its radioprotective properties. This could be accomplished by co-administration of $LTC_4$ with agents that reverse the behavioral disruption. Alternatively, it may be feasible to develop $LTC_4$ analogs that retain the radioprotective or other clinically beneficial properties without the production of concomitant behavioral side-effects. In addition, it is likely that a mixture of radioprotective agents that act by different mechanisms will be required to provide a radioprotective compound that will offer effective protection from ionizing radiation with minimal toxicity.

## Acknowledgements

We thank M. E. Cranford, N. K. Farzaneh and M. E. Faccioli for their assistance during this experiment. Portions of this work were presented at the 37th annual meeting of the Radiation Research Society, Seattle, WA in March 1989. This research was supported by the Armed Forces Radiobiology Research Institute, Defense Nuclear Agency, under work units 00159 and 00162. The views presented in this paper are those of the authors; no endorsement by the Defense Nuclear Agency has been given or should be inferred. Research was conducted according to the principles enunciated in the 'Guide for the Care and Use of Laboratory Animals' prepared by the Institute of Laboratory Animal Resources, National Research Council.

## References

1. Dahlen S-E, Bjork J, Hedqvist P, Arfors K-E, Hammarstrom S, Lindgren J A, Samuelsson B. Leukotrienes promote plasma leakage and leukocyte adhesion in postcapillary venules: *In vivo* effects with relevance to the acute inflammatory response. Proceedings of the National Academy of Sciences (USA) 78: 3887–3891, 1981.
2. Lippton H L, Armstead W M, Hyman A L, Kadowitz P J. Vasoconstrictor effects of leukotrienes $C_4$ and $D_4$ in the feline mesenteric vascular bed. Prostaglandins 27: 233–243, 1984.
3. Malik A B, Perlman M B, Cooper J A, Noonan T, Bizios R. Pulmonary microvascular effects of arachidonic acid metabolites and their role in lung vascular injury. Federation Proceedings 44: 36–42, 1985.
4. Berkowitz B A, Zabko-Potapovich B, Valocik R, Gleason J G. Effects of the leukotrienes on the vasculature and blood pressure of different species. Journal of Pharmacology and Experimental Therapeutics 229: 105–112, 1984.
5. Badr K F, Baylis C, Pferrer J M, Pfeffer M A,

Soberman R J, Lewis R A, Austen K F, Corey E J, Brenner B F. Renal and systemic hemodynamic responses to intravenous infusion of leukotriene $C_4$ in the rat. Circulation Research 54: 492–499, 1984.
6. Filep J, Foldes-Filep E, Frolich J C. Vascular responses to leukotriene $B_4$, $C_4$, and $D_4$ following FPL 55712, indomethacin, saralasin, phentolamine and verapamil in the conscious rat. British Journal of Pharmacology 90: 431–439, 1987.
7. Bisgaard H, Kristensen J, Sondergaard J. The effect of leukotriene $C_4$ and $D_4$ on cutaneous blood flow in humans. Prostaglandins 23: 797–801, 1982.
8. Palmer M R, Mathews R, Murphy R C, Hoffer B J. Leukotriene C elicits a prolonged excitation of cerebellar Purkinje neurons. Neuroscience Letters 18: 173–180, 1980.
9. Samuelsson B, Dahlen S-E, Lindgren J A, Rouzer C A, Serhan C N. Leukotrienes and lipoxins: structures, biosynthesis, and biological effects. Science 237: 1171–1176, 1987.
10. Hulting A L, Lindgren J A, Hokfelt T, Eneroth P, Werner S, Patrono C, Samuelsson B. Leukotriene $C_4$ as a mediator of lutenizing hormone release from rat anterior pituitary cells. Proceedings of the National Academy of Sciences (USA) 82: 3834–3838, 1985.
11. Dahlen S-E, Hedqvist P, Westund P, Granstrom E, Hammarstrom S, Lindgren J A, Radmark O. Mechanisms of leukotriene-induced contractions of guinea pig airways: Leukotriene $C_4$ has a potent direct action whereas leukotriene $B_4$ acts indirectly. Acta Physiologica Scandinavica 118: 393–403, 1983.
12. Samuelsson B, Leukotrienes: Mediators of immediate hypersensitivity reactions and inflammation. Science 220: 568–575, 1983.
13. Dahlen S-E, Hansson G, Hedqvist P, Bjorck T, Granstrom E, Dahlen B. Allergen challenge of the lung tissue from asthmatics elicits bronchial contraction that correlates with the release of leukotrienes $C_4$, $D_4$, and $E_4$. Proceedings of the National Academy of Sciences (USA) 80: 1712–1716, 1983.
14. Robertson R P, Characterization and regulation of prostaglandin and leukotriene receptors: An overview. Prostaglandins 31: 395–411, 1986.
15. Wolfe L S, Eicosanoids: Prostaglandins, thromboxanes, leukotrienes, and other derivatives of carbon-20 unsaturated fatty acids. Journal of Neurochemistry 38: 1–14, 1982.
16. Spector R, Goetzl E J. Commentary: The role of concentrative leukotriene transport systems in the central nervous system. Biochemical Pharmacology 35: 2849–2853, 1986.
17. Kiwak K J, Moskowitz M A, Levine L. Leukcotriene production in gerbil brain after ischemic insult, subarachnoid hemorrhage, and concussive injury. Journal of Neurosurgery 62: 865–869, 1985.
18. Wargovich T, Mehta J, Nichols W W, Pepine C J, Conti R. Reduction of blood flow in normal and narrowed coronary arteries of dogs by leukotriene $C_4$. Journal of the American College of Cardiology 6: 1047–1051, 1985.
19. Woodman O L, Dusting G J. Coronary vasoconstriction induced by leucotrienes in the anesthetized dog. European Journal of Pharmacology 86: 125–128, 1982.
20. Brus R, Krzeminsk-i T, Juraszczyk Z, Kurcok A, Felinska W, Kozik W. Central effects of leukotriene C4 and D4 in rats and mice. Biomedica Biochimica Acta 45: 1153-1158, 1986.
21. Walden T L Jr, Holahan E V, Catravas G N. Development of a model system to study leukotriene-induced modification of radiosensitivity in mammalian cells. Lipid Research 25: 587–590, 1986.
22. Walden T L Jr, Patchen M L, MaoVittie T J. Leukotriene-induced radioprotection of hematopoietic stem cells in mice. Radiation Research 113: 388–395, 1988.
23. Walden T L Jr, Pretreatment with leukotriene $C_4$ enhances the whole-animal survival of mice exposed to ionizing radiation. Annals of the New York Academy of Sciences 524: 431–433, 1988.
24. Landauer M R, Walden T L Jr, Davis H D, Dominitz J A, Alterations in locomotor activity induced by radioprotective doses of 16,16-dimethyl prostaglandin $E_2$, pp 244–251 in Prostaglandins and Lipid Metabolism in Radiation Injury (T L Walden Jr, H N Hughes eds) Plenum Press, New York, 1987.
25. Landauer M R, Walden T L Jr, Davis, H D. Behavioral effects of radioprotective agents in mice: Combination of WR-2721 and 16,16 dimethyl prostaglandin $E_2$. Proceedings of the 21 Annual Meeting of the European Society for Radiation Biology, in press.
26. Gilmore D P, Shakh A A, The effect of prostaglandin $E_2$ in inducing sedation in the rat. Prostaglandins 2: 143–152, 1972.
27. Walden T L Jr, Patchen M L, Snyder S L. 16,16-Dimethyl prostaglandin $E_2$ increases survival in mice following irradiation, Radiation Research 109: 440–448, 1987.
28. Landauer M R, Davis H D, Dominitz J D, Weiss J F, Dose and time relationships of the radioprotector WR-2721 on locomotor activity in mice, Pharmacology, Biochemistry and Behavior 27: 573–576, 1987.
29. Landauer M R, Davis H D, Dominitz J D, Weiss J F. Comparative behavioral toxicity of four sulfhydryl radioprotective compounds in mice: WR-2721, cysteamine, diethyldithiocarbamate, and N-acetylcysteamine, Pharmacology and Therapeutics 39: 97–100, 1988.
30. Landauer M R, Davis H D, Dominitz J D, Weiss J F. Long-term effects of radioprotector WR-2721 on locomotor activity and body weight of mice following exposure to ionizing radiation, Toxicology 49: 315–323, 1988.
31. O'Rourke S T, Rudy T A. Intracerebroventricular and preoptic injections of $LTC_4$, $D_4$, and $E_4$ in the rat: Lack of febrile effect. Brain Research 295: 283–288, 1984.
32. Mashburn T A Jr, Llanos-Q J, Ahokas R A, Blatteis C M. Thermal and acute-phase protein responses of guinea pigs to intrapreoptic injections of leukotrienes. Brain Research 376: 285–291, 1986.
33. Rees M C, DiMarzo V, Tippins J R, Morris H R, Turnbull A C. Leukotriene release by endometrium and myometrium throughout the menstrual cycle in dysmenorrhoea and menorrhagia. Journal of Endocrinology 113: 291–295, 1987.
34. Roth D M, Lefer D L, Hock C E, Lefer A M. Effects of peptide leukotrienes on cardiac dynamics in rat, cat, and guinea pig heart. American Journal of Physiology 249: 477–484, 1985.
35. Maisin J R, Protection against ionizing radiation by combinations of radioprotectors. Pharmacology and Therapeutics 39: 189–193, 1988.
36. Landauer M R, Patchen M L, Davis H D. Time course of behavioral effects in mice treated with soluble glucan. Abstracts of the 4th International Conference on Immunopharmacology, Osaka, Japan, p 91, 1988.

In: *Frontiers in Radiation Biology*, Edited by E. Riklis, VCH Publishers, New York, 1990, pp. 199-207.

# Behavioral effects of radioprotective agents in mice: combination of WR-2721 and 16,16 dimethyl prostaglandin $E_2$

MICHAEL R. LANDAUER[1], THOMAS L. WALDEN, JR[2] AND HIRSCH D. DAVIS[1]
*Departments of [1]Behavioral Sciences & [2]Radiation Biochemistry, Armed Forces Radiobiology Research Institute, Bethesda, MD 20814-5145 USA*

## Introduction

Although the radioprotective properties of a number of compounds have been investigated in the last 40 years (see Giambarresi and Jacobs, 1987; Weiss and Simic, 1988), the consideration and testing of the behavioral effects of these agents has only recently begun to be systematically investigated (Bogo, 1988; Landauer et al., 1987a, 1987c, 1988b, 1988c, 1988d, 1989). Behavioral toxicity of an agent that enhances radiotherapeutic efficacy is not necessarily a limiting factor in clinical use where small numbers of patients can be monitored and treated. However, an effective drug-screening program for radioprotective agents must evaluate the behavioral toxicity of those compounds that have potential use for humans in radiation accidents and in civil defense situations.

A program has been implemented in our laboratory to screen radioprotective agents for behavioral toxicity by quantitating their effects on spontaneous locomotor activity. Tests of locomotor activity (Reiter and MacPhail, 1982; Tilson and Mitchell, 1984) have been recommended for the evaluation of chemical compounds by such agencies as the United States Environmental Protection Agency and the World Health Organization (Sette and Levine, 1986; WHO, 1986). Locomotion in the adult animal is a naturally occurring behavior, and therefore measurement of this parameter does not involve long-term training procedures. Spontaneous locomotor behavior can be assessed without bias by using automated devices that detect movements by a series of infrared-sensitive photodetectors (Reiter and MacPhail, 1982). Locomotor activity has been determined to be a sensitive measure for the assessment of the behavioral toxicity of radioprotectors (Landauer et al., 1987a,

1987c, 1988b, 1988c; Liu et al., 1987; Tikal et al., 1979) as well as ionizing radiation (Kimmeldorf and Hunt, 1965; Landauer et al., 1987b, 1988a).

Sulfhydryl compounds such as S-2(3-aminopropylamino) ethylphosphorothioic acid (also known as WR-2721, ethiofos, or gammaphos) are among the leading radioprotectors (Davidson et al., 1980). The radioprotective effects of some prostaglandins such as 16,16 dimethyl prostaglandin $E_2$ ($DiPGE_2$), a methylated derivative of the naturally occurring prostaglandin $E_2$, are also well documented (Hanson and Thomas, 1983; Hanson and Ainsworth, 1985; Hanson, 1987; Hanson et al., 1988; Walden et al., 1987; Steel and Catravas, 1988). However, both WR-2721 (Bogo et al., 1985; Landauer et al., 1987a, 1988b; Liu et al., 1987) and $DiPGE_2$ (Landauer et al., 1987c) produce performance decrements at doses that are radioprotective. One method to minimize side effects of a compound while maximizing protection is through combinations with other radioprotective agents. Ideally, such combinations should provide additive or synergistic protection with minimal behavioral toxicity. Combinations of these agents have been found to increase radioprotection (Maisin, 1988; Patchen et al., 1988; Weiss et al., 1987), but little information is available on their behavioral effects. This study was undertaken to evaluate whether combinations of WR-2721 and $DiPGE_2$ would provide a higher degree of radioprotection than either drug alone, and to determine the behavioral toxicity associated with this treatment.

## Materials and Methods

### *Subjects*

Male CD2F1 mice, 6–8 weeks old were obtained from Charles River (Kingston, NY). All animals were quarantined for 2 weeks while representative animals were examined for physiological and serological indications of illness or *Pseudomonas* infections. Animals were housed 8–10 to a cage, maintained on a 12-hr light-dark cycle, and provided Wayne Rodent Blox diet and acidified (pH 2.5) water (McPherson, 1963) ad libitum. Animals weighed 20–25 grams at the time of the experiments.

### *Radioprotection*

Mice were placed in well-ventilated plastic restraint devices and irradiated in a bilateral cobalt-60 field at a dose rate of 1.0 Gy/min as previously described (Snyder et al., 1986). Before irradiation, animals were administered either saline (controls), WR-2721 (200 mg/kg, IP), $DiPGE_2$ (0.4 mg/kg, SC), or both compounds. WR-2721 was injected 15 min prior to radiation exposure, and $DiPGE_2$ 10 min before.

Control animals received vehicle alone. Radiation survival curves were determined for the control and treated animals with doses ranging from 7 to 22 Gy. A minimum of 30 mice were used for each dose at each time point. Irradiated animals were monitored for the fraction surviving 30 days postirradiation, and the LD50 values were determined by probit analysis. (Pilot studies indicated that a higher dose of $DiPGE_2$ (1.6 mg/kg) combined with 200 mg/kg WR-2721 resulted in extreme toxicity, with 43% of the mice dying within 30 min. Therefore, this combination was not examined further.

***Behavioral Testing***

Locomotor behavior was measured using a computerized animal activity monitor (Model RXYZCM-16, Omnitech Electronics, Columbus, Ohio), which recorded horizontal activity (ambulation) by means of infrared photodetectors. All mice received two injections. The first injection was either WR-2721 or the saline vehicle administered IP. The second injection, administered 5 min after the first, was either a SC dose of $DiPGE_2$ or the vehicle, 4% ethanol in saline. Four groups of animals were tested (N = 8–12/group). Group 1 animals received IP injections of 200 mg/kg WR-2721 followed by SC injections of 0.4 mg/kg $DiPGE_2$; group 2, two vehicle injections; group 3, 200 mg/kg WR-2721 IP followed by SC vehicle injections; and group 4, IP saline injections followed by 0.4 mg/kg $DiPGE_2$ SC. Mice were placed in the test apparatus immediately following the second injection. Locomotor activity was monitored at 5-min intervals for the first 60 min to determine the latency of onset of the drug. Thereafter, activity was recorded at 1-hr intervals for the next 6 hr, after which all groups returned to control values. Since the mouse is a nocturnal animal, all testing took place during the dark portion of the light-dark cycle.

Analysis of variance with repeated measures was performed on the locomotor activity data. Post hoc comparisons were made using Dunnett's test. Radiation survival data were analyzed by probit analysis, and the LD50/30 and 95% confidence intervals were determined.

## Results and Discussion

Coadministration of WR-2721 (200 mg/kg) and $DiPGE_2$ (0.4 mg/kg) provided a greater dose reduction factor (DRF) than either compound alone (see Table 1). The combination did not result in any lethality from the drugs alone. The LD50/30 of control mice was 8.35 Gy. Pretreatment with WR-2721 provided a DRF of 1.90, while pretreatment with $DiPGE_2$ increased survival with a DRF of 1.45. The LD50/30 for mice receiving the combined treatment was 17.91 Gy (DRF = 2.15).

Table 1: Radioprotective and behavioral effects of WR-2721 and 16,16 Dimethyl prostaglandin $E_2$ alone and in combination

| | LD50/30 (Gy) (95% confidence limits) | DRF | Behavioral onset | Duration of behavioral decrement | Diarrhea |
|---|---|---|---|---|---|
| Control | 8.35 (8.27–8.43) | – | – | – | No |
| WR-2721 (200 mg/kg) | 15.84 (15.37–16.23) | 1.90 | 15 min | 3 hr | No |
| $DiPGE_2$ (0.4 mg/kg) | 12.07 (11.56–12.53) | 1.45 | 5 min | 2 hr | Yes |
| WR-2721 + $DiPGE_2$ | 17.91 (17.54–18.22) | 2.15 | 5 min | 6 hr | Yes |

The time course of performance decrement as measured by alterations in locomotor activity was also assessed in nonirradiated mice receiving 200 mg/kg WR-2721 or 0.4 mg/kg $DiPGE_2$ alone or in combination. Each of the compounds separately and in combination induced almost complete cessation of locomotor activity. WR-2721 produced significant locomotor deficits within 15 min and lasted for 3 hr. Administration of 0.4 mg/kg $DiPGE_2$ resulted in significant decrements within 5 min of injection and persisted for 2 hr. The combination of WR-2721 and $DiPGE_2$ resulted in deficits within 5 min of injection and remained below control levels for 6 hr following drug administration.

Diarrhea was a noticeable side effect of $DiPGE_2$ when administered in a dose of 0.4 mg/kg. The severity of this condition has been shown to be dose-dependent (Walden et al., 1987), although this factor was not quantified in the present study. The combination of $DiPGE_2$ and WR-2721 did not appear to alter the production of diarrhea by the prostaglandin.

The results of this study indicate that following exposure to gamma radiation the combination of WR-2721 and $DiPGE_2$ provided a greater protective effect than either compound alone. However, when 453 mg/kg WR-2721 was combined with 0.4 mg/kg $DiPGE_2$ in female mice receiving neutron radiation, an enhanced protective ratio was not found (Steel et al., 1988). This may reflect differences in the dose of WR-2721 (200 vs. 453 mg/kg), the strain and sex of the mice used (CD2F1 males vs. B6D2F1 females), or the quality of radiation (gamma vs. neutron).

In studies where the behavioral toxicity of radioprotectors had been determined, higher degrees of protection are usually correlated with greater performance decrement. This relationship has been observed for sulfhydryl compounds such as WR-2721, cysteamine, N-acetylcysteine, and diethyldithiocarbamate (Landauer et al., 1988c). Similar effects have been observed for $DiPGE_2$ (Landauer et al., 1987c), leukotriene $C_4$ (Landauer et al., 1989) and platelet activating factor (Landauer, Hughes, Walden, and Davis, unpublished), as well as for biological response modifiers such as glucan (Landauer et al., 1988d). Within this group there are some qualitative differences. Some compounds provide better radioprotection at behaviorally tolerated doses than others.

WR-2721 is one of the most effective radioprotective agents in terms of its DRF. It appears to have some value in the treatment of cancer patients undergoing radiotherapy or chemotherapy (Glover et al., 1988). However, side effects including hypotension, emesis, somnolence, and hypocalcemia have been noted in clinical trials (Turrisi et al., 1983). Several studies in animals have used reduced doses of WR-2721 in combination with other protective agents in an attempt to provide maximal radioprotection with minimal toxicity. Each of these experiments, including our own, has still used behaviorally toxic doses of WR-2721. Patchen et al., (1988) reported enhanced protection with combinations of WR-2721 and glucan F. The dose of glucan (250 mg/kg, IV) used, however, produced locomotor decrements for approximately 6 hr postinjection (Landauer et al., 1988d). Mice treated with glucan and WR-2721 exhibited enhanced locomotor performance compared to animals treated with WR-2721 alone, but not until the third week following treatment (Landauer and Patchen, unpublished). Similarly, Weiss et al., (1987) were able to increase the protection and reduce the lethal toxicity of WR-2721 by combining it with selenium. The combination of doses that offered the best protection (400–600 mg/kg WR-2721 and 1.6 mg/kg selenium) were, however, also behaviorally toxic to the animals (Landauer and Weiss, unpublished). Moreover, as the current study indicates, combinations of agents that enhance radioprotection may also exacerbate acute behavioral toxicity. Attempts are being made to determine optimal doses of WR-2721 and agents used in combination (e.g., glucan, selenium) that will provide protection with minimal behavioral effects.

The duration of the radioprotective activity for both WR-2721 and $DiPGE_2$ has previously been demonstrated to be much shorter than the disruptive effects on locomotor activity. The hemodynamic effects of WR-2721 that have been shown to result in severe hypotension also persist longer (> 4 hr) than the radioprotective action (approximately 1 hr) of this drug (Kuna et al., 1983). A similar relationship has been observed for $DiPGE_2$ (Landauer et al., 1987c). The differences in the relatively short duration of the radioprotective effects compared to the longer acting,

detrimental behavioral and physiological side effects indicate that separate mechanisms of action are involved.

It is difficult from these experiments to determine whether the behavioral effects are mediated by a central mechanism. While prostaglandins are capable of passing the blood-brain barrier (Bito et al., 1976), WR-2721 is not (Utley et al., 1976). Indirect effects on the central nervous system may result from a decrease in cerebral blood flow following administration of $DiPGE_2$. $PGE_2$-induced sedation is believed to occur through this mechanism (Gilmore and Shakh, 1972).

A combination of WR-2721 and $DiPGE_2$ has been shown to protect murine intestinal crypt cells from radiation injury (Hanson et al., 1988). One possibility for the enhanced protection observed by the combined treatment in that study may be an altered biodistribution of WR-2721 by $DiPGE_2$. The optimal time for $DiPGE_2$ administration for intestinal crypt cell radioprotection is 1–3 hr prior to irradiation (Hanson and Thomas, 1983), while whole-animal survival is best when the drug is administered 5–30 min before whole-body radiation exposure (Walden et al., 1987). Therefore, the time of administration for WR-2721 and $DiPGE_2$ may be critical according to the mechanism(s) involved in the protection. In the present survival study, WR-2721 was administered 5 min before $DiPGE_2$. Radioprotective doses of $DiPGE_2$ produce profound increases in the hematocrit within 5–10 min postadministration (Walden et al., 1987), which could affect the biodistribution of WR-2721 and therefore alter its radioprotective effectiveness. When trying to determine the mechanism(s) involved in the resultant additional radioprotection, questions arise as to whether we are observing a minimally effective WR-2721 activity added to a maximal $DiPGE_2$ response, a small contribution of $DiPGE_2$ being added to a maximal WR-2721 response, or some other combination.

Both WR-2721 and $DiPGE_2$ suppressed locomotor activity for several hours and the combination exacerbated the duration of decrement. This makes it unlikely that these compounds administered at comparative doses for humans would be useful as radioprotectors when mental and physical alertness must be maintained. Since the duration of radioprotective efficacy and performance decrement of both these compounds differ significantly, it is likely they are producing their radioprotective and behavioral effects by different mechanisms. It may be possible, therefore, to mitigate the behavioral and physiological side effects by providing additional compounds to formulate a radioprotective cocktail that has the ability to maintain protection in the absence of behavioral decrements.

## Acknowledgements

We wish to thank Dr. Douglas Morton of The Upjohn Company for very

kindly supplying the prostaglandin used in this investigation and the Experimental Therapeutics Division, Walter Reed Army Institute of Research, Washington, DC for the WR-2721. Special thanks to Modeste Greenville and Catherine Sund for their editorial assistance. This research was supported by the Armed Forces Radiobiology Research Institute, Defense Nuclear Agency under Research Work Units 00159 and 00162. The views presented in this paper are those of the authors. No endorsement by the Defense Nuclear Agency has been given or should be inferred. Research was conducted according to the principles enunciated in the "Guide for the Care and Use of Laboratory Animals" prepared by the Institute of Animal Laboratory Resources, National Research Council.

## References

Bito, L.Z., Davson, H., and Hollingsworth, J.R. 1976. Facilitated transport of prostaglandins across the blood-cerebrospinal fluid and blood-brain barriers. *Journal of Physiology*, 253, 273–285.

Bogo, V. 1988. Behavioral radioprotection. Toxicology, 39, 73–78.

Bogo, V., Jacobs, A.J., and Weiss, J.F. 1985. Behavioral toxicity and efficacy of WR-2721 as a radioprotectant. *Radiation Research*, 104, 182–190.

Davidson, D.E., Grenan, M.M., and Sweeney, T.R. 1980. Biological characteristics of some improved radioprotectors. Radiation Sensitizers: Their Use in the Clinical Management of Cancer, edited by L.W. Brady, (New York: Masson) pp. 309–320.

Giambarresi, L., and Jacobs, A.J. 1987. Radioprotectants. Military Radiobiology, edited by J.J. Conklin and R.I. Walker, (New York: Academic Press) pp. 265–301.

Gilmore, D.P., and Shakh, A.A. 1972. The effect of prostaglandin $E_2$ in inducing sedation in the rat. *Prostaglandins 2, 143–151.*

Hanson, W.R. 1987. Radioprotection of murine intestine by WR-2721, 16,16 dimethyl prostaglandin $E_2$ and the combination of both agents. *Radiation Research*, 111, 361–373.

Hanson, W.R., and Ainsworth, E.J. 1985. 16,16-Dimethyl prostaglandin $E_2$ induced radioprotection in murine intestinal and hematopoietic stem cells. *Radiation Research*, 103, 196–203.

Hanson, W.R., Houseman, K.A., and Collins, P.W. 1988. Radiation protection *in vivo* by prostaglandins and related compounds of the arachidonic acid cascade. *Pharmacology and Therapeutics*, 39, 347–356.

Hanson, W.R., and Thomas, C. 1983. 16,16-Dimethyl prostaglandin $E_2$ increases survival of murine intestinal stem cells when given before photon radiation. *Radiation Research*, 96, 393–398.

Kimeldorf, D., and Hunt, E. 1965. Ionizing Radiation: Neural Function and Behavior. (New York: Academic Press).

Kuna, P., Volenec, K., Vodicka, I., and Dostal, M. 1983. Radioprotective and hemodynamic effects of WR-2721 and cystamine in rats: Time course studies. *Neoplasma*, 30, 349–357.

Glover, D., Fox, K.R., Weiler, C., Kligerman, M.M., Turrisi, A., and Glick, J.H. 1988. Clinical trials of WR-2721 prior to alkylating agent chemotherapy and radiotherapy. *Pharmacology and Therapeutics*, 39, 3–7.

Landauer, M.R., Davis, H.D., Dominitz, J.A., and Pierce, S.J. 1988a. Dose-dependent radiation-induced alterations in ambulation and rearing over a 30-day period in C57BL/6J mice. *FASEB Journal*, 2, A1569.

Landauer, M.R., Davis, H.D., Dominitz, J.A., and Weiss, J.F. 1987a. Dose and time relationships of the radioprotector WR-2721 on locomotor activity in mice. *Pharmacology, Biochemistry and Behavior*, 27, 573–576.

Landauer, M.R., Davis, H.D., Dominitz, J.A., and Weiss, J.F. 1988b. Long-term effects of radioprotector WR-2721 on locomotor activity and body weight of mice following exposure to ionizing radiation. *Toxicology*, 49, 315–323.

Landauer, M.R., Davis, H.D., Dominitz, J.A., and Weiss, J.F. 1988c. Comparative behavioral toxicity of four sulfhydryl radioprotective compounds in mice: WR-2721, cysteamine, diethyldithiocarbamate and N acetylcysteine. *Pharmacology and Therapeutics*, 39, 97–100.

Landauer, M.R., Ledney, G.D., and Davis, H.D. 1987b. Locomotor behavior in mice following exposure to fission-neutron irradiation and trauma. *Aviation, Space and Environmental Medicine*, 58, 1205–1210.

Landauer, M.R., Patchen, M.L., and Davis, H.D. 1988d. Time course of behavioral effects in mice treated with soluble glucan. Abstracts of the 4th International Conference on Immunopharmacology, Osaka, Japan, p. 91.

Landauer, M.R., Walden, T.L., Davis, H.D., Cranford, M.E., and Farzaneh, N.K. 1989. Behavioral and physiological effects of leukotriene $C_4$. Abstracts of the 37th Annual Meeting of the Radiation Research Society, Seattle, WA.

Landauer, M.R., Walden, T.L., Davis, H.D., and Dominitz, J.A. 1987c. Alterations in locomotor activity induced by radioprotective doses of 16,16-dimethyl prostaglandin $E_2$. In: Prostaglandin and Lipid Metabolism in Radiation Injury, edited by T.L. Walden and H.N. Hughes (New York: Plenum Press), pp. 245–251.

Liu, W.F., Shin, J.H., Lin, R.F., Ma, C., Lin, C.H., Liu, C.Y., Chang, C.C., and Wu, M.T. 1987. Relationship between radioprotective and neuromotor effects of S-2(3-aminopropyl-amino) ethylphosphorothioate (WR-2721) in mice. *Neurotoxicology and Teratology* 9, 333–337.

McPherson, C.W. 1963. Reduction of *Pseudomonas aeruginosa* ar coliform bacteria in mouse drinking water following treatment with hydrochloric acid or chlorine. *Laboratory Animal Care*, 13, 737–744.

Maisin, J.R. 1988. Protection against ionizing radiation by combinations of radioprotectors. *Pharmacology and Therapeutics*, 39, 189–193.

Patchen, M.L., D'Alesandro, M.M., Chirigos, M.A., and Weiss, J.F. 1988. Radioprotection by biological response modifiers alone and in combination with WR-2721. *Pharmacology and Therapeutics*, 39, 247–254.

Reiter, L.W., and Macphail, R.C. 1982. Factors influencing motor activity measurements in neurotoxicology. In: Nervous System Toxicology, edited by C.L. Mitchell (New York: Raven Press), pp. 45–65.

Sette, W.F., and Levine, T.E. 1986. Assessment of locomotor activity. In: Neurobehavioral Toxicology, edited by Z. Annau (Baltimore, MD: Johns Hopkins Univ Press), pp. 397–403.

Snyder, S.L., Walden, T.L., Jr., MacVittie, T.J., Patchen, M.L., and Fuchs, P. 1986. Radioprotective properties of detoxified lipid A from *Salmonella minnesota* R595. *Radiation Research*, 107, 107114.

Steel, L.K., and Catravas, G.N. 1988. Protection against ionizing radiation with eicosanoids. In: Eicosanoids and Radiation, edited by P. Polgar (Boston: Kluwer Academic Publishers), pp. 79–87.

Steel, L.K., Walden, T.L., Hughes, H.N., and Jackson, W.E., III. 1988. Protection of mice against mixed fission neutron-gamma (n:gamma = 1.1) irradiation by WR-2721, 16, 16 dimethyl $PGE_2$, and the combination of both agents. *Radiation Research*, 115, 605–608.

Tikal, K., Plevova, J., and Hvizdosva, J. 1979. Behavioural effects of cystamine and mexamine in rats. *Activitas Nervosa Superior*, 21, 59–62.

Tilson, H.A., and Mitchell, C.L. 1984. Neurobehavioral techniques to assess the effects of chemicals on the nervous system. *Annual Review of Pharmacology and Toxicology* 24, 425–450.

Turrisi, A.T., Kligermann, M.M., Glover, D.J., Glick, J.H., Norfleet, L., and Gramkowski, M. 1983. Experience with Phase I trials of WR-2721 preceding radiation therapy. In: Radioprotectors and Anticarcinogens, edited by O.F. Nygaard and M.G. Simic (New York: Academic Press), pp. 681–694.

Utley, J.F., Marlowe, C., Wadell, J.W. 1976. Distribution of S-35 labelled WR-2721 in normal and malignant tissues of the mouse. *Radiation Research*, 68, 284–291.

Walden, T.L., Jr., Patchen, M., and Snyder, S.L. 1987. 16,16-dimethyl prostaglandin $E_2$ increases survival in mice following irradiation. *Radiation Research*, 109, 440–448.

Weiss, J.F., Hoover, R.L., and Kumar, S.K. 1987. Selenium pretreatment enhances the radioprotective effect and reduces the lethal toxicity of WR-2721. Free Radical Research Communications, 3, 33–38.

Weiss, J.F., and Simic, M.G. 1988. editors, Special Issue: Perspectives in Radioprotection, Pharmacology and Therapeutics, 39, 1–414.

WHO. 1986. Environmental Health Criteria, Principles and Methods for the Assessment of Neurotoxicity Associated with Exposure to Chemicals. World Health Organization, Geneva.

# Onset of Behavioral Effects in Mice Exposed to 10 Gy $^{60}$Co Radiation

DONNA M. MAIER, M.A., Ph.D., and MICHAEL R. LANDAUER, M.S., Ph.D.

MAIER DM, LANDAUER MR. *Onset of behavioral effects in mice exposed to 10 Gy $^{60}$Co radiation.* Aviat. Space Environ. Med. 1990; 61:893–8.

**The effects of 10 Gray (Gy) $^{60}$Co radiation on social behavior, locomotor activity, and body weight were assessed in individually housed male Swiss-Webster mice. In Experiment 1, aggressive behavior was evaluated prior to irradiation and for 7 d postirradiation by placing an untreated intruder in the irradiated or sham-irradiated resident's home cage for 5 min. Offensive aggressive behavior was not affected significantly by radiation until day 7 postirradiation, when attack latency increased, the frequency and duration of fighting decreased, and the frequency of bites, lunges, and chases decreased. Untreated intruder mice paired with irradiated resident mice showed a decrease in the duration of defensive upright postures and a decrease in the frequency of defensive upright postures, squeaks, and escapes on day 7 postirradiation. In Experiment 2, locomotor activity and body weight were monitored for 7 d postirradiation. Body weight was decreased in irradiated mice beginning 4 d postirradiation. Locomotor activity was suppressed in irradiated animals 90 min after irradiation and remained depressed throughout the 7-d testing period.**

ACUTE ADMINISTRATION of radiation to humans (2–7.5 Gray [Gy]) produces a hematopoietic syndrome characterized by bone marrow damage that results in anemia, lowered immune response, and hemorrhage. If the damage to the blood forming organs is severe, the individual will die (25). Radiation doses of approximately 7.5–30 Gy produce symptoms characteristic of gastrointestinal involvement: nausea, vomiting, anorexia, diarrhea, and lethargy, followed by loss of body weight, dehydration, exhaustion, and death (25). The effects of the hematopoietic and gastrointestinal syndromes are likely to influence behavior. Assessing the acute effects of ionizing radiation on behavior is, therefore, important in the conduct of space missions and the cleanup of accidents involving nuclear material such as those at Chernobyl, USSR (12) and Goiania, Brazil (18).

In the present studies, the laboratory mouse was used as a model to investigate the effects of acute radiation (10 Gy $^{60}$Co) exposure on aggressive behavior, locomotor activity, and body weight. In this species, doses of approximately 5–10 Gy result in the development of the hematopoietic syndrome, while mice receiving 10–50 Gy exhibit symptoms characteristic of the gastrointestinal syndrome (22). The dose of radiation used in this study (10 Gy), therefore, produces a combination of the hematopoietic and gastrointestinal syndromes.

Previous studies have not examined the impact of radiation on social behavior in a sufficiently quantitative manner, or they have used inappropriate models of social interaction. The measures used to quantify aggressive behavior in these studies were not specified, nor was aggressive behavior their primary focus (3,13, 14,17). Preliminary research in 1950 conducted with mice [following 12–20 Gy X-rays administered in fractionated doses] indicated a tendency for decreased aggressive behavior shortly before death (24). More recent work, focusing on survivable doses (3 Gy, 5 Gy, and 7 Gy) of gamma radiation, reported a decrease in aggressive behavior in mice during the second week postirradiation (11). This decrease was presumably due to physical symptoms produced by hematopoietic effects at these radiation doses.

The purpose of this study (Experiment 1) was to investigate the effects of a radiation dose that would produce both the hematopoietic and the gastrointestinal syndromes, using a quantifiable, naturally occurring model of aggressive behavior. The resident-intruder paradigm, in which a resident mouse attacks an intruder mouse that has entered its territory, was chosen to measure aggressive behavior (16,23). This model has been widely used in the laboratory to study offensive aggressive behavior (observed in the resident as it attacks the intruder) and defensive aggressive behavior (observed in the intruder as it defends itself against the resident) and is ethologically valid, because territorial defense by dominant mice occurs in the natural environment (16).

From the Behavioral Sciences Department, Armed Forces Radiobiology Research Institute, Bethesda, MD.

This manuscript was received for review in August 1989. The revised manuscript was accepted for publication in February 1990.

Send reprint requests to: Dr. Michael Landauer, Behavioral Sciences Department, Armed Forces Radiobiology Research Institute, Bethesda, MD 20814-5145.

Decreases in general activity after radiation exposure have been previously reported for several species (5). Both gamma and neutron radiation have been shown to decrease spontaneous locomotor activity in the mouse (6–8). In Swiss-Webster mice receiving 7 Gy $^{60}$Co, locomotor activity was decreased at 15 d postirradiation, while lower doses did not have a significant effect. This dose also resulted in a biphasic decrease in body weight on days 2, 3, and 13–21 postirradiation (6). In Experiment 2 of this paper, both locomotor activity and body weight were monitored in male Swiss-Webster mice receiving 10 Gy $^{60}$Co. This study was conducted to ascertain the time course of changes produced in these parameters and to determine if they were related to alterations in aggressive behavior.

## MATERIALS AND METHODS

*Subjects:* Male Crl:CFW (SW)BR VAF/Plus Swiss-Webster albino mice, from the Charles River Breeding Laboratory (Raleigh, NC), 16–20 weeks of age, were used in these experiments. Animals were quarantined on arrival and representative animals were screened for evidence of disease. They were individually housed in plastic Micro-isolator cages on hardwood chip contact bedding in an AAALAC accredited facility on a reversed 12:12 h light/dark cycle with lights off at 0700. Commercial rodent chow (Wayne Lab Blox, Wayne, OH) and acidified water (pH 2.5 using HCl) were freely available. Temperature was maintained at 21°C ± 1°C with 50% ± 10% relative humidity. All mice were euthanized by inhalation of carbon dioxide at the end of the experiment.

*Radiation exposure:* The mice were placed in ventilated polycarbonate restraint devices for approximately 20 min during irradiation. Irradiation was accomplished with bilateral, whole-body exposure to gamma-ray photons from a $^{60}$Co source. The mice received 10 Gy of gamma radiation administered at a dose of 1 Gy/min. Sham-irradiated mice were treated exactly as the irradiated mice, but they were not exposed to radiation.

### *Experiment 1—Aggressive Behavior*

*Preirradiation testing:* The mice were individually housed 1 month prior to irradiation, because this has previously been reported to induce offensive aggressive behavior in resident mice (16,23). After 2 weeks of individual housing, each mouse was brought to the test room and paired with a weight-matched mouse to establish pairs in which one animal was clearly dominant over the other. While individually housed mice are often aggressive, some can be classified as timid (16). Timid mice show many defensive behaviors and fewer offensive behaviors than aggressive mice, and can be used as subordinate intruders in a resident-intruder paradigm.

Individually housed rather than group-housed animals were used as intruders because irradiated mice are highly susceptible to infections, and group housing can exacerbate transmission of pathogens. Subsequently, the dominant mouse in each pair was designated as the resident and the subordinate mouse as the intruder. The mice were kept in the same resident-intruder pair throughout the study. Resident-intruder pairs were randomly assigned to the two treatment groups. In the irradiated group (N = 8), the resident animal was irradiated (as described above), and in the control group (N = 8), the resident mouse was sham-irradiated. Intruder mice were not treated. Irradiated mice were monitored daily for mortality.

*Resident-intruder test:* The mice were habituated to the test room for 1 h. The intruder was placed in the resident's home cage (25.7 cm × 15.2 cm × 12.1 cm) for 5 min during the dark portion of the light-dark cycle, and the mice were videotaped under infrared light. The following behaviors displayed by the resident mouse were scored: latency to attack (a lunge, a bite, or a fight was considered to be an attack), number and duration of roll and tumble fights, and number of lunges and chases, bites and tail rattles (1,2). These behaviors were chosen based on previous studies that indicated they were most often displayed by attacking mice (1,2,16). Bites did not draw blood or leave any discernible mark on the intruder. The following behaviors displayed by the intruder mouse were scored: the number and duration of defensive upright postures, and the number of squeaks and escapes from the resident mouse (1,2). The criteria for these behaviors were based on the description provided by Benton *et al.* (1). Mice were tested in the resident-intruder model 2 d before irradiation (baseline test), at 1 h to 3 h postirradiation (day 0), and on days 2, 5, and 7 postirradiation. The aggressive interactions were videotaped and analyzed after the study was completed. The scorer did not know which animals had been irradiated.

### *Experiment 2—Locomotor activity and Body Weight*

Locomotor activity was measured using a computerized Digiscan Animal Activity Monitor (Omnitech Electronics, Columbus, OH) that recorded horizontal activity (ambulation) and the number of vertical movements (rearing) by infrared photodetectors. The area of the Plexiglas open field was 20.3 cm × 20.3 cm. Animals were placed in the activity monitors for 5 min during the dark portion of the light-dark cycle. The mice were tested 2 d prior to irradiation (baseline test), 90 min postirradiation (day 0), and on days 2, 5, and 7 postirradiation. Mice were habituated to the experimental room for 60 min before testing. Body weights of the animals were measured 2 d prior to irradiation, and on days 0, 2, 4, 5, 6, and 7 postirradiation. The animals were randomly assigned to either the irradiated (N = 12) or sham-irradiated (N = 12) group. All mice were isolated 1 wk before irradiation. Results from our laboratory indicate that there are no significant differences in locomotor activity between male Swiss-Webster mice housed in isolation for 1 week or 4 weeks (Davis, Maier, and Landauer, unpublished observations).

### *Statistical Analysis*

Data from Experiment 1 were nonparametric and were, therefore, analyzed using the Mann-Whitney U test (sham-irradiated vs. irradiated animals on each test day). Activity and body weight data from Experiment 2 were analyzed by *t*-tests (sham-irradiated vs. irradiated animals on each test day). A two-tailed alpha level of

0.05 was used to evaluate the statistics from Experiment 1. Based upon the results of previous studies (4,6,7, 8,10), a one-tailed alpha level of 0.05 was used to evaluate statistics from Experiment 2.

## RESULTS

### *Experiment 1—Aggressive Behavior*

Offensive aggressive behavior of the irradiated and sham-irradiated resident mice did not differ significantly until day 7 postirradiation (Fig. 1). On day 7, attack latency in the irradiated residents increased significantly [$U(8,7) = 53$, $p < 0.01$]. The number of bites [$U(8,7) = 53$, $p < 0.01$] and the number of lunges and chases [$U(8,7) = 54$, $p < 0.01$] in the irradiated resident mice decreased significantly on day 7 postirradiation. Both duration and number of fights decreased on day 7, although not significantly [for both measures $U(8,7) = 43.5$, $p = 0.09$]. The number of tail rattles by resident mice was not affected by irradiation at any time. One resident mouse died 7 d after irradiation and the remainder by day 10 postirradiation (mean ± S.E.M. time to death = 8.5 ± 0.3 days).

On day 7 postirradiation, defensive behaviors displayed by intruder mice paired with irradiated residents were significantly decreased when compared with intruders paired with sham-irradiated mice (Fig. 2). Both duration [$U(8,7) = 51$, $p < 0.01$] and number [$U(8,7) = 51.5$, $p < 0.01$] of defensive upright postures decreased

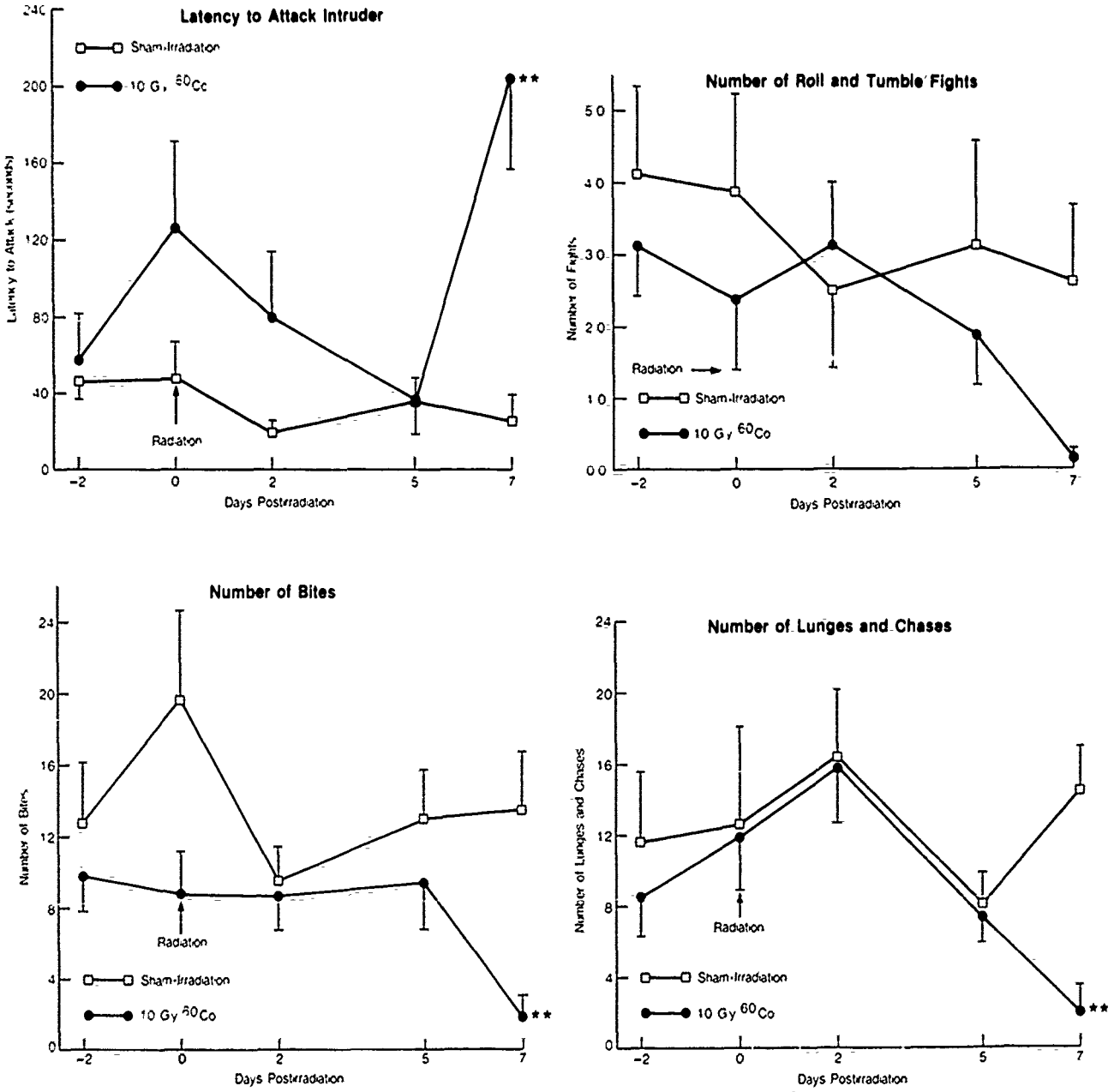


**Fig. 1. Offensive aggressive behaviors (mean ± S.E.M.) displayed by individually housed resident mice in a 5-min resident-intruder test. Resident mice were treated with 10 Gy $^{60}$Co radiation or were sham-irradiated on day 0; intruder mice were not irradiated. N = 8, except for irradiated group on day 7 when one animal died (N = 7); **$p < 0.01$.**

in intruder mice paired with irradiated residents. Number of escapes [U(8,7) = 52, $p < 0.01$] and squeaks [U(8,7) = 56, $p < 0.01$] in intruder mice paired with irradiated residents also decreased on day 7. The number of squeaks in intruder mice interacting with irradiated residents was significantly decreased on day 5 postirradiation when compared with intruders paired with sham-irradiated residents [U(8,8) = 54, $p < 0.05$]. No other defensive behaviors were significantly decreased at any time.

*Experiment 2—Locomotor Activity and Body Weight*

Ambulation of irradiated mice was significantly lower than that of sham-irradiated animals at 90 min (day 0) postirradiation [t(22) = 2.52, $p < 0.05$] and on days 2 [t(22) = 3.51, $p < 0.01$], 5 [t(22) = 2.24, $p < 0.05$], and 7 [t(22) = 6.71, $p < 0.01$] postirradiation (Fig. 3A). Rearing of irradiated mice was lower than that of sham-irradiated controls at 90 min postirradiation [t(22) = 4.26, $p < 0.01$] and on days 2 [t(22) = 1.92, $p < 0.05$], 5 [t(22) = 1.51, $p = 0.07$], and 7 [t(22) = 6.14, $p < 0.01$] postirradiation (Fig. 3B). Body weight of irradiated mice was significantly decreased on days 4 [t(22) = 2.39, $p < 0.05$], 5 [t(22) = 2.55, $p < 0.01$], 6 [t(22) = 3.42, $p < 0.01$], and 7 [t(22) = 4.03, $p < 0.01$] postirradiation (Fig. 4).

## DISCUSSION

Irradiated and sham-irradiated resident mice did not differ significantly in the amount or type of offensive

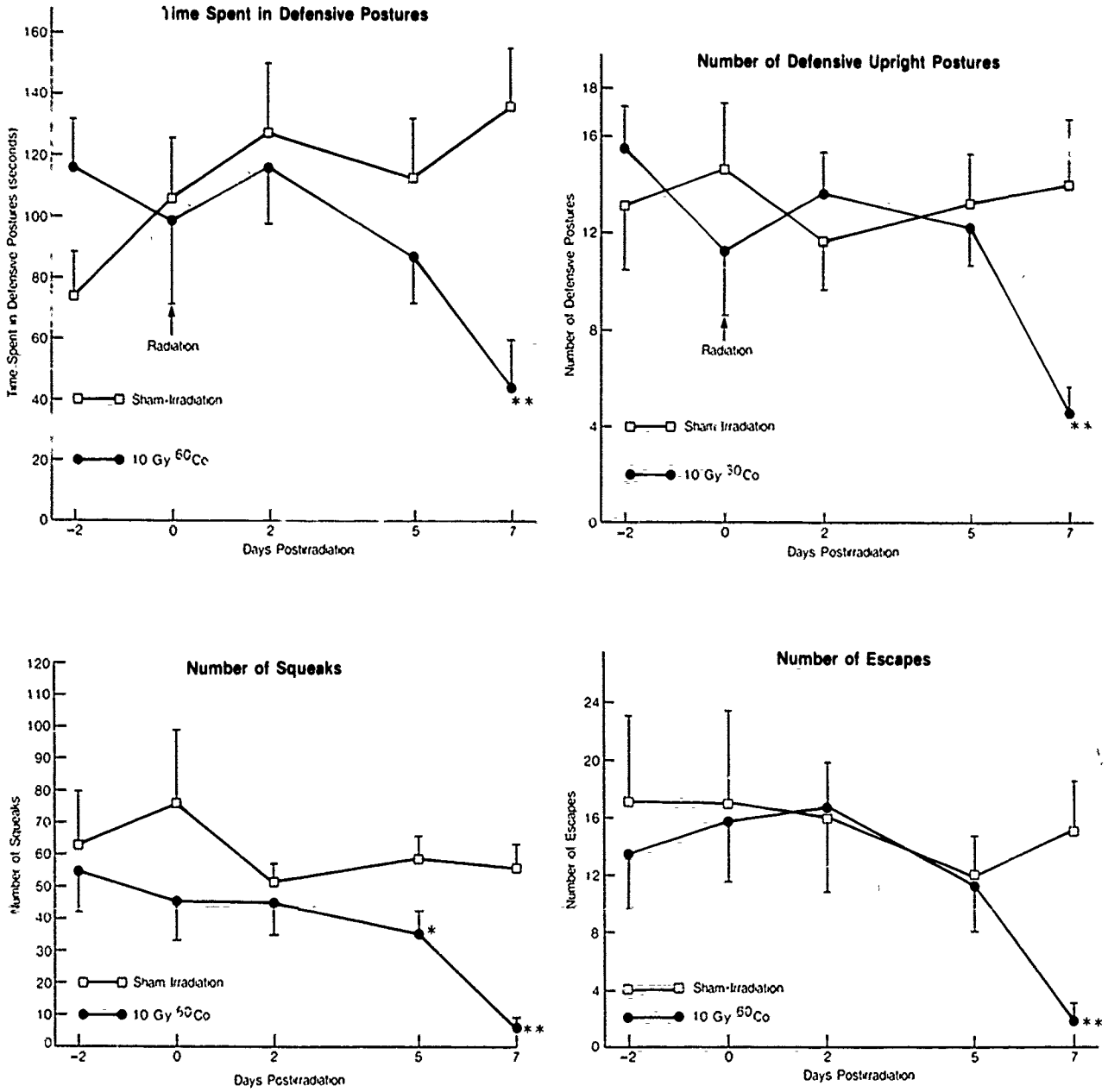


**Fig. 2. Defensive aggressive behaviors (mean ± S.E.M.) displayed by intruder mice in a 5-min resident-intruder test. Intruder mice were not irradiated; resident mice were treated with 10 Gy $^{60}$Co radiation or were sham-irradiated on day 0. N = 8, except for irradiated group on day 7 when one animal died (N = 7); *p < 0.05; **p < 0.01.**

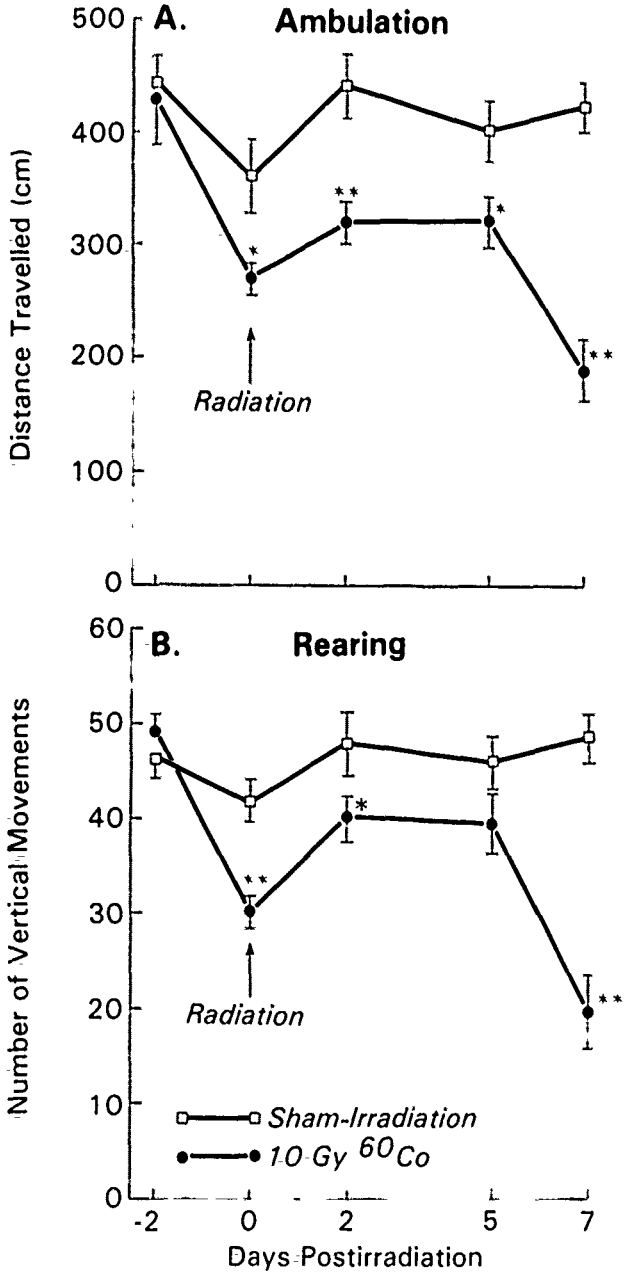


**Fig. 3. Locomotor activity (mean ± S.E.M.) displayed in irradiated (10 Gy $^{60}$Co) and sham-irradiated mice for 5 min in an open field. Animals were irradiated on day 0. A) Ambulation, B) Rearing. N = 12/group; *p < 0.05; **p < 0.01.**

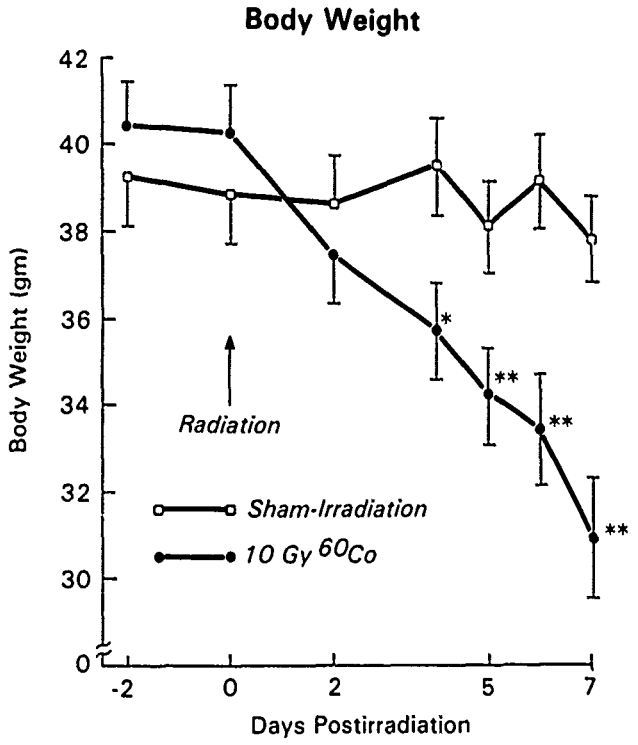


**Fig. 4. Body weight (mean ± S.E.M.) over time in irradiated (10 Gy $^{60}$Co) and sham-irradiated mice. Animals were irradiated on day 0. N = 12/group. *p < 0.05; **p < 0.01.**

aggressive behaviors that they displayed until 7 d postirradiation. At this time, irradiated resident mice showed a decrease in offensive aggressive behavior. This confirms results of a previous study (N = 5/group) in which offensive aggressive behavior was not affected until 7 d after exposure to 10 Gy $^{60}$Co radiation (Maier, unpublished results). Ambulation and rearing in an open field decreased in irradiated mice 90 min (day 0) after irradiation and remained below that of sham-irradiated controls on days 2, 5, and 7 postirradiation. It has previously been reported that 10 Gy $^{60}$Co produces significant decrements in open field activity beginning 45 min postirradiation in this mouse strain (4). Preliminary studies on older, individually housed male Swiss-Webster mice (aged 10 months, N = 8/group) tested during the first week after irradiation indicated that ambulation and rearing decreased 2–5 d postirradiation (10). Age may be important in determining the onset of radiation-induced suppression of locomotor behavior. Both age and strain have previously been shown to affect locomotor activity in mice (9).

In the present study and in previous work (10), aggressive behavior was maintained in irradiated mice for a longer period of time than spontaneous locomotor activity. While changes in locomotor activity preceded changes in aggressive behavior, it is doubtful that the decreases in activity were responsible for the subsequent decrements in aggressive behavior. Siegfried *et al.* (21), also failed to find a correlation between locomotor activity and aggressive behavior in mice. Therefore, it is not likely that radiation-induced decrements in locomotor activity underlie subsequent deficits in aggressive behavior.

Motivational factors may influence the different time courses observed for radiation-induced deficits in aggressive behavior and locomotor activity. The motivation of animals has previously been shown to be important in the production of radiation-induced behavioral decrements (5). Tasks that are aversively motivated, such as those that use shock, have been shown to be relatively resistant to radiation-induced decrement. For example, once animals have recovered from an early transient incapacitation (which occurs within minutes after exposure to high doses of radiation), performance of shock-avoidance tasks persists until death is imminent (15). Rhesus monkeys receiving 10 Gy mixed neutron-gamma radiation did not exhibit deficits in performance of a shock-avoidance lever-press task until 6–7 d

postirradiation (20). In addition, after exposure to 100 Gy X-rays, monkeys continued to perform a shock-avoidance lever-press task until they were severely debilitated and close to death (19). The maintenance of both shock avoidance and aggressive behavior until the animal is moribund contrasts with the earlier onset of radiation-induced suppression of spontaneous locomotor activity. Differences in the motivational aspects of these behaviors may, therefore, contribute to differences in the onset and duration of radiation-induced performance decrements.

Intruder mice paired with irradiated and sham-irradiated resident mice did not differ in the amount or type of defensive aggressive behaviors that they displayed until 7 d postirradiation. At this time, there was a decrease in the aggressive behavior of the intruders paired with the irradiated resident mice. This may reflect the decline in offensive aggressive behaviors of the irradiated residents paired with them. Intruders interacting with irradiated resident mice exhibited a decrease in defensive behavior on day 7, indicating that the intruder was sensitive to the amount and type of behavior displayed by the resident animal, and altered its own behavior accordingly.

In summary, irradiated and sham-irradiated resident mice did not differ significantly in the amount or type of offensive aggressive behavior that they displayed until 7 d postirradiation, when a decrease was observed in irradiated resident mice. Ambulation and rearing in an open field were suppressed beginning on the day of irradiation. Body weight significantly decreased by 4 d postirradiation, indicating either that food consumption had dropped because of radiation-induced anorexia, or that the mice were no longer physiologically capable of deriving the full nutritional value of their food due to erosion of gastrointestinal cells (22,25). Unlike locomotor activity and maintenance of body weight, aggressive behavior was maintained until the irradiated mouse was moribund. These results may be influenced by the motivational aspects and the different physiological/neural substrates underlying these behaviors. Research is continuing in our laboratory to elucidate the behavioral consequences associated with ionizing radiation.

ACKNOWLEDGMENTS

The authors would like to thank Mr. Hirsch Davis, Mr. Jason Dominitz, Ms. Catherine Sund and Ms. Gloria Ruggiero for their valuable assistance in the preparation of this manuscript. Research was conducted according to the principles enunciated in the *Guide for the Care and Use of Laboratory Animals* prepared by the Institute of Laboratory Animal Resources, National Research Council. Views presented in this paper are those of the authors; no endorsement by the Defense Nuclear Agency has been given or should be inferred.

REFERENCES

1. Benton D, Brain P, Jones S, Colebrook E, Grimm V. Behavioral examinations of the anti-aggressive drug Flupazine. Behav. Brain Res. 1983; 10:325–38.
2. Blanchard RJ, O'Donnell V, Blanchard DC. Attack and defensive behaviors in the albino mouse. Aggressive Behav. 1979; 5:341–52.
3. Dahlstrom A, Haggendal J, Rosengren B. The effect of roentgen irradiation on monoamine containing neurons in the rat brain. Acta. Radiol. 1973; 12:191–200.
4. Davis HD, Maier DM, Landauer MR. Early activity decrements in grouped and isolated mice after exposure to ionizing radiation. Soc. Neurosci. 1988; 14:1221.
5. Kimeldorf DJ, Hunt EL. Ionizing radiation, neural function and behavior. New York: Academic Press, 1965.
6. Landauer MR, Davis HD, Dominitz JA, Pierce SJ. Effects of acute radiation exposure on locomotor activity in Swiss-Webster mice. Toxicologist 1987; 7:253.
7. Landauer MR, Davis HD, Dominitz JA, Weiss JF. Long-term effects of radioprotector WR-2721 on locomotor activity and body weight of mice following exposure to ionizing radiation. Toxicology 1988; 49:315–23.
8. Landauer MR, Ledney GD, Davis HD. Locomotor behavior in mice following exposure to fission-neutron irradiation and trauma. Aviat. Space Environ. Med. 1987; 58:1205–10.
9. Lhotellier L, Cohen-Salmon C. Genetics and senescence. I. Age-related changes in activity and exploration in three inbred strains of mice. Physiol. Behav. 1989; 45:491–3.
10. Maier DM, Landauer MR. Radiation-induced alterations in fighting behavior and locomotor activity in mice. In: Brain PF, Olivier B, Mos J, Benton D, Bronstein PM, eds. Multidisciplinary studies on aggression. Swansea, Wales: International Society for Research on Aggression, 1988:74.
11. Maier DM, Landauer MR. Effects of acute sublethal gamma radiation exposure on aggressive behavior in male mice, a dose-response study. Aviat. Space Environ. Med. 1989; 60:774–8.
12. Marshall E. Reactor explodes amid Soviet silence. Science 1986; 232:814–5.
13. Mattsson JL, Yochmowitz MG. Radiation-induced emesis in monkeys. Radiat. Res. 1980; 82:191–9.
14. McDowell AA, Davis RT, Steele JP. Application of systematic direct observational methods to analysis of the radiation syndrome in monkeys. Percept. Mot. Skills. 1956; 6:117–30.
15. Mickely GA, Bogo V, Landauer MR, Mele PC. Current trends in behavioral radiobiology. In: McCormack PD, Swenberg C, Bucker H, eds. Terrestrial space radiation and its biological effects. New York: Plenum, 1988:517–36.
16. Miczek KA, Krsiak M. Pharmacological analysis of attack and flight. In: Brain PF, Benton D, eds. Multidisciplinary approaches to aggression research. New York, Elsevier/North Holland Biomedical Press, 1981:341–54.
17. O'Boyle M. Suppression of mouse-killing in rats following irradiation. Percept. Mot. Skills. 1976; 42:511–4.
18. Roberts L. Radiation accident grips Goiania. Science 1987; 238:1028–31.
19. Sharp JC, Daoust DL. The effects of massive doses of ionizing radiation upon conditioned avoidance behavior of the primate Washington, DC, Behavioral Radiobiology Laboratory, Walter Reed Army Institute of Research, 1964; Report No. 3.
20. Sharp JC, Keller BK. A comparison between the effects of exposure to a mixed fission spectrum delivered in a single "pulse" and X-rays delivered at a slower rate upon the conditioned avoidance behavior of primates. Washington, DC: Behavioral Radiology Laboratory, Walter Reed Army Institute of Research, 1965; Report No. 4.
21. Siegfried B, Alleva E, Oliverio A, Puglisi-Allegra S. Effects of isolation on activity, reactivity, excitability, and aggressive behavior in two inbred strains of mice. Behav. Brain Res. 1981; 2:211–8.
22. Storer JB, Fry RJM, Ulrich RL. Somatic effects of radiation. In: Foster HL, Small JD, Fox JG, eds. The mouse in biomedical research. Volume IV: Experimental biology and oncology. New York: Academic Press, 1982:133–46.
23. Thurmond JB, Lasley SM. The development of territorial-induced intermale agonistic behavior in albino laboratory mice. Aggressive Behav. 1979; 5:163–71.
24. Vogel HH. The effect of X irradiation on fighting behavior of male mice. Anat. Rec. 1950; 108:547.
25. Young RW. Acute radiation syndrome. In: Conklin JJ, Walker RI, eds. Miltiary radiobiology. New York: Academic Press, 1987:165–90.

Exp. Hematol. 18:1042–1048 (1990)




*Experimental* Hematology

# Survival Enhancement and Hemopoietic Regeneration Following Radiation Exposure: Therapeutic Approach Using Glucan and Granulocyte Colony-stimulating Factor

Myra L. Patchen,[1] Thomas J. MacVittie,[1] Brian D. Solberg,[1] and Larry M. Souza[2]

[1]Department of Experimental Hematology, Armed Forces Radiobiology Research Institute, Bethesda, Maryland; and [2]AMGen, Thousand Oaks, California, USA

*(Received 15 January 1990; in revised form 29 March 1990; accepted 13 April 1990)*

**Abstract.** C3H/HeN female mice were exposed to whole-body cobalt-60 radiation and administered soluble glucan (5 mg i.v. at 1 h following exposure), recombinant human granulocyte colony-stimulating factor (G-CSF; 2.5 μg/day s.c., days 3–12 following exposure), or both agents. Treatments were evaluated for their ability to enhance hemopoietic regeneration, and to increase survival after radiation-induced myelosuppression. Both glucan and G-CSF enhanced hemopoietic regeneration alone; however, greater effects were observed in mice receiving both agents. For example, on day 17 following a sublethal 6.5-Gy radiation exposure, mice treated with saline, G-CSF, glucan, or both agents, respectively, exhibited 36%, 65%, 50%, and 78% of normal bone marrow cellularity, and 84%, 175%, 152%, and 212% of normal splenic cellularity. At this same time, granulocyte–macrophage colony-forming cell (GM-CFC) values in saline, G-CSF, glucan, or combination-treated mice, respectively, were 9%, 46%, 26%, and 57% of normal bone marrow values, and 57%, 937%, 364%, and 1477% of normal splenic values. Endogenous spleen colony formation was also increased in all treatment groups, with combination-treated mice exhibiting the greatest effects. Likewise, although both glucan and G-CSF alone enhanced survival following an 8-Gy radiation exposure, greatest survival was observed in mice treated with both agents. These studies suggest that glucan, a macrophage activator, can synergize with G-CSF to further accelerate hemopoietic regeneration and increase survival following radiation-induced myelosuppression.

**Key words:** Glucan — G-CSF — Hemopoiesis — Irradiation — Myelosuppression

Hemopoietic and immune depression and subsequent susceptibility to potentially lethal opportunistic infections are well-documented phenomena following chemotherapy and/or radiotherapy [1–5]. Methods to therapeutically mitigate radiation- and drug-induced myelosuppression could offer great clinical utility.

We have previously demonstrated that glucan, a beta-1,3-polysaccharide immunomodulator, is capable of enhancing hemopoietic regeneration and increasing survival when administered to mice following irradiation [6–8]. Specifically, glucan therapy was demonstrated to accelerate the repopulation of pluripotent hemopoietic stem cells (spleen colony-forming units, CFU-s), as well as committed granulocyte-macrophage (granulocyte–macrophage colony-forming cells, GM-CFC), pure macropnage (macrophage colony-forming cells, M-CFC), and erythroid (erythroid colony-forming units, CFU-e and erythroid burst-forming units, BFU-e) hemopoietic progenitor cells. The survival-enhancing and hemopoietic activities of glucan could be correlated with its ability to activate macrophages, resulting in enhanced macrophage-mediated defense against opportunistic infections following irradiation, as well as the production of macrophage-derived hemopoietic growth factors [9–11].

Granulocytes also play a critical role in host defense against microbial invasion [12, 13]. Granulocyte colony-stimulating factor (G-CSF) is a glycoprotein regulator of granulocyte proliferation, differentiation, and function [14–18]. Human G-CSF has been purified [19], molecularly cloned [20], and expressed as a recombinant protein [21]. Recently, recombinant human G-CSF has also been demonstrated to accelerate hemopoietic regeneration and to enhance survival in irradiated mice and canines [22–26].

Because glucan and G-CSF appear to target different cell populations in mediating survival enhancement following irradiation, we hypothesized that the use of these agents in combination may further increase hemopoietic regeneration and survival following irradiation. In this study, the therapeutic effect of combined glucan and G-CSF treatment was evaluated in a murine model of radiation-induced myelosuppression.

## Materials and methods

*Glucan and G-CSF.* Endotoxin-free soluble glucan [27] was purchased from Tulane University School of Medicine (New Orleans, Louisiana) and administered i.v. at 5 mg/mouse 1 h after irradiation. Recombinant human G-CSF was provided by AMGen (Thousand Oaks, California) and administered s.c. at 2.5 μg/mouse on days 3–12 following irradiation. This G-CSF (lot no. 600) was *Escherichia coli*-derived and had a specific activity of $10^8$ U/mg as assayed by the GM-CFC assay. Endotoxin contamination was undetectable based on the *Limulus* amebocyte assay.

*Mice.* C3H/HeN female mice (~20 g) were purchased from Charles River Laboratories (Raleigh, North Carolina). Mice were maintained in a facility accredited by the American Association for the Accreditation of Laboratory Animal Care (AAALAC) in micro-isolator cages

*Address offprint requests to:* Dr. Myra L. Patchen, Department of Experimental Hematology, Armed Forces Radiobiology Research Institute, Building #42 NNMC, Bethesda, MD 20814-5145, USA.

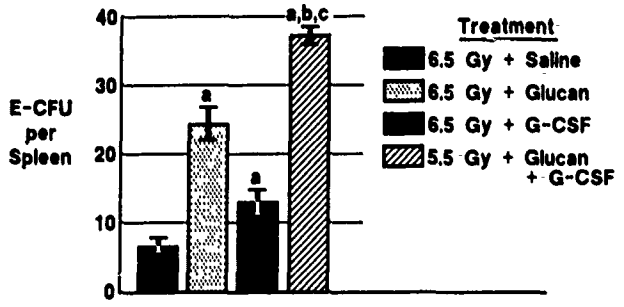


**Fig. 1.** Effect of glucan, G-CSF, and glucan plus G-CSF on endogenous spleen colony formation in C3H/HeN mice irradiated with 6.5 Gy. Mice received glucan at 1 h following irradiation (5 mg, i.v.) and G-CSF on days 3–12 following irradiation (2.5 μg/day, s.c.). Data are represented as mean ± SE of values obtained from a total of at least 15 mice. [a], significantly different from saline values. [b], significantly different from glucan values. [c], significantly different from G-CSF values.

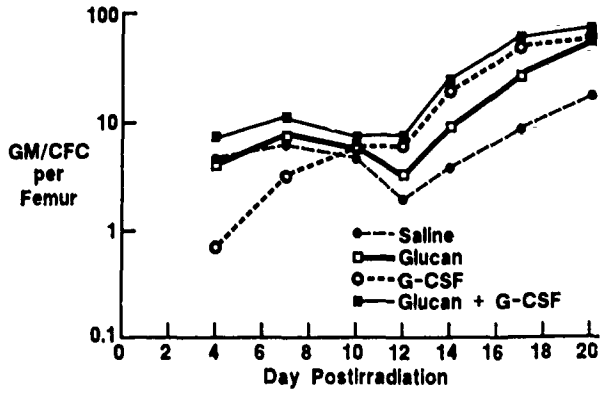


**Fig. 2.** Effect of glucan, G-CSF, and glucan plus G-CSF on GM-CFC per femur in C3H/HeN mice irradiated with 6.5 Gy. Mice received glucan at 1 h following irradiation (5 mg, i.v.) and G-CSF on days 3–12 following irradiation (2.5 μg/day, s.c.). Data are represented as a percentage of femoral GM-CFC content in nonirradiated (normal control) mice. Glucan values differ significantly from saline values on days 12 ($p = 0.0065$), 14 ($p = 0.0007$), 17 ($p = 0.0003$), and 20 ($p = 0.0001$). G-CSF values differ significantly from saline values on days 4 ($p = 0.0235$), 7 ($p = 0.0205$), 12 ($p = 0.0011$), 14 ($p = 0.0001$), 17 ($p = 0.0001$), and 20 ($p = 0.0177$). Glucan plus G-CSF values differ significantly from saline values on days 4 ($p = 0.0496$), 7 ($p = 0.0451$), 10 ($p = 0.0493$), 12 ($p = 0.0012$), 14 ($p = 0.0001$), 17 ($p = 0.0001$), and 20 ($p = 0.0001$). Glucan plus G-CSF values differ significantly from glucan values on days 4 ($p = 0.0426$), 7 ($p = 0.0448$), 12 ($p = 0.0057$), 14 ($p = 0.0001$), 17 ($p = 0.0008$), and 20 ($p = 0.0211$). Glucan plus G-CSF values differ significantly from G-CSF values on days 4 ($p = 0.0133$), 7 ($p = 0.0171$), 17 ($p = 0.0413$), and 20 ($p = 0.0481$).

on hardwood-chip contact bedding, and they were provided commercial rodent chow and acidified water (pH 2.5) ad libitum. Animal rooms were equipped with full-spectrum light from 0600 to 1800 hours, and they were maintained at 21° ± 1°C with 50% ± 10% relative humidity using at least ten air changes per hour of 100% conditioned fresh air. Upon arrival, all mice were tested for *Pseudomonas* and quarantined until test results were obtained. Only healthy mice were released for experimentation. All animal experiments were approved by the Institute Animal Care and Use Committee prior to performance.

*Irradiation.* The cobalt-60 source at the Armed Forces Radiobiology Research Institute was used to administer bilateral total-body gamma radiation. Mice were placed in ventilated Plexiglas containers and irradiated at a dose rate of 0.4 Gy/min. Dosimetry was determined by ionization chambers [28]. Hemopoietic and survival studies were performed following 6.5- and 8.0-Gy irradiations, respectively.

*Survival assays.* Irradiated mice were returned to the animal facility and cared for routinely. Survival was checked and recorded daily for 30 days; on day 31, surviving mice were euthanized by cervical dislocation. Each treatment group consisted of ten mice. Experiments were repeated three times.

*GM-CFC assay.* Hemopoietic progenitor cells committed to granulocyte and/or macrophage development were assayed using a previously described agar GM-CFC assay [29]. Mouse endotoxin serum (5% vol/vol) was added to feeder layers as a source of colony-stimulating activity. Colonies (>50 cells) were counted after 10 days of incubation in a 37°C humidified environment containing 5% $CO_2$. The cell suspensions used for these assays represented tissues from three normal, irradiated, or treated and irradiated mice at each time point. Femurs and spleens were removed from mice euthanized by cervical dislocation. Cells were flushed from femurs with 3 ml of McCoy's 5A medium (Flow Laboratories, McLean, Virginia) containing 10% heat-inactivated fetal bovine serum (Hyclone, Logan, Utah). Spleens were pressed through stainless-steel mesh screen, and the cells were washed from the screen with 6 ml of medium. The numbers of nucleated cells in the suspensions were determined using a Coulter counter. Experiments were repeated three times.

*Peripheral blood cell counts.* Blood was obtained from cervically dislocated mice via cardiac puncture using a heparinized syringe attached to a 20-gauge needle. White blood cell (WBC), red blood cell (RBC), and platelet (PLT) counts were performed using a Coulter counter.

*Endogenous spleen colony-forming unit (E-CFU) assay.* The E-CFU assay [30] was used to determine the effects of glucan, G-CSF, and glucan plus G-CSF therapy on endogenous hemopoietic stem cell recovery in irradiated mice. Mice were exposed to 6.5 Gy of radiation to partially ablate endogenous hemopoietic stem cells. Twelve days later, mice were euthanized by cervical dislocation and spleens were removed. The spleens were fixed in Bouin's solution, and grossly visible spleen colonies arising from the clonal proliferation of surviving endogenous hemopoietic stem cells were counted. Each treatment group consisted of five mice. Experiments were repeated three times.

*Statistics.* Student's *t*-test was used to determine statistical differences in all but survival data; survival data were analyzed using the generalized Savage (Mantel-Cox) procedure. Significance level was set at $p < 0.05$. Saline data were pooled because responses of saline-treated mice controlling for glucan injection (i.e., 1 h following irradiation, i.v.), G-CSF injections (i.e., days 3–12 following irradiation, s.c.), or both injections, did not statistically differ.

## Results

### *Glucan, G-CSF, and glucan plus G-CSF treatments enhance E-CFU formation*

The E-CFU assay was used as a general indicator of the ability of glucan, G-CSF, and glucan plus G-CSF treatments to stimulate hemopoiesis. Compared to 6.8 ± 0.8 colonies observed in saline-treated mice, glucan and G-CSF treatments significantly increased E-CFU numbers to 23.4 ± 2.3 and 12.5 ± 1.4, respectively (Fig. 1). Combined treatment with glucan plus G-CSF further increased E-CFU numbers to 36.7 ± 1.2. In addition, spleens obtained from mice receiving glucan plus G-CSF treatment were approximately twice as large as spleens obtained from glucan- or G-CSF-treated mice.

**Table 1.** Effect of glucan, G-CSF, and glucan plus G-CSF therapies on bone marrow and splenic cellularity following 6.5-Gy irradiation (percent normal control)

| Cellularity per femur | Day after irradiation | | | | | | |
|---|---|---|---|---|---|---|---|
| | 4 | 7 | 10 | 12 | 14 | 17 | 20 |
| Saline | 23.9 ± 2.0 | 43.5 ± 3.7 | 54.9 ± 3.5 | 52.8 ± 1.2 | 47.2 ± 3.7 | 35.6 ± 2.6 | 42.9 ± 1.8 |
| Glucan[a] | 12.8 ± 1.2[b] | 51.8 ± 1.8 | 56.9 ± 3.9 | 68.9 ± 3.7[b] | 54.0 ± 3.8 | 50.4 ± 3.6[b] | 59.5 ± 4.7[b] |
| G-CSF[c] | 16.7 ± 0.8[b] | 27.6 ± 0.8[b] | 43.1 ± 7.3 | 57.1 ± 3.3 | 52.8 ± 1.8 | 64.6 ± 2.8[b] | 76.5 ± 1.8[b] |
| Glucan plus G-CSF[a,c] | 14.2 ± 2.0[b] | 39.4 ± 4.5[d,e] | 50.6 ± 6.1 | 63.8 ± 2.8[b] | 60.8 ± 3.0[b,e] | 78.0 ± 4.1[b,d,e] | 89.6 ± 3.3[b,d,e] |

| Cellularity per spleen | Day after irradiation | | | | | | |
|---|---|---|---|---|---|---|---|
| | 4 | 7 | 10 | 12 | 14 | 17 | 20 |
| Saline | 7.5 ± 0.6 | 9.0 ± 0.3 | 14.9 ± 1.3 | 20.4 ± 0.4 | 36.1 ± 2.9 | 83.5 ± 5.2 | 153.7 ± 3.5 |
| Glucan[a] | 8.6 ± 1.1 | 10.7 ± 1.1 | 20.0 ± 1.2[b] | 40.0 ± 2.1[b] | 60.8 ± 9.5[b] | 151.6 ± 12.6[b] | 110.1 ± 5.7[b] |
| G-CSF[c] | 9.7 ± 0.3[b] | 10.4 ± 0.4[b] | 25.1 ± 5.0[b] | 36.0 ± 4.2[b] | 44.3 ± 1.8[b] | 175.0 ± 6.8[b] | 155.6 ± 5.0 |
| Glucan plus G-CSF[a,c] | 13.3 ± 1.3[b,d,e] | 16.8 ± 2.2[b,d,e] | 29.8 ± 1.6[b,d] | 48.1 ± 3.7[b,d,e] | 105.5 ± 11.2[b,d,e] | 211.8 ± 14.2[b,d,e] | 143.3 ± 10.3[d] |

Average cellularities per femur and spleen in normal C3H/HeN mice were 4.92 ± 0.22 × $10^6$ and 106.90 ± 5.20 × $10^6$, respectively.
[a] Glucan (5 mg, i.v.) administered 1 h after irradiation.
[b] Significantly different from saline values; $p < 0.05$.
[c] G-CSF (2.5 μg/day, s.c.) administered on days 3–12 after irradiation.
[d] Significantly different from glucan values; $p < 0.05$.
[e] Significantly different from G-CSF values; $p < 0.05$.

### *Glucan, G-CSF, and glucan plus G-CSF treatments accelerate hemopoietic regeneration in irradiated mice*

To evaluate the ability of glucan, G-CSF, and glucan plus G-CSF therapies to accelerate hemopoietic recovery following radiation injury, femoral and splenic cellularity and GM-CFC content were assayed on days 4, 7, 10, 12, 14, 17, and 20 following a sublethal 6.5-Gy radiation exposure. Compared to saline-treated mice, significantly increased femoral and splenic cellularities were observed in all treatment groups; the greatest increases, however, were generally observed in mice receiving glucan plus G-CSF therapy (Table 1).

The increased bone marrow and splenic cellularity observed in mice receiving glucan, G-CSF, or combination therapy was at least partially due to an increase in GM-CFC progenitors (Figs. 2 and 3). Compared to saline-treated mice, significantly increased femoral GM-CFC numbers were observed in glucan-treated mice by day 12 following exposure, in G-CSF-treated mice also by day 12 following exposure, and in combination-treated mice as early as day 4 following exposure (Fig. 2). Interestingly, femoral GM-CFC numbers in G-CSF-treated mice were lower than those in saline-treated mice on days 4 and 7 following exposure. In part, this may have been attributed to increased mobilization of progenitor cells from the marrow into the peripheral circulation; however, because peripheral blood was used to perform cell counts, not enough blood remained to evaluate this possibility. After day 12, GM-CFC numbers progressively increased in all treatment groups with combination therapy > G-CSF therapy > glucan therapy > saline therapy. By day 20 after irradiation, bone marrow GM-CFC content in combination-treated mice had recovered to 71.0% ± 6.2% of normal control values, compared with 57.5% ± 3.4% in G-CSF-treated mice 52.6% ± 2.9% in glucan-treated mice, and 16.7% ± 2.9% in saline-treated mice. In the spleen, GM-CFC recovery remained undetectable in any treatment group until day 10 following irradiation. However, dramatically accelerated splenic GM-CFC recovery was detected in all treatment groups from day 10 to day 20, with glucan plus G-CSF treatment producing the greatest effect (Fig. 3). By day 17 after exposure, splenic GM-CFC numbers in glucan plus G-CSF-treated mice had recovered to 1477.9% ± 120.0% of normal control values, compared with 936.9% ± 70.1% in G-CSF-treated mice, 363.8% ± 40.9% in glucan-treated mice, and only 56.9% ± 9.5% in saline-treated mice.

In addition to effects on progenitor cells, accelerated recovery of mature peripheral blood WBC, RBC, and PLT was observed in mice treated with glucan, G-CSF, and glucan plus G-CSF (Figs. 4–6). RBC and WBC recoveries were accelerated most in combination-treated mice, whereas PLT recovery was accelerated most in mice receiving only G-CSF therapy. WBC in treated mice consisted primarily of neutrophilic granulocytes.

### *Glucan, G-CSF, and glucan plus G-CSF treatments enhance survival in irradiated mice*

Consistent with the ability of glucan, G-CSF, and glucan plus G-CSF treatments to accelerate hemopoietic regeneration following irradiation, all three of these therapies also significantly increased survival in severely irradiated (8 Gy) mice (Fig. 7). Compared with 27% ± 3% survival observed in saline-treated mice, glucan, G-CSF, and glucan plus G-CSF treatments resulted in 63% ± 7%, 57% ± 3%, and 83% ± 4% survival, respectively.

## Discussion

It is well known that radiation exposure can predispose a host to life-threatening endogenous and exogenous infections

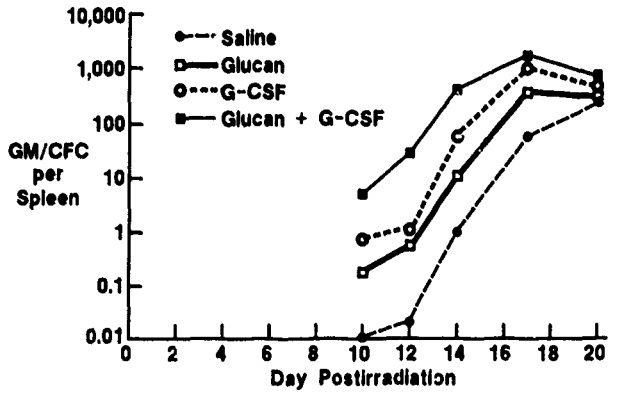


Fig. 3. Effect of glucan, G-CSF, and glucan plus G-CSF on GM-CFC per spleen in C3H/HeN mice irradiated with 6.5 Gy. Mice received glucan at 1 h following irradiation (5 mg, i.v.) and G-CSF on days 3–12 following irradiation (2.5 μg/day, s.c.). Data are represented as a percentage of splenic GM-CFC content in nonirradiated (normal control) mice. Glucan values differ significantly from saline values on days 10 ($p = 0.0056$), 12 ($p = 0.0004$), 14 ($p = 0.0001$), 17 ($p = 0.0001$), and 20 ($p = 0.0158$). G-CSF values differ significantly from saline values on days 10 ($p = 0.0042$), 12 ($p = 0.0001$), 14 ($p = 0.0001$), 17 ($p = 0.0001$), and 20 ($p = 0.0038$). Glucan plus G-CSF values differ significantly from saline values on days 10 ($p = 0.0001$), 12 ($p = 0.0001$), 14 ($p = 0.0001$), 17 ($p = 0.0001$), and 20 ($p = 0.0010$). Glucan plus G-CSF values differ significantly from glucan values on days 10 ($p = 0.0001$), 12 ($p = 0.0068$), 14 ($p = 0.0012$), 17 ($p = 0.0001$), and 20 ($p = 0.0001$). Glucan plus G-CSF values differ significantly from G-CSF on days 10 ($p = 0.0001$), 12 ($p = 0.0075$), 14 ($p = 0.0028$), 17 ($p = 0.0032$), and 20 ($p = 0.0451$). No splenic GM-CFC were detected in any treatment group on days 4 or 7 following irradiation.

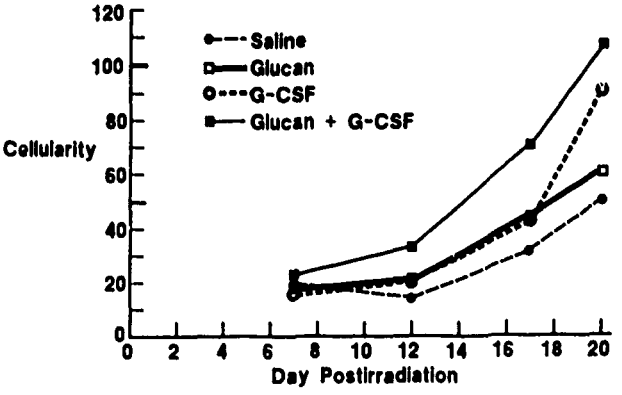


Fig. 4. Effect of glucan, G-CSF, and glucan plus G-CSF on peripheral white blood cellularity in C3H/HeN mice irradiated with 6.5 Gy. Mice received glucan at 1 h following irradiation (5 mg, i.v.) and G-CSF on days 3–12 following irradiation (2.5 μg/day, s.c.). Data are represented as a percentage of counts obtained in nonirradiated (normal control) mice. Glucan values differ significantly from saline values on days 12 ($p = 0.0086$), 17 ($p = 0.0073$), and 20 ($p = 0.0083$). G-CSF values differ significantly from saline values on days 12 ($p = 0.0092$), 17 ($p = 0.0076$), 20 ($p = 0.0043$). Glucan plus G-CSF values differ significantly from saline values on days 12 ($p = 0.0034$), 17 ($p = 0.0002$), and 20 ($p = 0.0019$). Glucan plus G-CSF values differ significantly from glucan values on days 12 ($p = 0.0501$), 17 ($p = 0.0319$), and 20 ($p = 0.0012$). Glucan plus G-CSF values differ significantly from G-CSF values on days 7 ($p = 0.0497$), 12 ($p = 0.0499$), 17 ($p = 0.0324$), and 20 ($p = 0.0296$).

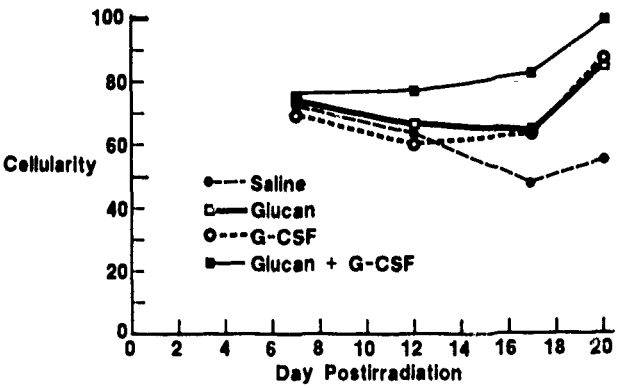


Fig. 5. Effect of glucan, G-CSF, and glucan plus G-CSF on red blood cellularity in C3H/HeN mice irradiated with 6.5 Gy. Mice received glucan at 1 h following irradiation (5 mg, i.v.) and G-CSF on days 3–12 following irradiation (2.5 μg/day, s.c.). Data are represented as a percentage of counts obtained in nonirradiated (normal control) mice. Glucan values differ significantly from saline values on days 17 ($p = 0.0014$) and 20 ($p = 0.0004$). G-CSF values differ significantly from saline values on days 17 ($p = 0.0135$) and 20 ($p = 0.0007$). Glucan plus G-CSF values differ significantly from saline values on days 12 ($p = 0.0469$), 17 ($p = 0.0001$), and 20 ($p = 0.0001$). Glucan plus G-CSF values differ significantly from glucan values on days 12 ($p = 0.0499$), 17 ($p = 0.0213$), and 20 ($p = 0.0393$). Glucan plus G-CSF values differ significantly from G-CSF values on days 7 ($p = 0.0100$), 12 ($p = 0.0024$), 17 ($p = 0.0243$), and 20 ($p = 0.0400$).

as a result of hemopoietic stem cell damage and subsequent abolition of the ability to generate mature WBC critical for effective antimicrobial host defenses [4, 5, 31]. In vivo, hemopoiesis is regulated by specific molecules produced within specialized accessory cells constituting the hemopoietic microenvironment [32–3. ]. Hence, hemopoietic regeneration following radiation exp sure is dependent both on the sparing of a critical number of hemopoietic stem cells and on the sparing of accessory cells necessary for the production of essential hemopoietic growth factors.

The sparing of hemopoietic stem cells directly depends on radiation dose [36, 37]; the greater the radiation dose, the greater the proportion of stem cells destroyed and the longer the time required for the regeneration of mature functional hemopoietic cells. Following radiation doses that theoretically could require weeks for hemopoietic regeneration, death due to infection generally occurs before signs of hemopoietic reconstitution are detectable. However, if infection can be mitigated and survival time extended, for example, by the administration of substitutional therapy such as antibiotics and fluids or replacement therapy such as PLT and RBC [38–40], hemopoietic recovery eventually occurs, even following some otherwise lethal radiation exposures. Thus, by keeping the host from succumbing to infection, some therapies "buy time" to allow the production of new functional mature WBC that are ultimately responsible for enhancing survival. As opposed to "buying time" to allow normal hemopoietic regeneration to occur, an alternative approach to enhancing survival is to reduce the period of time required for hemopoietic regeneration to occur. For example, following otherwise lethal radiation exposures that permit the survival of only a small number of endogenous hemopoietic stem cells, administration of individual hemopoietic growth factors or immunomodulators capable of inducing endogenous hemopoietic growth factor production has been demonstrated

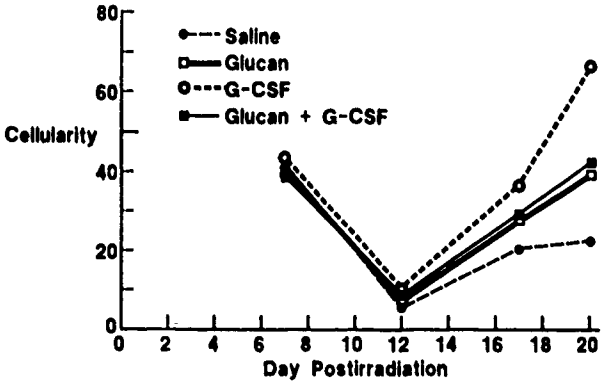


Fig. 6. Effect of glucan, G-CSF, and glucan plus G-CSF on PLT cellularity in C3H/HeN mice irradiated with 6.5 Gy. Mice received glucan at 1 h following irradiation (5 mg, i.v.) and G-CSF on days 3–12 following irradiation (2.5 μg/day, s.c.). Data are represented as a percentage of counts obtained in nonirradiated (normal control) mice. Glucan values differ significantly from saline values on days 17 ($p = 0.0424$) and 20 ($p = 0.0014$). G-CSF values differ significantly from saline values on days 12 ($p = 0.0442$), 17 ($p = 0.0001$), and 20 ($p = 0.0001$). Glucan plus G-CSF values differ significantly from saline values on days 12 ($p = 0.0501$), 17 ($p = 0.0193$), and 20 ($p = 0.0015$). Glucan plus G-CSF values differ significantly from G-CSF values on days 17 ($p = 0.0447$) and 20 ($p = 0.0001$).

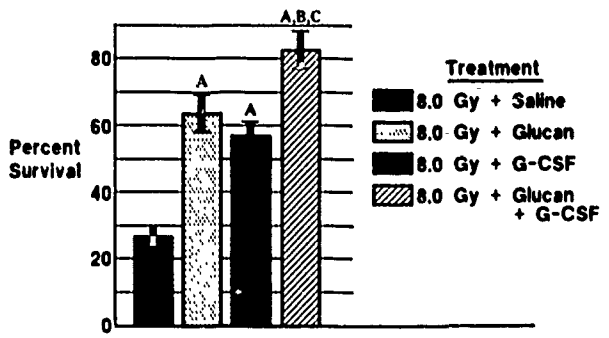


Fig. 7. Effect of glucan, G-CSF, and glucan plus G-CSF on survival in C3H/HeN mice irradiated with 8.0 Gy. Mice received glucan at 1 h following irradiation (5 mg, i.v.) and G-CSF on days 3–12 following irradiation (2.5 μg/day, s.c.). Each group represents a total of 30 mice. [a], significantly different from saline values. [b], significantly different from glucan values. [c], significantly different from G-CSF values.

to accelerate hemopoietic regeneration and to enhance survival [25, 26, 29, 40–42]. Furthermore, when substitutional and replacement therapies such as antibiotics and PLT have been combined with hemopoietic growth factor or immunomodulator therapy, even better survival enhancement than that produced by either individual therapy has been demonstrated [26, 40, 42]. In the studies described in this paper, we evaluated the ability of glucan and G-CSF, two hemopoietic stimulants that individually can enhance survival in irradiated mice [8, 24], to further accelerate hemopoietic regeneration and enhance survival when administered in combination.

The survival-enhancing capability of G-CSF has been thought to be mediated by its ability to accelerate the regeneration of mature granulocytes necessary for effective antimicrobial host defenses [43]. Presumably, this occurs through the ability of G-CSF to directly stimulate the regenerative capacity of GM-CFC progenitor pools [22-24, 26]. However, recent murine data demonstrate that in vivo administration of G-CSF also enhances the regeneration of CFU-s, BFU-e, and megakaryocyte colony-forming cells (Meg-CFC) [23]; these effects may be indirectly mediated following administration of G-CSF. Our findings confirm the multiple lineage effects of G-CSF administration in mice because WBC, RBC, and PLT recoveries were all accelerated following G-CSF therapy.

The survival-enhancing capability of glucan, to a large extent, has also been attributed to its ability to stimulate hemopoietic regeneration, following irradiation. However, as opposed to G-CSF, which no doubt has direct stimulating effects on at least GM-CFC precursors, the hemopoietic effects of glucan are presumed to be indirectly mediated through its ability to induce endogenous hemopoietic growth factor production from predominantly radioresistant macrophage cell populations [10, 44]. For example, both GM-CSF [10, 11] and interleukin (IL-1) [45] production have been demonstrated following in vivo glucan administration. Glucan therapy following irradiation has been demonstrated to accelerate the regeneration of not only CFU-s but also GM-CFC, M-CFC, BFU-e, CFU-e, and hemopoietic stromal cells [6]. In addition, even prior to detection of hemopoietic effects, glucan-treated irradiated mice exhibit reduced bacterial translocation, which is mediated via glucan-activated host macrophage populations [9]. Hence, glucan appears to function as a therapy that "buys time," as well as a therapy capable of stimulating hemopoietic regeneration.

It is because of the somewhat different mechanisms through which glucan and G-CSF appear to mediate their survival-enhancing effects that it was suspected that these agents might further enhance survival if used in combination in irradiated mice. The data presented in this paper affirm this hypothesis. In addition, our studies confirm that, individually, glucan and G-CSF therapy can accelerate hemopoietic regeneration and enhance survival in irradiated mice. In general, G-CSF therapy resulted in better hemopoietic regeneration than glucan therapy; however, glucan therapy was slightly more effective in enhancing survival than G-CSF therapy. These results again suggest that multiple mechanisms contribute to survival enhancement following radiation injury. When used in combination, glucan plus G-CSF therapy not only resulted in better survival enhancement than either agent alone (Fig. 7), but it also resulted in better hemopoietic regeneration than either agent used individually (Table 1 and Figs. 2–5). Similar synergistic hemopoietic regenerative effects have been observed with G-CSF administered in combination with GM-CSF [23], IL-1 [46], and dolichyl phosphate [47] in radiation- or chemotherapy-treated mice. In contrast to some of these other combination therapies, however, glucan plus G-CSF therapy not only best accelerated hemopoietic regeneration following radiation exposure, but also reduced the severity of the GM-CFC, WBC, and RBC nadirs following radiation exposure (Figs. 2–5). The mechanisms through which this occurs remain to be evaluated.

Platelet recovery was the one exception where combined glucan plus G-CSF therapy did not result in the best recovery (Fig. 6). Mice treated with G-CSF alone consistently demonstrated the best platelet recovery. One explanation for this could be that glucan, through its ability to activate macrophage populations and to increase reticuloendothelial clearance capacity in irradiated mice [9], may (in spite of potentially stimulating platelet regeneration) also promote platelet clearance/destruction through enhanced reticuloendothelial clearance mechanisms. Interestingly, a similar phenomenon was also transiently observed in irradiated mice treated with G-CSF used in combination with GM-CSF [23].

In conclusion, the data presented in this paper suggest that hemopoietic and survival-enhancing agents that act through different immuno/hemopoietic mechanisms may be successfully used in combination to further accelerate hemopoietic repopulation following irradiation and increase survival. Such combined therapeutic approaches may have great value in mitigating radiation- or drug-induced myelosuppression and subsequent lethality in the clinic.

## Acknowledgments

We are grateful to Ms. Barbara Calabro and Ms. Sheryl Reilly for excellent technical assistance and to Ms. Carolyn Wooden for editorial assistance. This work was supported by the Armed Forces Radiobiology Research Institute, Defense Nuclear Agency, under Research Work Unit 00132. Views presented in this paper are those of the authors; no endorsement by the Defense Nuclear Agency has been given or should be inferred. Research was conducted according to the principles enunciated in the Guide for the Care and Use of Laboratory Animals prepared by the Institute of Laboratory Animal Resources, National Research Council.

## References

1. Blackett NM, Marsh JC, Gordon MY, Okell SF, Aguado M (1978) Simultaneous assay by six methods of the effect on hemopoietic precursor cells of adriamycin, methyl-CCNU, $^{60}$Co gamma rays, vinblastine, and cytosine arabinoside. Exp Hematol 6:2
2. Lohrmann HP, Schreml W (1982) Cytotoxic drugs and the granulopoietic system. Recent Results Cancer Res 81:1
3. Broerse JJ, MacVittie TJ (1984) Response of different species to total body irradiation. Dordrecht: Martinus Nijhoff
4. Benacerraf B (1960) Influence of irradiation on resistance to infection. Bacteriol Rev 24:35
5. Hammond CW, Tompkins M, Miller CP (1954) Studies on susceptibility to infection following ionizing radiation; time of onset and duration of endogenous bacteremias in mice. J Exp Med 99:405
6. Patchen ML, MacVittie TJ, Wathen LM (1984) Effect of pre- and post-irradiation glucan treatment on pluripotent stem cells, granulocyte, macrophage and erythroid progenitor cells, and hemopoietic stromal cells. Experientia 40:1240
7. Patchen ML, D'Alesandro MM, Chirigos MA, Weiss JF (1988) Radioproteciton by biological response modifiers alone and in combination with WR-2721. Pharmacol Ther 39:247
8. Patchen ML, MacVittie TJ, Jackson WE (1989) Postirradiation glucan administration enhances the radioprotective effects of WR-2721. Radiat Res 117:59
9. Patchen ML, D'Alesandro MM, Brook I, Blakely WF, MacVittie TJ (1987) Glucan: mechanisms involved in its "radioprotective" effect. J Leukocyte Biol 42:95
10. Patchen ML, Lotzova E (1981) The role of macrophages and T-lymphocytes in glucan-mediated alteration of murine hemopoiesis. Biomedicine 34:71
11. Patchen ML, MacVittie TJ (1986) Hemopoietic effects of intravenous soluble glucan administration. Int J Immunopharmacol 8:407
12. Tatsukawa K, Mitsuyama M, Takeya K, Nomoto K (1979) Differing contribution of polymorphonuclear cells and macrophages to protection of mice against *Listeria monocytogenes* and *Pseudomonas aeruginosa*. J Gen Microbiol 115:161
13. Hirsch JG (1975) The phagocytic cells in host resistance: a perspective summation. In: Bellanti JA, Dayton DH (eds) The phagocytic cell in host resistance. New York: Raven Press, p 333
14. Metcalf D (1987) The molecular control of normal and leukaemic granulocytes and macrophages. Proc R Soc Lond B Biol Sci 230:389
15. Cohen AM, Zsebo KM, Inoue H, Hines D, Boone TC, Chazin VR, Tsai L, Ritch T, Souza LM (1987) In vivo stimulation of granulopoiesis by recombinant human granulocyte colony-stimulating factor. Proc Natl Acad Sci USA 84:2484
16. Nicola NA, Vadas M (1984) Hemopoietic colony-stimulating factors. Immunol Today 5:76
17. Lopez AF, Nicola NA, Burgess AW, Metcalf D, Battye FL, Sewell WA, Vadas M (1983) Activation of granulocyte cytotoxic function by purified mouse colony-stimulating factors. J Immunol 131:2983
18. Vadas MA, Nicola NA, Metcalf D (1983) Activation of antibody-dependent cell-mediated cytoxicity of human neutrophils and eosinophils by separate colony-stimulating factors. J Immunol 130:795
19. Welte K, Platzer E, Lu L, Gabrilove JL, Levi E, Mertelsmann R, Moore MAS (1985) Purification and biochemical characterization of human pluripotent hemopoietic colony-stimulating factor. Proc Natl Acad Sci USA 82:1526
20. Zsebo KM, Cohen AM, Murdock DC, Boone TC, Inoue H, Chazin VR, Hines D, Souza LM (1986) Recombinant human granulocyte colony-stimulating factor: molecular and biological characterization. Immunobiology 172:175
21. Souza LM, Boone TC, Gabrilove J, Lai PH, Zsebo KM, Murdock DC, Chazin VR, Bruszewski J, Lu H, Chen KK, Barendt J, Platzer E, Moore MAS, Mertelsmann R, Welte K (1986) Recombinant human granulocyte colony-stimulating factor: effects on normal and leukemic myeloid cells. Science 232:61
22. Kobayashi Y, Okabe T, Urabe A, Suzuki N, Takaku F (1987) Human granulocyte colony-stimulating factor produced by *Escherichia coli* shortens the period of granulocytopenia induced by irradiation in mice. Jpn J Cancer Res 78:763
23. Tanikawa S, Nakao I, Tsuneoka K, Nara N (1989) Effects of recombinant granulocyte colony-stimulating factor (rG-CSF) and recombinant granulocyte-macrophage colony-stimulating factor (rGM-CSF) on acute radiation hemopoietic injury in mice. Exp Hematol 17:883
24. Patchen ML, MacVittie TJ, Solberg BD, Souza LM (1990) Therapeutic administration of recombinant human granulocyte colony-stimulating factor accelerates hemopoietic regeneration and enhances survival in a murine model of radiation-induced myelosuppression. Int J Cell Cloning 8:107
25. Schuenig FG, Storb R, Goehle S, Graham TC, Appelbaum FR, Hackman R, Souza LM (1989) Effect of recombinant human granulocyte colony-stimulating factor on hemotopoiesis of normal dogs and on hemopoietic recovery after otherwise lethal total body irradiation. Blood 74:1308
26. MacVittie TJ, Monroy RL, Patchen ML, Souza LM (1990) Therapeutic use of recombinant human G-CSF (rhG-CSF) in a canine model of sublethal whole-body irradiation. Int J Radiat Biol 57:723
27. DiLuzio NR, Williams DL, McNamee RB, Edwards BF, Kitahama A (1979) Comparative tumor-inhibitory and anti-bacterial activity of soluble and particulate glucan. Int J Cancer 24: 773
28. Schulz J, Almond PR, Cunningham JR, Holt JG, Loevinger R, Suntharalingam N, Wright KA, Nath R, Lempert D (1983) A protocol for the determination of absorbed dose from high energy proton and electron beams. Med Phys 10:741
29. Patchen ML, MacVittie TJ (1985) Stimulated hemopoiesis and enhanced survival following glucan treatment in sublethally and lethally irradiated mice. Int J Immunopharmacol 7:923

30. Till J, McCulloch E (1963) Early repair processes in marrow cells irradiated and proliferating in vivo. Radiat Res 18:96
31. Durack DT (1982) Infection in compromised hosts. In: Lachmann PJ, Peters DK (eds) Clinical aspects of immunology. Oxford: Blackwell Scientific, p 1713
32. Broudy V, Kaushansky K, Segal G, Harlan J (1986) Tumor necrosis factor type alpha stimulates human endothelial cells to produce granulocyte–macrophage colony-stimulating factor. Proc Natl Acad Sci USA 83:7467
33. Moore RN, Oppenheim JJ, Farrar JJ, Carter CS, Waheed A. Shadduck RK (1980) Production of lymphocyte-activating factor (interleukin-1) by macrophages activated with colony-stimulating factors. J Immunol 125:1302
34. Sieff CA (1987) Hemopoietic growth factors. J Clin Invest 79: 1549
35. Le PT, Tuck DT, Dinarello CA, Hynes BF, Singer KH (1987) Human thymic epithelial cells produce interleukin 1. J Immunol 138:2520
36. Carsten AL (1984) Acute lethality: the hemopoietic syndrome in different species. In: Broerse JJ, MacVittie TJ (eds) Response of different species to total body irradiation. Dordrecht: Martinus Nijhoff, p 59
37. MacVittie TJ, Monroy RL, Patchen ML, Darden JH (1984) Acute lethality and radiosensitivity of the canine hemopoietic system to cobalt-60 gamma and mixed neutron-gamma irradiation. In: Broerse JJ, MacVittie TJ (eds) Response of different species to total body irradiation. Dordrecht: Martinus Nijhoff, p 113
38. Sorensen DK, Bond VP, Cronkite EP, Perman V (1960) An effective therapeutic regimen for the hemopoietic phase of the acute radiation syndrome in dogs. Radiat Res 13:669
39. Perman V, Sorensen DK, Usenik EA, Bond VP, Cronkite EP (1962) Hemopoietic regeneration in control and recovery of heavily irradiated dogs following severe hemorrhage. Blood 19: 738
40. MacVittie TJ, Monroy RL Potential improvement in the management of seriously irradiated persons. In: Ricks RC, Fry SA (eds) The medical basis for radiation accident preparedness: clinical experiences and follow-up since 1979. New York: Elsevier Scientific (in press)
41. Patchen ML, Chirigos MA, Brook I (1988) Use of glucan-P and sixteen other immunopharmaceutical agents in prevention of acute radiation injury. Comments Toxicol 2:217
42. Madonna GS, Ledney GD, Elliott TB, Brook I, Ulrich JT, Myers KR, Patchen ML, Walker RI (1989) Trehalose dimycolate enhances resistance to infection in neutropenic animals. Infect Immun 57:2495
43. Matsumoto M, Matsubara S, Matsuno T, Tamura M, Hattori K, Nomura H, Ono M, Yokota T (1987) Protective effect of human granulocyte colony-stimulating factor on microbial infection in neutropenic mice. Infect Immun 55:2715
44. Gallin EK, Patchen ML, Green SW, Schwartz GN Comparative effects of particulate and soluble glucan in C3H/HeN and C3H/HeJ mice: possible role of macrophage stimulation in glucan-mediated radioprotection. J Leukocyte Biol (submitted)
45. Sherwood E, Williams D, DiLuzio N (1986) Glucan stimulates production of antitumor cytolytic/cytostatic factor(s) by macrophages. J Biol Response Mod 5:504
46. Moore MA, Warren DS (1987) Synergy of interleukin-1 and granulocyte colony-stimulating factor: in vivo stimulation of stem cell recovery and hemopoietic regeneration following 5-fluorouracil treatment of mice. Proc Natl Acad Sci USA 84:7134
47. Shimamura M, Takigawa T, Urabe A, Okabe T, Souza L, Takaku F (1988) Synergistic effect of dolichyl phosphate and human recombinant granulocyte colony-stimulating factor on recovery from neutropenia in mice treated with anti-cancer drugs. Exp Hematol 16:681